PB81-124000

REPORT NO.
UCB/EERC-80/17
JULY 1980

EARTHQUAKE ENGINEERING RESEARCH CENTER

DYNAMIC RESPONSE OF SIMPLE ARCH DAMS INCLUDING HYDRODYNAMIC INTERACTION

by
CRAIG S. PORTER
ANIL K. CHOPRA

A report on research conducted under
Grants ATA74-20554 and ENV76-80073
from the National Science Foundation.

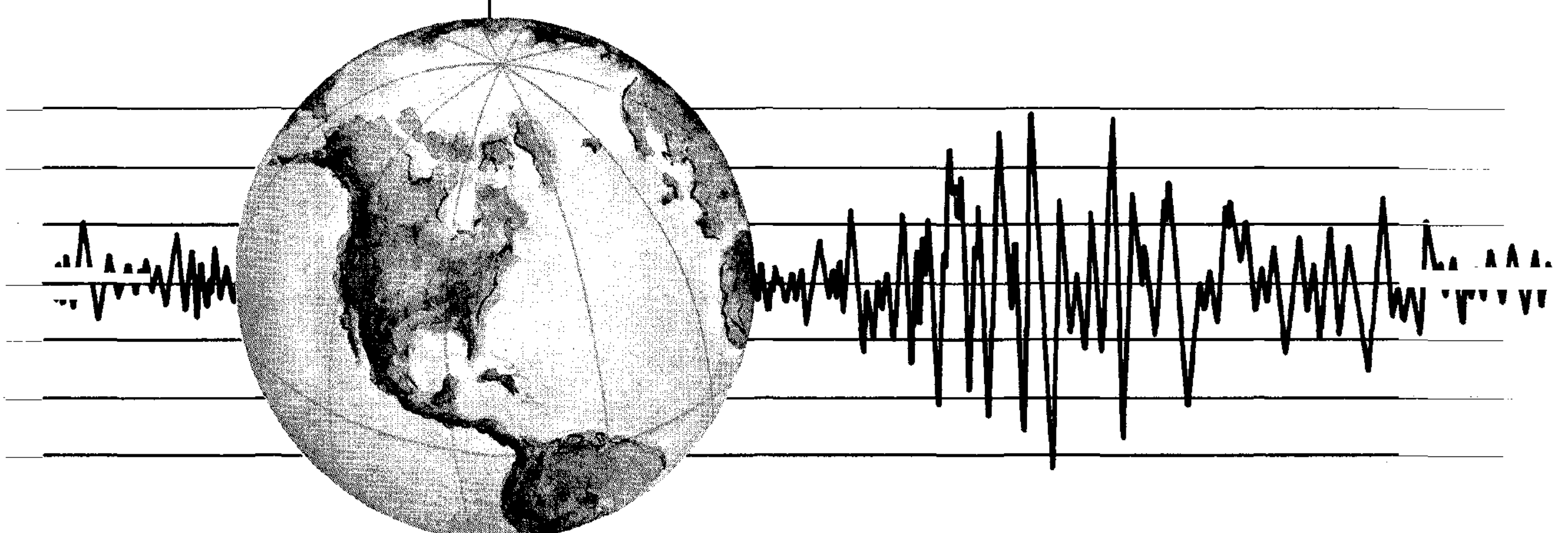

COLLEGE OF ENGINEERING

UNIVERSITY OF CALIFORNIA · Berkeley, California

For sale by the National Technical Information Service, U.S. Department of Commerce, Springfield, Virginia 22161.

See back of report for up to date listing of EERC reports.

DISCLAIMER

50272-101

REPORT DOCUMENTATION PAGE	1. REPORT NO. NSF/RA-800291	2.	3. Recipient's Accession No. PB81 124000

4. Title and Subtitle Dynamic Response of Simple Arch Dams Including Hydrodynamic Interaction	5. Report Date July 1980
	6.
7. Author(s) Craig S. Porter and Anil K. Chopra	8. Performing Organization Rept. No. UCB/EERC-80/17
9. Performing Organization Name and Address Earthquake Engineering Research Center University of California, Richmond Field Station 47th and Hoffman Blvd. Richmond, California 94804	10. Project/Task/Work Unit No. 11. Contract(C) or Grant(G) No. (C) (G) ATA74-20554 ENV76-80073
12. Sponsoring Organization Name and Address National Science Foundation 1800 G Street, N.W. Washington, D. C. 20550	13. Type of Report & Period Covered 14.

15. Supplementary Notes

16. Abstract (Limit: 200 words)

The substructure method is adapted and generalized for response analysis of arch dams subjected to upstream-downstream, cross-stream and vertical components of ground motion. The arch dam is assumed to be a segment of a circular cylinder, bounded by vertical, radial banks of the river valley enclosing a central angle of 90°. The arch dam and impounded water are treated as two substructures of the total system and displacements of the dam are represented as a linear combination of the first few natural modes of vibration of the dam alone. For this simple geometry of the arch dam and fluid domain, mathematical solutions of the wave equation are presented to determine the hydrodynamic terms in the finite element equations for the dam. Responses to arbitrary ground motion can be obtained by Fourier synthesis procedures applied to the complex frequency response functions determined by the analysis procedures developed in this report.

Numerical results are presented for the complex frequency response functions for hydrodynamic pressures on rigid dams due to each of the three ground motion components. The variation of these pressures with excitation frequency, depth below the free surface of water and circumferential location on the upstream face of the dam is studied, and compared with the hydrodynamic pressures on straight gravity dams.

The responses of three arch dams, with different radius to height ratios, are analysed for three conditions: the dam alone without water, and the dam with full reservoir, considering water to be compressible in one case and neglecting water compressibility in the other case. The complex frequency response functions for accelerations at the dam crest due to the three components of ground motion -- upstream-downstream component, cross-stream component and vertical component -- are presented. These response results are discussed in detail.

18. Availability Statement Release Unlimited	19. Security Class (This Report)	21. No. of Pages
	20. Security Class (This Page)	22. Price

(ANSI-Z39.18) See Instructions on Reverse

OPTIONAL FORM 272 (4-77)
(Formerly NTIS-35)
Department of Commerce

DYNAMIC RESPONSE OF SIMPLE ARCH DAMS INCLUDING HYDRODYNAMIC INTERACTION

by

Craig S. Porter
Anil K. Chopra

A Report on Research Conducted Under
Grants ATA74-20554 and ENV76-80073
from the National Science Foundation

Report No. UCB/EERC-80/17
Earthquake Engineering Research Center
University of California
Berkeley, California

July 1980

ABSTRACT

The substructure method is adapted and generalized for response analysis of arch dams subjected to upstream-downstream, cross-stream and vertical components of ground motion. The arch dam is assumed to be a segment of a circular cylinder, bounded by vertical, radial banks of the river valley enclosing a central angle of 90°. The arch dam and impounded water are treated as two substructures of the total system and displacements of the dam are represented as a linear combination of the first few natural modes of vibration of the dam alone. For this simple geometry of the arch dam and fluid domain, mathematical solutions of the wave equation are presented to determine the hydrodynamic terms in the finite element equations for the dam. Responses to arbitrary ground motion can be obtained by Fourier synthesis procedures applied to the complex frequency response functions determined by the analysis procedures developed in this report.

Numerical results are presented for the complex frequency response functions for hydrodynamic pressures on rigid dams due to each of the three ground motion components. The variation of these pressures with excitation frequency, depth below the free surface of water and circumferential location on the upstream face of the dam is studied, and compared with the hydrodynamic pressures on straight gravity dams.

The responses of three arch dams, with different radius to height ratios, are analysed for three conditions: the dam alone without water, and the dam with full reservoir, considering water to be compressible in one case and neglecting water compressibility in the other case. The complex frequency response functions for accelerations

at the dam crest due to the three components of ground motion -- upstream-downstream component, cross-stream component and vertical component -- are presented. These response results lead to the following conclusions.

In general, hydrodynamic effects and water compressibility should be considered in analyzing the dynamic response of arch dams.

Water in the reservoir causes a decrease in the resonant frequencies of the dam; as much as 30 percent reduction was observed in in the cases analyzed. The decrease in a resonant frequency depends on the depth of water, mode number, whether the mode is symmetric or anti-symmetric and the radius to height ratio of the dam. Greater reductions are observed for dams with higher radius to height ratios and in the lower modes of vibration.

For all three components of ground motion, water compressibility has little influence on the response of the dam at excitation frequencies ω much smaller than ω_1^r, the fundamental resonant frequency of the fluid domain. At excitation frequencies $\omega > \omega_1^r$ the response to upstream-downstream and vertical components of ground motion is reduced by water compressibility effects. However, these effects may lead to an increase or decrease in the response to cross-stream ground motion, depending on the excitation frequency.

Dam-water interaction, considering water compressibility, affects the radial acceleration response of dams to upstream-downstream and cross-stream ground motions to a similar degree. However, the response to vertical ground motion is greatly increased by these effects. Just as in the case of gravity dams, vertical ground motion causes significant hydrodynamic pressures, which act in the horizontal plane on a cylindrical dam face, thus causing significant additional response.

The additional hydrodynamic forces caused by bank motions in the upstream-downstream or cross-stream directions may significantly affect the dynamic response of arch dams at some excitation frequencies. However, these effects of bank motions are generally smaller than the effects of dam-water interaction or of water compressibility. The effects of bank motion on dam response are roughly similar in magnitude for the two howizontal components of ground motion. In the case of vertical ground motion, the motion of the vertical banks produces no additional hydrodynamic forces and hence has no influence on the dam response.

ACKNOWLEDGEMENTS

This research investigation was conducted under grants from the National Science Foundation: Grants ATA74-20554 and ENV76-80073.

This report also constitutes Craig S. Porter's doctoral dissertation which has been submitted to the University of California, Berkeley. The dissertation committee consisted of Professors A.K. Chopra (Chairman), R.W. Clough and E.J. Pinney. Appreciation is expressed to Professors Clough and Pinney for reviewing the manuscript.

TABLE OF CONTENTS

Page

1. INTRODUCTION

1.1 Objectives

The dynamic response behavior of concrete arch dams is complicated because of their three dimensional geometry and the effects of impounded water. Improved understanding of the effects of the impounded water on the dynamics of concrete arch dams is essential to develop reliable procedures for computing the dynamic deformations and stresses in a dam subjected to prescribed ground motion. The objective of this work is to study the dynamic structural behavior and response of arch dams to ground motion, with special emphasis on identifying hydrodynamic effects in the response behavior.

1.2 Review of Past Work

During the past 25 years the finite element method has become the standard procedure for analysis of all types of complex civil engineering structures. Employing three-dimensional solid elements and thick shell elements, computer programs for finite element analysis of earthquake response of arch dams have been developed [1]. The principal limitation of computer programs presently available lies in the treatment of the dynamic effects of the impounded water; they have either been ignored or simplified to an extent that the results may be unreliable.

Early results of Westergaard's and Zangar's analyses of earthquake induced hydrodynamic pressures on rigid, straight dams with vertical upstream face [2] and sloping upstream face [3] provided a basis for added mass representation of hydrodynamic effects in analysis of dams. Because corresponding results for arch dams have not been available in appropriate form, the results for straight gravity dams have been extrapolated and adapted in analyses of arch dams [4].

Under the assumption that the arch dam is a segment of a rigid cylinder -- thus having a constant radius -- bounded by vertical, radial banks of the river valley enclosing a central angle of 90°, the wave equation governing the hydrodynamic pressures was solved mathematically for prescribed harmonic motions of the boundaries [5]. This result along with Fourier Transform procedures permitted evaluation of hydrodynamic pressures due to arbitrary earthquake motions [6]. Although the dam was assumed to be rigid and only one direction of ground motion was considered in these studies, it was shown that water compressibility as well as curvature of the arch dam in plan has significant influence on hydrodynamic pressures.

Electrical analogue [7] and finite difference [8,9] procedures have been employed to model arbitrary, three-dimensional geometry of the reservior and dam. Neglecting water compressibility, hydrodynamic pressures due to prescribed accelerations of rigid dams [8] or flexible dams [9] were determined by these procedures.

The assumption of a rigid dam in the above mentioned analyses of hydrodynamic pressures omits fundamental features of the problem. The ground motion and the deformations of the upstream face of the dam will cause hydrodynamic pressures, and the structural deformations in turn will be affected by the hydrodynamic pressures on the upstream face of the dam. To break this closed cycle of cause and effect, the problem formulation must recognize the dynamic interaction between the dam and water.

A finite element or finite difference analysis of the complete dam-water system can account for the interaction effects [10,11,12].

However, these approaches appear to require prohibitive computational effort for problems of practical size. In other approaches to include hydrodynamic interaction effects, the equations of motion for the dam are numerically solved in the time domain with the hydrodynamic terms determined from finite difference solutions of the fluid domain [8].

Methods recently developed for analysis of gravity dams including hydrodynamic interaction contain two key ideas [13]. Firstly, the dam and the fluid domain are treated as two substructures of the total system, with the effects of the fluid expressed as frequency-dependent terms in the governing equations for the dam. Secondly, these equations are transformed in terms of the first few modes of vibration of the dam, thus enabling drastic reduction in the number of unknowns leading to highly efficient solutions. The hydrodynamic terms in the structural equations are determined as solutions of the wave equation over the fluid domain for appropriate motions of the boundary. In analysis of gravity dam monoliths, two dimensional solutions for the wave equation had to be obtained. Explicit mathematical solutions were possible under the assumption that the upstream face is vertical and the reservoir extends to infinity in the upstream direction [13,14].

The earliest analyses [14,15] of response of gravity dams including hydrodynamic effects, a special case of the general procedure developed later [13], considered only the fundamental mode of vibration of the dam. Following identical steps, the corresponding one-mode analysis for arch dams subjected to upstream-downstream ground motion has been developed [16]. In this analysis explicit mathematical solutions for the fluid domain with the idealized geometry mentioned earlier were employed. Results of this analysis indicated that the earthquake response of arch dams with full reservoir is much larger than the response with no water; and that water compressibility has significant influence on the hydrodynamic effects in response of dams.

The analysis procedure presented here is a generalization of the work mentioned above [16], being capable of including any number of modes of vibration of the dam thus making it possible to obtain results to any desired degree of accuracy; and considering the responses to all three -- upstream-downstream, cross-stream and vertical -- components of ground motion. The substructure method for formulating the governing equations in the frequency domain and their transformation to modal coordinates, which has proven to be an effective approach in two-dimensional analysis of concrete gravity dams, is adapted and generalized for three dimensional analysis of arch dams.

1.3 Scope

The ground motion assumptions and description of the idealized geometry of the arch dam and reservoir are described in Chapter 2.

Chapter 3 presents the equations of motion governing the dam including fluid interaction. These equations are transformed to the undamped modal coordinates of the dam. Equations of motion governing the hydrodynamic pressure in the fluid are also presented.

In Chapters 4, 5 and 6 the equations governing the hydrodynamic pressures on the dam are solved for upstream-downstream, cross-stream and vertical components of ground motion, respectively. Results are presented and discussed for the special case of hydrodynamic pressures on rigid arch dams. In each of these chapters the hydrodynamic terms are then incorporated into the modal equations of motion of the dam. Versions of these equations are presented for the cases of no fluid, incompressible fluid and compressible fluid in the reservoir.

Using the analysis procedures of Chapters 3 thru 6, nondimensional numerical results for the harmonic response of arch dams having three different sets of geometric properties are presented in Chapter 7. Effects of hydrodynamic interaction, compressibility of water and bank motion on dam response are identified.

The more important conclusions of this investigation are summarized in Chapter 8.

Using the analysis procedures of Chapters 3 thru 6, nondimensional numerical results for the harmonic response of arch dams having three different sets of geometric properties are presented in Chapter 7. Effects of hydrodynamic interaction, compressibility of water and bank motion on dam response are identified.

The more important conclusions of this investigation are summarized in Chapter 8.

2. SYSTEM AND GROUND MOTION

The arch dam-water system investigated is shown in Fig. 2.1. The upstream face of the arch dam is a segment of a circular cylinder, radius R and height H_d, contained within radially extending banks enclosing a central angle of 90°. In addition, the geometry and the mass, stiffness and damping properties of the dam are all assumed to be symmetrical about the x-z ($\theta = 0$) plane. Except for these restrictions, the geometry and these properties of the arch dam are arbitrary. The reservoir, which has a horizontal bottom, is filled to a height H with water extending to infinity in the x (upstream) direction. The dam is presumed to be fixed at the base and at the banks.

In analyzing the earthquake response of the system, the dam material is considered to be linearly elastic and the deformation of the dam small, resulting in linear force-deformation relations for the dam. Water is considered to be compressible and inviscid, and only linear effects are included.

The earthquake ground motion is defined by the upstream-downstream (x), cross-stream (y) and vertical (z) translational components or ground motion; the first two are horizontal and the latter is vertical. The upstream-downstream component of ground motion is along the plane of symmetry of the dam. The cross-stream (y) component is perpendicular to the plane of symmetry (Fig. 2.1). At any instant of time, the ground motion is identical throughout the reservoir bottom and banks, but the motion varies with time.

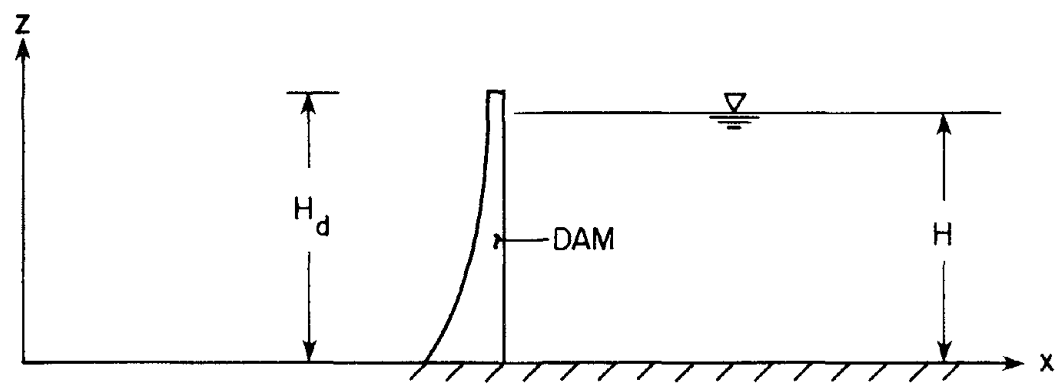

(a) SECTION ALONG X AXIS

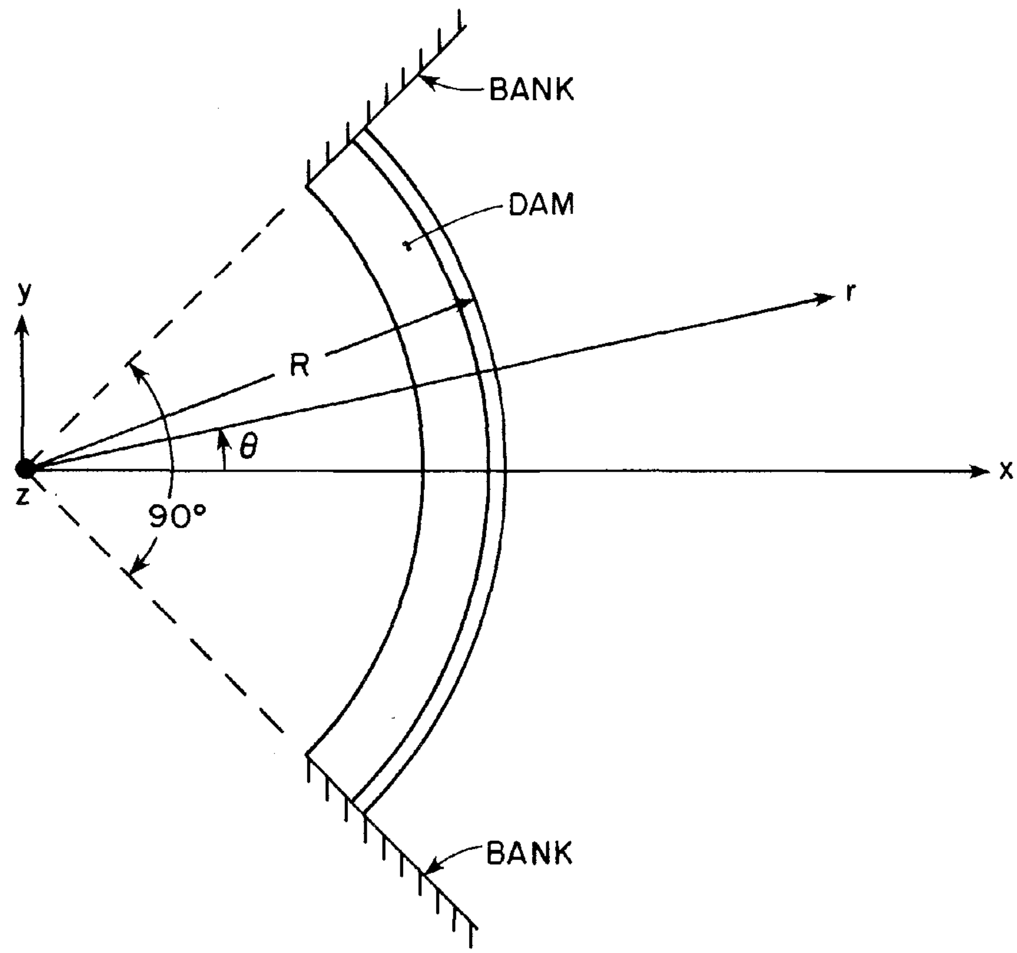

(b) PLAN VIEW

FIG. 2.1 ARCH DAM-RESERVOIR SYSTEM

3. EQUATIONS OF MOTION

3.1 Finite Element Idealization

A finite element idealization for an arch dam must reproduce the three-dimensional structural behavior of the dam. Many different types of finite elements have been proposed for analysis of three-dimensional structures. For arbitrary solids the eight-node isoparametric brick element with internal incompatible modes has proven to be very efficient - it provides a good approximation of the stress distribution with a minimum number of degrees of freedom (DOF). However, for an arch dam, significantly better performance can be obtained for a given cost of computation by modeling the dam with higher order elements that can better represent the complex geometric shape and can more closely approximate the thick shell structural behavior of the dam. In this study, the dam is idealized as an assemblage of curved thick shell elements - 16 node isoparametric brick elements with internal incompatible modes to improve bending behavior, see Appendix B. This element was selected from available element types used in ADAP (Arch Dam Analysis Program) [1].

3.2 Equations of Motion: Dam

The equations of motion for an arch dam, idealized as a thick-shell finite element system and subjected to earthquake ground motion, including hydrodynamic effects, are:

$$\underline{m}\,\ddot{\underline{v}} + \underline{c}\,\dot{\underline{v}} + \underline{k}\,\underline{v} = -\,\underline{m}\,\underline{e}^x\,\ddot{v}_g^x(t) - \underline{m}\,\underline{e}^y\,\ddot{v}_g^y(t) - \underline{m}\,\underline{e}^z\,\ddot{v}_g^z(t) - \underline{Q}(t) \qquad (3.1)$$

In this equation, $\underline{v}$ is the vector of nodal point displacement relative to the ground, and

$$\underline{v}^T = < v_1^x, v_1^y, v_1^z, v_2^x, v_2^y, v_2^z, \ldots, v_n^x, v_n^y, v_n^z, \ldots, v_N^x, v_N^y, v_N^z >$$

where v_n^x, v_n^y, and v_n^z are, respectively, the x-, y-, and z-components of the displacement of nodal point "n" (Fig. 3.1) and N is the number of unrestrained nodal points, those above the base and not on the banks, in the finite element idealization. The nodal point velocity and acceleration vectors are denoted by $\dot{\underline{v}}$ and $\ddot{\underline{v}}$ and the consistent mass, damping, and stiffness matrices for the finite element system by $\underline{m}$, $\underline{c}$, and $\underline{k}$, respectively. Neglected in the effective load terms of Eq. 3.1 is the mass matrix $\underline{m}_g$ coupling DOF of the restrained nodal points, those on the base or on the banks, with the DOF of the unrestrained nodal points [17]. The pseudo-static influence vectors $\underline{e}^x$, $\underline{e}^y$, and $\underline{e}^z$, associated with three components of ground motion, are defined by:

$$\{e^x\}^T = < 1,0,0,1,0,0,\ldots 1,0,0,\ldots 1,0,0 >$$

$$\{e^y\}^T = < 0,1,0,0,1,0,\ldots 0,1,0,\ldots 0,1,0 >$$

$$\{e^z\}^T = < 0,0,1,0,0,1,\ldots 0,0,1,\ldots 0,0,1 >$$

The x-, y-, and z-components of earthquake ground acceleration are denoted by $v_g^x(t)$, $v_g^y(t)$, and $v_g^z(t)$, respectively.

In Eq. 3.1 $\underline{Q}(t)$ is the vector of nodal point loads associated with hydrodynamic pressures. As these pressures act only on the upstream face of the dam, the elements in $\underline{Q}(t)$ corresponding to nodal points not on the upstream face are zero. The subvector of $\underline{Q}(t)$ associated with the DOF of the nodal points on the upstream face, in contact with the water, is denoted by $\underline{Q}^f(t)$. Because the hydrodynamic pressures act normal to the upstream face, which is a segment of a

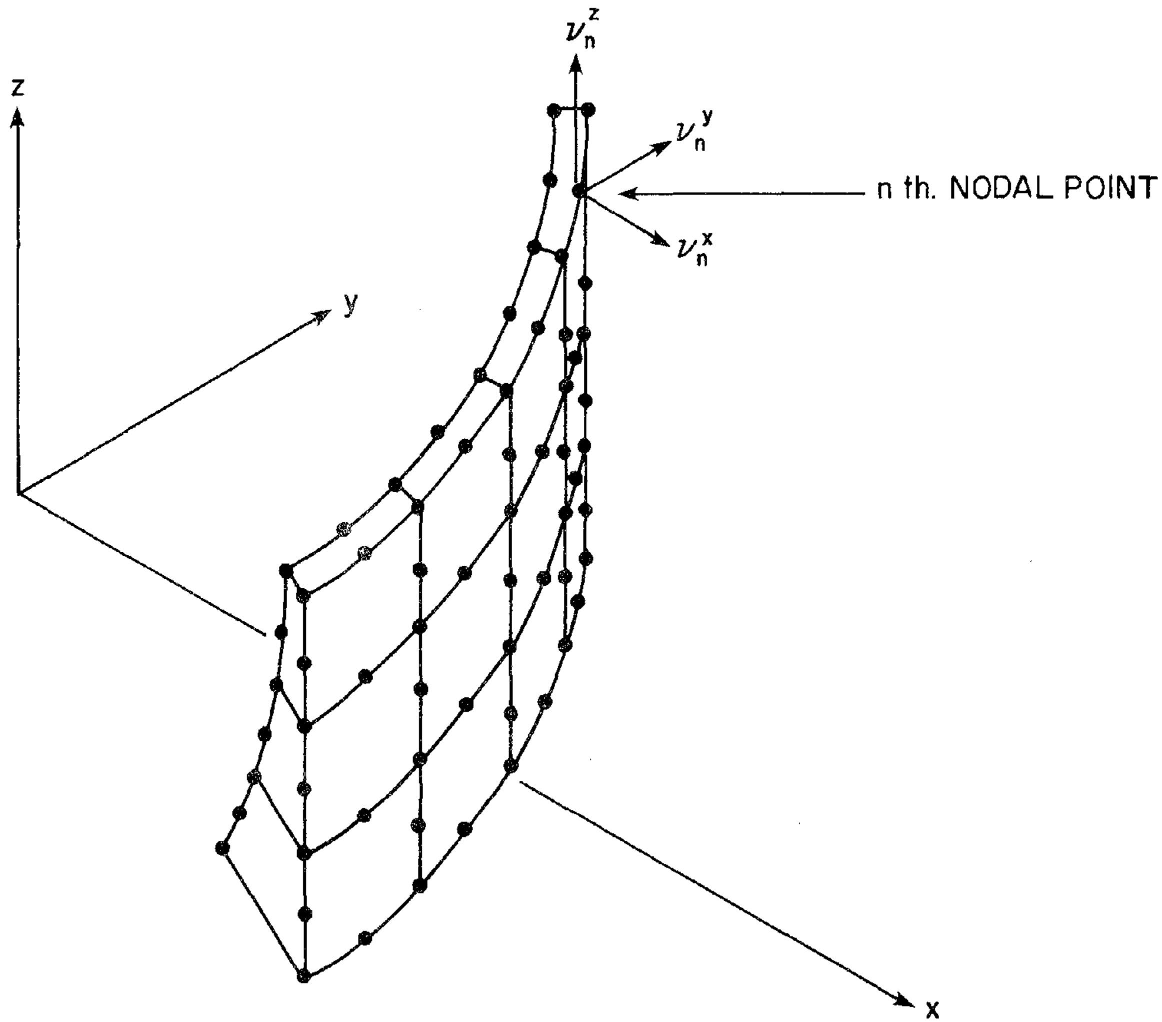

FIG. 3.1 FINITE ELEMENT IDEALIZATION OF AN ARCH DAM

segment of a circular cylinder, the elements of $\underset{\sim}{Q}^f$ associated with the vertical (z) DOF will be zero.

Standard procedures are available to evaluate the mass and stiffness properties of the finite element assemblage [18-20], which need not be described here; moreover the damping properties are best expressed in terms of the damping ratios, as will be described later, so that there is no need to evaluate the damping matrix.

Following procedures presented earlier for analysis of gravity dams [13] and axisymmetric towers [21], the displacements of the arch dam, including hydrodynamic interaction effects, are expressed as a linear combination of the natural modes of vibration $\underset{\sim}{\phi}_j$ of the dam (without water):

$$\underset{\sim}{v}(t) = \sum_{j=1}^{J} Y_j(t)\ \underset{\sim}{\phi}_j \tag{3.2}$$

in which $Y_j(t)$ is the generalized displacement in the j^{th} mode. These natural vibration modes are the solutions of the following eigenvalue problem

$$\underset{\sim}{k}\ \underset{\sim}{\phi}_j = \omega_j^2\ \underset{\sim}{m}\ \underset{\sim}{\phi}_j \tag{3.3}$$

where ω_j denotes the j^{th} natural frequency of vibration of the dam. The expansion given in Eq. 3.2 is complete if J is equal to 3N, the total number of DOF of the finite element system, because the vectors $\underset{\sim}{\phi}_j$ are linearly independent and span the space of dimension 3N. All modes contributing significantly to the response should be included in Eq. 3.2. Generally, the number of modes necessary is a small fraction of the total number of DOF.

Substituting Eq. 3.2 in Eq. 3.1 and utilizing the orthogonality properties of mode shapes, the equation governing the generalized displacement Y_j in the j^{th} mode is

$$M_j \ddot{Y}_j(t) + C_j \dot{Y}_j(t) + K_j Y_j(t) = P_j(t) \qquad j = 1,2,3,\ldots,J \qquad (3.4)$$

in which

$M_j = \underline{\phi}_j^T \underline{m} \underline{\phi}_j$ is the generalized mass

$C_j = \underline{\phi}_j^T \underline{c} \underline{\phi}_j = 2\xi_j \omega_j M_j$ is the generalized damping

ξ_j = the damping ratio for the j^{th} natural mode of vibration of the dam (without water)

$K_j = \underline{\phi}_j^T \underline{k} \underline{\phi}_j = \omega_j^2 M_j$ is the generalized stiffness

$P_j(t) = -\underline{\phi}_j \underline{m} \underline{e}^x \ddot{v}_g^x(t) - \underline{\phi}_j \underline{m} \underline{e}^y \ddot{v}_g^y(t) - \underline{\phi}_j \underline{m} \underline{e}^z \ddot{v}_g^z(t)$
$- \{\phi_j^f\}^T \underline{Q}^f(t)$ is the generalized load

The vector $\underline{\phi}_j^f$ is a sub-vector of the j^{th} mode shape $\underline{\phi}_j$ containing elements associated with the DOF on the upstream face of the dam. Two sub-vectors of $\underline{\phi}_j^f$ are introduced for use in section 4.3: $\underline{\phi}_j^{xf}$ and $\underline{\phi}_j^{yf}$, containing elements associated respectively with the x and y DOF of the nodal points on the upstream face.

3.3 Equations of Motion: Fluid Domain

Assuming water to be linearly compressible and inviscid, the pressures associated with small amplitude irrotational motion are governed by the wave equation in cylindrical coordinates (Fig. 2.1)

$$\frac{\partial^2 p}{\partial r^2} + \frac{1}{r}\frac{\partial p}{\partial r} + \frac{1}{r^2}\frac{\partial^2 p}{\partial \theta^2} + \frac{\partial^2 p}{\partial z^2} = \frac{1}{C^2}\frac{\partial^2 p}{\partial t^2} \qquad (3.5)$$

in which $p(r,\theta,z,t)$ is the hydrodynamic pressure (in excess of hydrostatic pressure) and C is the velocity of sound in water. The following expressions relate the hydrodynamic pressure and displacements of any particle of water

$$\frac{w}{g}\frac{\partial^2 v^r}{\partial t^2} = -\frac{\partial p}{\partial r}$$

$$\frac{w}{g}\frac{\partial^2 v^\theta}{\partial t^2} = -\frac{1}{r}\frac{\partial p}{\partial \theta} \qquad (3.6)$$

$$\frac{w}{g}\frac{\partial^2 v^z}{\partial t^2} = -\frac{\partial p}{\partial z}$$

where v^r, v^θ, and v^z are, respectively, the radial, tangential, and vertical components of water particle displacement; w is the unit weight of water, and g is the acceleration due to gravity.

Equation 3.5 together with appropriate boundary conditions at the reservoir boundaries -- the upstream face of the dam, the reservoir bottom, the free surface of the water, and the reservoir banks -- defines the problem for the fluid domain.

The nodal force vector $\underset{\sim}{Q}^f(t)$ is the static equivalent of the hydrodynamic pressures on the upstream face $p_c(\theta,z,t) \equiv p(R,\theta,z,t)$. It may be computed from the pressures using the principle of virtual work wherein the variation of displacements between the nodal points is defined by the finite element interpolation functions. Appropriate coordinate transformations are necessary in carrying out these computations because the pressures are defined in the cylindrical coordinate system whereas the nodal loads are in the cartesian coordinate system.

4. ANALYSIS OF DAM RESPONSE TO HARMONIC UPSTREAM-DOWNSTREAM GROUND MOTION

4.1 Equations of Motion

The normal modes of vibration of arch dams with mass, stiffness, damping and geometric properties symmetric about the x-z ($\theta = 0$) plane fall into two categories: symmetric and antisymmetric relative to the same plane. Only the symmetric modes will be excited by the upstream-downstream component of ground motion. For this excitation, the equations of motion are a special case of Eq. 3.4:

$$M_j \ddot{Y}_j^x(t) + C_j \dot{Y}_j^x(t) + K_j Y_j^x(t) = - \underline{\phi}_j^T \underline{m}\, \underline{e}^x \ddot{v}_g^x(t) - \{\phi_j^f\}^T \underline{Q}^f(t) \qquad j = 1,2,3,\ldots,J \qquad (4.1)$$

in which $Y_j^x(t)$ is the generalized displacement associated with the j^{th} symmetric mode of vibration.

4.2 Fluid Domain: Boundary Conditions

As defined in Section 3.2, $\underline{Q}^f(t)$ in Eq. 4.1 is the vector of nodal forces associated with hydrodynamic pressures on the upstream face of the dam. These pressures, acting in the radial direction (normal to the upstream face which is a segment of a circular cylinder) are governed by the wave equation (Eq. 3.5) together with the following boundary conditions:

- The radial component of fluid motion at the upstream face of the dam (boundary $r = R$) is the same as the radial motion of the upstream face of the dam.
- The fluid motion normal to the banks (boundaries $\theta = \pm \pi/4$) is the same as the normal component of motion of the banks.

- There is no vertical motion of the fluid at the bottom of the reservoir.
- Fluid pressure at the free surface is zero. This implies that the effects of waves at the free surface are ignored; the associated errors are known to be small [6,22,23].
- Since the system, symmetrical about the x-z ($\theta = 0$) plane, is excited by the x-component of ground motion, the hydrodynamic pressures must be symmetric about the same plane.
- The radiation boundary condition not permitting any reflected waves applies at the upstream end ($r = \infty$) of the reservoir.

4.3 Complex Frequency Responses

It is a property of linear time invariant systems that when the excitation is simple harmonic motion, the steady state response is also simple harmonic motion at the same frequency. The complex frequency response function $\bar{r}(\omega)$ describes the frequency dependence of the amplitude and phase of the response $r(t)$. It has the property that when the excitation is the real part of $e^{i\omega t}$, the response is the real part of $\bar{r}(\omega)\ e^{i\omega t}$.

In studying the effects of structure-fluid interaction on the dynamics of arch dams, it is most appropriate and convenient to consider harmonic ground motion and to develop procedures to determine the complex frequency response functions for various response quantities of interest.

The response to harmonic ground acceleration in the x-direction, $\ddot{v}_g^x(t) = e^{i\omega t}$, can be expressed as follows:

• Hydrodynamic pressures on the dam face,

$$p_c(\theta,z,t) = \bar{p}_c(\theta,z,\omega)\ e^{i\omega t} \tag{4.2a}$$

• Generalized accelerations,

$$\ddot{Y}_j^x(t) = \bar{\ddot{Y}}_j^x(\omega)\ e^{i\omega t} \tag{4.2b}$$

• Radial accelerations of the upstream face of the dam,

$$\ddot{v}^r(R,\theta,z,t) = \left\{\cos\theta + \sum_{j=1}^{J}\left[\phi_j^{xf}(\theta,z)\cos\theta + \phi_j^{yf}(\theta,z)\sin\theta\right]\bar{\ddot{Y}}_j^x(\omega)\right\}e^{i\omega t} \quad \text{......(4.2c)}$$

Where $\phi_j^{xf}(\theta,z)$ and $\phi_j^{yf}(\theta,z)$ are the continuous function analogues for the vectors $\underline{\phi}_j^{xf}$ and $\underline{\phi}_j^{yf}$, defined in Section 3.2. These functions are obtained from the vectors and the finite element interpolation functions (see Appendix D).

4.3.1 Boundary Conditions

Using Eqs. 3.6 and 4.2, the boundary conditions of Section 4.2 can be expressed analytically as follows:

$$\frac{\partial p}{\partial r}(R,\theta,z,t) = -\frac{w}{g}\left\{\cos\theta + \sum_{j=1}^{J}\left[\phi_j^{xf}(\theta,z)\cos\theta + \phi_j^{yf}(\theta,z)\sin\theta\right]\bar{\ddot{Y}}_j^x(\omega)\right\}e^{i\omega t} \quad \text{......(4.3a)}$$

$$\frac{\partial p}{r\partial\theta}\left(r,\frac{\pi}{4},z,t\right) = \frac{w}{g}\sin\frac{\pi}{4}\ e^{i\omega t} \tag{4.3b}$$

$$\frac{\partial p}{\partial z}(r,\theta,0,t) = 0 \tag{4.3c}$$

$$p(r,\theta,H,t) = 0 \tag{4.3d}$$

$$\frac{\partial p}{r\partial\theta}(r,0,z,t) = 0 \tag{4.3e}$$

In addition to these boundary conditions, no wave reflections are permitted at the upstream end of the reservoir ($r = \infty$).

Because the governing wave equation as well as the boundary conditions are linear, the principle of superposition applies. The complex frequency response function for the hydrodynamic pressures on the dam face $\bar{p}_c(\theta,z,t)$ can therefore be expressed as:

$$\bar{p}_c(\theta,z,\omega) = \bar{p}^x_{0D}(\theta,z,\omega) + \bar{p}^x_{0B}(\theta,z,\omega) + \sum_{j=1}^{J} \bar{\ddot{Y}}^x_j(\omega)\ \bar{p}^x_j(\theta,z,\omega) \qquad (4.4)$$

The complex frequency response functions $\bar{p}^x_{0D}$, $\bar{p}^x_{0B}$, and $\bar{p}^x_j$ in Eq. 4.4 are defined as follows. $p^x_{0D}(\theta,z,t) = \bar{p}^x_{0D}(\theta,z,\omega)\ e^{i\omega t}$ is the solution of the wave equation (Eq. 3.5) at $r = R$ (upstream face of the dam) for the following boundary conditions:

$$\frac{\partial p}{\partial r}(R,\theta,z,t) = -\frac{w}{g}\cos\theta\ e^{i\omega t} \qquad (4.5a)$$

$$\frac{\partial p}{r\partial\theta}\left(r, \frac{\pi}{4}, z, t\right) = 0 \qquad (4.5b)$$

and those specified by Eqs. 4.3c to 4.3e. $p^x_{0B}(\theta,z,t) = \bar{p}^x_{0B}(\theta,z,\omega)\ e^{i\omega t}$ is the solution of the wave equation at $r = R$ for the following boundary conditions:

$$\frac{\partial p}{\partial r}(R,\theta,z,t) = 0 \qquad (4.6a)$$

$$\frac{\partial p}{r\partial\theta}\left(r, \frac{\pi}{4}, z, t\right) = \frac{1}{\sqrt{2}}\ \frac{w}{g}\ e^{i\omega t} \qquad (4.6b)$$

and those specified by Eqs. 4.3c to 4.3e. $p^x_j(\theta,z,t) = \bar{p}^x_j(\theta,z,\omega)\ e^{i\omega t}$ is the solution of the wave equation at $r = R$ for the following boundary conditions:

$$\frac{\partial p}{\partial r}(R,\theta,z,t) = -\frac{w}{g}\left[\phi_j^{xf}(\theta,z)\cos\theta + \phi_j^{yf}(\theta,z)\sin\theta\right]e^{i\omega t} \qquad (4.7a)$$

$$\frac{\partial p}{r\partial\theta}\left(r, \frac{\pi}{4}, z, t\right) = 0 \qquad (4.7b)$$

and those specified by Eqs. 4.3c to 4.3e.

The complex frequency response functions $\bar{p}_{0D}^{x}(\theta,z,\omega)$, $\bar{p}_{0B}^{x}(\theta,z,\omega)$, and $\bar{p}_{j}^{x}(\theta,z,\omega)$ are for the hydrodynamic pressures on the upstream face of the dam for the following three excitations, respectively: (i) Acceleration of rigid dam in the x-direction but the reservoir banks remain stationary, (ii) Acceleration of only the reservoir banks in the x-direction, (iii) Acceleration $\ddot{\bar{Y}}_j^{x}(\omega) = 1$ in the j^{th} symmetrical natural mode of vibration of the dam (without water) but there is no motion of the dam base or reservoir banks.

4.3.2 Hydrodynamic Pressures: Analytical Results

The solutions of the wave equation for the three sets of boundary conditions presented in Section 4.3.1 are derived in Appendix C. The final expressions for $\bar{p}_{0D}^{x}(\theta,z,\omega)$, $\bar{p}_{0B}^{x}(\theta,z,\omega)$, and $\bar{p}_{j}^{x}(\theta,z,\omega)$ are as follows:

$$\bar{p}_{0D}^{x}(\theta,z,\omega) = \frac{16\sqrt{2}\,wR}{g\pi^2}\sum_{m=1}^{\infty}\sum_{n=0}^{\infty}\frac{(-1)^m}{(2m-1)}\frac{\varepsilon_n(-1)^n}{(1-16n^2)}\left[C_n(\lambda_m R) + iD_n(\lambda_m R)\right]\cos 4n\theta\,\cos\alpha_m z \qquad \ldots\ldots(4.8)$$

$$\bar{p}_{0B}^{x}(\theta,z,\omega) = \frac{2\sqrt{2}\,wR}{g\pi}\left\{\sum_{m=1}^{\infty}\left[E_m(\lambda_m R) + iF_m(\lambda_m R)\right]\cos\alpha_m z + \frac{8}{\pi}\sum_{m=1}^{\infty}\sum_{n=0}^{\infty}\varepsilon_n\left[U_{mn}(\lambda_m R) + iV_{mn}(\lambda_m R)\right]\cos 4n\theta\,\cos\alpha_m z\right\} \qquad \ldots\ldots(4.9)$$

$$\bar{p}_j^x(\theta,z,\omega) = -\frac{16wR}{g\pi}\sum_{m=1}^{\infty}\sum_{n=0}^{\infty}\varepsilon_n I_{mn}^j\left[C_n(\lambda_m R) + iD_n(\lambda_m R)\right]\cos 4n\theta \cos\alpha_m z \qquad \text{.......(4.10)}$$

where

R = radius of the upstream face of the dam

H = depth of water in the reservoir

C = velocity of sound in water (4720 ft/sec)

ω = excitation frequency

$$\varepsilon_n = \begin{cases} 1 & n = 0 \\ 2 & n \neq 0 \end{cases}$$

$J_n(x)$ = Bessel function of the first kind of order n

$Y_n(x)$ = Bessel function of the second kind of order n

$K_n(x)$ = modified Bessel function of the second kind of order n

$\omega_1^r = \frac{\pi C}{2H}$ = the first resonant frequency of the water in the reservoir

$$\alpha_m = \frac{(2m-1)\cdot\pi}{2H} \qquad (4.11a)$$

$$\lambda_m R = R\sqrt{\left|\alpha_m^2 - \frac{\omega^2}{C^2}\right|} = \frac{\pi R}{2H}\sqrt{\left|(2m-1)^2 - \left(\frac{\omega}{\omega_1^r}\right)^2\right|} \qquad (4.11b)$$

$$I_{mn}^j = \frac{1}{H}\int_0^{\pi/4}\int_0^H\left[\phi_j^{xf}(\theta,z)\cos\theta + \phi_j^{yf}(\theta,z)\sin\theta\right]\cos 4n\theta \cos\alpha_m z \, dz d\theta \qquad \text{......(4.11c)}$$

m_ℓ = the largest integer "m" satisfying the inequality $\frac{\omega}{\omega_1^r} > (2m-1)$

Expressions for functions C_n, D_n, E_m, F_m, U_{mn}, and V_{mn} differ depending on whether m is smaller or larger than m_ℓ. For $m \leq m_\ell$ they are as follows:

$$C_n(\lambda_m R) = \frac{[A_n(\lambda_m R)\ J_{4n}(\lambda_m R) + B_n(\lambda_m R)\ Y_{4n}(\lambda_m R)]}{\lambda_m R\ [A_n^2(\lambda_m R) + B_n^2(\lambda_m R)]} \tag{4.11d}$$

$$D_n(\lambda_m R) = \frac{[B_n(\lambda_m R)\ J_{4n}(\lambda_m R) - A_n(\lambda_m R)\ Y_{4n}(\lambda_m R)]}{\lambda_m R\ [A_n^2(\lambda_m R) + B_n^2(\lambda_m R)]} \tag{4.11e}$$

$$E_m(\lambda_m R) = \frac{(-1)^m}{(2m-1)\lambda_m R} \left\{\sin[\lambda_m R\ \sin(\frac{\pi}{4} - \theta)] + \sin[\lambda_m R\ \sin(\frac{\pi}{4} + \theta)]\right\} \quad \ldots\ldots\ldots(4.11f)$$

$$F_m(\lambda_m R) = \frac{(-1)^m}{(2m-1)\lambda_m R} \left\{\cos[\lambda_m R\ \sin(\frac{\pi}{4} - \theta)] + \cos[\lambda_m R\ \sin(\frac{\pi}{4} + \theta)]\right\} \quad \ldots\ldots\ldots(4.11g)$$

$$U_{mn}(\lambda_m R) = \frac{(-1)^m(-1)^n}{(2m-1)} \left\{T_n(\lambda_m R)\ C_n(\lambda_m R) + \frac{\pi}{4} A_n(\lambda_m R)\ D_n(\lambda_m R)\right\} \quad \ldots\ldots\ldots(4.11h)$$

$$V_{mn}(\lambda_m R) = \frac{(-1)^m(-1)^n}{(2m-1)} \left\{T_n(\lambda_m R)\ D_n(\lambda_m R) - \frac{\pi}{4} A_n(\lambda_m R)\ C_n(\lambda_m R)\right\} \quad \ldots\ldots\ldots(4.11i)$$

where:

$$A_n(\lambda_m R) = J_{4n-1}(\lambda_m R) - J_{4n+1}(\lambda_m R) \tag{4.11j}$$

$$B_n(\lambda_m R) = Y_{4n-1}(\lambda_m R) - Y_{4n+1}(\lambda_m R) \tag{4.11k}$$

$$T_n(\lambda_m R) = \sum_{k=0}^{\infty} \varepsilon_{2k} J_{2k}(\lambda_m R)\ \frac{(16n^2+4k^2-1)}{(16n^2-4k^2-4k-1)(16n^2-4k^2+4k+1)} \quad \ldots\ldots\ldots(4.11\ell)$$

For $m > m_\ell$ the above listed functions are as follows:

$$C_n(\lambda_m R) = \frac{-K_{4n}(\lambda_m R)}{\lambda_m R\ [K_{4n-1}(\lambda_m R) + K_{4n+1}(\lambda_m R)]} \tag{4.11m}$$

$$D_n(\lambda_m R) = 0. \tag{4.11n}$$

$$E_m(\lambda_m R) = \frac{-(-1)^m}{(2m-1)\lambda_m R}\left[e^{-\lambda_m R\ \sin(\pi/4-\theta)} + e^{-\lambda_m R\ \sin(\pi/4+\theta)}\right] \quad \ldots\ldots.(4.11o)$$

$$F_m(\lambda_m R) = 0. \tag{4.11p}$$

$$U_{mn}(\lambda_m R) = \frac{-(-1)^m}{(2m-1)}\ G_n(\lambda_m R)\quad C_n(\lambda_m R) \tag{4.11q}$$

$$V_{mn}(\lambda_m R) = 0. \tag{4.11r}$$

where:

$$G_n(\lambda_m R) = \int_0^{\pi/4}\left[\sin(\tfrac{\pi}{4}-\theta)\ e^{-\lambda_m R \sin(\pi/4-\theta)} + \sin(\tfrac{\pi}{4}+\theta)\ e^{-\lambda_m R \sin(\pi/4+\theta)}\right]\cos 4n\theta\ d\theta \quad \ldots\ldots.(4.11s)$$

In the above equations the Bessel functions are grouped so that the expressions for $C_n(\lambda_m R)$ and $D_n(\lambda_m R)$, Eqs. 4.11d,e and m, are well behaved functions (Appendix D).

The above solutions of the wave equation for the three sets of boundary conditions presented in Section 4.3.1 are for fluid domains described by Fig. 2.1. The fluid is bounded by the upstream face of the dam, which is a segment of a circular cylinder of radius R, and by radially extending banks enclosing a central angle of 90°. For arbitrary central angles standard analytical procedures are able to provide solutions of the wave equation for $\bar{p}^x_{0D}(\theta,z,\omega)$ but not for $\bar{p}^x_{0B}(\theta,z,\omega)$ [5].

As the central angle approaches 180° and $R \to \infty$, representing a straight dam in the limit, $\bar{p}^x_{0D}(\theta,z,\omega)$ approaches the previously obtained [22] two-dimensional solution of the wave equation for a straight gravity dam (Appendix E).

An eigen-frequency of the wave equation in the particular fluid domain under consideration corresponds to each pair of functions $\cos 4n\theta$, $n = 0, 1, 2, \ldots\ldots$ and $\cos\alpha_m z$, $m = 1, 2, 3, \ldots\ldots$ The hydrodynamic pressures $\bar{p}^x_{0D}(\theta,z,\omega)$, $\bar{p}^x_{0B}(\theta,z,\omega)$, and $\bar{p}^x_j(\theta,z,\omega)$ are unbounded at the eigen-frequencies corresponding to $n = 0$ with $m = 1, 2, 3, \ldots\ldots$ At all the other eigen-frequencies, the pressures are bounded and, as will be seen later, do not resonate. The resonant frequencies, the eigen-frequencies corresponding to $n = 0$ and $m = 1, 2, 3, \ldots\ldots$ are $\omega^r_m = (2m-1)\,\pi C/2H$. They are the same as the resonant frequencies obtained for two-dimensional fluid domains [22].

4.3.3 Hydrodynamic Pressures and Forces on Rigid Dams: Numerical Results

The complex valued frequency response functions $\bar{p}^x_{0D}(\theta,z,\omega)$ and $\bar{p}^x_{0B}(\theta,z,\omega)$ are for the hydrodynamic pressures on a rigid dam due to separate accelerations of the dam and of the banks, respectively, in the upstream-downstream direction. The response function for the total pressure $\bar{p}^x_{0T}(\theta,z,\omega)$ is the sum of the two functions. Numerical results for the absolute value (or modulus) of these frequency response functions are presented for the arch dam-water system of Fig. 2.1 with $R/H = 1.5$. For several values of the normalized excitation frequency, these functions are plotted over the upstream face at the base of the dam and over the depth valiable z at two selected values of the angular coordinate $\theta = 0$ (crown) and $\theta = 45°$ (bank). Because the pressures are symmetric about the x-z ($\theta = 0$) plane, pressures over only half of the base arch are presented. Each of Figs. 4.1 - 4.3 contains results for a particular normalized excitation frequency.

The complex-valued frequency response functions for hydrodynamic forces, acting in the radial direction, per unit length of circumference are:

$$\bar{F}_{0\ell}(\theta,\omega) = \int_0^H \bar{p}^x_{0\ell}(\theta,z,\omega)\ dz \quad , \quad \ell = D,B,T \tag{4.12}$$

Variation of the absolute value (or modulus) of the complex-valued hydrodynamic forces (Eq. 4.12) with excitation frequency is presented in Fig. 4.4 for the arch dam-water system with R/H = 1.5 at $\theta = 0°$ (crown), $\theta = 22\frac{1}{2}°$ and $\theta = 45°$ (banks).

In Figs. 4.1 to 4.4 hydrodynamic pressures and forces have been normalized with respect to hydrostatic pressure at the base of the dam and hydrostatic force per unit of circumferential length $F_s = WH^2/2$, respectively. The excitation frequency is normalized with respect to the fundamental resonant frequency of the fluid domain, ω_1^r. When presented in this form, the results apply to all arch dam-fluid systems with the particular value of R/H; in this case R/H = 1.5.

Figures 4.1 to 4.4 also show the complex frequency response functions for hydrodynamic forces and pressures on rigid straight gravity dams due to ground motion acceleration transverse to the dam axis. These results were obtained for gravity dams with vertical upstream face [22].

The hydrodynamic forces (and pressures) on arch dams depend strongly on the excitation frequency: they increase as the excitation frequency approaches from above or below a resonant frequency ω_m^r of the

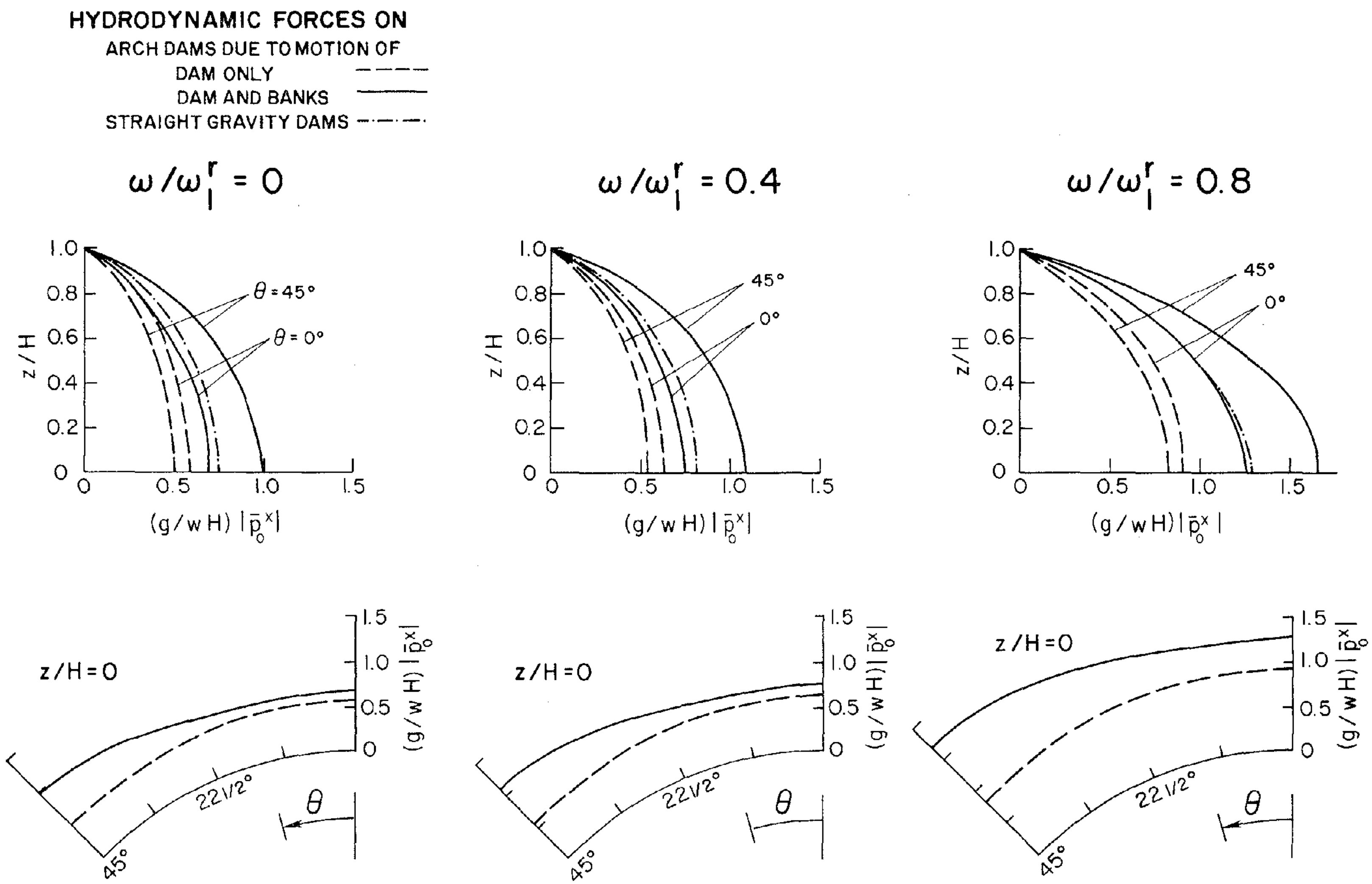

FIG. 4.1 COMPLEX FREQUENCY RESPONSES FOR HYDRODYNAMIC PRESSURES ON RIGID DAMS DUE TO UPSTREAM-DOWNSTREAM GROUND MOTION. RESULTS ARE FOR ARCH DAMS WITH R/H = 1.5 AND STRAIGHT GRAVITY DAMS.

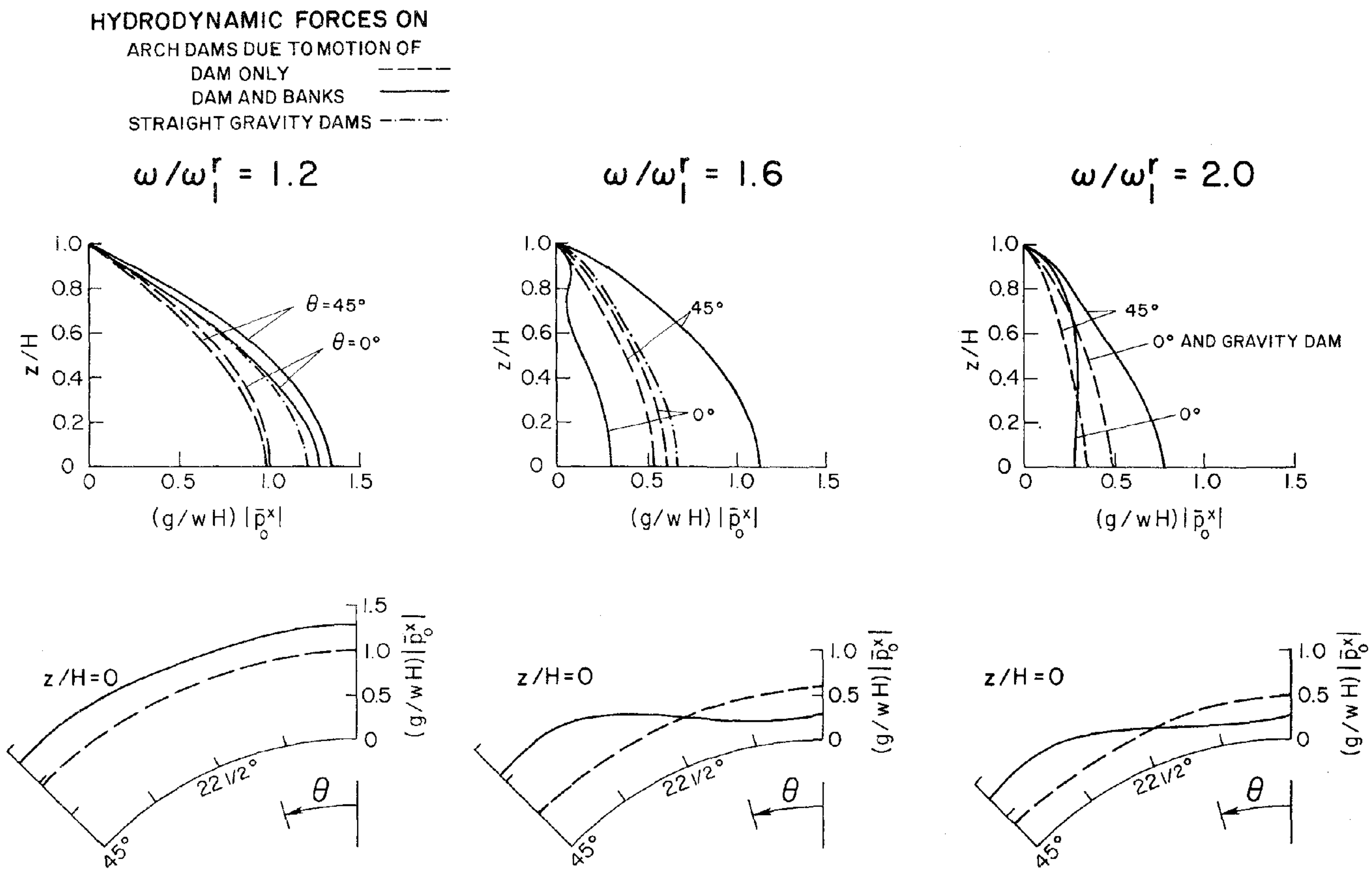

FIG. 4.2 COMPLEX FREQUENCY RESPONSES FOR HYDRODYNAMIC PRESSURES ON RIGID DAMS DUE TO UPSTREAM-DOWNSTREAM GROUND MOTION. RESULTS ARE FOR ARCH DAMS WITH R/H = 1.5 AND STRAIGHT GRAVITY DAMS.

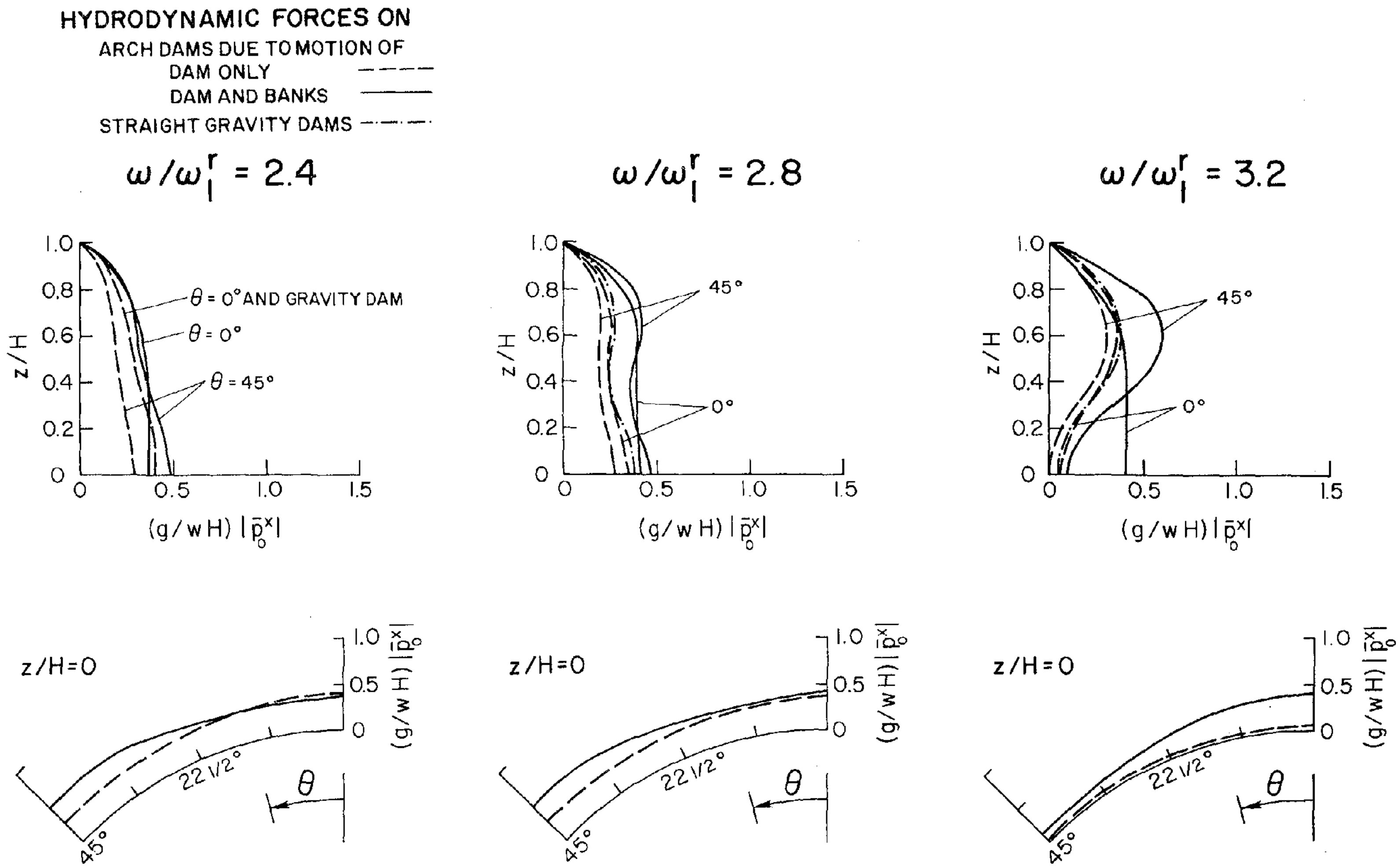

FIG. 4.3 COMPLEX FREQUENCY RESPONSES FOR HYDRODYNAMIC PRESSURES ON RIGID DAMS DUE TO UPSTREAM-DOWNSTREAM GROUND MOTION. RESULTS ARE FOR ARCH DAMS WITH R/H = 1.5 AND STRAIGHT GRAVITY DAMS.

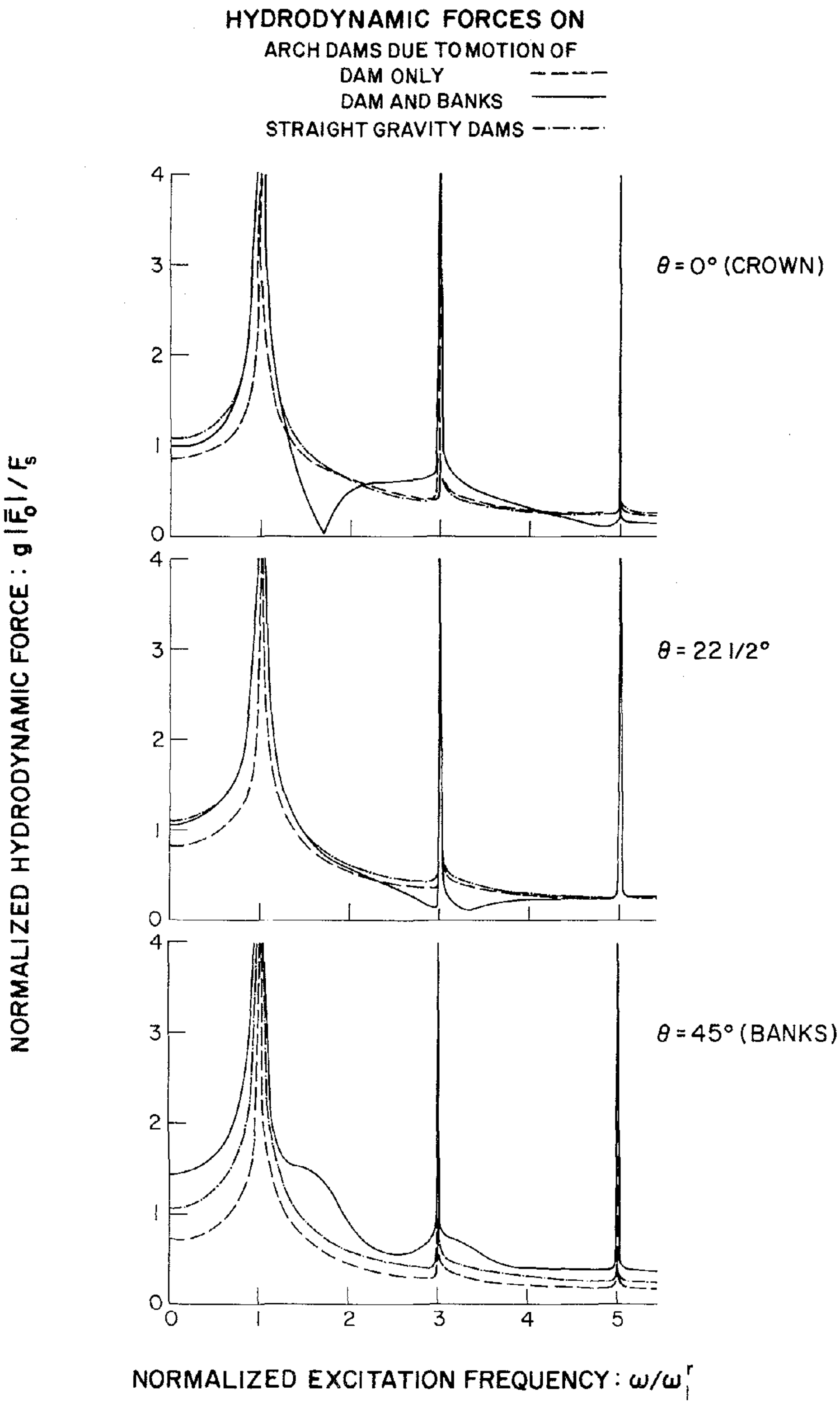

FIG. 4.4 COMPLEX FREQUENCY RESPONSES FOR HYDRODYNAMIC FORCE ON RIGID DAMS DUE TO UPSTREAM-DOWNSTREAM COMPONENT OF GROUND MOTION. RESULTS ARE FOR ARCH DAMS WITH R/H = 1.5 AND STRAIGHT GRAVITY DAMS.

fluid domain. The forces are unbounded at these resonant frequencies. The response amplification becomes increasingly sharp and narrow banded at higher resonant frequencies. But for these very localized amplifications at the higher resonant frequencies, the response tends to decrease as the excitation frequency increases beyond the fundamental resonant frequency.

By comparing with results for straight gravity dams, it is apparent that the resonant frequencies are the same (see Section 4.3.2) but the hydrodynamic forces due to motion of the dam alone are influenced by the curvature of the dam. The forces are reduced at most excitation frequencies in a manner that the variation of forces with excitation frequency are affected little by curvature, at least for dams with $R/H = 1.5$.

The motion of banks modifies the hydrodynamic forces, increasing them for some excitation frequencies, decreasing them for others. The curvature of the dam influences the total -- due to motion of the dam and banks -- hydrodynamic force, resulting in larger forces at most excitation frequencies. At some frequencies, however, the forces are greatly reduced.

The variation of hydrodynamic pressures with depth and position along the arch depends on the excitation frequency (Figs. 4.1 to 4.3). The following observations are based on these results for arch dam-water systems shown in Fig. 2.1 with $R/H = 1.5$.

The hydrodynamic pressures due to motion of the dam alone vary little with θ, decreasing slightly from the crown to the banks. However, the pressures due to motion of the dam and banks vary significantly with θ, increasing from crown to banks for smaller excitation frequencies but decreasing for the higher frequencies.

At the crown and banks of arch dams, the pressures due to motion of the dam alone, and motion of both dam and banks at smaller excitation frequencies ($\omega/\omega_1^r < 1.2$), vary with depth in a manner similar to the pressure-depth curve for straight gravity dams. The pressures on arch dams due to motion of the dam alone vary with depth similarly to pressures on straight dams even at higher excitation frequencies ($\omega/\omega_1^r > 1.2$). At higher excitation frequencies ($\omega/\omega_1^r > 2$), the pressures at all depths on the crown due to motion of the dam only are virtually identical to those on straight gravity dams.

At excitation frequencies $\omega < \omega_1^r$, the contributions of the motion of the banks lead to increases in hydrodynamic pressures on the dam. However, at $\omega > \omega_1^r$, there is no apparent systematic trend in the contribution of the motion of the banks to the hydrodynamic pressures. For a particular excitation frequency, and fixed θ, the pressures may increase at some depths and decrease at others; for a fixed depth below the water surface, the pressures may increase for some θ values and decrease for others.

4.3.4 Dam Response

As mentioned earlier $\underset{\sim}{Q}^f(t)$ is the vector of loads at the nodal points on the upstream face of the dam associated with hydrodynamic pressures $p_c(\theta,z,t)$. These hydrodynamic loads due to harmonic ground acceleration are of the form $\underset{\sim}{Q}^f(t) = \bar{\underset{\sim}{Q}}^f(\omega)\ e^{i\omega t}$. The complex frequency response function for this load vector can, from Eq. 4.4, be expressed as:

$$\bar{\underset{\sim}{Q}}^f(\omega) = \bar{\underset{\sim}{Q}}^x_{0D}(\omega) + \bar{\underset{\sim}{Q}}^x_{0B}(\omega) + \sum_{k=1}^{J} \bar{\bar{Y}}^x_k(\omega)\ \bar{\underset{\sim}{Q}}^x_k(\omega) \tag{4.13}$$

where the force vectors $\bar{\underline{Q}}^{x}_{0D}(\omega)$, $\bar{\underline{Q}}^{x}_{0B}(\omega)$, and $\bar{\underline{Q}}^{x}_{k}(\omega)$ are static equivalents of the corresponding pressure functions $\bar{p}^{x}_{0D}(\theta,z,\omega)$, $\bar{p}^{x}_{0B}(\theta,z,\omega)$, and $\bar{p}^{x}_{k}(\theta,z,\omega)$ and may be computed by applying the principle of virtual work, wherein the finite element interpolation functions describe the variation of displacement between nodal points. In Eq. 4.14 the hydrodynamic forces on the dam have been expressed in terms of the unknown generalized coordinate responses $\bar{Y}^{x}_{k}(\omega)$.

For excitation $\ddot{v}^{x}_{g}(t) = e^{i\omega t}$, Eq. 4.1, after substitution of Eq. 4.13, becomes:

$$[-\omega^2 M_j + i\omega C_j + K_j]\bar{Y}^{x}_{j}(\omega) = -\underline{\phi}^{T}_{j}\underline{m}\,\underline{e}^{x} - \{\phi^{f}_{j}\}^{T}\left\{\bar{\underline{Q}}^{x}_{0D}(\omega) + \bar{\underline{Q}}^{x}_{0B}(\omega) - \omega^2 \sum_{k=1}^{J} \bar{Y}^{x}_{k}(\omega)\,\bar{\underline{Q}}^{x}_{k}(\omega)\right\} \qquad \text{.......(4.14)}$$

This set of equations may be expressed in matrix form as:

$$\begin{bmatrix} S_{11}(\omega) & S_{12}(\omega) & \cdots\cdots & S_{1J}(\omega) \\ S_{21}(\omega) & S_{22}(\omega) & \cdots\cdots & S_{2J}(\omega) \\ \vdots & & & \vdots \\ S_{J1}(\omega) & S_{J2}(\omega) & \cdots\cdots & S_{JJ}(\omega) \end{bmatrix} \begin{Bmatrix} \bar{Y}^{x}_{1}(\omega) \\ \bar{Y}^{x}_{2}(\omega) \\ \vdots \\ Y^{u}_{J}(\omega) \end{Bmatrix} = \begin{Bmatrix} L^{x}_{1}(\omega) \\ L^{x}_{2}(\omega) \\ \vdots \\ L^{u}_{J}(\omega) \end{Bmatrix} \qquad (4.15a)$$

or

$$\underline{S}(\omega)\ \bar{\underline{Y}}^{x}(\omega) = \underline{L}^{x}(\omega) \qquad (4.15b)$$

where,

$$\left.\begin{aligned} S_{jk}(\omega) &= -\omega^2 \{\phi_j^f\}^T \bar{\underset{\approx}{Q}}_k^x(\omega) \quad ; \quad j \neq k \\ S_{jj}(\omega) &= -\omega^2 M_j + i\omega C_j + K_j - \omega^2 \{\phi_j^f\}^T \bar{\underset{\approx}{Q}}_j^x(\omega) \\ L_j^x(\omega) &= -\underline{\phi}_j^T \underline{m}\, \underline{e}^x - \{\underline{\phi}_j^f\}^T \{\bar{\underset{\approx}{Q}}_{0D}^x(\omega) + \bar{\underset{\approx}{Q}}_{0B}^x(\omega)\} \end{aligned}\right\} \begin{aligned} & \\ & \\ j &= 1,2,3,\ldots,J \\ k &= 1,2,3,\ldots,J \end{aligned} \tag{4.16}$$

The frequency dependent matrix $\underline{S}(\omega)$ in Eq. 4.15 relates the generalized displacement vector $\underline{\bar{Y}}^x(\omega)$ to the corresponding generalized loads $\underline{L}^x(\omega)$. Unlike in classical modal analysis the matrix $\underline{S}(\omega)$ is not diagonal because the vectors $\underline{\phi}_j$ are not the normal modes of the dam-fluid system; they are the modes of the dam alone (without water). It can be shown that $\underline{S}(\omega)$ is a symmetric matrix (see Appendix F).

Solutions of Eq. 4.15 for a range of values of the excitation frequency ω would provide the complex frequency response functions for all the generalized displacements $\bar{Y}_j^x(\omega)$, $j = 1,2,\ldots,J$. The frequency responses for generalized accelerations may be obtained from:

$$\bar{\ddot{Y}}_j^x(\omega) = -\omega^2 \bar{Y}_j^x(\omega) \tag{4.17}$$

The complex frequency responses for acceleration at the nodal points of the dam are

$$\underline{\bar{\ddot{v}}}^x(\omega) = \sum_{j=1}^{J} \underline{\bar{\ddot{v}}}_j^x(\omega) \tag{4.18}$$

The contribution of the j^{th} vibration mode of the dam to these accelerations is

$$\underline{\bar{\ddot{v}}}_j^x(\omega) = \bar{\ddot{Y}}_j^x(\omega)\, \underline{\phi}_j \tag{4.19}$$

4.4 Singularities of the Solution

The hydrodynamic pressure functions $\bar{p}^x_{0D}(\theta,z,\omega)$, $\bar{p}^x_{0B}(\theta,z,\omega)$, and $\bar{p}^x_j(\theta,z,\omega)$ are unbounded at $\omega = \omega^r_m$, where $\omega^r_m = (2m-1)\pi C/2H$, $m = 1,2,3,\ldots.$ is the m^{th} resonant frequency of the fluid contained in the reservoir. Consequently, the elements of $\underline{S}(\omega)$ and $\underline{L}^x(\omega)$ defined in Eq. 4.16 are unbounded at these frequencies.

When $J = 1$, i.e. only the first vibration mode is included in the analysis, Eq. 4.16 reduces to one equation and the response at a resonant frequency can be obtained through a limiting process. If the excitation is only the motion of the base of the dam and the banks are stationary (i.e. $\bar{p}^x_{0B}(\theta,z,\omega) = 0$ and $\bar{\underline{Q}}^x_{0B}(\omega) = 0$), the result of the limiting process is (see Appendix E)

$$\lim_{\omega\to\omega^r_m} \bar{\ddot{Y}}^x_1(\omega) = \frac{\sqrt{2}\ (-1)^m}{\pi(2m-1)\ I^1_{m0}} \tag{4.20}$$

where I^1_{m0} was defined in Section 4.3.2. However, the limiting process leads to unbounded response when the excitation includes the simultaneous motion of the dam base and reservoir banks.

When more than one vibration mode is included in the analysis, the limiting process leads to a system of equations such that $\underline{S}(\omega)$ is singular -- in particular all the J equations become identical -- and no solution can be obtained at frequencies ω^r_m. However, numerical solutions to the equations can be obtained for values of ω arbitrarily near these frequencies.

The set of governing equations, corresponding to Eq. 4.15, for concrete gravity dams were also singular at the resonant frequencies of the undamped fluid domain [13]. As discussed therein, such singularities are characteristic of the results from a substructure method of analysis applied to a system with no damping in one of the substructures, in this case the fluid domain.

4.5 Analysis Neglecting Compressibility of Water

Only the hydrodynamic terms are altered in Eq. 4.15 if water is assumed as incompressible. In this case the hydrodynamic pressure functions $\bar{p}^x_{0D}(\theta,z,\omega)$, $\bar{p}^x_{0B}(\theta,z,\omega)$ and $\bar{p}^x_j(\theta,z,\omega)$ are independent of frequency and they may be obtained by taking limits of these functions (Eq. 4.8 - 4.10) as $C \to \infty$ or as values of these functions at $\omega = 0$:

$$\bar{p}^x_{0D}(\theta,z,0) = \frac{16\sqrt{2}\,WR}{g\pi^2} \sum_{m=1}^{\infty} \sum_{n=0}^{\infty} \frac{(-1)^m}{(2m-1)} \frac{\varepsilon_n(-1)^n}{(1-16n^2)} C_n(\alpha_m R)\cos 4n\theta \, \cos\alpha_m z \quad \text{.......(4.21)}$$

$$\bar{p}^x_{0B}(\theta,z,0) = \frac{2\sqrt{2}\,WR}{g\pi} \left\{ \sum_{m=1}^{\infty} E_m(\alpha_m R)\cos\alpha_m z + \frac{8}{\pi} \sum_{m=1}^{\infty} \sum_{n=0}^{\infty} \varepsilon_n U_{mn}(\alpha_m R)\cos 4n\theta \, \cos\alpha_m z \right\} \quad \text{.......(4.22)}$$

$$\bar{p}^x_j(\theta,z,0) = -\frac{16WR}{\pi g} \sum_{m=1}^{\infty} \sum_{n=0}^{\infty} \varepsilon_n I^j_{mn} \, C_n(\alpha_m R)\cos 4n\theta \, \cos\alpha_m z \qquad (4.23)$$

where all quantities except the following are defined in Section 4.3.2:

$$C_n(\alpha_m R) = \frac{-K_{4n}(\alpha_m R)}{\alpha_m R\,[K_{4n-1}(\alpha_m R) + K_{4n+1}(\alpha_m R)]} \qquad (4.24a)$$

$$E_m(\alpha_m R) = \frac{-(-1)^m}{(2m-1)\alpha_m R}\left[e^{-\alpha_m R \sin(\pi/4-\theta)} + e^{-\alpha_m R \sin(\pi/4+\theta)}\right] \qquad (4.24b)$$

$$U_{mn}(\alpha_m R) = \frac{-(-1)^m}{(2m-1)} \; G_n(\alpha_m R)\; C_n(\alpha_m R) \qquad (4.24c)$$

$$G_n(\alpha_m R) = \int_0^{\pi/4} \left[\sin(\frac{\pi}{4}-\theta)\, e^{-\alpha_m R \sin(\pi/4-\theta)} + \sin(\frac{\pi}{4}+\theta)\, e^{-\alpha_m R \sin(\pi/4+\theta)}\right] \cos 4n\theta \, d\theta \qquad ....(4.24d)$$

In general, the functions $\bar{p}^x_{0D}$, $\bar{p}^x_{0B}$ and $\bar{p}^x_j$ are complex valued and depend on the excitation frequency (Eqs. 4.8, 4.9 and 4.10), but they are real valued and independent of frequency if compressibility of water is neglected. Equation 4.15 then becomes

$$-\omega^2(\underline{M} + \underline{M}^a)\ \underline{\bar{Y}}^x(\omega) + i\omega\underline{C}\ \underline{\bar{Y}}^x(\omega) + \underline{K}\ \underline{\bar{Y}}^k(\omega) = \underline{L}^{0x} + \underline{L}^{ax} \qquad (4.25)$$

where $\underline{M}$, $\underline{C}$ and $\underline{K}$ are generalized mass, generalized damping and generalized stiffness matrices respectively; each is a diagonal matrix. $\underline{L}^{0x} = -\ \underline{\phi}_j^T \underline{m}\ \underline{e}^x\ \underline{M}^a$ is an "added mass" matrix defined by

$$M^a_{jk} = \{\phi^f_j\}^T\ \underline{\underline{\bar{Q}}}^x_k(0) \quad ; \quad j,k = 1,2,3,....,J \qquad (4.26a)$$

$\underline{L}^{ax}$ is an "added load" vector defined by

$$L^{ax}_j = -\ \{\phi^f_j\}^T\{\underline{\underline{\bar{Q}}}^x_{0D}(0) + \underline{\underline{\bar{Q}}}^x_{0B}(0)\} \quad j = 1,2,....,J \qquad (4.26b)$$

When water is assumed to be incompressible, the hydrodynamic effects are thus equivalent to frequency independent added mass and load terms. Consequently, unlike the case including water compressibility and involving hydrodynamic terms that depend on frequency (Eqs. 4.15 - 4.16), Eq. 4.25 can be written directly in the time domain as:

$$(\underline{M} + \underline{M}^a)\ddot{\underline{Y}}^x(t) + \underline{C}\ \dot{\underline{Y}}^x(t) + \underline{K}\ \underline{Y}^x(t) = (\underline{L}^{0x} + \underline{L}^{ax})\ddot{v}^x_g(t) \qquad (4.27)$$

4.6 Dam With Empty Reservoir

Equations for complex frequency responses of the dam with no water in the reservoir may be obtained as a special case from Eqs. 4.16 and 4.17 simply by setting to zero the hydrodynamic loads $\bar{\underline{Q}}^x_{0D}$, $\bar{Q}^x_{0B}$, and $\bar{\underline{Q}}^x_j$. The coefficients of Eq. 4.15 will then be:

$$
\begin{aligned}
S_{jk}(\omega) &= 0 \qquad j \neq k \\
S_{jj}(\omega) &= -\omega^2 M_j + i\omega C_j + K_j \qquad\qquad (4.28) \\
L^x_j(\omega) &= -\underline{\phi}^T_j \, \underline{m} \, \underline{e}^x = L^{0x}_j(\omega)
\end{aligned}
$$

The matrix $\underline{S}(\omega)$ is now diagonal since the natural modes of vibration of the dam, in terms of which Eq. 4.16 is developed, are also the natural modes of the system considered. Comparing Eqs. 4.16 and 4.28, it is apparent that the presence of water introduces added load terms in $\underline{L}^x(\omega)$ and modifies $\underline{S}(\omega)$. The diagonal terms in $\underline{S}(\omega)$ are modified by an additive quantity and off-diagonal terms appear. Because the natural modes of vibration of the dam are not the normal coordinates of the dam-fluid system, the equations in terms of Y^x_j (Eq. 4.15) are coupled.

4.7 Computer Program

Based on the analytical procedures described in this Chapter and Chapters 5 and 6, a computer program (Appendices H and I) has been written in FORTRAN IV to numerically evaluate the response of arch dams including reservoir interaction effects to horizontal and vertical components of harmonic ground motion. As the program is capable of including any number of modes of vibration of the dam, results can be obtained to any desired degree of accuracy. Analysis with compressibility of water neglected or with the reservoir water absent are included in the program as special cases. This program generated the results in Chapter 7.

5. ANALYSIS OF DAM RESPONSE TO HARMONIC CROSS-STREAM GROUND MOTION

5.1 Equations of Motion

The analytical procedures and results developed in this Chapter for response of the dam to the cross-stream component of ground motion closely parallel those of Chapter 4. At the expense of some duplication, the presentation in this Chapter is self-contained.

Only the antisymmetric natural modes of vibration of the dam (see Section 4.1) will be excited by the y-component of ground motion. For this excitation, the equations of motion are a special case of Eq. 3.4:

$$M_j \ddot{Y}_j^y(t) + C_j \dot{Y}_j^y(t) + K_j Y_j^y(t) = -\underline{\phi}_j^T \underline{m}\, \underline{e}^y \ddot{v}_g^y(t) - \{\phi_j^f\}^T \underline{Q}^f(t)$$

$$j = 1,2,3,\ldots,J \qquad (5.1)$$

in which $Y_j^y(t)$ is the generalized displacement associated with the j^{th} antisymmetric mode of vibration.

5.2 Fluid Domain: Boundary Conditions

As defined in Section 3.2, $\underline{Q}^f(t)$ in Eq. 5.1 is the vector of nodal forces associated with hydrodynamic pressures on the upstream face of the dam. These pressures, acting in the radial direction (normal to the upstream face) are governed by the wave equation (Eq. 3.5) together with the following boundary conditions.

- The radial component of fluid motion at the upstream face of the dam (boundary r = R) is the same as the radial motion of the upstream face of the dam.

- The fluid motion normal to the banks (boundaries $\theta = \pm \pi/4$) is the same as the normal component of motion of the banks.
- There is no vertical motion of the fluid at the bottom of the reservoir.
- Fluid pressure at the free surface is zero.
- Since the system, symmetrical about the x - z ($\theta = 0$) plane, is excited by the y-component of ground motion, the hydrodynamic pressures must be antisymmetric about the same plane.
- The radiation boundary condition not permitting any reflected wave applies at the upstream end ($r = \infty$) of the reservoir.

5.3 Complex Frequency Response

The response to harmonic ground acceleration in the y-direction, $\ddot{v}_g^y(t) = e^{i\omega t}$, can be expressed as follows:

- Hydrodynamic pressures on the dam face,

$$p_c(\theta,z,t) = \bar{p}_c(\theta,z,t)\ e^{i\omega t} \tag{5.2a}$$

- Generalized accelerations,

$$\ddot{Y}_j^y(t) = \bar{\ddot{Y}}_j^y(\omega)\ e^{i\omega t} \tag{5.2b}$$

- Radial accelerations of the upstream face of the dam,

$$\ddot{v}^r(R,\theta,z,t) = \left\{ \sin\theta + \sum_{j=1}^{J} \left[\phi_j^{xf}(\theta,z)\ \cos\theta + \phi_j^{yf}(\theta,z)\ \sin\theta \right] \bar{\ddot{Y}}_j^y(\omega) \right\} e^{i\omega t} \qquad \ldots\ldots\ (5.2c)$$

where $\phi_j^{xf}(\theta,z)$ and $\phi_j^{yf}(\theta,z)$ are the continuous function analogues (Section 4.2) for the vectors $\underline{\phi}_j^{xf}$ and $\underline{\phi}_j^{yf}$ defined in Section 3.2.

5.3.1 Boundary Conditions

Using Eqs. 3.6 and 5.2, the boundary conditions of Section 5.2 can be expressed analytically as follows:

$$\frac{\partial p}{\partial r}(R,\theta,z,t) = -\frac{w}{g}\left\{\sin\theta + \sum_{j=1}^{J}\left[\phi_j^{xf}(\theta,z)\ \cos\theta + \phi_j^{yf}(\theta,z)\ \sin\theta\right]\bar{\ddot{Y}}_j^{y}(\omega)\right\}e^{i\omega t} \qquad \text{.......(5.3a)}$$

$$\frac{\partial p}{r\partial\theta}(r, \frac{\pi}{4}, z, t) = -\frac{w}{g}\cos(\frac{\pi}{4})\ e^{i\omega t} \tag{5.3b}$$

$$\frac{\partial p}{\partial z}(r,\theta,0,t) = 0 \tag{5.3c}$$

$$p(r,\theta,H,t) = 0 \tag{5.3d}$$

$$p(r,0,z,t) = 0 \tag{5.3e}$$

In addition to these boundary conditions, no wave reflections at the upstream end of the reservoir ($r = \infty$) are permitted.

Because the governing wave equation as well as the boundary conditions are linear, the principle of superposition applies. The complex frequency response function for the hydrodynamic pressures on the dam face $p_c(\theta,z,t)$ can therefore be expressed as:

$$\bar{p}_c(\theta,z,\omega) = \bar{p}_{0D}^{y}(\theta,z,\omega) + \bar{p}_{0B}^{y}(\theta,z,\omega) + \sum_{j=1}^{J}\bar{\ddot{Y}}_j^{y}(\omega)\ \bar{p}_j^{y}(\theta,z,\omega) \tag{5.4}$$

The complex frequency response functions $\bar{p}_{0D}^{y}$, $\bar{p}_{0B}^{y}$, and $\bar{p}_j^{y}$ in Eq. 5.4 are defined as follows. $p_{0D}^{y}(\theta,z,t) = \bar{p}_{0D}^{y}(\theta,z,\omega)\ e^{i\omega t}$ is the solution of the wave equation (Eq. 3.5) at $r = R$ (upstream face of the dam) for the following boundary conditions:

$$\frac{\partial p}{\partial r}(R,\theta,z,t) = -\frac{w}{g} \sin\theta \; e^{i\omega t} \tag{5.5a}$$

$$\frac{\partial p}{r\partial\theta}(r, \frac{\pi}{4}, z, t) = 0 \tag{5.5b}$$

and those specified by Eqs. 5.3c to 5.3e. $p_{0B}^{y}(\theta,z,t) = \bar{p}_{0B}^{y}(\theta,z,\omega)\; e^{i\omega t}$ is the solution of the wave equation at $r = R$ for the following boundary conditions:

$$\frac{\partial p}{\partial r}(R,\theta,z,t) = 0 \tag{5.6a}$$

$$\frac{\partial p}{r\partial\theta}(r, \frac{\pi}{4}, z, t) = -\frac{1}{\sqrt{2}} \; \frac{w}{g} \; e^{i\omega t} \tag{5.6b}$$

and those specified by Eqs. 5.3c to 5.3e. The solution of the wave equation at $r = R$ is $p_j^{y}(\theta,z,t) = \bar{p}_j^{y}(\theta,z,\omega)\; e^{i\omega t}$ for the following boundary conditions:

$$\frac{\partial p}{\partial r}(R,\theta,z,t) = -\frac{w}{g}\left[\phi_j^{xf}(\theta,z)\cos\theta + \phi_j^{yf}(\theta,z)\sin\theta\right] e^{i\omega t} \tag{5.7a}$$

$$\frac{\partial p}{r\partial\theta}(r, \frac{\pi}{4}, z, t) = 0 \tag{5.7b}$$

and those specified by Eqs. 5.3c to 5.3e.

The complex frequency response functions $\bar{p}_{0D}^{y}(\theta,z,\omega)$, $\bar{p}_{0B}^{y}(\theta,z,\omega)$, and $\bar{p}_j^{y}(\theta,z,\omega)$ are for the hydrodynamic pressures on the upstream face of the dam for the following three excitations, respectively: (i) accelerations of the rigid dam in the y-direction but the banks remain stationary, (ii) acceleration of only the reservoir banks in the y-direction, (iii) acceleration $\bar{\ddot{Y}}_j^{y}(\omega) = 1$ in the j^{th} antisymmetric natural mode of vibration of the dam (without water) but there is no motion of the dam base or reservoir banks.

5.3.2 Hydrodynamic Pressures: Analytical Results

The solution of the wave equation for the three sets of boundary conditions presented in Section 5.3.1 are derived in Appendix C. The final expression for $\bar{p}^y_{0D}(\theta,z,\omega)$, $\bar{p}^y_{0B}(\theta,z,\omega)$ and $\bar{p}^y_j(\theta,z,\omega)$ are as follows:

$$\bar{p}^y_{0D}(\theta,z,\omega) = \frac{32\sqrt{2}\,wR}{g\pi^2} \sum_{m=1}^{\infty} \sum_{n=0}^{\infty} \frac{(-1)^m}{(2m-1)} \frac{(-1)^n}{(\mu_n^2-1)} \left[C_n(\lambda_m R) + iD_n(\lambda_m R)\right] \sin\mu_n\theta \, \cos\alpha_m z \qquad \text{......(5.8)}$$

$$\bar{p}^y_{0B}(\theta,z,\omega) = \frac{2\sqrt{2}\,wR}{g\pi} \left\{ \sum_{m=1}^{\infty} \left[E_m(\lambda_m R) + iF_m(\lambda_m R)\right] \cos\alpha_m z + \frac{16}{\pi} \sum_{m=1}^{\infty} \sum_{n=0}^{\infty} \left[U_{mn}(\lambda_m R) + iV_{mn}(\lambda_m R)\right] \sin\mu_n\theta \, \cos\alpha_m z \right\} \qquad \text{......(5.9)}$$

$$\bar{p}^y_j(\theta,z,\omega) = -\frac{32wR}{g\pi} \sum_{m=1}^{\infty} \sum_{n=0}^{\infty} I^j_{mn} \left[C_n(\lambda_m R) + iD_n(\lambda_m R)\right] \sin\mu_n\theta \, \cos\alpha_m z \qquad \text{.......(5.10)}$$

where:

R = radius of the upstream face of the dam

H = depth of water in the reservoir

C = velocity of sound in water (4720 ft/sec)

ω = excitation frequency

$$\varepsilon_{2k} = \begin{cases} 1 & k = 0 \\ 2 & k \neq 0 \end{cases}$$

$J_{\mu_n}(x)$ = Bessel function of the first kind of order μ_n

$Y_{\mu_n}(x)$ = Bessel function of the second find of order μ_n

$K_{\mu_n}(x)$ = modified Bessel function of the second kind of order μ_n

$\omega^r_1 = \frac{\pi C}{2H}$ = the first eigen-frequency of the water in the reservoir

$$\alpha_m = \frac{(2m-1)\pi}{2H} \tag{5.11a}$$

$$\lambda_m R = R\sqrt{\left|\alpha_m^2 - \frac{\omega^2}{C^2}\right|} = \frac{\pi R}{2H}\sqrt{\left|(2m-1)^2 - \left(\frac{\omega}{\omega_1^r}\right)^2\right|} \tag{5.11b}$$

$$I_{mn}^j = \frac{1}{H}\int_0^{\pi/4}\int_0^H \left[\phi_j^{xf}(\theta,z)\cos\theta + \phi_j^{yf}(\theta,z)\sin\theta\right]\sin\mu_n\theta\,\cos\alpha_m z\,dzd\theta \quad \ldots\ldots. \tag{5.11c}$$

$$\mu_n = 4n + 2 \tag{5.11d}$$

m_ℓ = the largest integer "m" satisfying the inequality $\frac{\omega}{\omega_1^r} > (2m-1)$

Expressions for functions C_n, D_n, E_m, F_m, U_{mn}, and V_{mn} differ depending on whether m is smaller or larger than m_ℓ. For $m \leq m_\ell$ they are as follows:

$$C_n(\lambda_m R) = \frac{\left[A_n(\lambda_m R)\ J_{\mu_n}(\lambda_m R) + B_n(\lambda_m R)\ Y_{\mu_n}(\lambda_m R)\right]}{\lambda_m R\left[A_n^2(\lambda_m R) + B_n^2(\lambda_m R)\right]} \tag{5.11e}$$

$$D_n(\lambda_m R) = \frac{\left[B_n(\lambda_m R)\ J_{\mu_n}(\lambda_m R) - A_n(\lambda_m R)\ Y_{\mu_n}(\lambda_m R)\right]}{\lambda_m R\left[A_n^2(\lambda_m R) + B_n^2(\lambda_m R)\right]} \tag{5.11f}$$

$$E_m(\lambda_m R) = \frac{(-1)^m}{(2m-1)\lambda_m R}\left\{\sin[\lambda_m R\sin(\frac{\pi}{4}+\theta)] - \sin[\lambda_m R\sin(\frac{\pi}{4}-\theta)]\right\} \quad \ldots\ldots. \tag{5.11g}$$

$$F_m(\lambda_m R) = \frac{(-1)^m}{(2m-1)\lambda_m R}\left\{\cos[\lambda_m R\sin(\frac{\pi}{4}+\theta)] - \cos[\lambda_m R\sin(\frac{\pi}{4}-\theta)]\right\} \quad \ldots\ldots. \tag{5.11h}$$

$$U_{mn}(\lambda_m R) = \frac{(-1)^m(-1)^n}{(2m-1)}\left\{T_n(\lambda_m R)\ C_n(\lambda_m R) + \frac{\pi}{4}A_n(\lambda_m R)\ D_n(\lambda_m R)\right\} \tag{5.11i}$$

$$V_{mn}(\lambda_m R) = \frac{-(-1)^m(-1)^n}{(2m-1)} \left\{ T_n(\lambda_m R)\ D_n(\lambda_m R) - \frac{\pi}{4} A_n(\lambda_m R)\ C_n(\lambda_m R) \right\} \quad (5.11j)$$

where:

$$A_n(\lambda_m R) = J_{\mu_n - 1}(\lambda_m R) - J_{\mu_n + 1}(\lambda_m R) \quad (5.11k)$$

$$B_n(\lambda_m R) = Y_{\mu_n - 1}(\lambda_m R) - Y_{\mu_n + 1}(\lambda_m R) \quad (5.11\ell)$$

$$T_n(\lambda_m R) = \sum_{k=0}^{\infty} \varepsilon_{2k}\ J_{2k}(\lambda_m R) \frac{(\mu_n^2 + 4k^2 - 1)}{(\mu_n^2 - 4k^2 - 4k - 1)(\mu_n^2 - 4k^2 + 4k - 1)} \quad (5.11m)$$

For $m > m_\ell$ the above listed functions are as follows:

$$C_n(\lambda_m R) = \frac{-K_{\mu_n}(\lambda_m R)}{\lambda_m R \left[K_{\mu_n - 1}(\lambda_m R) + K_{\mu_n + 1}(\lambda_m R)\right]} \quad (5.11n)$$

$$D_n(\lambda_m R) = 0. \quad (5.11o)$$

$$E_m(\lambda_m R) = \frac{-(-1)^m}{(2m-1)\lambda_m R} \left[e^{-\lambda_m R \sin(\pi/4+\theta)} - e^{-\lambda_m R \sin(\pi/4-\theta)} \right]$$

.......(5.11p)

$$F_m(\lambda_m R) = 0.$$

(5.11q)

$$U_{mn}(\lambda_m R) = \frac{-(-1)^m}{(2m-1)} G_n(\lambda_m R)\ C_n(\lambda_m R)$$

$$V_{mn}(\lambda_m R) = 0. \quad (5.11r)$$

where:

$$G_n(\lambda_m R) = \int_0^{\pi/4} \left[\sin(\tfrac{\pi}{4}+\theta)\ e^{-\lambda_m R \sin(\pi/4+\theta)} - \sin(\tfrac{\pi}{4}-\theta)\ e^{-\lambda_m R \sin(\pi/4-\theta)} \right] \sin\mu_n\theta\, d\theta$$

.......(5.11s)

For ground motion in the "y" direction and for the particular fluid domain under consideration an eigen-frequency of the wave equation corresponds to each pair of functions $\sin\mu_n\theta$, $n = 0,1,2,3,\ldots,$ and $\cos\alpha_m z$, $m = 1,2,3,\ldots,$. The hydrodynamic pressures $\bar{p}^y_{0D}(\theta,z,\omega)$, $\bar{p}^y_{0B}(\theta,z,\omega)$, and $\bar{p}^y_j(\theta,z,\omega)$ are bounded at all eigen-frequencies. This contrasts with the results for ground motion in the "x" direction in which case the pressure functions are unbounded at eigen-frequencies corresponding to $n = 0$, $m = 1,2,3,\ldots,$.

The eigenfunctions $\cos 4n\theta$ and $\cos\alpha_m z$ define the distribution of hydrodynamic pressures on the face of the dam due to the x-component of ground motion. For $n = 0$ and $m = 1,2,3,\ldots,$ the pressures are unbounded and independent of angular coordinate. The eigenfunctions $\sin\mu_n\theta$ defines the angular distribution of pressures due to the y-component of ground motion. Because this antisymmetric excitation produces antisymmetric eigenfunctions there are no eigenfunctions that are independent of angular coordinate and resonance (unbounded response) does not occur at any eigen-frequency. Furthermore, the antisymmetric excitation of the banks causes a canceling of pressures due to motion of the banks $\theta = +\pi/4$ with the pressures due to motion of the bank $\theta = -\pi/4$. Because of this canceling effect $\bar{p}^y_{0B}(\theta,z,\omega)$ remains bounded at all eigen-frequencies.

5.3.3 Hydrodynamic Pressures and Forces on Rigid Dams: Numerical Results

The complex frequency response functions for hydrodynamic pressures and forces on rigid arch dams with $R/H = 1.5$ due to cross-stream (y) acceleration of the dam alone as well as of dam and banks are presented in Figs. 5.1 - 5.4. These results are presented in a manner parallel to those for the upstream-downstream motion (Section 4.3.3 and Figs. 4.1 - 4.4). The pressures are now antisymmetric about

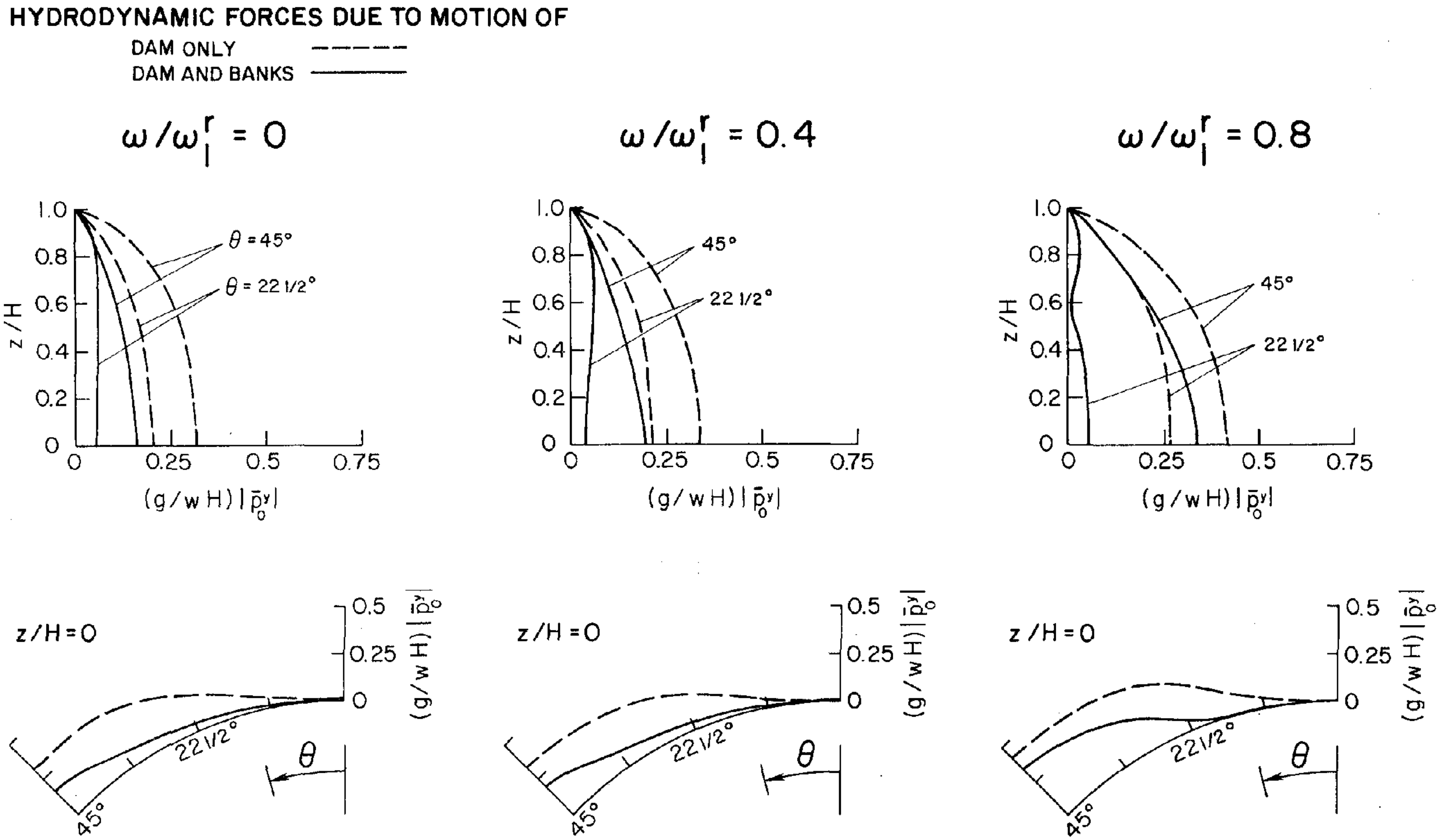

FIG. 5.1 COMPLEX FREQUENCY RESPONSES FOR HYDRODYNAMIC PRESSURES ON RIGID ARCH DAMS, R/H = 1.5, DUE TO THE CROSS-STREAM COMPONENT OF GROUND MOTION.

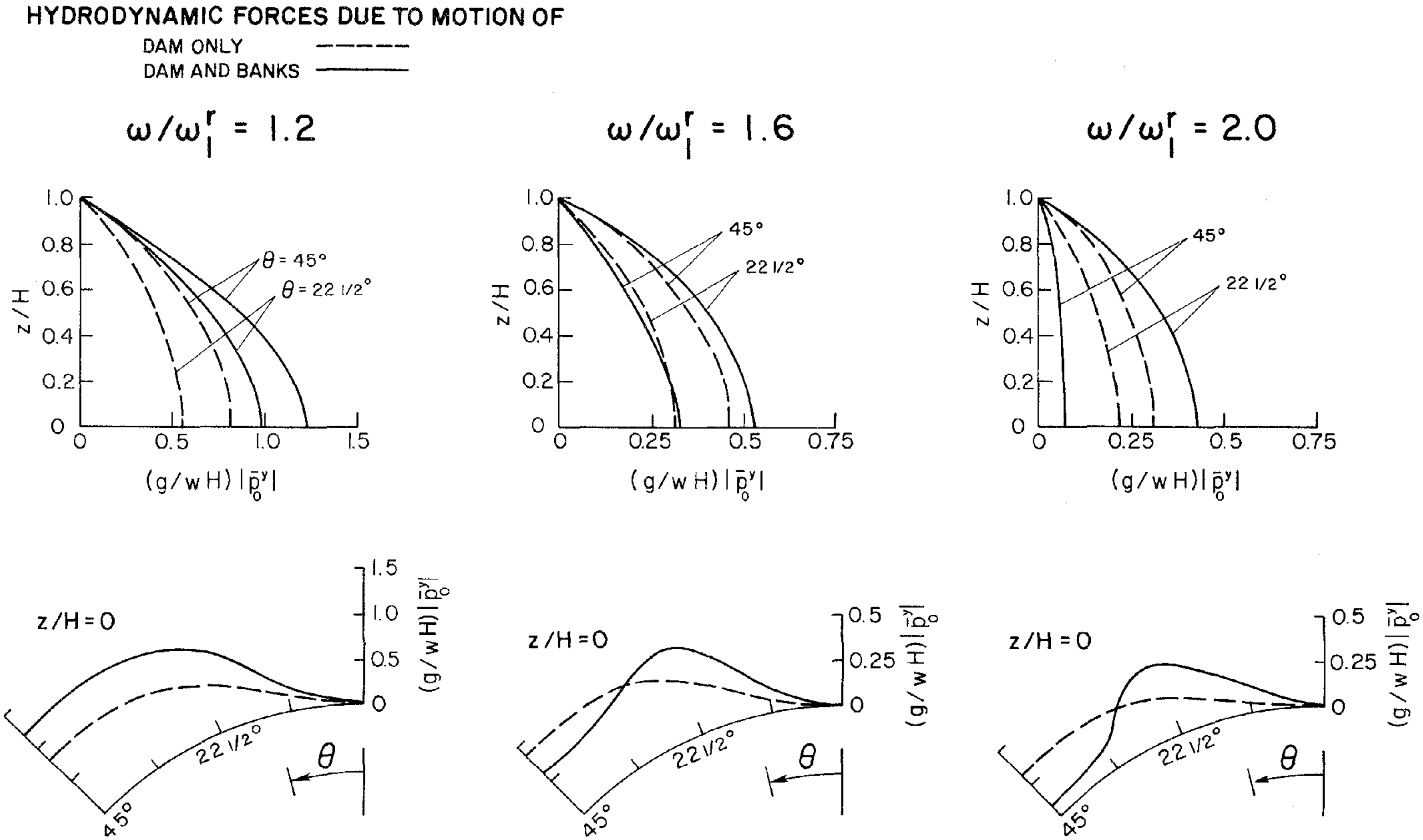

FIG. 5.2 COMPLEX FREQUENCY RESPONSES FOR HYDRODYNAMIC PRESSURE ON RIGID ARCH DAMS, R/H = 1.5, DUE TO THE CROSS-STREAM COMPONENT OF GROUND MOTION.

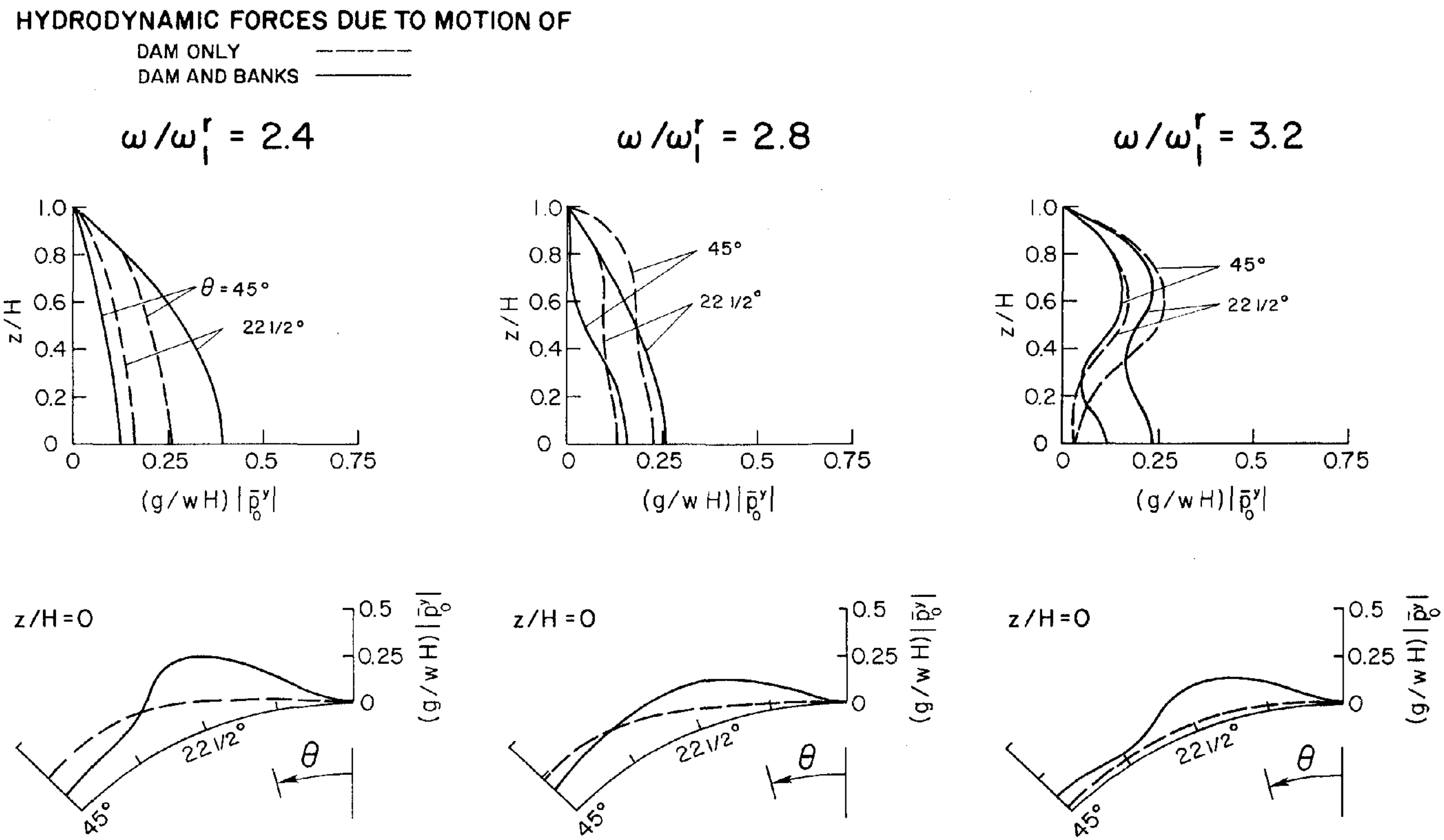

FIG. 5.3 COMPLEX FREQUENCY RESPONSES FOR HYDRODYNAMIC PRESSURES ON RIGID ARCH DAMS, R/H = 1.5, DUE TO THE CROSS-STREAM COMPONENT OF GROUND MOTION.

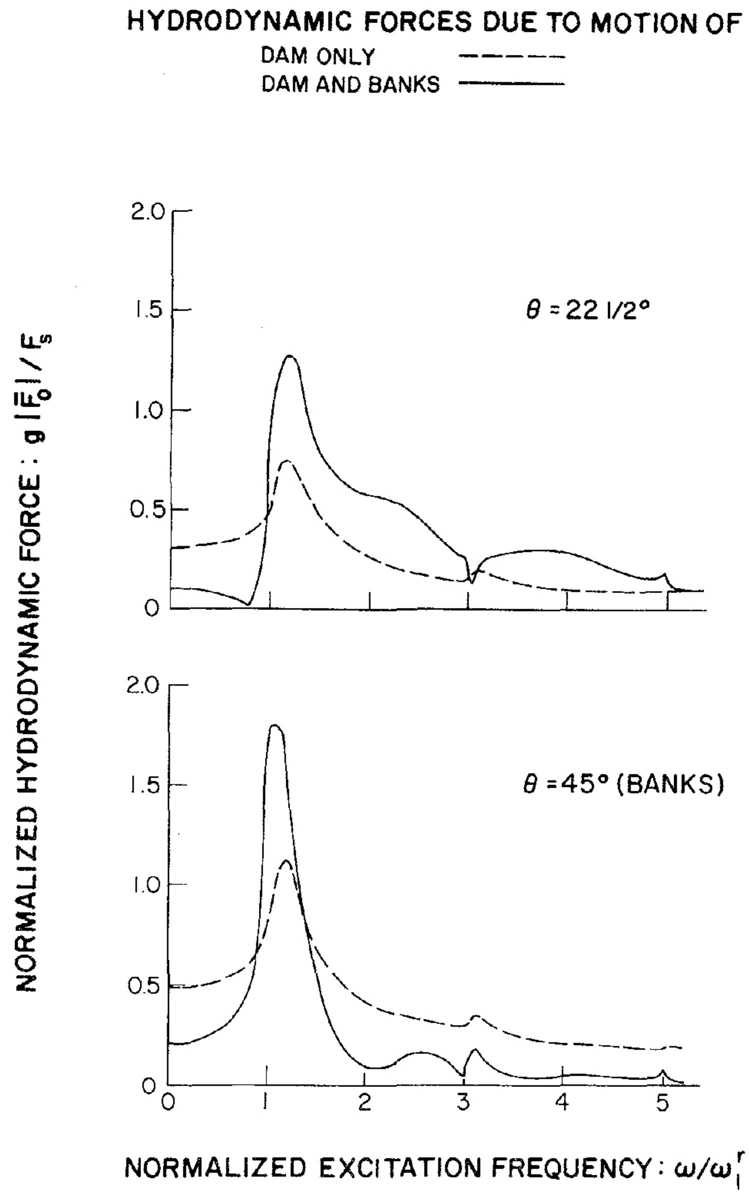

FIG. 5.4 COMPLEX FREQUENCY RESPONSES FOR HYDRODYNAMIC FORCE ON RIGID ARCH DAMS, R/H = 1.5, DUE TO THE CROSS-STREAM COMPONENT OF GROUND MOTION.

the x-z ($\theta = 0$) plane, being zero on that plane. The pressures on straight gravity dams due to cross-stream motion are also zero.

The hydrodynamic forces (and pressures) associated with cross-stream motion depend significantly on the excitation frequency. However, in contrast to the results for upstream-downstream motion, the hydrodynamic forces due to cross-stream motion are bounded at all excitation frequencies with maximum response at or near $\omega/\omega_1^r = 1.0$. The forces due to cross-stream motion are considerably smaller than those due to upstream-downstream motion. The motion of banks modifies the hydrodynamic forces -- increasing them for some excitation frequencies, decreasing them for others.

The hydrodynamic pressures at the base of the dam due to motion of the dam alone increase from zero at the crown to a maximum value at the banks. The pressures due to motion of the dam and banks also attain their maximum value at the banks for smaller excitation frequencies but close to the mid-angle between the crown and the banks for the higher frequencies.

At excitation frequencies $\omega < \omega_1^r$, the contributions of the motion of the banks lead to reduction in hydrodynamic pressures on the dam. However, at $\omega > \omega_1^r$ there is no apparent systematic trend in the contribution of the bank motion to the hydrodynamic pressures. For a particular excitation frequency and fixed θ, the pressures may increase at some depths and decrease at others. For a fixed depth below the water surface, the pressures may increase for some θ values and decrease for others.

5.3.4 Dam Response

The vector of nodal point loads $\underset{\sim}{Q}^f(t)$ on the upstream face of the dam are associated with the hydrodynamic pressure $p_c(\theta,z,t)$. These hydrodynamic loads due to harmonic ground acceleration are of the form $\underline{Q}^f(t) = \bar{\underline{Q}}^f(\omega)\, e^{i\omega t}$. The complex frequency response function for this load vector can, from Eq. 5.4, be expressed as:

$$\bar{\underline{Q}}^f(\omega) = \bar{\underline{Q}}^y_{0D}(\omega) + \bar{\underline{Q}}^y_{0B}(\omega) + \sum_{k=1}^{J} \bar{\ddot{Y}}^y_k(\omega)\, \bar{\underline{Q}}^y_k(\omega) \tag{5.12}$$

where the force vectors $\bar{\underline{Q}}^y_{0D}(\omega)$, $\bar{\underline{Q}}^y_{0B}(\omega)$, and $\bar{\underline{Q}}^y_k(\omega)$ are static equivalents (see Section 4.3.4) of the corresponding pressure functions $\bar{p}^y_{0D}(\theta,z,\omega)$, $\bar{p}^y_{0B}(\theta,z,\omega)$, and $\bar{p}^y_k(\theta,z,\omega)$.

For excitation $\ddot{v}^y_g(t) = e^{i\omega t}$, Eq. 5.1, after substitution of Eq. 5.12, becomes

$$[-\omega^2 M_j + i\omega C_j + K_j]\bar{Y}^y_j(\omega) = -\underline{\phi}^T_j \underline{m}\, \underline{e}^y - \{\phi^f_j\}^T \left\{\bar{\underline{Q}}^y_{0D}(\omega) + \bar{\underline{Q}}^y_{0B}(\omega) - \omega^2 \sum_{k=1}^{J} \bar{Y}^y_k(\omega)\, \bar{\underline{Q}}^y_k(\omega)\right\} \quad \ldots\ldots.(5.13)$$

This set of equations may be expressed in matrix form as

$$\underline{S}(\omega)\ \bar{\underline{Y}}^y(\omega) = \underline{L}^y(\omega) \tag{5.14}$$

where:

$$\left.\begin{aligned} S_{jk}(\omega) &= -\omega^2 \{\phi^f_j\}^T\, \bar{\underline{Q}}^y_k(\omega) \qquad ; \qquad j \neq k \\ S_{jj}(\omega) &= -\omega^2 M_j + i\omega C_j + K_j - \omega^2 \{\phi^f_j\}^T\, \bar{\underline{Q}}^y_j(\omega) \\ L^y_j(\omega) &= -\underline{\phi}^T_j\, \underline{m}\, \underline{e}^y - \{\phi^f_j\}^T\{\bar{\underline{Q}}^y_{0D}(\omega) + \bar{\underline{Q}}^y_{0B}(\omega)\} \end{aligned}\right\} \quad \begin{aligned} j &= 1,2,3,\ldots,J \\ k &= 1,2,3,\ldots,J \end{aligned} \tag{5.15}$$

The frequency dependent matrix $\underline{S}(\omega)$ in Eq. 5.14 relates the generalized displacement vector $\bar{\underline{Y}}^y(\omega)$ to the corresponding generalized load vector $\underline{L}^y(\omega)$. For reasons mentioned in Section 4.3.4 the matrix $\underline{S}(\omega)$ is not diagonal. It can be shown that $\underline{S}(\omega)$ is a symmetric matrix (see Appendix F).

Solutions of Eq. 5.14 for a range of values of the excitation frequency, ω, would provide the complex frequency response functions for all the generalized displacements $\bar{Y}_j^y(\omega)$, $j = 1,2,3,\ldots,J$. The frequency responses for generalized accelerations may be obtained from

$$\bar{\ddot{Y}}_j^y(\omega) = -\omega^2 \bar{Y}_j^y(\omega) \tag{5.16}$$

The complex frequency responses for acceleration at the nodal points of the dam are

$$\bar{\ddot{\underline{v}}}^y(\omega) = \sum_{j=1}^{J} \bar{\ddot{\underline{v}}}_j^y(\omega) \tag{5.17}$$

where the contribution of the $j^{\underline{th}}$ vibration mode of the dam to the acceleration is

$$\bar{\ddot{\underline{v}}}_j^y(\omega) = \bar{\ddot{Y}}_j^y(\omega)\ \underline{\phi}_j \tag{5.18}$$

5.4 Analysis Neglecting Compressibility of Water

Only the hydrodynamic terms are altered in Eq. 5.14 and 5.15 if water is assumed as incompressible. In this case, the hydrodynamic pressure functions $\bar{p}_{0D}^y(\theta,z,\omega)$, $\bar{p}_{0B}^y(\theta,z,\omega)$ and $\bar{p}_j^y(\theta,z,\omega)$ are independent of frequency and they may be obtained by taking limits of these functions (Eqs. 5.8 - 5.10) as $C \to \infty$ or as these functions at $\omega = 0$.

$$\bar{p}_{0D}^y(\theta,z,0) = \frac{32\sqrt{2}\ wR}{g\pi^2} \sum_{m=1}^{\infty} \sum_{n=0}^{\infty} \frac{(-1)^m}{(2m-1)} \frac{(-1)^n}{(\mu_n^2-1)} C_n(\alpha_m R)\ \sin\mu_n\theta\ \cos\alpha_m z \quad \ldots\ldots.(5.19)$$

$$\bar{p}_{0B}^y(\theta,z,0) = \frac{2\sqrt{2}\ wR}{g\pi} \left\{ \sum_{m=1}^{\infty} E_m(\alpha_m R)\cos\alpha_m z + \frac{16}{\pi} \sum_{m=1}^{\infty} \sum_{n=0}^{\infty} U_{mn}(\alpha_m R)\sin\mu_n\theta\ \cos\alpha_m z \right\} \quad \ldots\ldots.(5.20)$$

$$\bar{p}_j^y(\theta,z,0) = -\frac{32wR}{g\pi}\sum_{m=1}^{\infty}\sum_{n=0}^{\infty} I_{mn}^j\; C_n(\alpha_m R)\; \sin\mu_n\theta\; \cos\alpha_m z \tag{5.21}$$

where all quantities except the following are defined in Section 5.3.2

$$C_n(\alpha_m R) = \frac{-K_{\mu_n}(\alpha_m R)}{\alpha_m R\left[K_{\mu_n-1}(\alpha_m R) + K_{\mu_n+1}(\alpha_m R)\right]} \tag{5.22a}$$

$$E_m(\alpha_m R) = \frac{-(-1)^m}{(2m-1)\alpha_m R}\left[e^{-\alpha_m R\sin(\pi/4+\theta)} - e^{-\alpha_m R\sin(\pi/4-\theta)}\right] \tag{5.22b}$$

$$U_{mn}(\alpha_m R) = \frac{-(-1)^m}{(2m-1)}\, G_n(\alpha_m R)\;\; C_n(\alpha_m R) \tag{5.22c}$$

where:

$$G_n(\alpha_m R) = \int_0^{\pi/4}\left[\sin(\tfrac{\pi}{4}+\theta)\; e^{-\alpha_m R\sin(\pi/4+\theta)} - \sin(\tfrac{\pi}{4}-\theta)\; e^{-\alpha_m R\sin(\pi/4-\theta)}\right]\sin\mu_n\theta\; d\theta$$

.......(5.22d)

In general, the functions $\bar{p}_{0D}^y$, $\bar{p}_{0B}^y$ and $\bar{p}_j^y$ are complex valued and depend on the excitation frequency (Eqs. 5.8, 5.9 and 5.10), but they are real valued and independent of frequency if compressibility of water is neglected. Equation 5.16 then becomes

$$-\omega^2[\underline{M} + \underline{M}^a]\bar{\underline{Y}}^y(\omega) + i\,\omega\,\underline{C}\;\bar{\underline{Y}}^y(\omega) + \underline{K}\;\bar{\underline{Y}}^y(\omega) = \underline{L}^{0y} + \underline{L}^{ay} \tag{5.23}$$

where $\underline{M}$, $\underline{C}$, and $\underline{K}$ are generalized mass, generalized damping and generalized stiffness matrices respectively; each is a diagonal matrix. $\underline{L}^{0y} = -\underline{\phi}_j^T\;\underline{M}\;\underline{e}^y$. $\underline{M}^a$ is an "added mass" matrix defined by

$$M_{jk}^a = \{\phi_j^f\}^T\;\underline{\bar{Q}}_k^y(0) \qquad ; \qquad j,k = 1,2,3,\ldots.,J \tag{5.24a}$$

and $\underline{L}^{ay}$ is an "added load" vector defined by

$$L_j^{ay} = - \{\phi_j^f\}^T \{\bar{\underline{Q}}_{0D}^y(0) + \bar{\underline{Q}}_{0B}^y(0)\} \quad ; \quad j = 1,2,3,....,J \quad (5.24b)$$

When water is assumed to be incompressible the hydrodynamic effects are thus equivalent to frequency independent added mass and load terms. Consequently, unlike the case including water compressibility and involving hydrodynamic terms that depend on frequency (Eqs. 5.14 and 5.15), Eq. 5.23 can be written directly in the time domain as

$$[\underline{M} + \underline{M}^a]\ddot{\underline{Y}}^y(t) + C\,\dot{\underline{Y}}^y(t) + K\,\underline{Y}^y(t) = [\underline{L}^{0y} + \underline{L}^{ay}]\ddot{v}_g^y(t) \qquad (5.25)$$

6. ANALYSIS OF DAM RESPONSE TO HARMONIC VERTICAL GROUND MOTION

6.1 Equations of Motion

The analytical procedures and results developed in this chapter for response of the dam to the vertical (z-) component of ground motion closely parallel those of Chapters 4 and 5. Although at the expense of some repetition, the presentation in this chapter is self-contained.

Only the symmetric natural modes of vibration of the dam (see Section 4.1) will be excited by the z-component of ground motion. For this excitation, the equation of motion (Eq. 3.4) specializes to:

$$M_j \ddot{Y}_j^z(t) + C_j \dot{Y}_j^z(t) + K_j Y_j^z(t) = -\underline{\phi}_j^T \underline{m}\, \underline{e}^z \ddot{v}_g^z(t) - \{\phi_j^f\}^T \underline{Q}^f(t) \; ; \quad j = 1,2,3,\ldots,J \tag{6.1}$$

where $Y_j^z(t)$ is the generalized displacement associated with the j^{th} symmetric mode of vibration.

6.2 Fluid Domain: Boundary Conditions

In Eq. 6.1 $\underline{Q}^f(t)$ is the vector of nodal forces associated with hydrodynamic pressures on the upstream face of the dam. These pressures acting in the radial direction are governed by the wave equation (Eq. 3.5) together with the following boundary conditions:

- The radial component of fluid motion at the upstream face of the dam (boundary $r = R$) is the same as the radial motion of the upstream face of the dam.
- There is no fluid motion normal to the banks (boundaries $\theta = \pm \pi/4$)

- The vertical motion of the fluid at the bottom of the reservoir (boundary $z = 0$) is prescribed by the vertical component of ground acceleration.
- Fluid pressure at the free surface is zero.
- Since the system, symmetrical about the x-z ($\theta = 0$) plane, is excited by the z-component of ground motion the hydrodynamic pressures must be symmetric about $\theta = 0$.
- The radiation boundary condition not permitting any reflected waves applies at the upstream end ($r = \infty$) of the reservoir.

6.3 Complex Frequency Response

The response to harmonic ground acceleration in the vertical direction, $\ddot{v}_g^z(t) = e^{i\omega t}$, can be expressed as follows:

- Hydrodynamic pressures at the dam face,

$$p_c(\theta,z,t) = \bar{p}_c(\theta,z,\omega)\ e^{i\omega t} \tag{6.2a}$$

- Generalized accelerations,

$$\ddot{Y}_j^z(t) = \bar{\ddot{Y}}_j^z(\omega)\ e^{i\omega t} \tag{6.2b}$$

- Radial accelerations on the upstream face of the dam

$$\ddot{v}^r(R,\theta,z,t) = \left\{ \sum_{j=1}^{J} [\phi_j^{xf}(\theta,z)\ \cos\theta + \phi_y^{yf}(\theta,z)\ \sin\theta]\ \bar{\ddot{Y}}_j^z(\omega) \right\} e^{i\omega t} \tag{6.2c}$$

where $\phi_j^{xf}(\theta,z)$ and $\phi_j^{yf}(\theta,z)$ are the continuous analogue functions (see Section 4.2) for the vectors $\underline{\phi}_j^{xf}$ and $\underline{\phi}_j^{yf}$ defined in Section 3.2.

6.3.1 Boundary Conditions

Using Eqs. 3.6 and 6.2; the boundary conditions of Section 6.2 can be expressed analytically as follows:

$$\frac{\partial p}{\partial r}(R,\theta,z,t) = -\frac{w}{g}\left\{\sum_{j=1}^{J} [\phi_j^{xf}(\theta,z) \cos\theta + \phi_j^{yf}(\theta,z) \sin\theta] \; \bar{\ddot{Y}}_j^{y}(\omega)\right\} e^{i\omega t} \quad (6.3a)$$

$$\frac{\partial p}{r\partial\theta}(r, \frac{\pi}{4}, z, t) = 0 \quad (6.3b)$$

$$\frac{\partial p}{\partial z}(r,\theta,0,t) = -\frac{w}{g}\, e^{i\omega t} \quad (6.3c)$$

$$p(r,\theta,H,t) = 0 \quad (6.3d)$$

$$\frac{\partial p}{r\partial\theta}(r,0,z,t) = 0 \quad (6.3e)$$

In addition to these boundary conditions, no wave reflections at the upstream end of the reservoir ($r = \infty$) are permitted.

Because the governing wave equation as well as the boundary conditions are linear, the principle of superposition applies. The complex frequency response function for the hydrodynamic pressures on the dam face $p_c(\theta,z,t)$ can therefore be expressed as:

$$\bar{p}_c(\theta,z,t) = \bar{p}_0^{z}(\theta,z,t) + \sum_{j=1}^{J} \bar{\ddot{Y}}_j^{z}(\omega) \; \bar{p}_j^{z}(\theta,z,\omega) \quad (6.4)$$

The complex frequency response functions $\bar{p}_0$ and $\bar{p}_j$ in Eq. 6.4 are defined as follows. The solution of the wave equation (Eq. 3.5) at $r = R$ (upstream face of the dam) is $p_0^z(\theta,z,t) = \bar{p}_0^z(\theta,z,t)\; e^{i\omega t}$ for the following boundary conditions:

$$\frac{\partial p}{\partial r}(R,\theta,z,t) = 0 \quad (6.5)$$

and those specified by Eqs. 6.3b to 6.3e. The solution of the wave equation at r = R is $p_j^z(\theta,z,t) = \bar{p}_j^z(\theta,z,t)\, e^{i\omega t}$ for the following boundary conditions:

$$\frac{\partial p}{\partial z}(r,\theta,0,t) = 0 \tag{6.6}$$

and those specified by Eqs. 6.3a, 6.3b, 6.3d and 6.3e.

The complex frequency response functions $\bar{p}_0^z(\theta,z,\omega)$ and $\bar{p}_j^z(\theta,z,\omega)$ are for hydrodynamic pressures on the upstream face of the dam due to two excitations. $\bar{p}_0^z(\theta,z,\omega)$ corresponds to vertical, rigid-body accelerations of dam, the reservoir bottom and the banks. Because the banks and the upstream face of the dam are vertical, these pressures result only from excitation of the reservoir bottom. $\bar{p}_j^z(\theta,z,\omega)$ corresponds to acceleration $\ddot{\bar{Y}}_j^z(\omega) = 1$ in the j^{th} symmetric mode of vibration of the dam (without water) but there is no motion of the dam base, banks or reservoir bottom.

6.3.2 Hydrodynamic Pressures: Analytical Results

The boundary conditions in Section 6.3.1 for which $\bar{p}_j^z(\theta,z,\omega)$ is the solution of the wave equation also arose in the analysis for the x-component of ground motion (Section 4.3.1). The solution has been presented in Eq. 4.10.

The solution of the wave equation for the first set of boundary conditions in Section 6.3.1 is derived in Appendix C. The final expression for $\bar{p}_0^z(\theta,z,\omega)$ is:

$$\bar{p}_0^z(\theta,z,\omega) = \frac{2wH}{g\pi}\,\frac{\sin\left[\frac{\pi}{2}\frac{\omega}{\omega_1^r}\left(1-\frac{z}{H}\right)\right]}{\frac{\omega}{\omega_1^r}\cos\left[\frac{\pi}{2}\frac{\omega}{\omega_1^r}\right]} \tag{6.7}$$

This result for $\bar{p}_0^z(\theta,z,\omega)$ was obtained with the assumption that the reservoir bottom is rigid, resulting in complete reflection of the hydrodynamic waves at that boundary. This result is identical to the two-dimensional solution obtained for hydrodynamic pressures on gravity dams due to vertical ground motion [22,24]. The hydrodynamic pressures are unbounded at frequencies $\omega = \omega_m^r$, $m = 1,2,3,\ldots.$ where $\omega_m^r = (2m-1)\,\frac{\pi c}{2H}$.

Analytical studies [22,24] indicated that the hydrodynamic pressures on rigid gravity dams due to earthquake motions when computed using Eq. 6.7 are unrealistically large. Thus Eq. 6.7 was modified to account for the deformability of the reservoir bottom and the partial reflection and refraction of the hydrodynamic waves at that boundary. The modification to $\bar{p}_0^z(\theta,z,\omega)$ was accomplished by solving a one-dimensional problem in which the rock under the reservoir was assumed to be an elastic, isotropic homogeneous half space [25]. The resulting complex frequency response function for the pressure is:

$$\bar{p}_0^z(\theta,z,\omega) = \frac{2wH}{g\pi\left(\dfrac{\omega}{\omega_1^r}\right)} \frac{(1+\alpha)\sin\left[\dfrac{\pi}{2}\dfrac{\omega}{\omega_1^r}\left(1-\dfrac{z}{H}\right)\right]}{(1+\alpha)\cos\left[\dfrac{\pi}{2}\dfrac{\omega}{\omega_1^r}\right] + i(1-\alpha)\sin\left[\dfrac{\pi}{2}\dfrac{\omega}{\omega_1^r}\right]} \tag{6.8}$$

where α is a reflection constant given by $\alpha = (k-1)/(k+1)$, where $k = C_r w_r / C_w$ with w_r being the unit weight of rock and C_r the P-wave velocity in rock. For the case of rigid rock at the reservoir bottom $\alpha = 1$ and Eq. 6.8 reduces to the earlier result (Eq. 6.7). In contrast to Eq. 6.7, the pressures given by Eq. 6.8 are bounded at all excitation frequencies. This investigation employs Eq. 6.8, thereby accounting for the influence of deformability of the foundation rock on the hydrodynamic pressures.

The solutions given in Eqs. 6.7 and 6.8 are independent of the angular coordinate, θ, and of the upstream radius of the dam, R. For a particular excitation frequency, the hydrodynamic pressures thus vary only with the z (depth) coordinate.

6.3.3 Hydrodynamic Pressures and Forces on Rigid Dams: Numerical Results

The complex valued frequency response function $\bar{p}_0^z(\theta,z,\omega)$ is for the hydrodynamic pressures on a rigid dam due to vertical ground motion. The hydrodynamic force, $\bar{F}_0$, acting per unit length of circumference is the integral of $\bar{p}_0^z$ over the depth of water. As noted earlier, $\bar{p}_0^z$ is independent of the angular coordinate θ and the radius R of the upstream face of the dam. Hence, $\bar{F}_0$ also is independent of θ and R. Thus the results shown in Figs. 6.1 and 6.2 apply to all values of θ and all dam-water systems of Fig. 2.1. The results have been appropriately normalized so that they also apply to all arch dam-water systems independent of water depth H. The pressures and forces of Figs. 6.1 and 6.2 were computed from Eq. 6.8 with $\alpha = 0.85$, an appropriate value for the reflection constant.

The hydrodynamic forces (and pressures) depend strongly on the excitation frequency. Starting with the hydrodynamic value at very low excitation frequencies, the force is amplified several times at the fundamental resonant frequency. Because the partial refraction of hydrodynamic waves at the bottom of the reservoir has been considered, resonant response is finite. The hydrodynamic force at higher resonant frequencies is also finite, and much smaller than at the fundamental resonant frequency. Except for the local amplification near the higher resonant frequencies, the hydrodynamic force decreases as the excitation frequency increases beyond the fundamental resonant frequency.

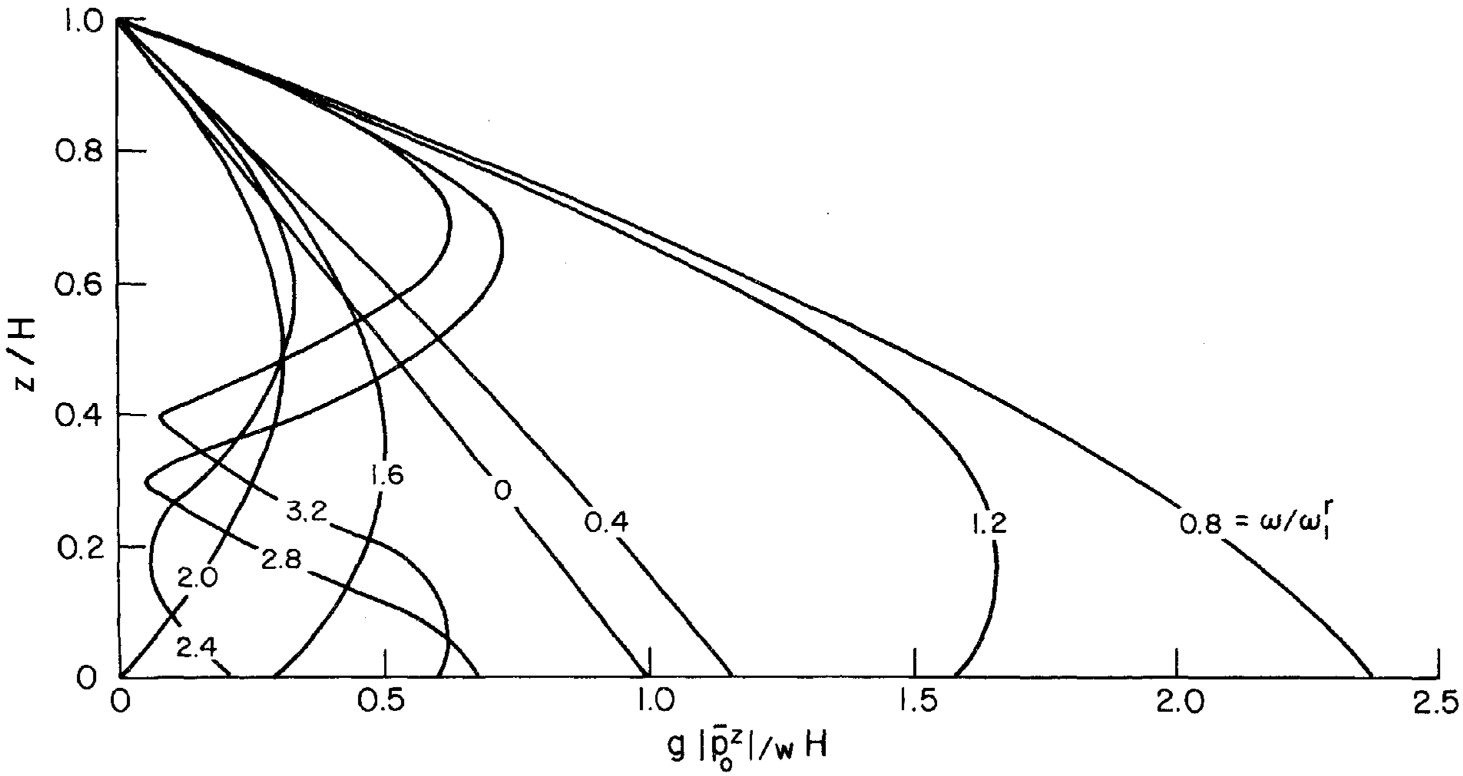

FIG. 6.1 COMPLEX FREQUENCY RESPONSES FOR HYDRODYNAMIC PRESSURES ON RIGID ARCH DAMS DUE TO VERTICAL GROUND MOTION; $\alpha = 0.85$. RESULTS ARE INDEPENDENT OF θ AND VALID FOR ALL R/H.

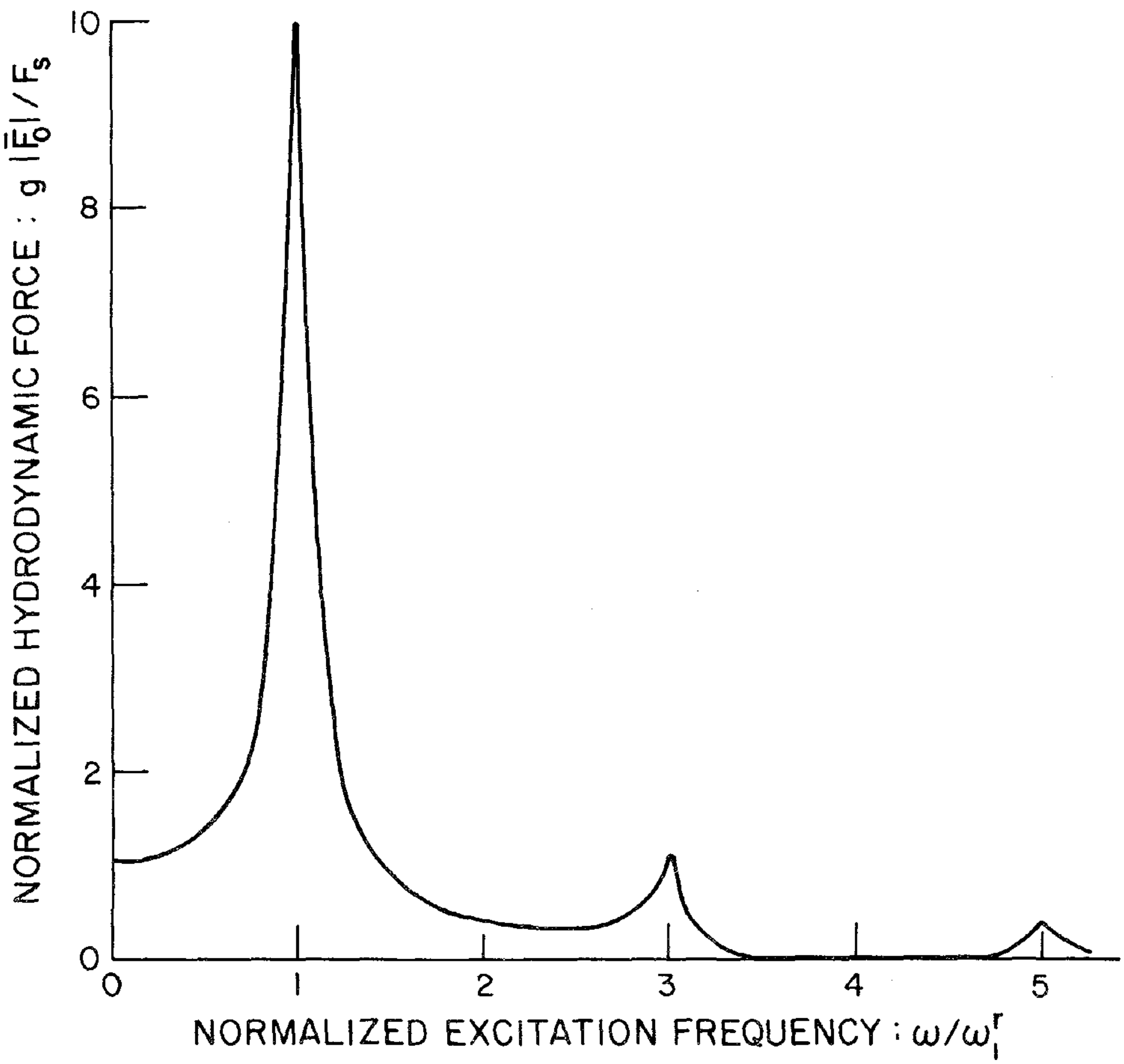

FIG. 6.2 COMPLEX FREQUENCY RESPONSE FOR HYDRODYNAMIC FORCE ON RIGID ARCH DAMS DUE TO VERTICAL GROUND MOTION; $\alpha = 0.85$. RESULTS ARE INDEPENDENT OF θ AND VALID FOR ALL R/H.

The variation of hydrodynamic pressure over depth depends strongly on the excitation frequency. At zero excitation frequency the hydrostatic pressure distribution is a straight line varying from zero at the free surface to a maximum value at the reservoir bottom. Starting with this straight line variation at zero frequency, the pressure distribution becomes increasingly complex with increasing excitation frequency.

6.3.4 Dam Response

The vector of nodal point loads, $\underset{\sim}{Q}^f(t)$, on the upstream face of the dam are associated with the hydrodynamic pressures $p_c(\theta,z,t)$. These hydrodynamic loads due to harmonic ground acceleration are of the form $\underset{\sim}{Q}^f(t) = \bar{\underset{\sim}{Q}}^f(\omega)\ e^{i\omega t}$. The complex frequency response function for this load vector can, from Eq. 6.4, by expressed as:

$$\bar{\underset{\sim}{Q}}^f(\omega) = \bar{\underset{\sim}{Q}}_0^z(\omega) + \sum_{k=1}^{J} \bar{\bar{Y}}_k^z(\omega)\ \bar{\underset{\sim}{Q}}_k^z(\omega) \tag{6.9}$$

where the force vectors $\bar{\underset{\sim}{Q}}_0^z(\omega)$ and $\bar{\underset{\sim}{Q}}_k^z(\omega)$ are static equivalents (see Section 4.3.4) of the corresponding pressure functions $\bar{p}_0^z(z,\omega)$ and $\bar{p}_k^z(\theta,z,\omega)$.

For excitation $\ddot{v}_g^z(t) = e^{i\omega t}$, Eq. 6.1, after substitution of Eq. 6.9, becomes:

$$[-\omega^2 M_j + i\omega C_j + K_j]\bar{Y}_j^z(\omega) = -\phi_j^T \underset{\sim}{m}\ \underset{\sim}{e}^z - \{\phi_j^f\}^T\{\bar{\underset{\sim}{Q}}_0^z(\omega) - \omega^2 \sum_{k=1}^{J} \bar{Y}_k^z(\omega)\ \bar{\underset{\sim}{Q}}_k^z(\omega)\} \quad \ldots\ldots\ (6.10)$$

This set of equations can be expressed in matrix form as:

$$\underset{\sim}{S}(\omega)\ \bar{\underset{\sim}{Y}}^z(\omega) = \underset{\sim}{L}^z(\omega) \tag{6.11}$$

where:

$$\left.\begin{aligned} S_{jk}(\omega) &= -\,\omega^2\ \{\phi_j^f\}^T\ \bar{\underset{\sim}{Q}}{}_k^z(\omega) \qquad ; \qquad j \neq k \\ S_{jj}(\omega) &= -\,\omega^2 M_j + i\omega C_j + k_j - \omega^2\ \{\phi_j^f\}^T\ \bar{\underset{\sim}{Q}}{}_j^z(\omega) \\ L_j^z(\omega) &= -\,\underset{\sim}{\phi}{}_j^T\ \underset{\sim}{m}\ \underset{\sim}{e}^z - \{\phi_j^f\}^T\ \bar{\underset{\sim}{Q}}{}_0^z(\omega) \end{aligned}\right\} \begin{aligned} &j = 1,2,3,\ldots\ldots,J \\ &k = 1,2,3,\ldots\ldots,J \end{aligned} \qquad (6.12)$$

This coefficient matrix $\underset{\sim}{S}(\omega)$ is identical to the matrix in Eq. 4.16 for the x-component of ground motion but different than the matrix in Eq. 5.15 for the y-component of ground motion.

The frequency dependent matrix $\underset{\sim}{S}(\omega)$ in Eq. 6.12 relates the generalized displacement vector $\bar{\underset{\sim}{Y}}{}^z(\omega)$ to the corresponding generalized loads $\underset{\sim}{L}^z(\omega)$. For reasons mentioned in Section 4.3.4, $\underset{\sim}{S}(\omega)$ is not diagonal. It can be shown that $\underset{\sim}{S}(\omega)$ is a symmetric matrix (Appendix F).

Solutions of Eq. 6.11 for a range of values of the excitation frequency, ω, would provide the complex frequency response function for all the generalized displacements $\bar{Y}_j^z(\omega)$, $j = 1,2,3,\ldots\ldots,J$. The frequency responses for generalized accelerations may be obtained from:

$$\bar{\ddot{Y}}{}_j^z(\omega) = -\,\omega^2\ \bar{Y}_j^z(\omega) \qquad (6.13)$$

The complex frequency responses for acceleration at the nodal points of the dam are

$$\bar{\ddot{\underset{\sim}{v}}}{}^z(\omega) = \sum_{j=1}^{J} \bar{\ddot{\underset{\sim}{v}}}{}_j^z(\omega) \qquad (6.14)$$

where the contribution of the j^{th} vibration mode of the dam to the acceleration is

$$\bar{\ddot{\underset{\sim}{v}}}{}_j^z(\omega) = \bar{\ddot{Y}}{}_j^z(\omega)\ \underset{\sim}{\phi}{}_j \qquad (6.15)$$

6.4 Analysis Neglecting Compressibility of Water

Only the hydrodynamic terms are altered in Eqs. 6.11 and 6.12 if water is assumed to be incompressible. In this case, the hydrodynamic pressure functions are obtained by taking the limits of $\bar{p}_0^z(z,\omega)$ and $\bar{p}_j^z(\theta,z,\omega)$ as $C \to \infty$ or as these functions at $\omega = 0$:

$$\bar{p}_0^z(z,0) = \frac{wH}{g}\left(1 - \frac{z}{H}\right) \tag{6.16}$$

and $\bar{p}_j^z(\theta,z,0)$ is given by Eq. 4.23.

In general, the functions $\bar{p}_0^z(z,\omega)$ and $\bar{p}_j^z(\theta,z,\omega)$ are complex valued and depend on the excitation frequency, but they are real valued and independent of frequency if compressibility of water is neglected. Equation 6.11 them becomes:

$$-\omega^2 (\underline{M} + \underline{M}^a)\, \bar{\underline{Y}}^z(\omega) + i\,\omega\, \underline{C}\, \bar{\underline{Y}}^z(\omega) + \underline{K}\, \bar{\underline{Y}}^z(\omega) = \underline{L}^{0z} + \underline{L}^{az} \tag{6.17}$$

where $\underline{M}$, $\underline{C}$, and $\underline{K}$ are generalized mass, generalized damping and generalized stiffness matrices respectively; each is a diagonal matrix. $\underline{L}^{0z} = -\underline{\phi}_j^T\, \underline{m}\, \underline{e}^z$. $\underline{M}^a$ is an "added mass" matrix defined by:

$$M_{jk}^a = \{\phi_j^f\}^T\, \bar{\underline{\underline{Q}}}_k^z(0) \quad ; \quad j,k = 1,2,3,\dots,J \tag{6.18a}$$

$\underline{L}^{az}$ is an "added load" vector defined by:

$$L_j^{az} = -\{\phi_j^f\}^T\, \bar{\underline{\underline{Q}}}_0^z(0) \quad ; \quad j = 1,2,3,\dots,J \tag{6.18b}$$

When water is assumed to be incompressible the hydrodynamic effects are thus equivalent to frequency independent added mass and load terms. Consequently, Eq. 6.17 can be written directly in the time domain as:

$$(\underline{M} + \underline{M}^a)\ddot{\underline{Y}}^z(t) + \underline{C}\,\dot{\underline{Y}}^z(t) + \underline{K}\,\underline{Y}^z(t) = (\underline{L}^{0z} + \underline{L}^{az})\ddot{v}_g^z(t) \tag{6.19}$$

7. HYDRODYNAMIC INTERACTION EFFECTS

7.1 Scope of Chapter

Using the analysis procedures developed in Chapters 3 - 6, numerical results for response of three arch dams with different radius to height ratios are presented in this chapter. Acceleration responses to harmonic ground motion applied separately in the x (upstream-downstream), y (cross-stream), and z (vertical) directions are presented. Based on these results, the effects of hydrodynamic interaction, compressibility of water and bank motion on dam response are identified.

7.2 Fundamental Parameters

The analysis procedure developed in Chapters 4 - 6 is for the idealized arch dams described in Chapter 2. The upstream face of the arch dam is a segment of a circular cylinder, radius R and height H_d, contained within radially extending banks enclosing a central angle of 90°. In addition, the geometry as well as mass, stiffness, and damping properties of the dam are all assumed to be symmetrical about the x-z (θ=0) plane. But for these restrictions, the geometric and material properties of the arch dam are arbitrary. Results presented in this chapter are for arch dams with trapezoidal radial section, the radial thickness varying linearly from B_1 at the crest to B_2 at the base.

As shown in Appendix G the frequency ω_j and mode shape $\underline{\phi}_j$ of the j^{th} natural mode of vibration of the dam without water and the complex frequency response for generalized acceleration $\ddot{\bar{Y}}_j$ in the j^{th} mode can be expressed in terms of dimensionless parameters as follows:

$$\omega_j = \frac{1}{H_d} \sqrt{\frac{Eg}{w_d}}\; f\left(\nu, \frac{B_1}{H_d}, \frac{B_2}{H_d}, \frac{R}{H_d}\right) \tag{7.1}$$

$$\underset{\sim}{\phi}_j = \underset{\sim}{\phi}_j \left(\frac{z}{H_d}, \theta, \frac{r}{H_d}, \frac{B_1}{H_d}, \frac{B_2}{H_d}, \frac{R}{H_d}, \nu\right) \tag{7.2}$$

$$\bar{\ddot{Y}}_j = \bar{\ddot{Y}}_j \left(\frac{\omega}{\omega_1}, \nu, \frac{B_1}{H_d}, \frac{B_2}{H_d}, \frac{R}{H_d}, \xi_j, \frac{w}{w_d}, \frac{\omega_1^r}{\omega_1}, \frac{H}{H_d}, \alpha\right) \tag{7.3}$$

where

f = symbol for "a function of"

B_1 = radial thickness of dam at the crest

B_2 = radial thickness of dam at the base

E = modulus of elasticity of the dam concrete

g = acceleration of gravity

H = depth of water

H_d = height of the dam

R = radius of upstream face of the dam

r, θ, z = cylindrical coordinates of points on the dam

w_d = unit weight of dam concrete

w = unit weight of water

α = reflection constant at reservoir bottom for hydrodynamic pressure waves defined in Section 6.3.2; pertinent only for vertical ground motion

ν = Poisson's ratio

ξ_j = damping ratio for the j^{th} mode of vibration of the dam

ω = excitation frequency

ω_1 = fundamental frequency of the dam

ω_1^r = fundamental eigen-frequency of the fluid domain

Unlike gravity dams [13], the fundamental mode of vibration for thin arch dams does not necessarily provide the most significant response. Thus when studying thin arch dam response, several vibration modes that contribute significantly to the response should be considered. This combined response is

$$\ddot{\underline{v}} = \sum_{j=1}^{J} \ddot{Y}_j \underline{\phi}_j = \ddot{\underline{v}}\left(\frac{\omega}{\omega_1},\ \nu,\ \frac{z}{H_d},\ \theta,\ \frac{r}{H_d},\ \frac{B_1}{H_d},\ \frac{B_2}{H_d},\ \frac{R}{H_d},\ \xi_j,\ \frac{w}{w_d},\ \frac{\omega_1^r}{\omega_1},\ \frac{H}{H_d},\ \alpha\right) \quad (7.4)$$

The parameters of Eqs. 7.3 and 7.4 -- not all are mutually independent -- are selected to be useful for interpreting response results and hydrodynamic interaction effects. For example, ω_1^r/ω_1 can be expressed in terms of other parameters as

$$\frac{\omega_1^r}{\omega_1} = \sqrt{\frac{C^2 w_d}{Eg}}\ \frac{H_d}{H}\ f\left(\nu,\ \frac{B_1}{H_d},\ \frac{B_2}{H_d},\ \frac{R}{H_d}\right) \quad (7.5)$$

7.3 Systems Analyzed

7.3.1 System Properties

The results presented in this chapter are obtained from specific numerical values of the parameters given in Section 7.2. Based on a survey of geometry of thin arch dams, the crest and base widths are fixed at $B_1/H_d = 0.035$ and $B_2/H_d = 0.200$ but three different values of $R/H_d = 0.5$, 1.5, and 2.5 are selected. The properties chosen for mass concrete of the dam are $E = 5 \times 10^6$ psi, $\nu = 0.17$, and $w_d = 150$ pcf. For water in the reservoir, $C = 4720$ fps and $w = 62.5$ pcf. The damping ratio ξ_j for all normal modes of vibration of the dam are assumed to be the same and equal to 0.05. In the analysis of response to vertical ground motion, the reflection constant $\alpha = 0.85$. Results are presented for two values of the height parameter; for a full reservoir $H/H_d = 1.0$, for an empty reservoir $H/H_d = 0.0$. The normalized excitation frequency ω/ω_1 is varied from 0.0 to 4.0.

Because the dam properties are symmetrical about the x-z (θ=0) plane, only one-half of the dam with appropriate boundary conditions on the plane of symmetry is considered in the analysis. Half of the dam is idealized as an assemblage of 36 three-dimensional elements as shown in Fig. 7.1. Every element has a height of $H_d/6$, and an included angle of 7.5° which extends throughout the thickness of the dam. The finite element system is analyzed by the procedures presented in Chapters 4 - 6 including 10 natural modes of vibration of the dam.

7.3.2 Natural Frequencies and Mode Shapes of Vibration

Because the geometry and material properties of the dam are symmetric about the x-z (θ=0) plane, the natural modes of vibration can be separated into two categories: symmetric or antisymmetric about the same plane. As mentioned earlier, the symmetric modes are excited by ground motions in the upstream-downstream and vertical directions: whereas the antisymmetric modes are excited by cross stream ground motion. The first six symmetric and first six antisymmetric mode shapes and natural frequencies of vibration for the three dams -- $R/H_d = 0.5$, 1.5, and 2.5 -- under consideration are presented in Figs. 7.2 - 7.7. These are vibration properties of the dam without water.

In Figs. 7.2 to 7.7, mode shapes are plotted along the upstream face of the dam at the crest ($Z/H_d = 1.0$) and the radial component is

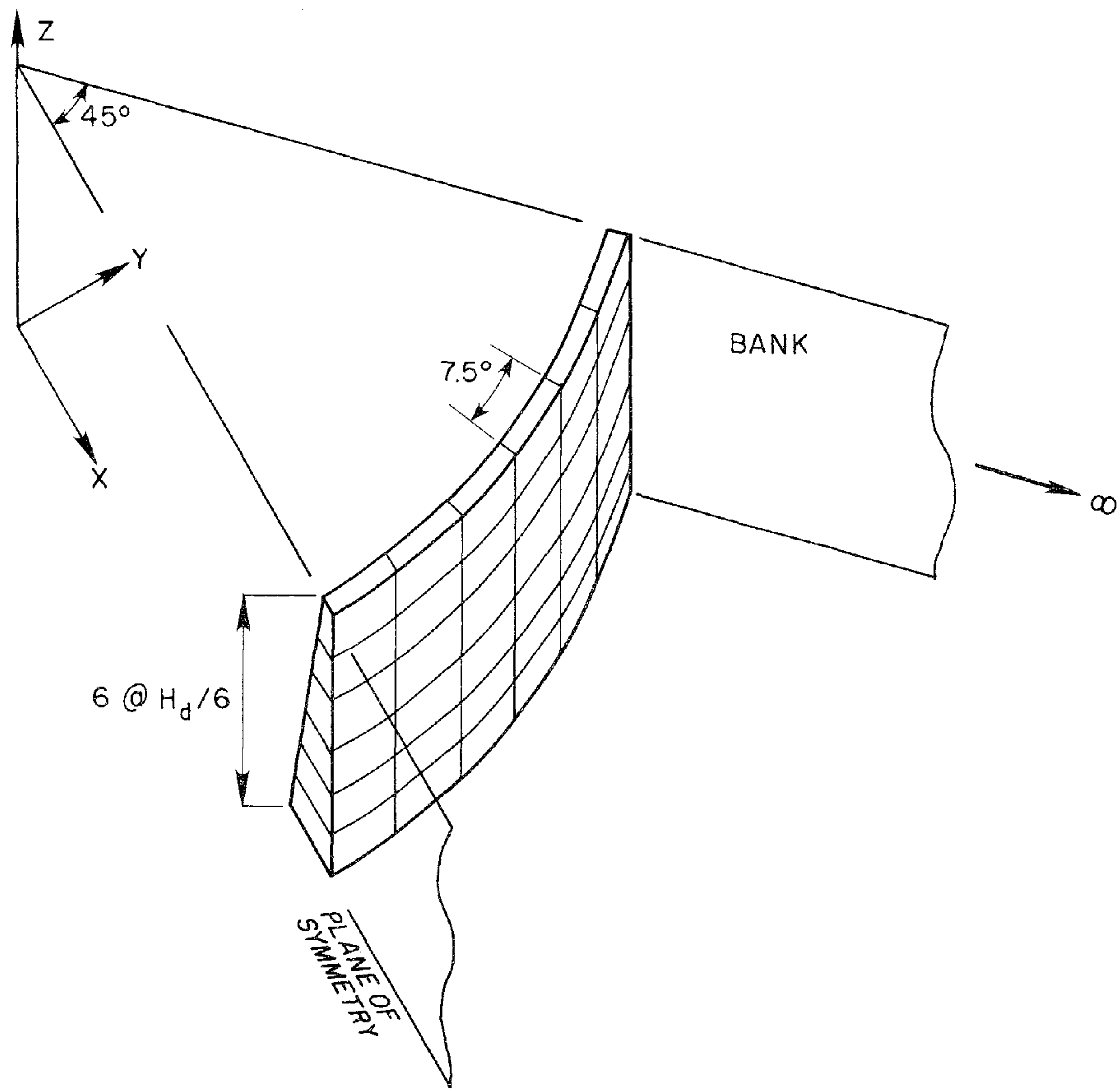

FIG. 7.1 FINITE ELEMENT IDEALIZATION OF HALF THE DAM USING SHELL ELEMENTS

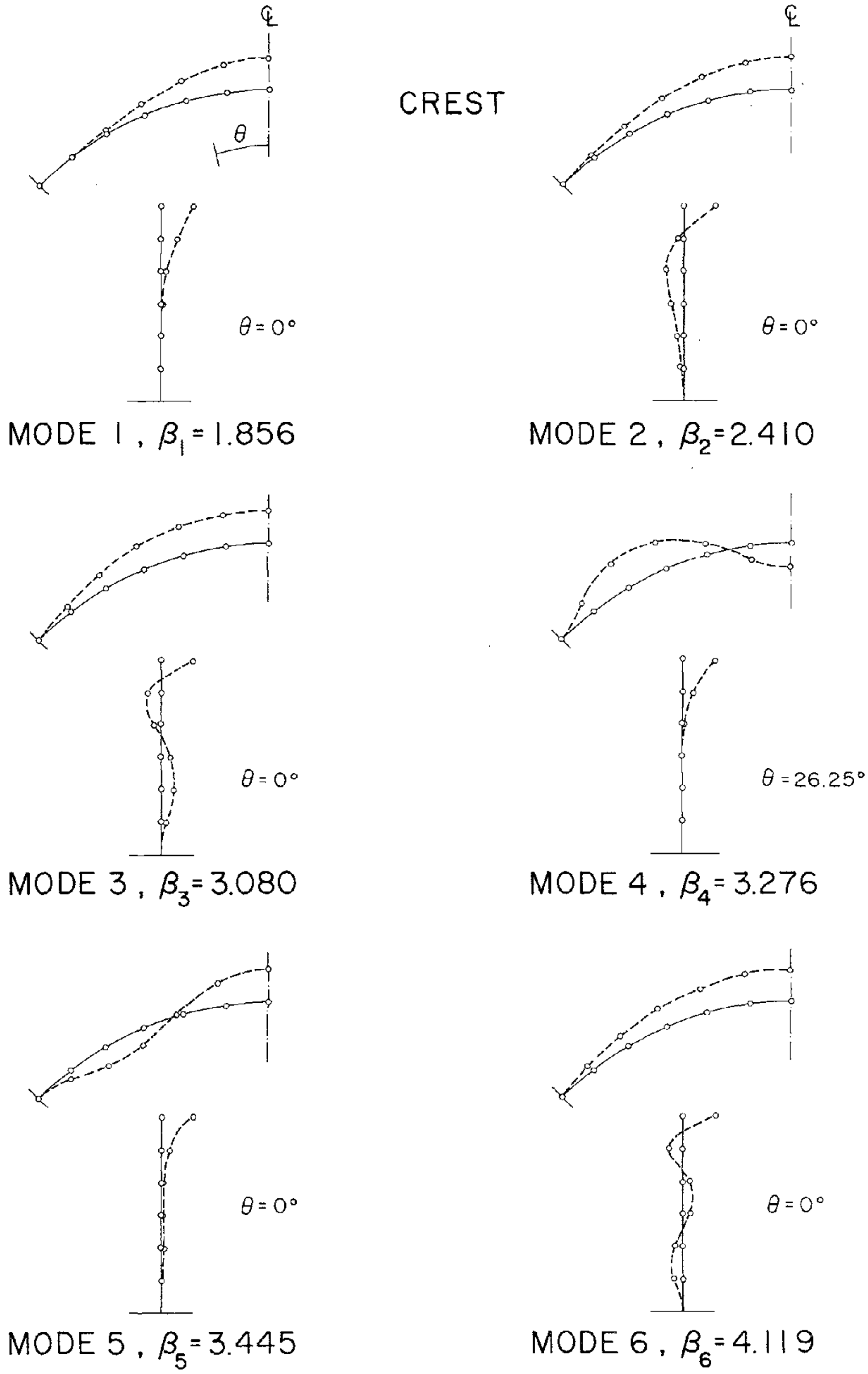

FIG. 7.2 NATURAL FREQUENCIES AND SHAPES OF SYMMETRIC VIBRATION MODES OF ARCH DAMS WITH $R/H_d = 0.5$. FREQUENCY OF j^{th} MODE $\omega_j = (\beta_j/H_d)\sqrt{gE/w_d}$

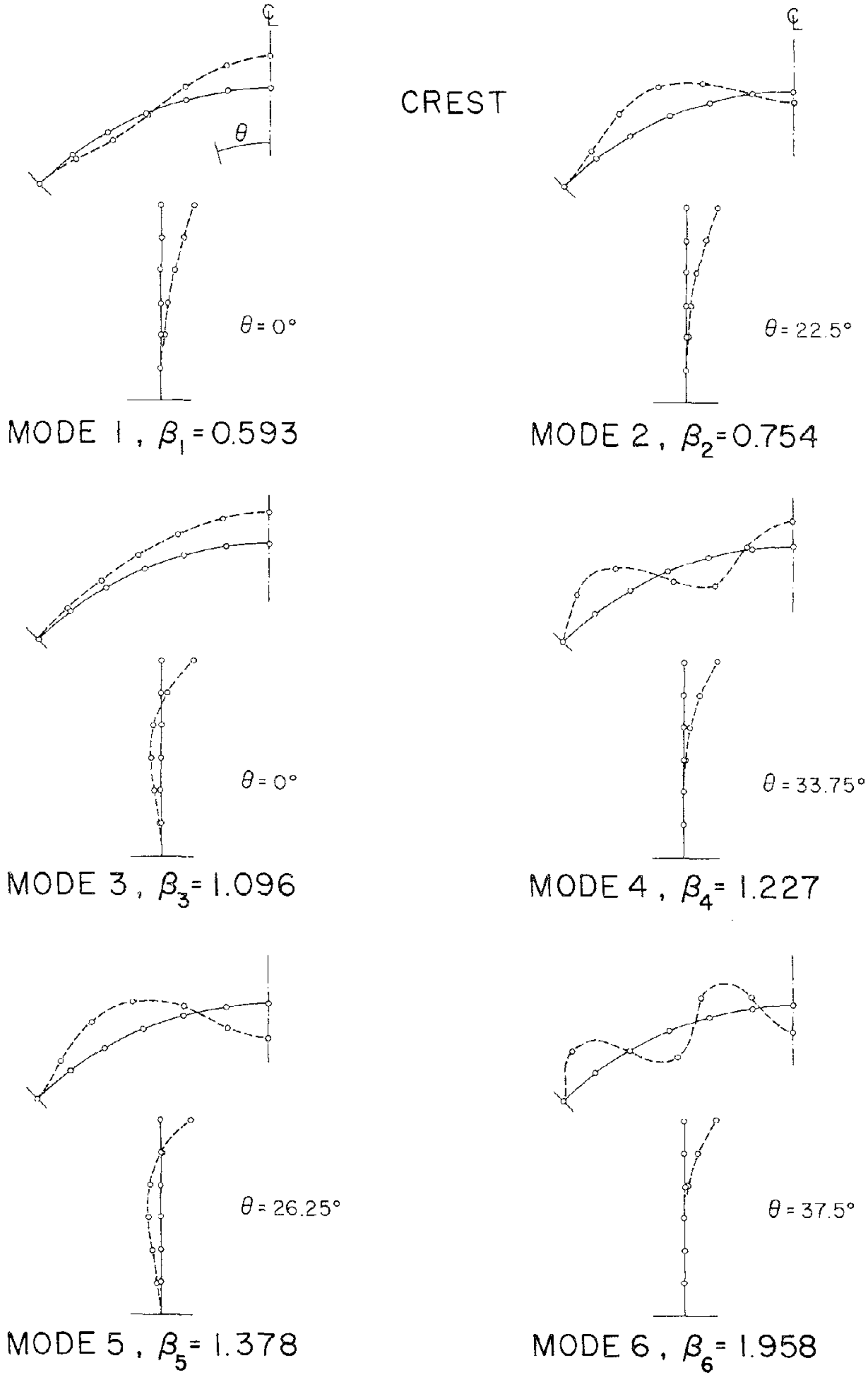

FIG. 7.3 NATURAL FREQUENCIES AND SHAPES OF SYMMETRIC VIBRATION MODES OF ARCH DAMS WITH $R/H_d = 1.5$. FREQUENCY OF j^{th} MODE $\omega_j = (\beta_j/H_d)\sqrt{gE/w_d}$

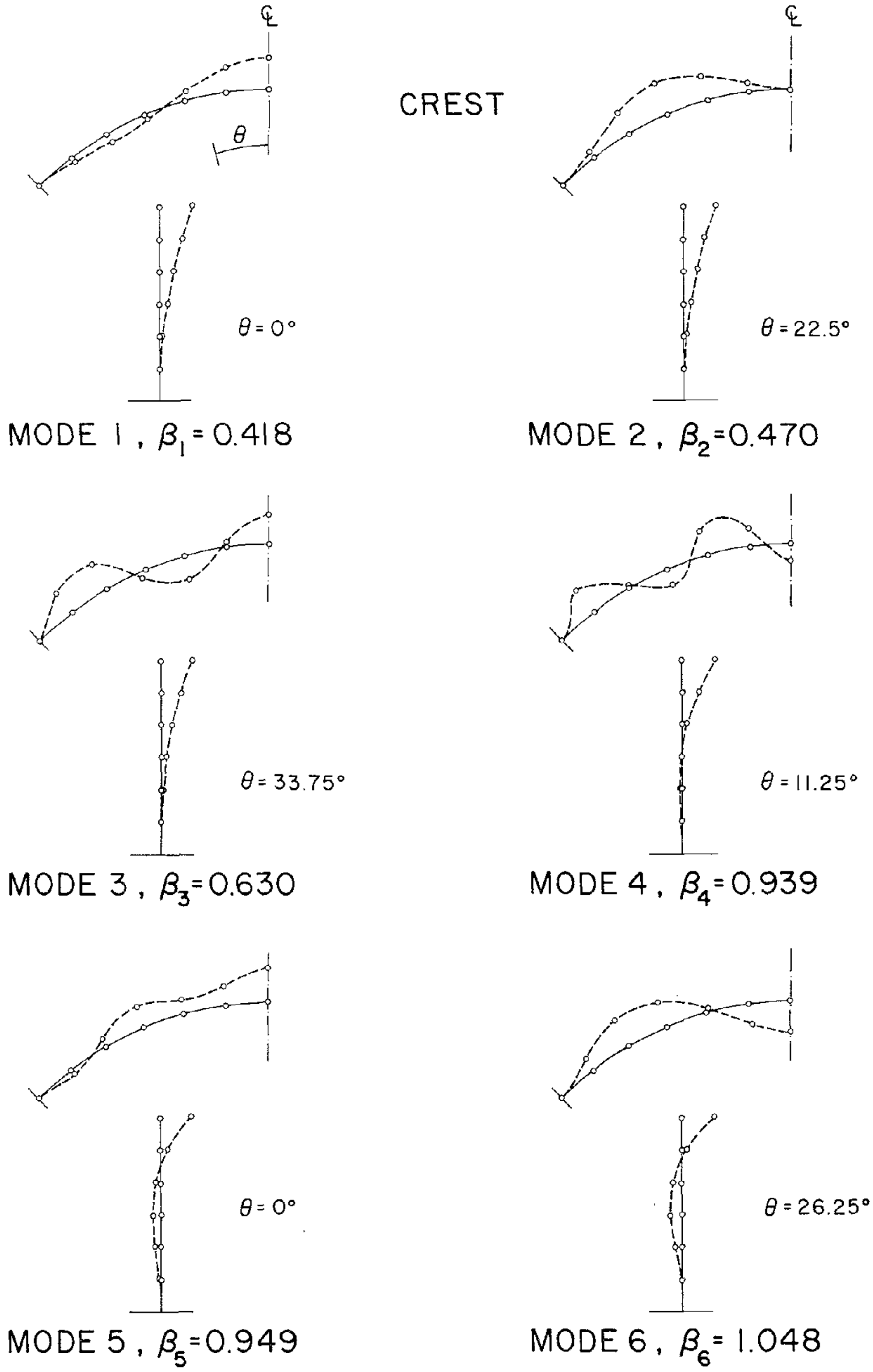

FIG. 7.4 NATURAL FREQUENCIES AND SHAPES OF SYMMETRIC VIBRATION MODES OF ARCH DAMS WITH $R/H_d = 2.5$. FREQUENCY OF j^{th} MODE $\omega_j = (\beta_j/H_d)\sqrt{gE/w_d}$

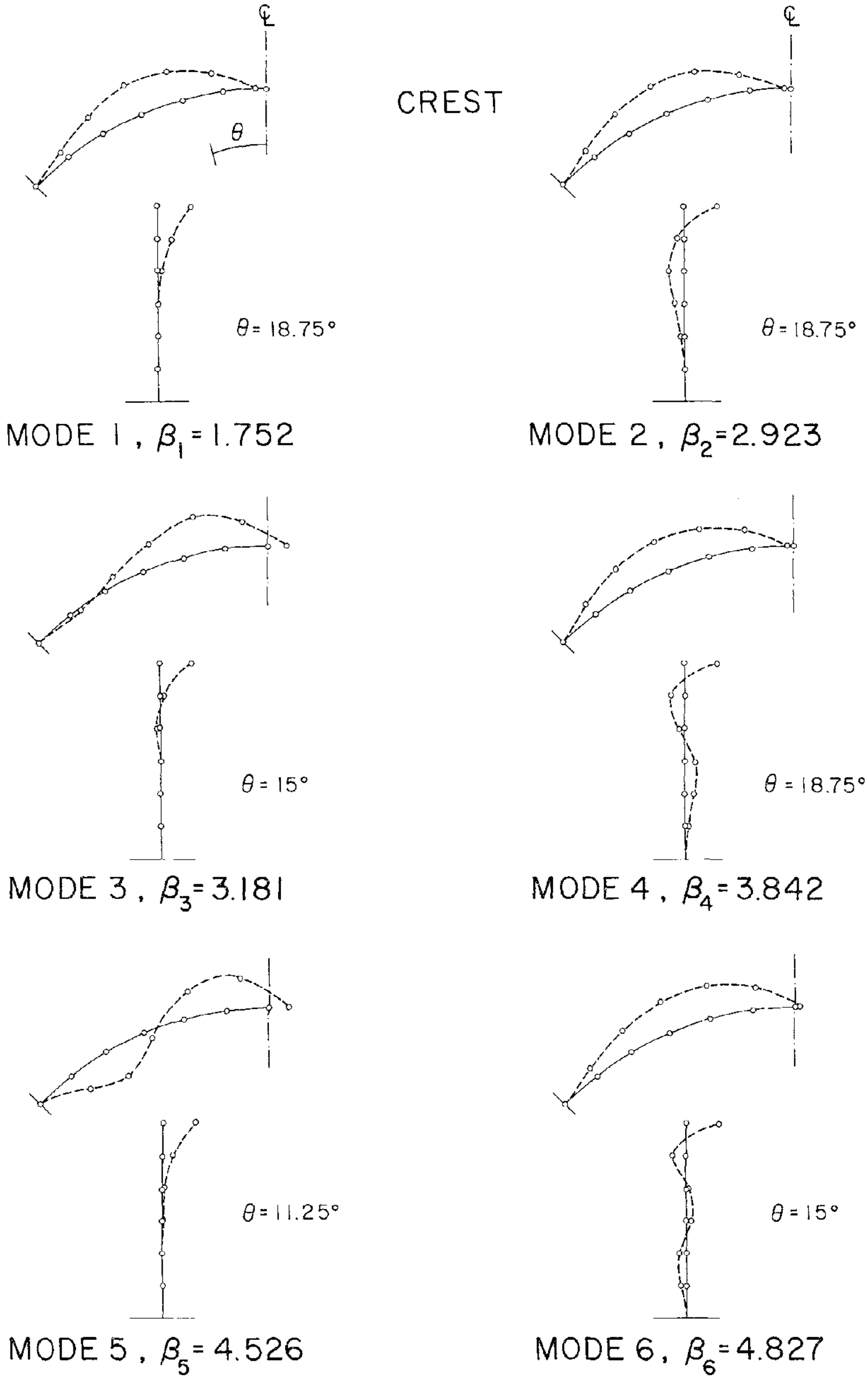

FIG. 7.5 NATURAL FREQUENCIES AND SHAPES OF ANTISYMMETRIC VIBRATION MODES OF ARCH DAMS WITH $R/H_d = 0.5$. FREQUENCY OF j^{th} MODE $\omega_j = (\beta_j/H_d)\ \sqrt{gE/w_d}$

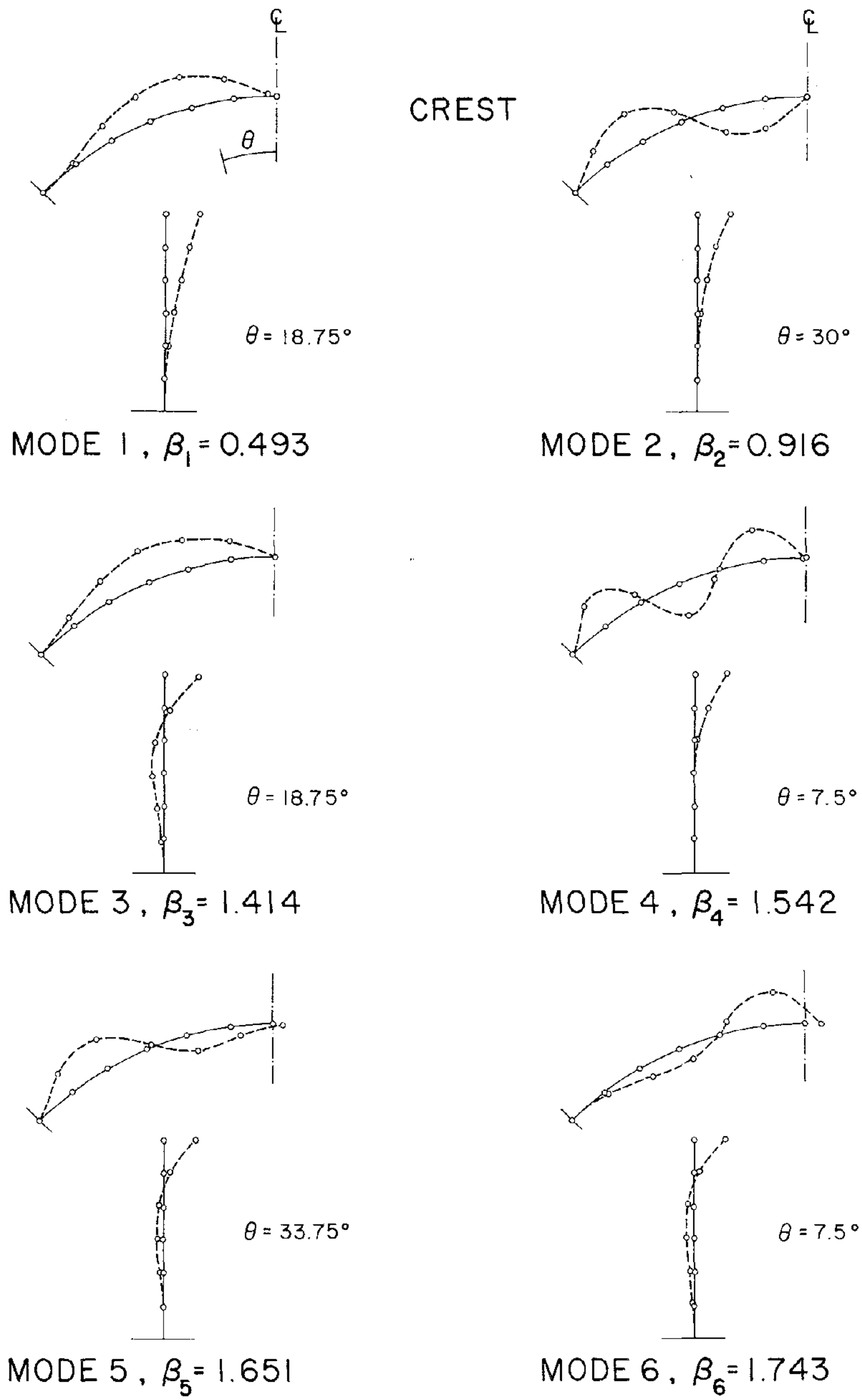

FIG. 7.6 NATURAL FREQUENCIES AND SHAPES OF ANTISYMMETRIC VIBRATION MODES OF ARCH DAMS WITH $R/H_d = 1.5$. FREQUENCY OF j^{th} MODE $\omega_j = (\beta_j/H_d)\sqrt{gE/w_d}$

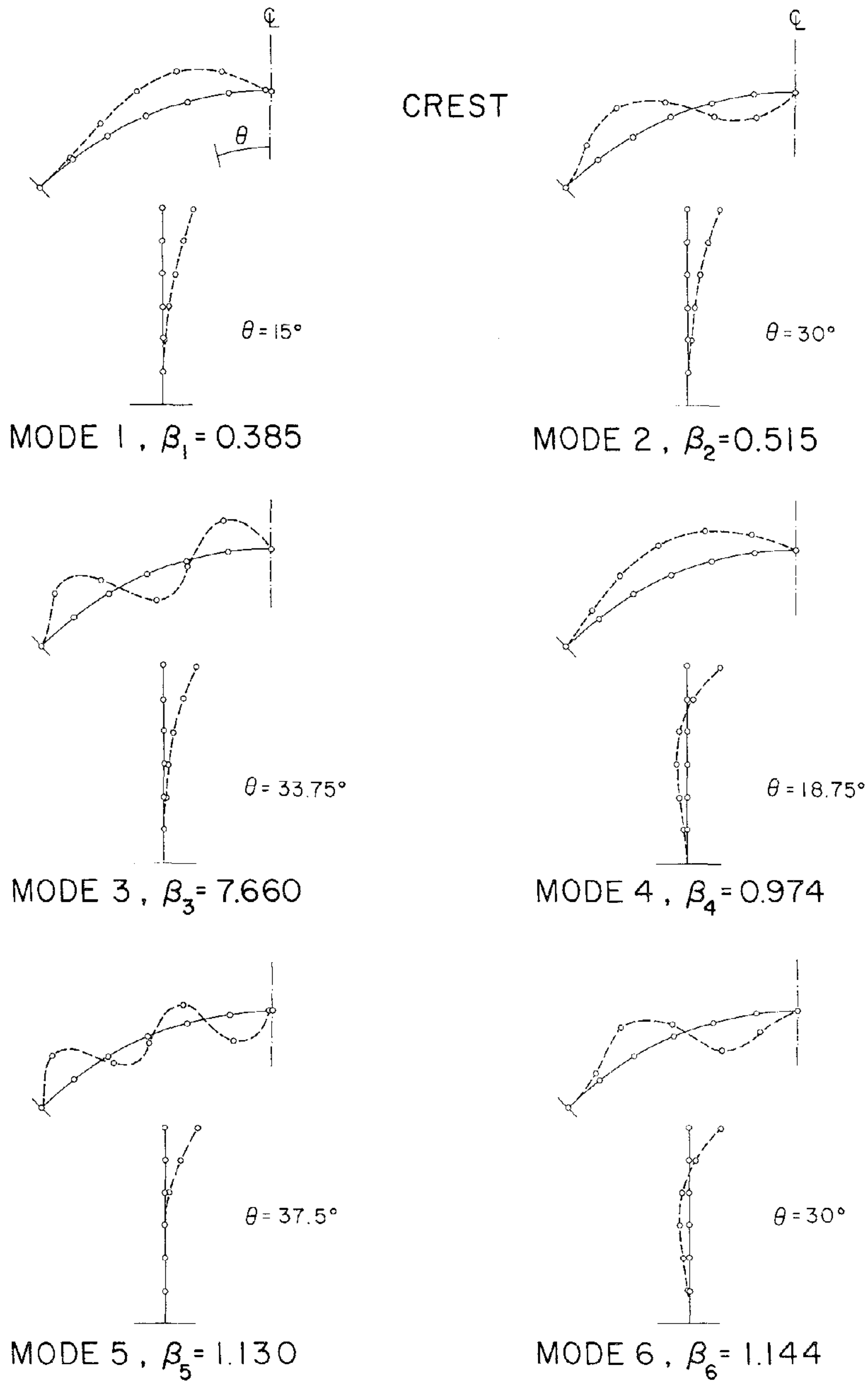

FIG. 7.7 NATURAL FREQUENCIES AND SHAPES OF ANTISYMMETRIC VIBRATION MODES OF ARCH DAMS WITH $R/H_d = 2.5$. FREQUENCY OF j^{th} MODE $\omega_j = (\beta_j/H_d)\sqrt{gE/w_d}$

plotted over the depth at the particular value of θ where the mode shape attains its maximum value. Because the mode shapes are either symmetric or antisymmetric about the x-z (θ=0) plane, they are displayed over only half the dam. Similar to Eq. 7.1, the natural frequencies associated with each mode are shown in dimensionless form. The mode shapes apply to a dam of any height, modulus of elasticity and density, provided it has the same idealized geometry, same value of R/H_d, and same Poisson's ratio for which the results have been presented.

It is seen from Figs. 7.2 - 7.7 that the vibration frequencies and mode shapes change significantly with R/H_d. In particular, the fundamental frequency decreases as R/H_d increases. The vibration mode shapes may be visualized as a combination of vibration modes of the crest arch and of vertical cantilevers fixed at the base of the dam. For example, the sixth symmetric mode for dams with R/H_d = 0.5 (Fig. 7.2) can be described as a combination of the first arch mode and the fourth cantilever mode.

Dams with the smallest R/H_d are relatively stiff in the arch direction compared to the cantilever direction. Thus, the first arch mode combines with three cantilever modes to produce the first three vibration modes of the dam (Figs. 7.2 and 7.5). In contrast, dams with the largest R/H_d are relatively flexible in the arch direction compared to the cantilever direction. As a result, the first cantilever mode combines with three arch modes to produce the first three vibration modes of the dam (Figs. 7.4 and 7.7).

7.4 Presentation of Response Results

In order to identify the effects of the impounded water on the dynamic response of dams, each of the three dams (Section 7.3.1) is analyzed for three conditions: the dam alone without water ($H/H_d = 0$), and the dam with water at a depth equal to the dam height ($H/H_d = 1$) considering water as compressible in one case and neglecting water compressibility effects in another case. The response of the dam to the three components of ground motion -- upstream-downstream component, cross-stream component, and vertical component -- was analyzed by the procedures of Chapters 4, 5, and 6, respectively.

For the symmetric dam-reservoir systems considered in this work, the natural modes of symmetric vibration of the dam are excited by ground motions in the upstream-downstream and vertical directions; whereas the antisymmetric modes are excited by cross stream ground motion. Considering the first ten natural modes of vibration, symmetric or antisymmetric as appropriate, the response of the three arch dams described in Section 7.3.1 to harmonic ground acceleration in each of the three directions, applied individually, was computed.

The acceleration response at selected locations on the crest of the three dams are presented in Figs. 7.8 to 7.31. The responses to upstream-downstream ground motion are presented in Figs. 7.8 to 7.16, to cross-stream ground motion in Figs. 7.17 to 7.25, and to vertical ground motion in Figs. 7.26 to 7.31. In each figure, the absolute value or modulus of the complex frequency response function for crest acceleration is plotted against the excitation frequency normalized relative to the fundamental natural frequency of the dam, in symmetric or antisymmetric vibration as appropriate. When presented in this form, the plots apply to dams of any height with the properties specified in Section 7.3.1. Furthermore, the response results excluding hydrodynamic effects or neglecting compressibility of water are independent of the

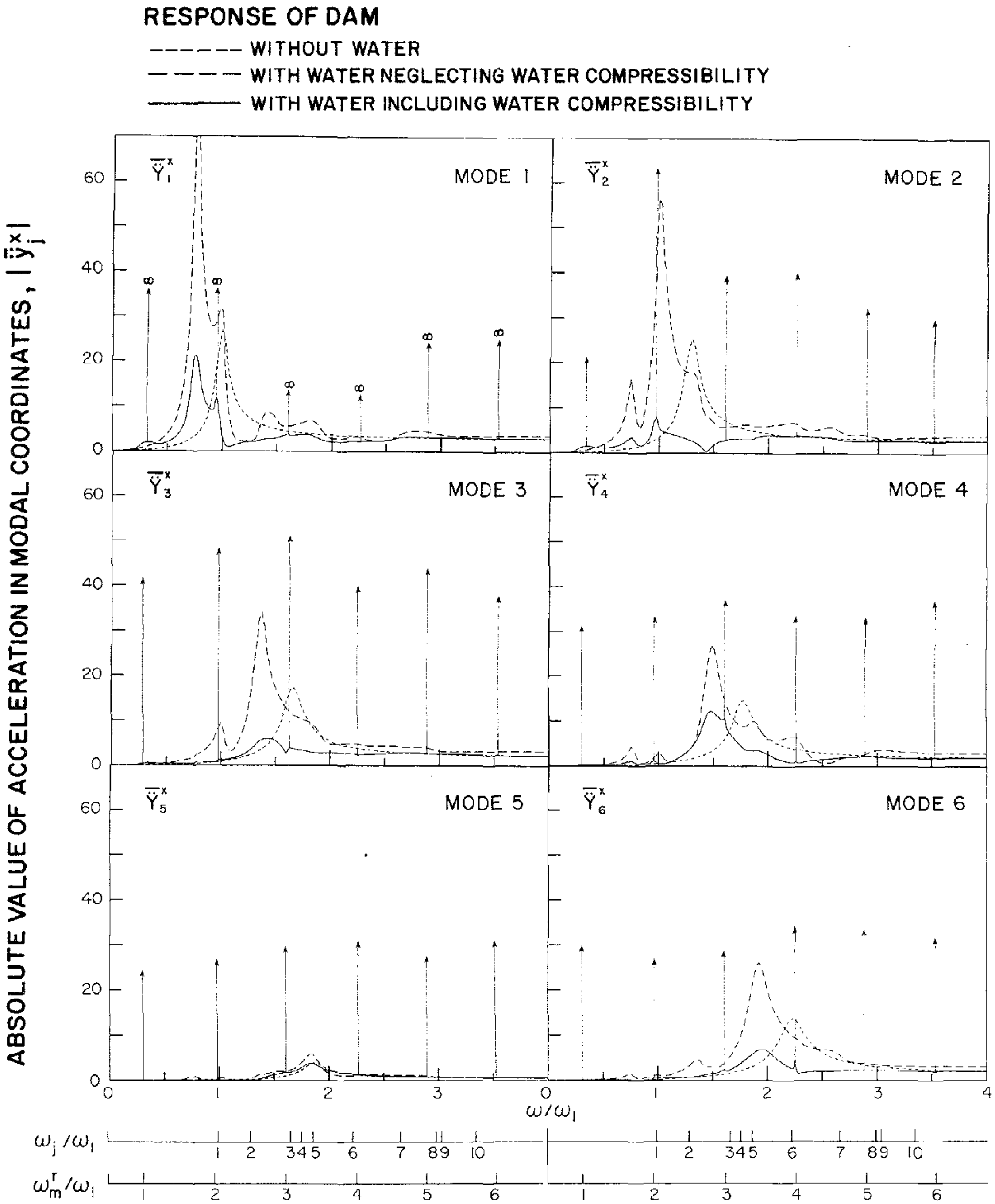

FIG. 7.8 COMPLEX FREQUENCY RESPONSES IN MODAL COORDINATES DUE TO UPSTREAM-DOWNSTREAM GROUND MOTION. RESULTS ARE FOR ARCH DAMS WITH $R/H_d = 0.5$

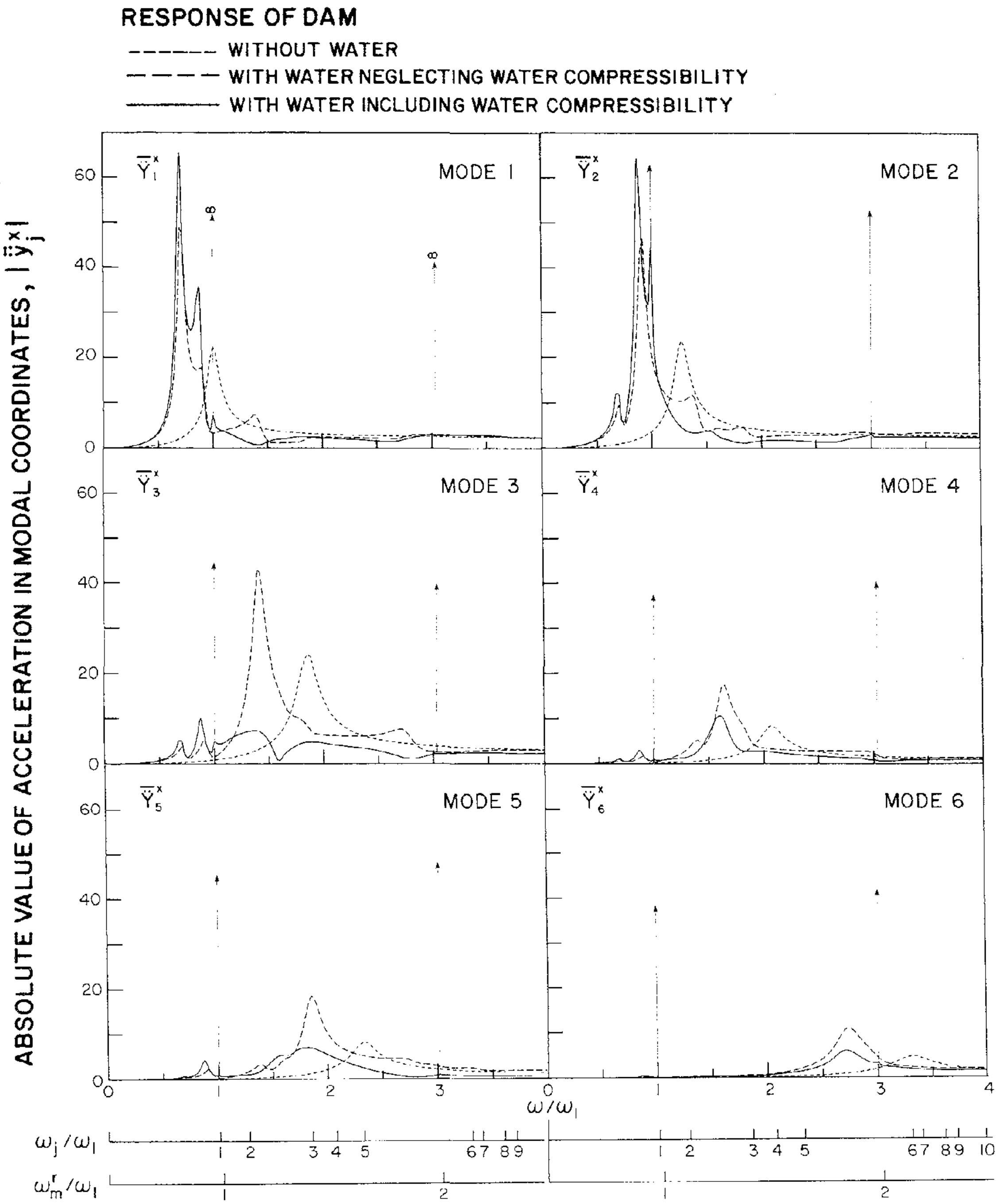

FIG. 7.9 COMPLEX FREQUENCY RESPONSES IN MODAL COORDINATES DUE TO UPSTREAM-DOWNSTREAM GROUND MOTION. RESULTS ARE FOR ARCH DAMS WITH $R/H_d = 1.5$

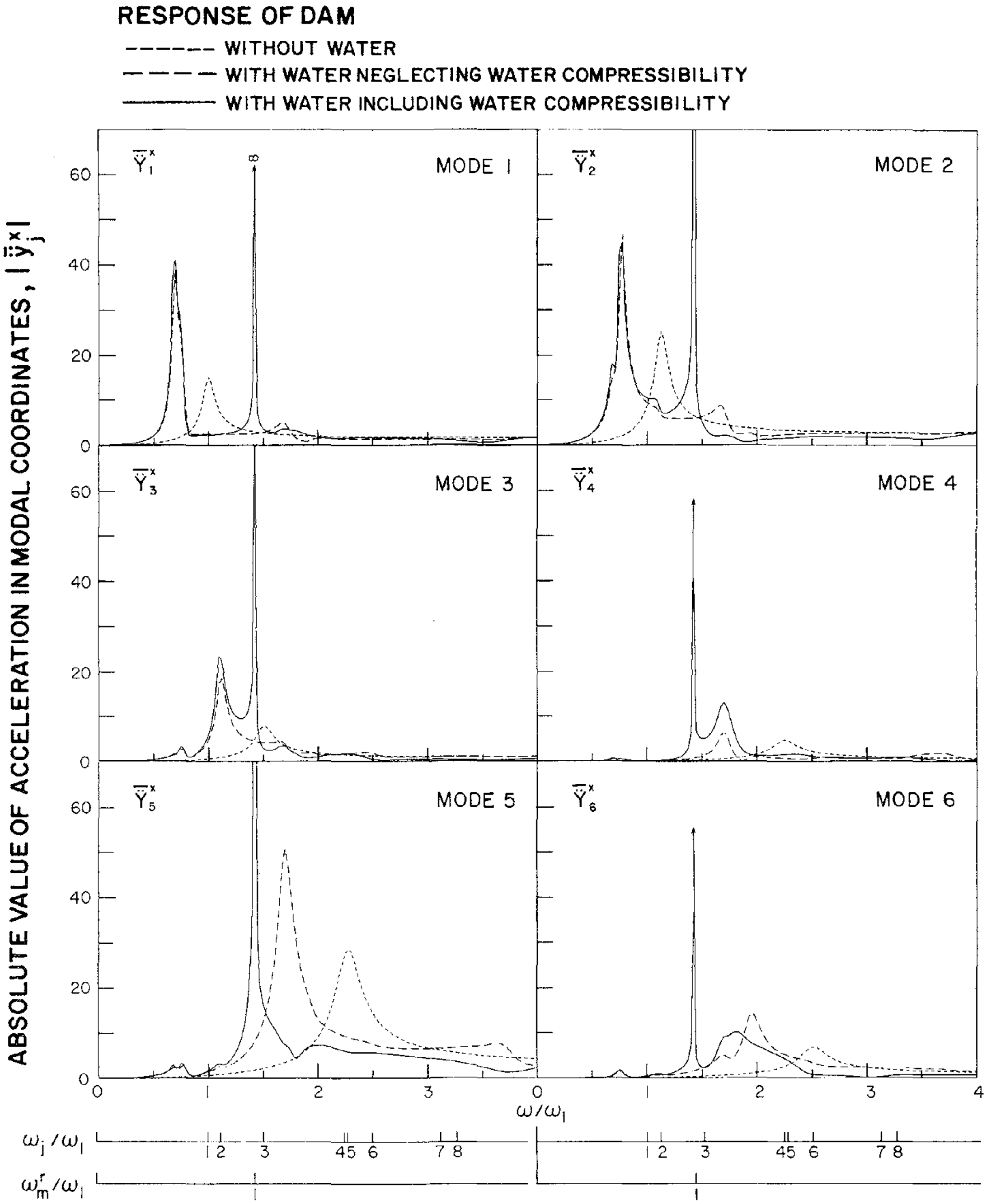

FIG. 7.10 COMPLEX FREQUENCY RESPONSES IN MODAL COORDINATES DUE TO UPSTREAM-DOWNSTREAM GROUND MOTION. RESULTS ARE FOR ARCH DAMS WITH $R/H_d = 2.5$

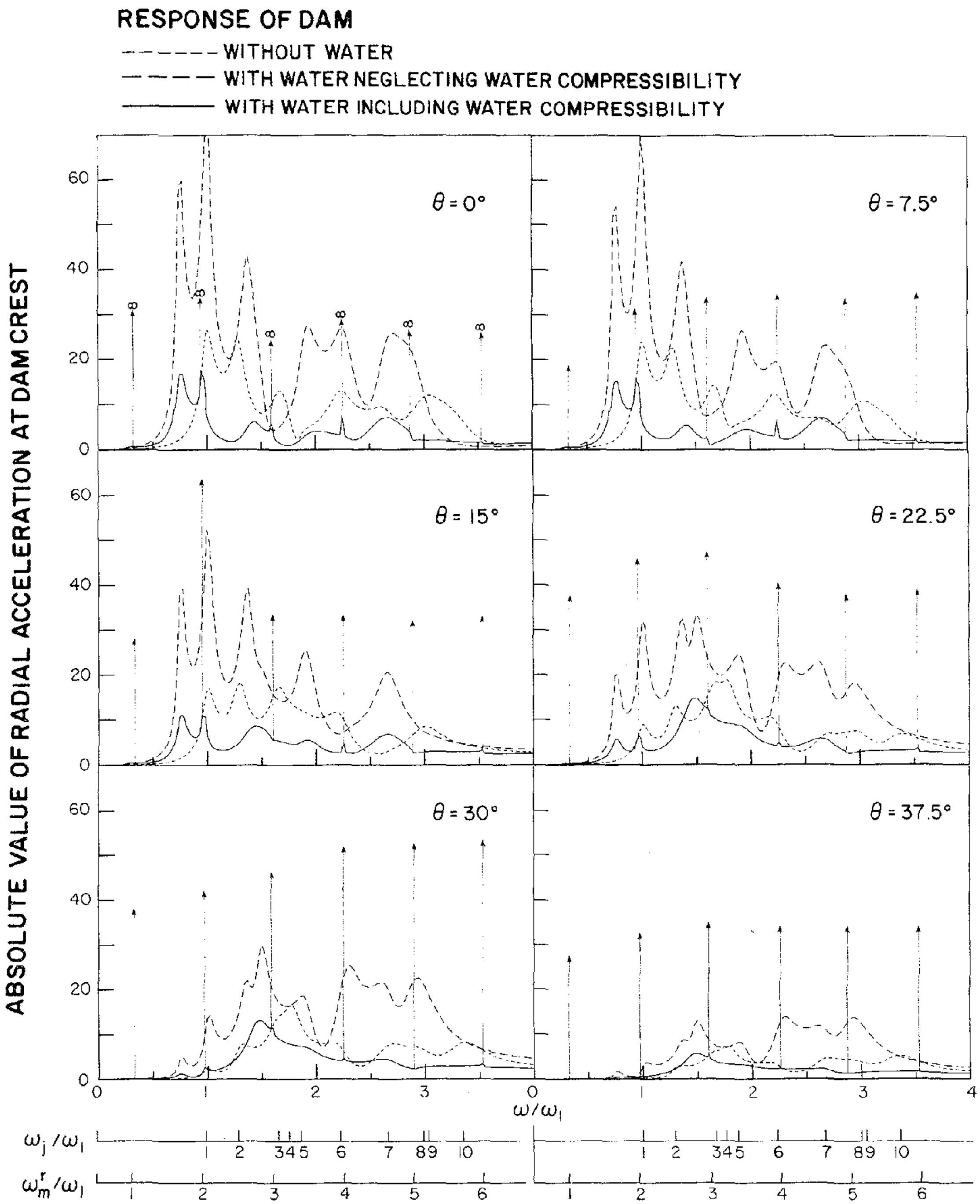

FIG. 7.11 COMPLEX FREQUENCY RESPONSES FOR RADIAL ACCELERATION AT $\Theta = 0^\circ$, 7.5°, 15°, 22.5°, 30°, AND 37.5° ALONG CREST OF THE DAM DUE TO UPSTREAM-DOWNSTREAM GROUND MOTION. RESULTS ARE FOR ARCH DAMS WITH $R/H_d = 0.5$

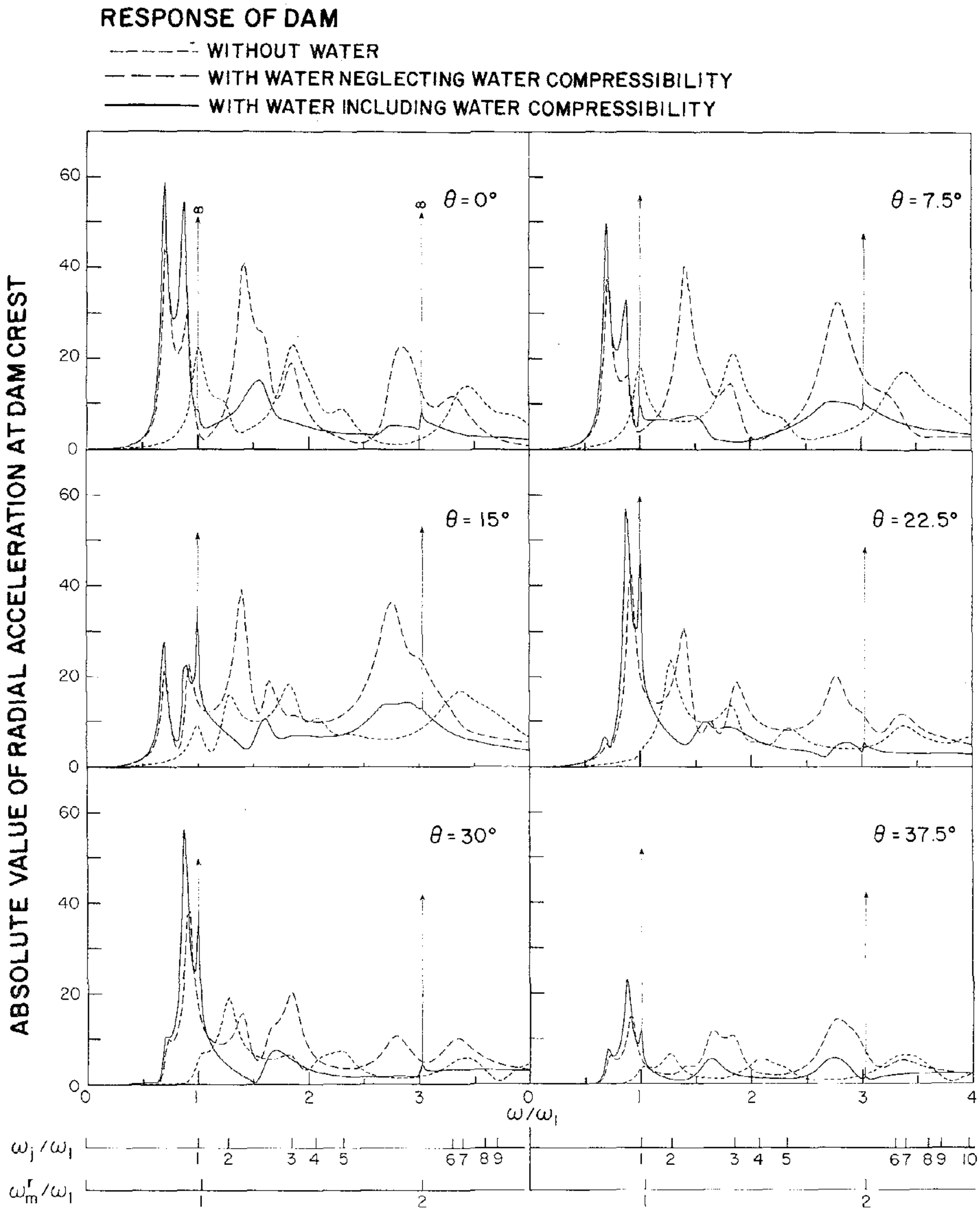

FIG. 7.12 COMPLEX FREQUENCY RESPONSES FOR RADIAL ACCELERATION AT $\theta = 0^{\circ}$, 7.5°, 15°, 22.5°, 30°, AND 37.5° ALONG CREST OF THE DAM DUE TO UPSTREAM-DOWNSTREAM GROUND MOTION. RESULTS ARE FOR ARCH DAMS WITH $R/H_d = 1.5$

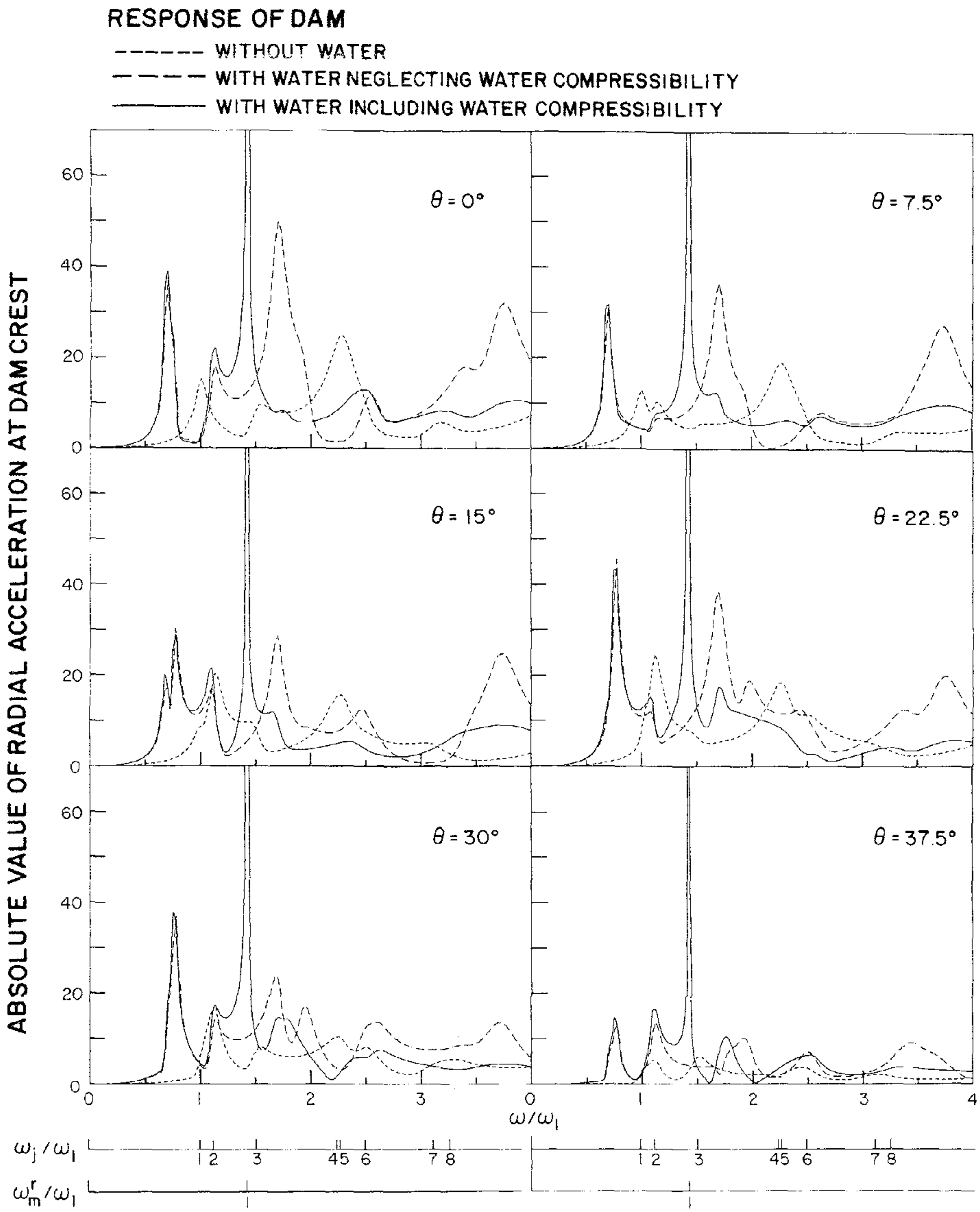

FIG. 7.13 COMPLEX FREQUENCY RESPONSES FOR RADIAL ACCELERATION AT $\Theta = 0^{\circ}$, 7.5°, 15°, 22.5°, 30°, AND 37.5° ALONG CREST OF THE DAM DUE TO UPSTREAM-DOWNSTREAM GROUND MOTION. RESULTS ARE FOR ARCH DAMS WITH $R/H_d = 2.5$

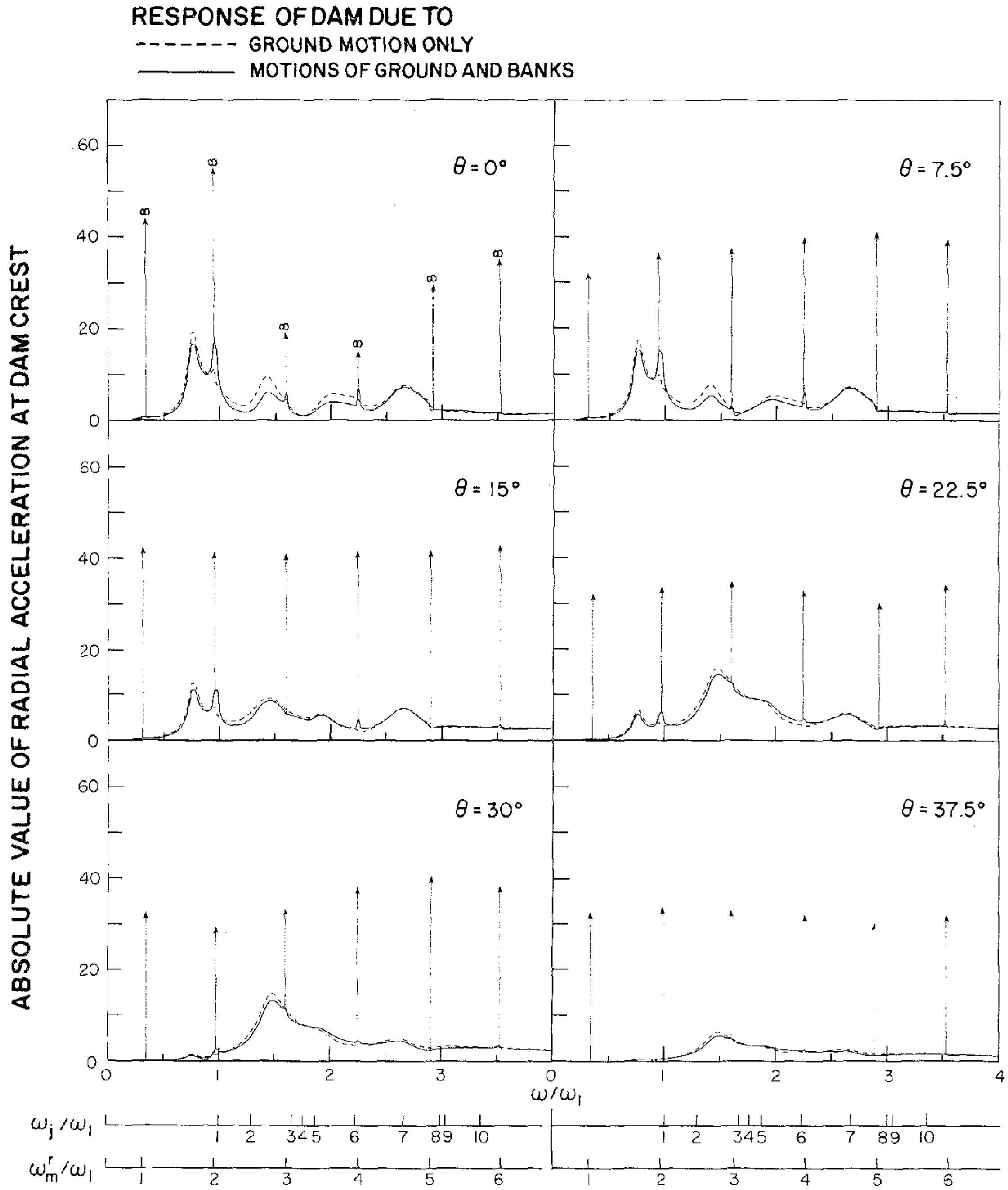

FIG. 7.14 COMPLEX FREQUENCY RESPONSES FOR RADIAL ACCELERATION AT $\Theta = 0^{\circ}$, 7.5°, 15°, 22.5°, 30°, AND 37.5° ALONG CREST OF THE DAM. EXCITATIONS ARE (1) UPSTREAM-DOWNSTREAM GROUND MOTION ONLY, AND (2) UPSTREAM-DOWNSTREAM MOTIONS OF GROUND AND BANKS. RESULTS ARE FOR ARCH DAMS WITH $R/H_d = 0.5$

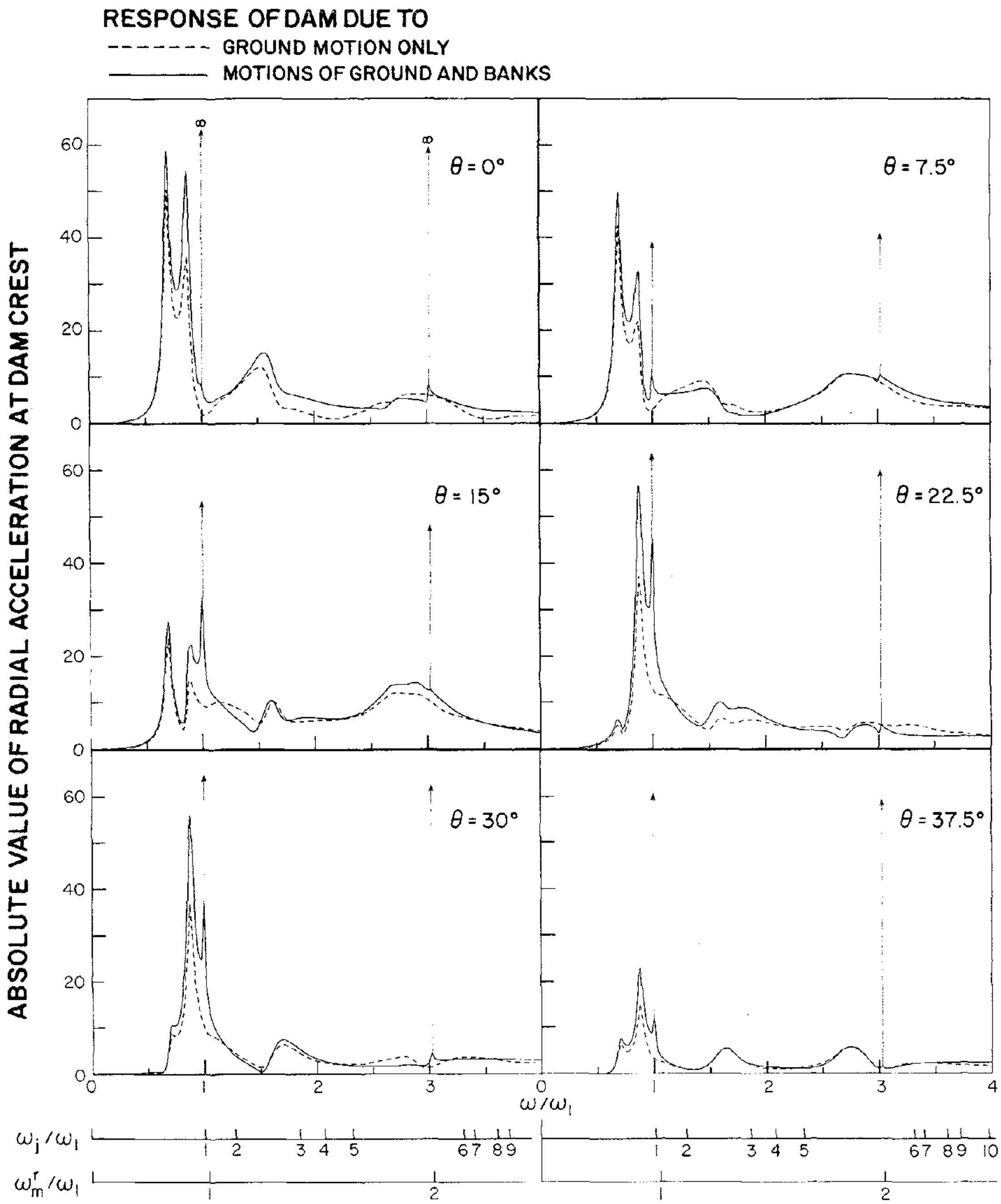

FIG. 7.15 COMPLEX FREQUENCY RESPONSES FOR RADIAL ACCELERATION AT $\Theta = 0^\circ$, 7.5°, 15°, 22.5°, 30°, AND 37.5° ALONG CREST OF THE DAM. EXCITATIONS ARE (1) UPSTREAM-DOWNSTREAM GROUND MOTION ONLY, AND (2) UPSTREAM-DOWNSTREAM MOTIONS OF GROUND AND BANKS. RESULTS ARE FOR ARCH DAMS WITH $R/H_d = 1.5$

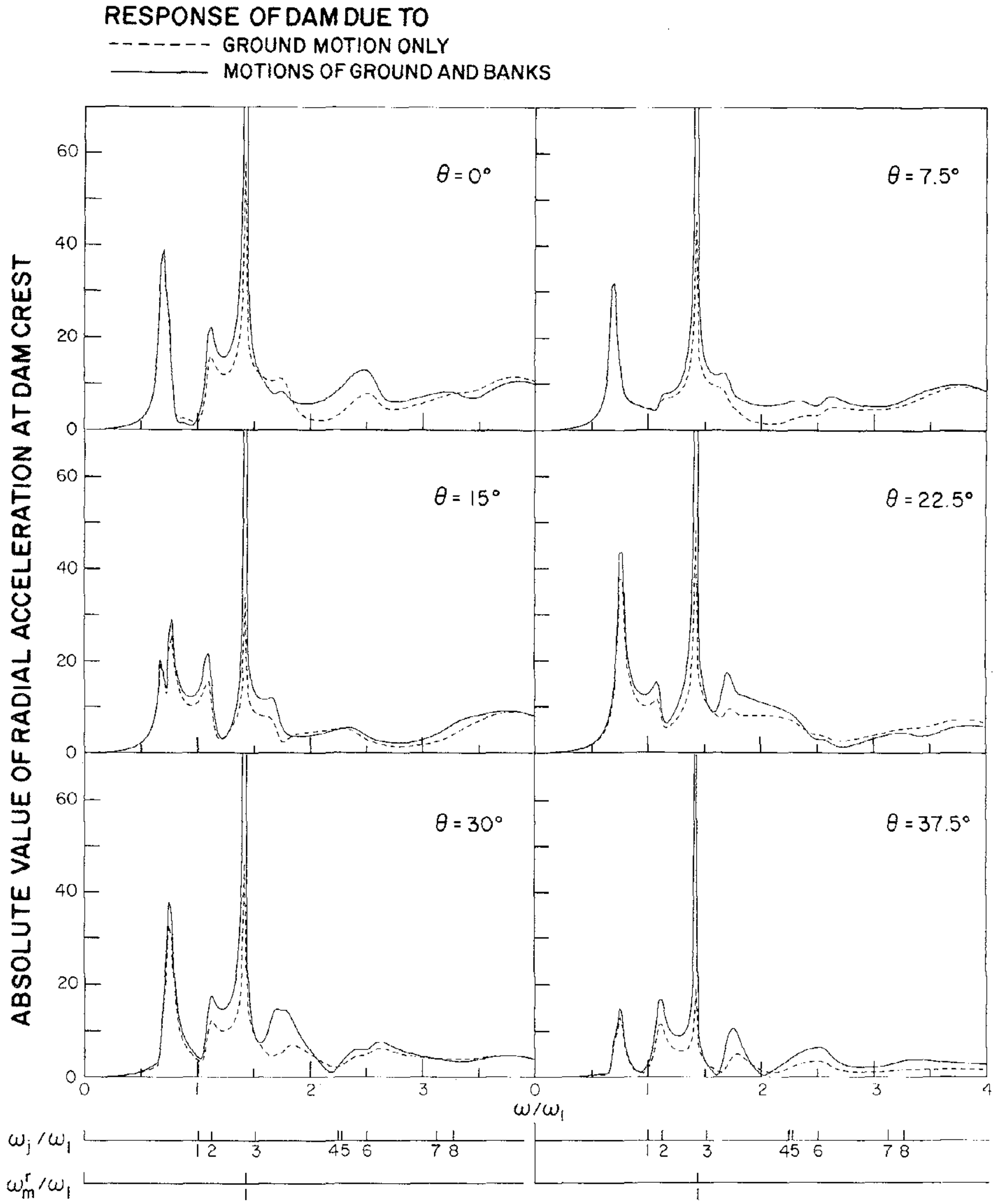

FIG. 7.16 COMPLEX FREQUENCY RESPONSES FOR RADIAL ACCELERATION AT $\Theta = 0^{\circ}, 7.5^{\circ}, 15^{\circ}, 22.5^{\circ}, 30^{\circ}$, AND 37.5° ALONG CREST OF THE DAM. EXCITATIONS ARE (1) UPSTREAM-DOWNSTREAM GROUND MOTION ONLY, AND (2) UPSTREAM-DOWNSTREAM MOTIONS OF GROUND AND BANKS. RESULTS ARE FOR ARCH DAMS WITH $R/H_d = 2.5$

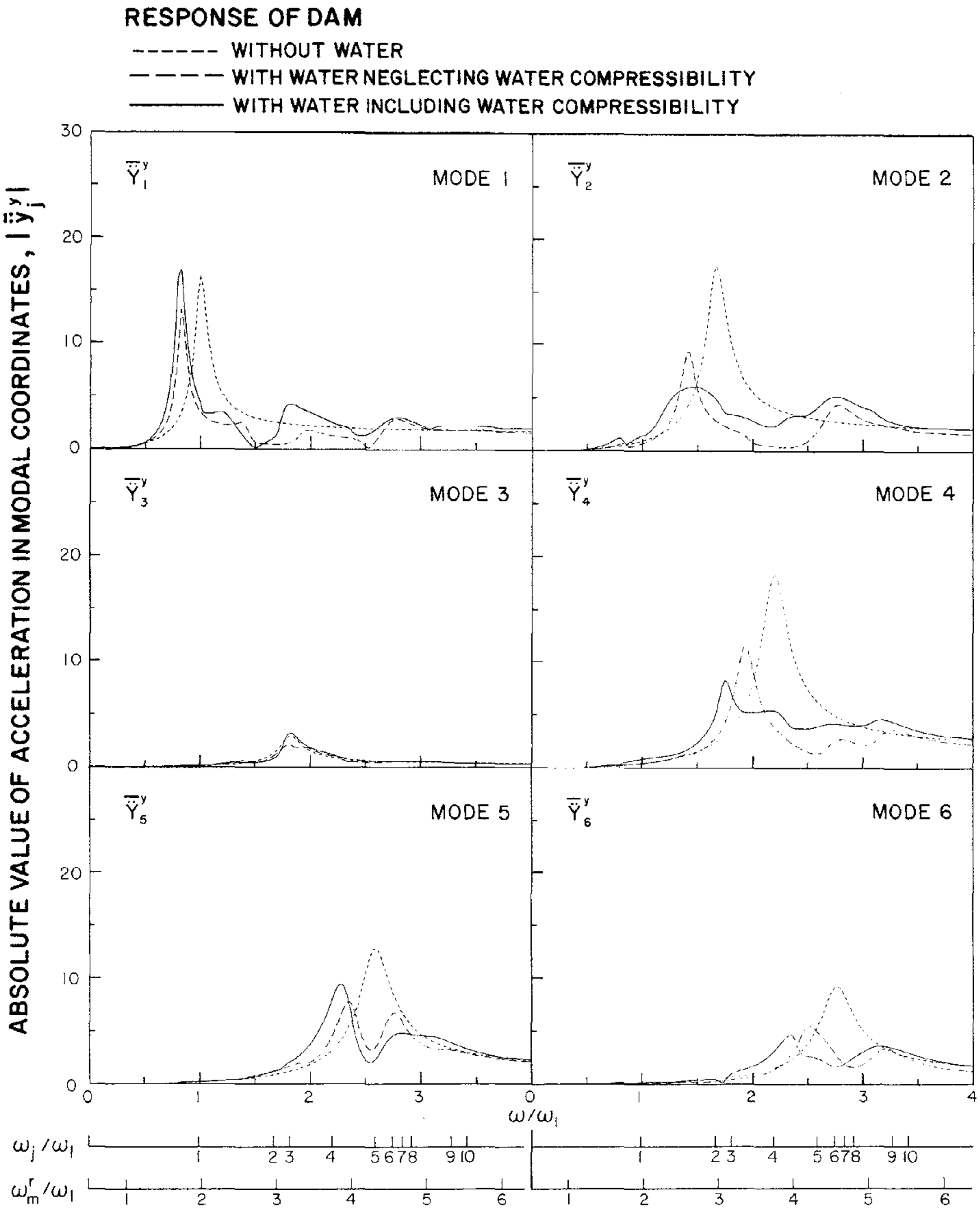

FIG. 7.17 COMPLEX FREQUENCY RESPONSES IN MODAL COORDINATES DUE TO CROSS-STREAM GROUND MOTION. RESULTS ARE FOR ARCH DAMS WITH $R/H_d = 0.5$

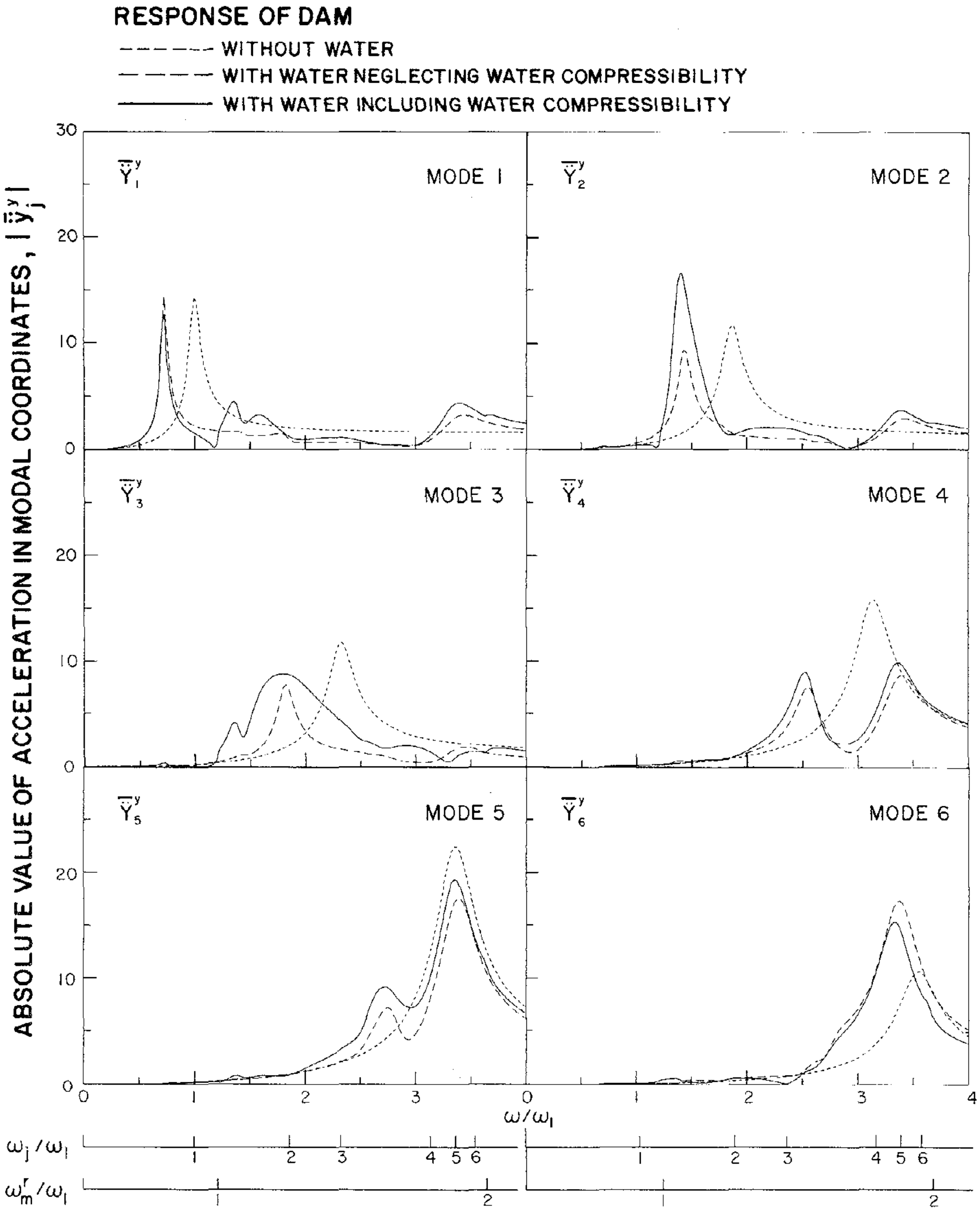

FIG. 7.18 COMPLEX FREQUENCY RESPONSES IN MODAL COORDINATES DUE TO CROSS-STREAM GROUND MOTION. RESULTS ARE FOR ARCH DAMS WITH $R/H_d = 1.5$

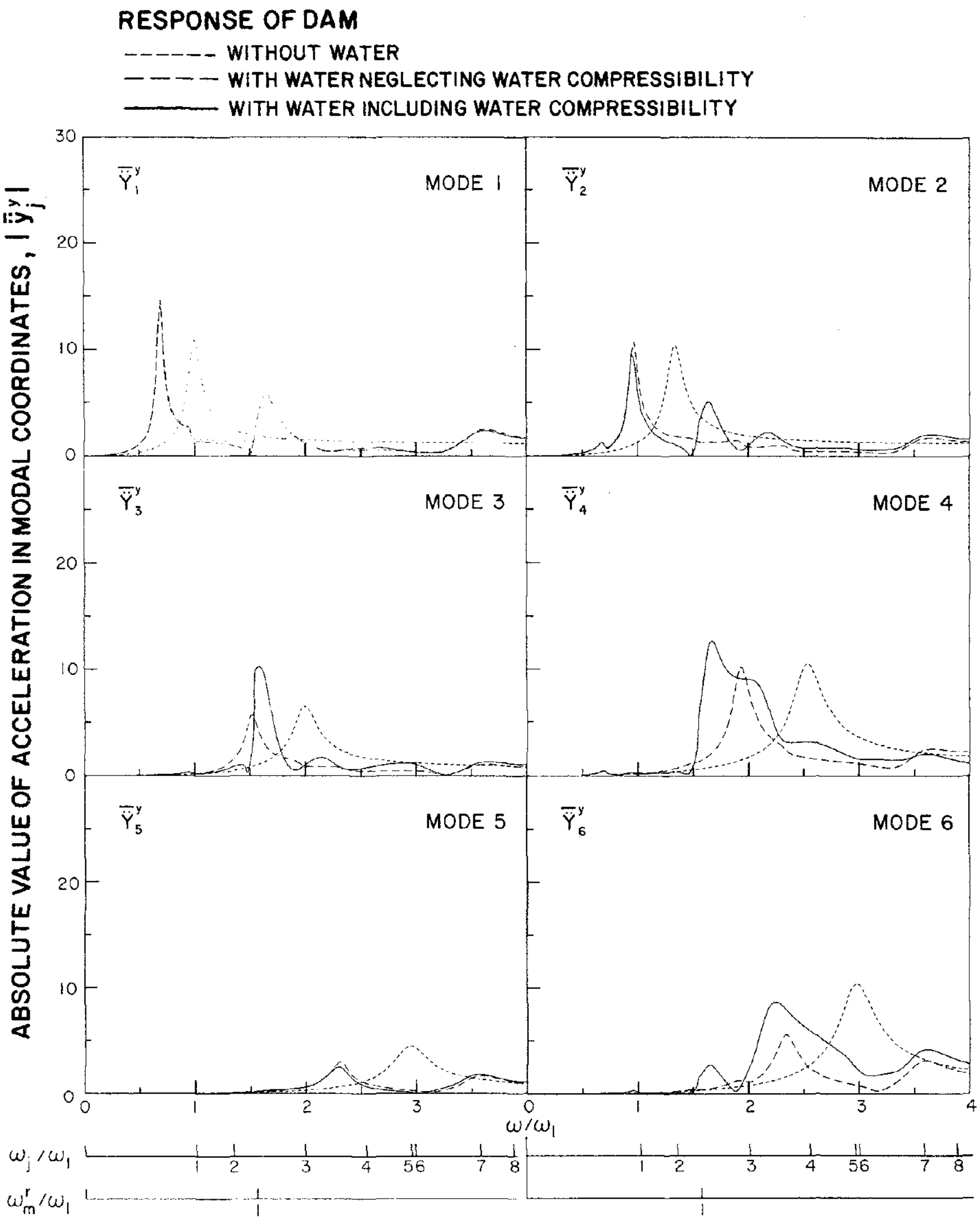

FIG. 7.19 COMPLEX FREQUENCY RESPONSES IN MODAL COORDINATES DUE TO CROSS-STREAM GROUND MOTION. RESULTS ARE FOR ARCH DAMS WITH $R/H_d = 2.5$

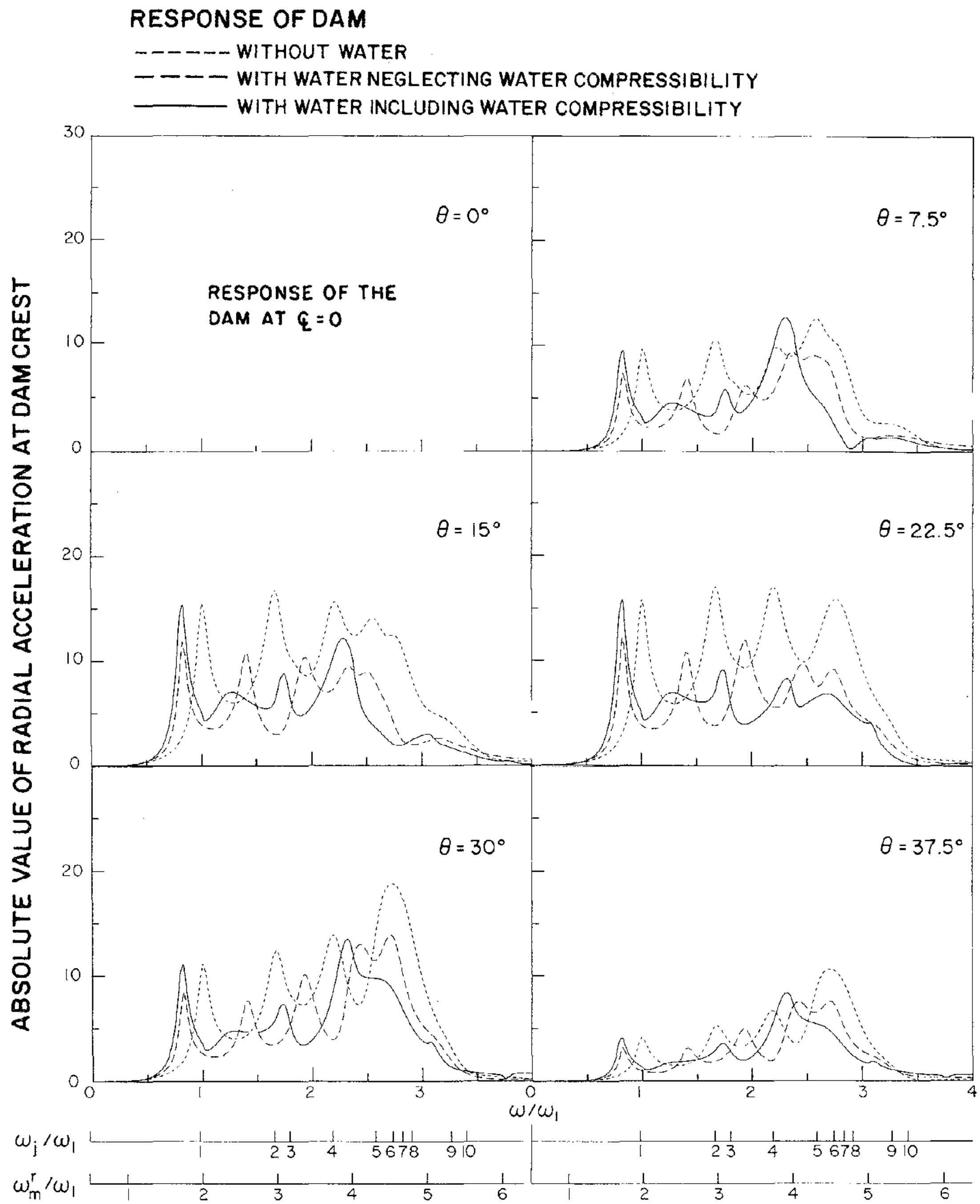

FIG. 7.20 COMPLEX FREQUENCY RESPONSES FOR RADIAL ACCELERATION AT $\Theta = 7.5^{\circ}$, 15°, 22.5°, 30°, AND 37.5° ALONG CREST OF THE DAM DUE TO CROSS-STREAM GROUND MOTION. RESULTS ARE FOR ARCH DAMS WITH $R/H_d = 0.5$

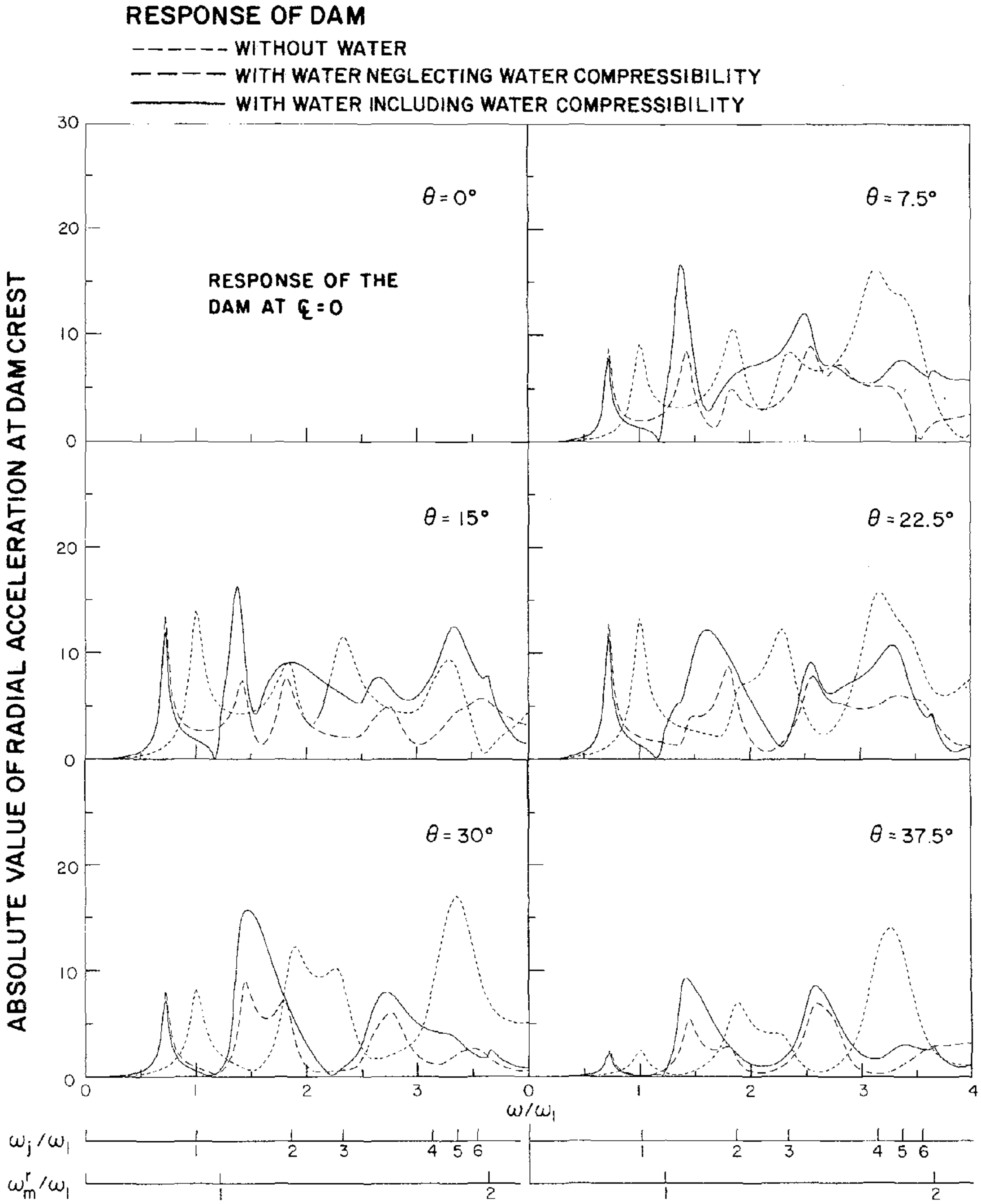

FIG. 7.21 COMPLEX FREQUENCY RESPONSES FOR RADIAL ACCELERATION AT $\Theta = 7.5^{\circ}$, 15°, 22.5°, 30°, AND 37.5° ALONG CREST OF THE DAM DUE TO CROSS-STREAM GROUND MOTION. RESULTS ARE FOR ARCH DAMS WITH $R/H_d = 1.5$

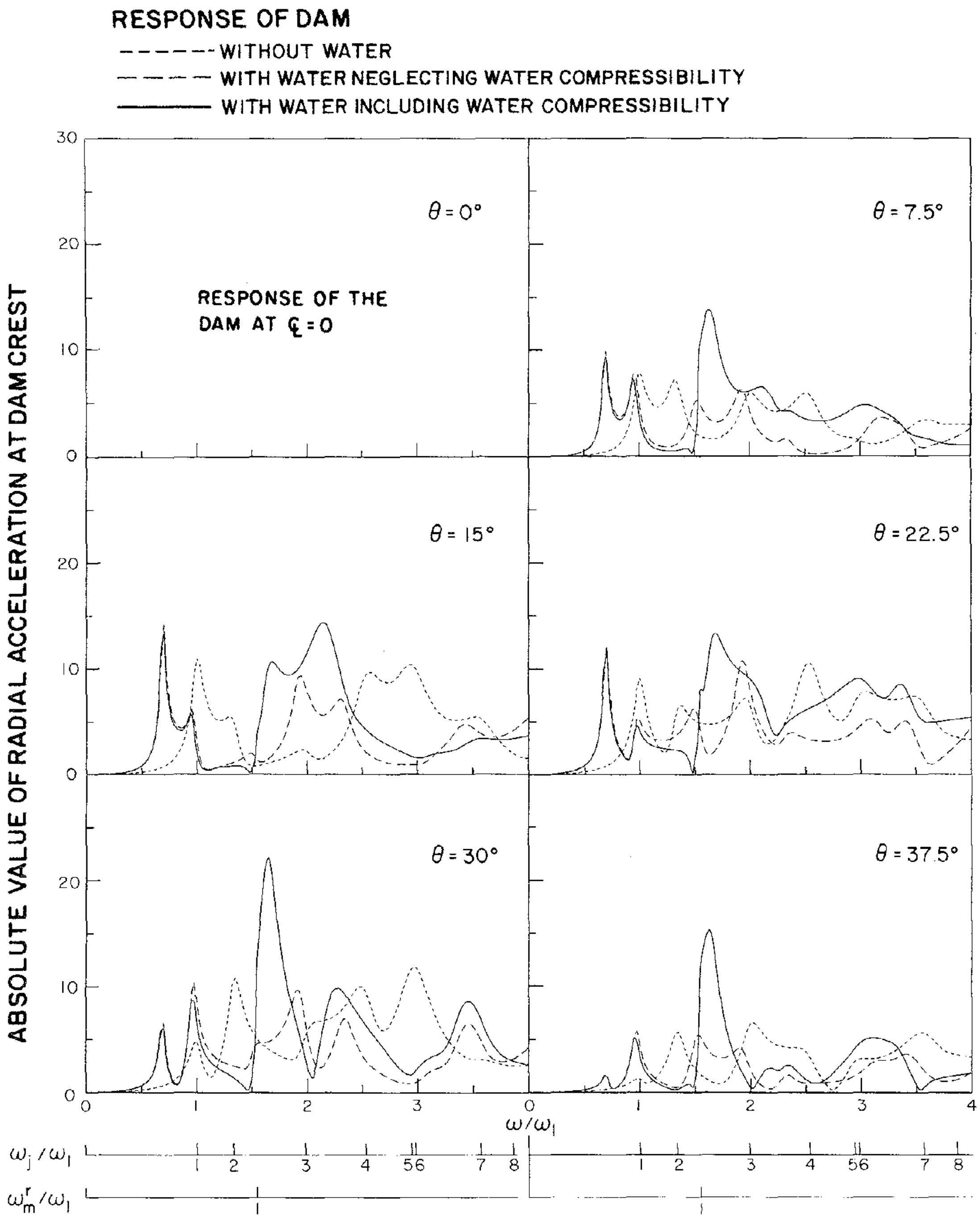

FIG. 7.22 COMPLEX FREQUENCY RESPONSES FOR RADIAL ACCELERATION AT $\theta = 7.5^\circ, 15^\circ, 22.5^\circ, 30^\circ$, AND 37.5° ALONG CREST OF THE DAM DUE TO CROSS-STREAM GROUND MOTION. RESULTS ARE FOR ARCH DAMS WITH $R/H_d = 2.5$

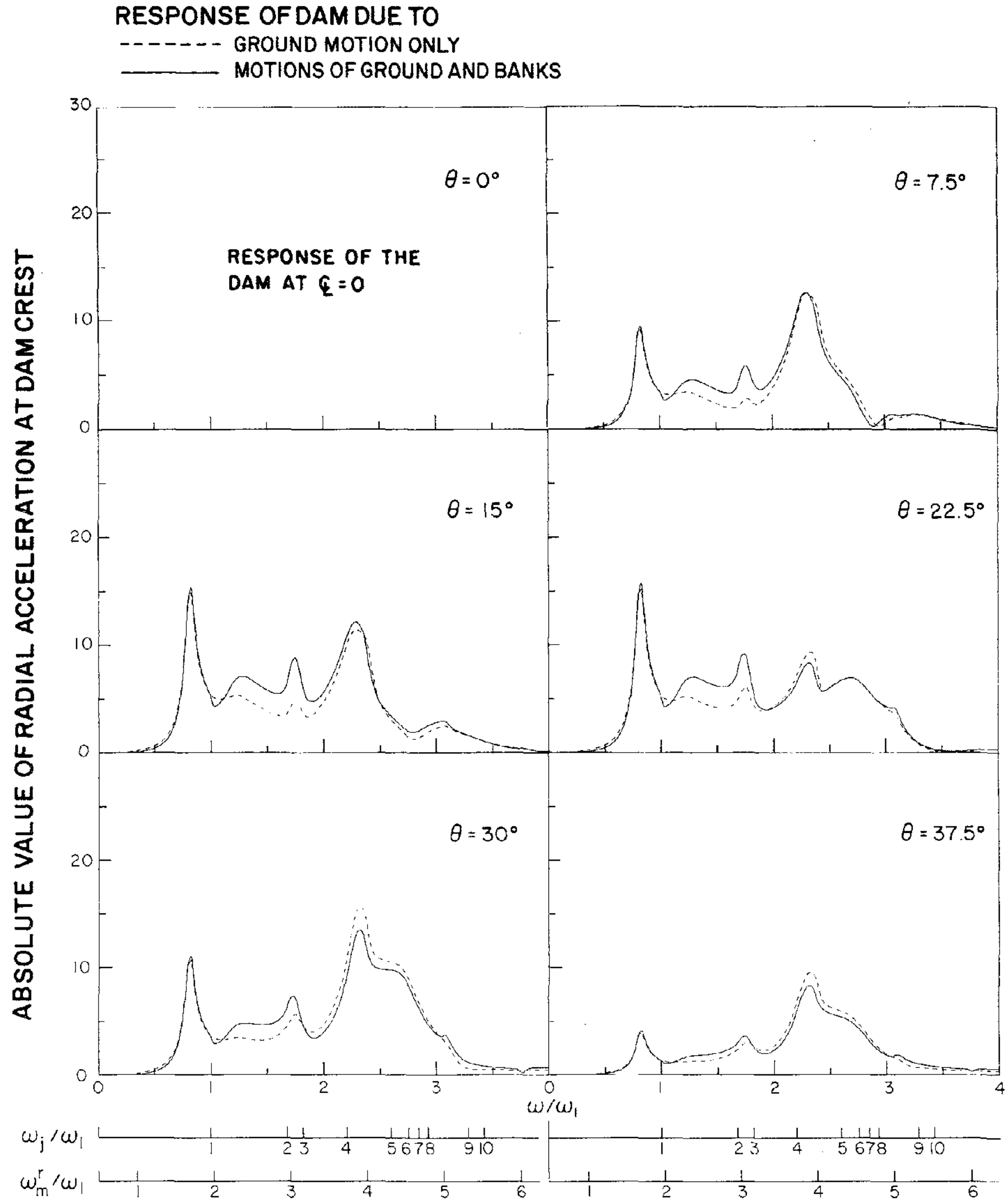

FIG. 7.23 COMPLEX FREQUENCY RESPONSES FOR RADIAL ACCELERATION AT Θ = 7.5°, 15°, 22.5°, 30°, AND37.5° ALONG CREST OF THE DAM. EXCITATIONS ARE (1) CROSS-STREAM GROUND MOTION ONLY, AND (2) CROSS-STREAM MOTIONS OF GROUND AND BANKS. RESULTS ARE FOR ARCH DAMS WITH $R/H_d = 0.5$

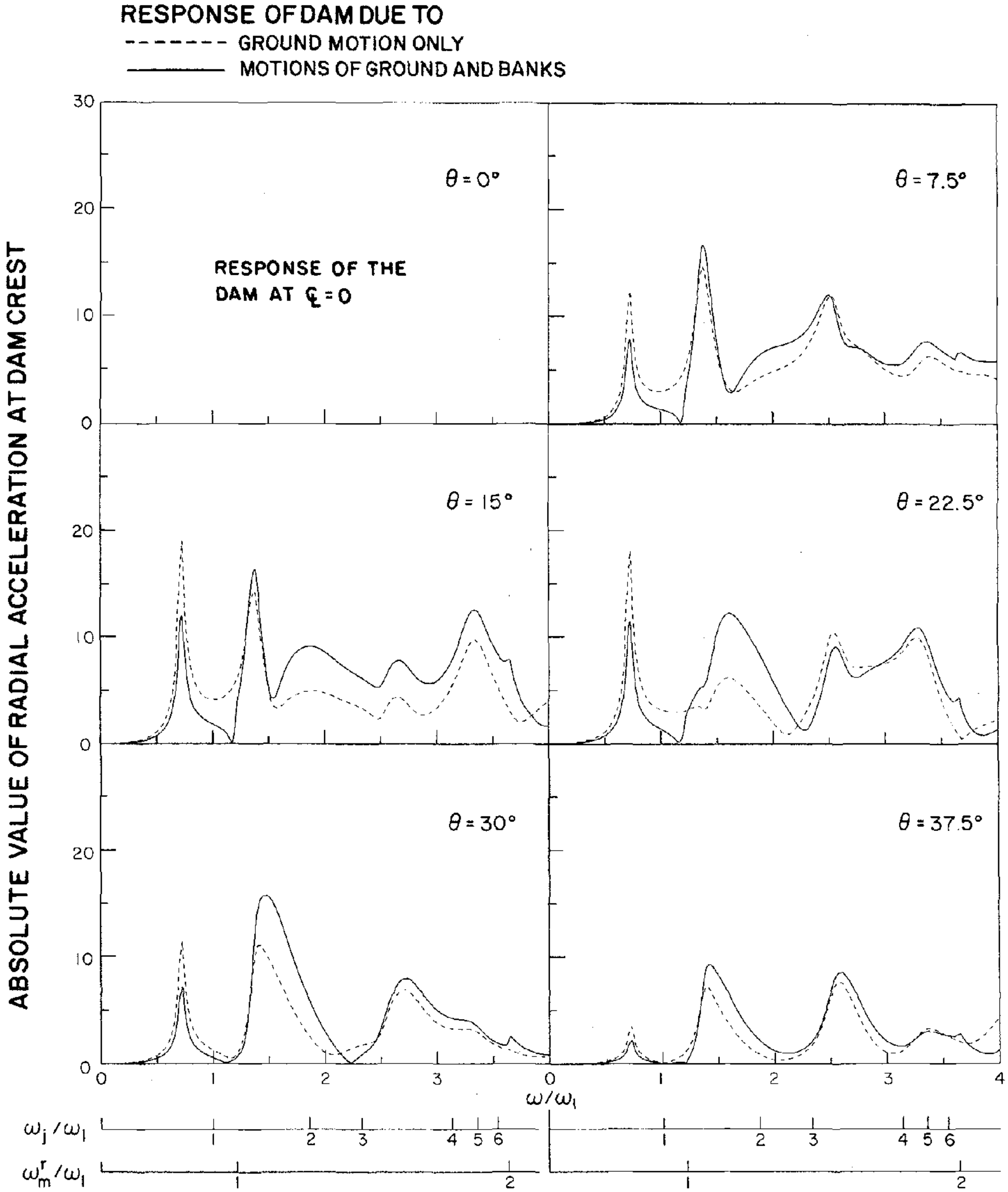

FIG. 7.24 COMPLEX FREQUENCY RESPONSES FOR RADIAL ACCELERATION AT $\Theta = 7.5^{\circ}$, 15°, 22.5°, 30°, AND 37.5° ALONG CREST OF THE DAM. EXCITATIONS ARE (1) CROSS-STREAM GROUND MOTION ONLY, AND (2) CROSS-STREAM MOTIONS OF GROUND AND BANKS. RESULTS ARE FOR ARCH DAMS WITH $R/H_d = 1.5$

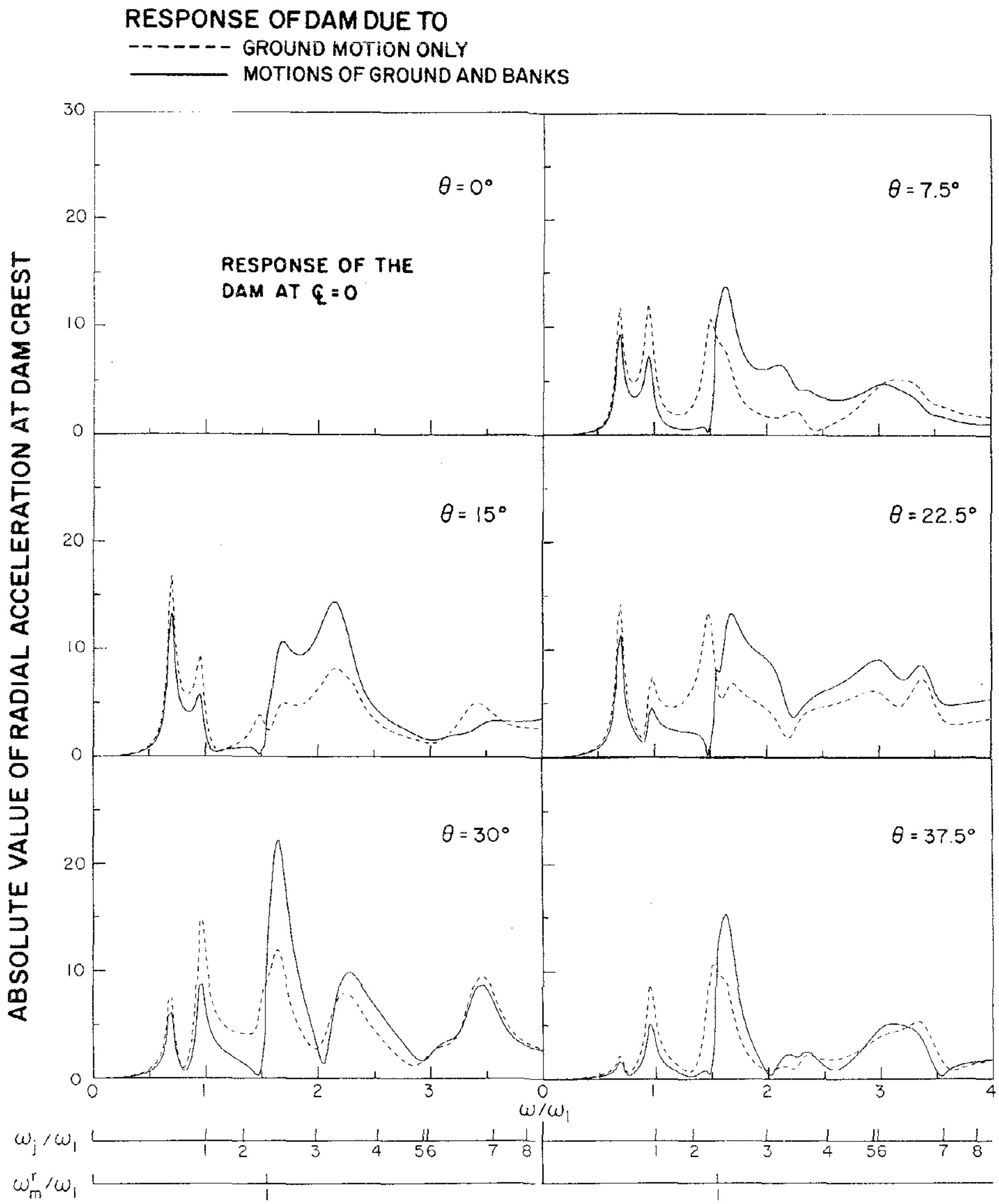

FIG. 7.25 COMPLEX FREQUENCY RESPONSES FOR RADIAL ACCELERATION AT $\Theta = 7.5^{\circ}$, 15°, 22.5°, 30°, AND 37.5° ALONG CREST OF THE DAM. EXCITATIONS ARE (1) CROSS-STREAM GROUND MOTION ONLY, AND (2) CROSS-STREAM MOTIONS OF GROUND AND BANKS. RESULTS ARE FOR ARCH DAMS WITH $R/H_d = 2.5$

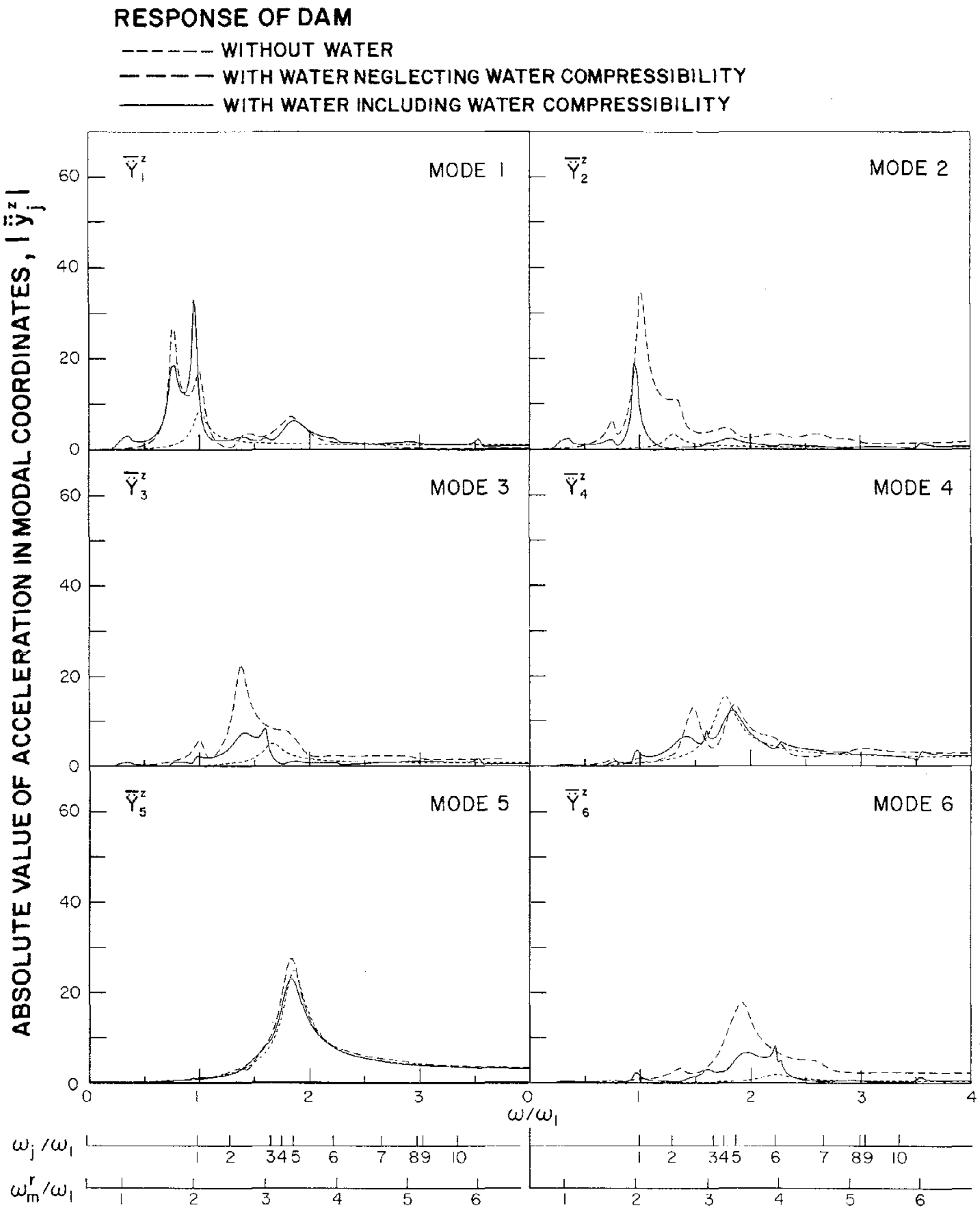

FIG. 7.26 COMPLEX FREQUENCY RESPONSES IN MODAL COORDINATES DUE TO VERTICAL GROUND MOTION. RESULTS ARE FOR ARCH DAMS WITH $R/H_d = 0.5$

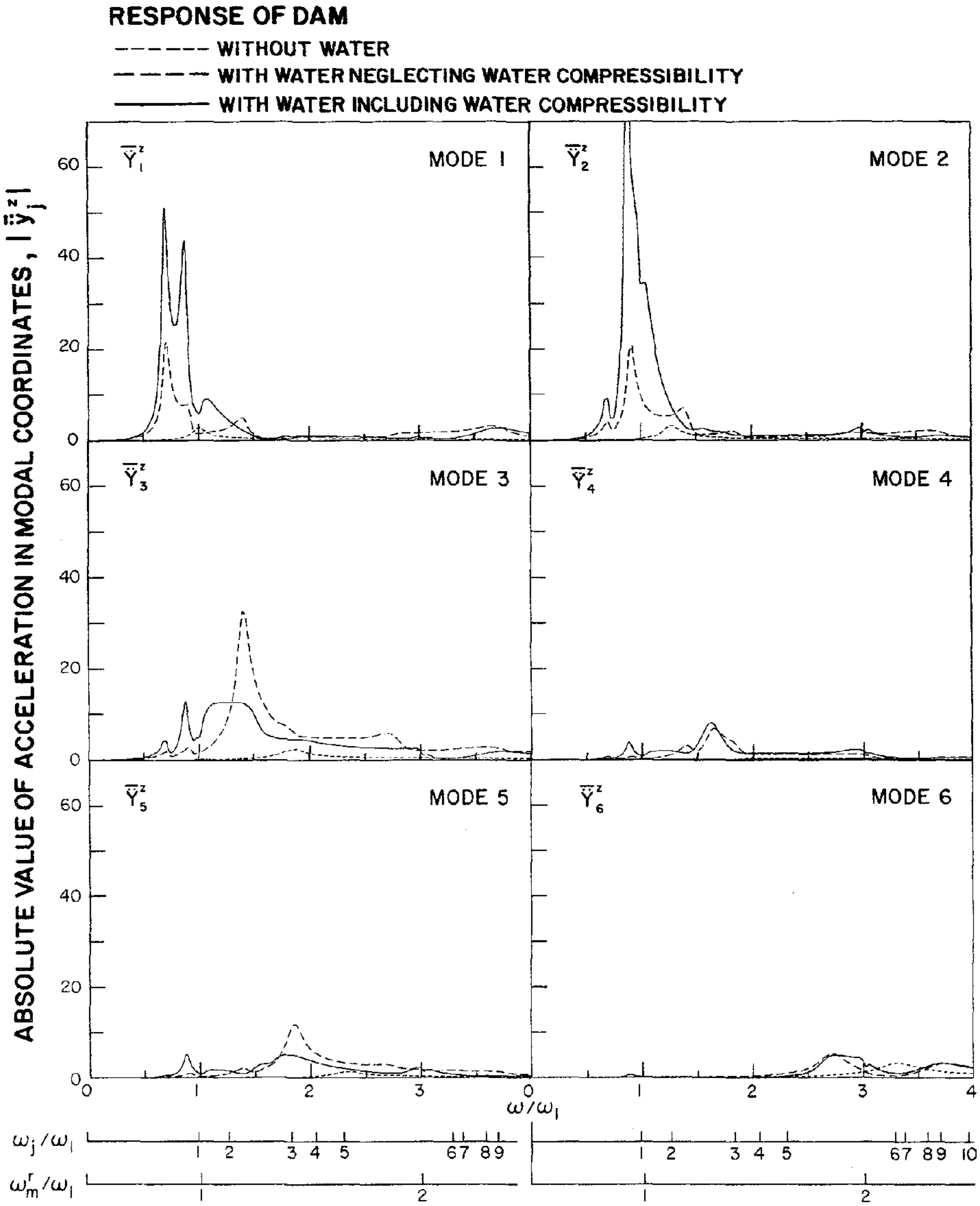

FIG. 7.27 COMPLEX FREQUENCY RESPONSES IN MODAL COORDINATES DUE TO VERTICAL GROUND MOTION. RESULTS ARE FOR ARCH DAMS WITH $R/H_d = 1.5$

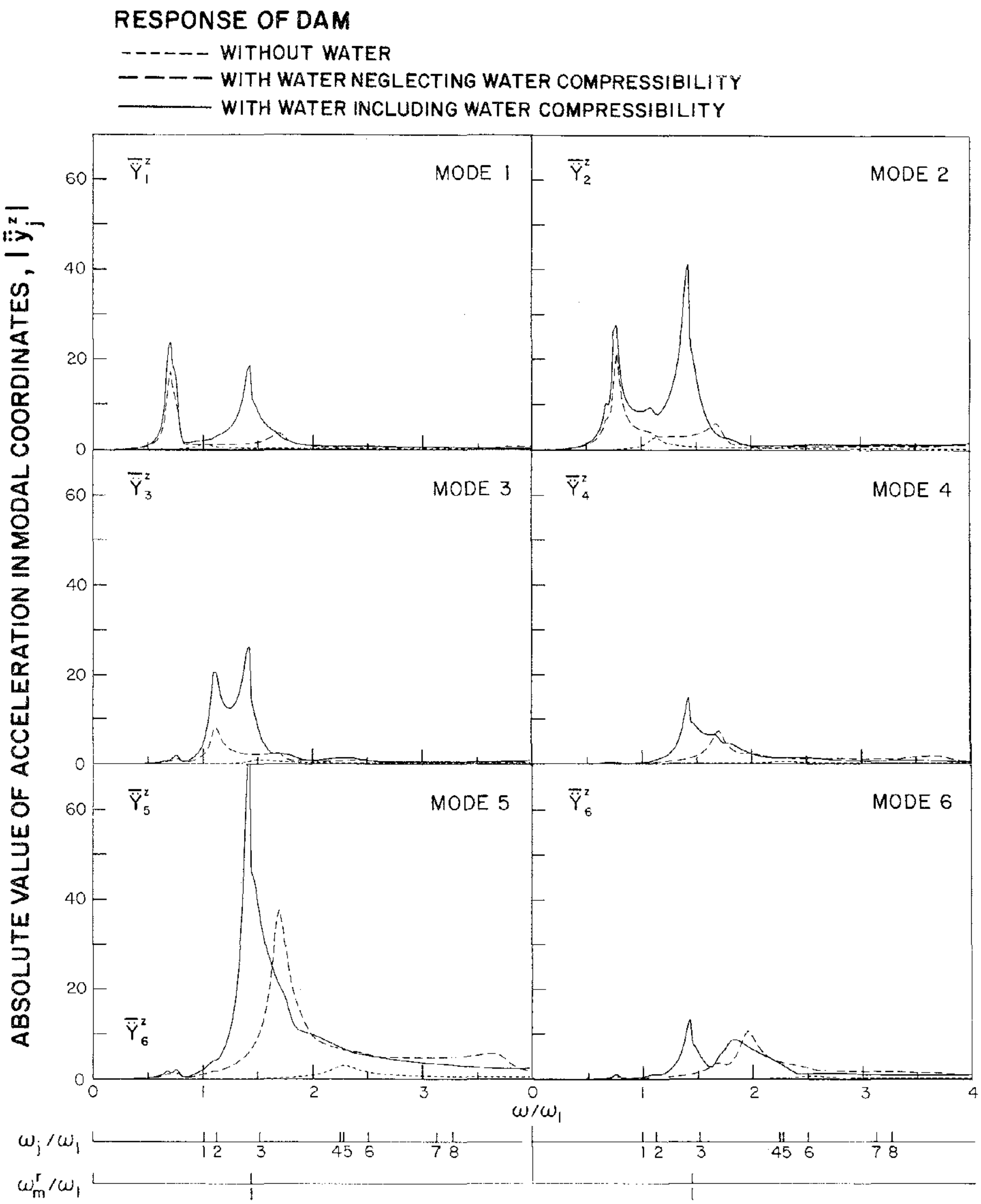

FIG. 7.28 COMPLEX FREQUENCY RESPONSES IN MODAL COORDINATES DUE TO VERTICAL GROUND MOTION. RESULTS ARE FOR ARCH DAMS WITH $R/H_d = 2.5$

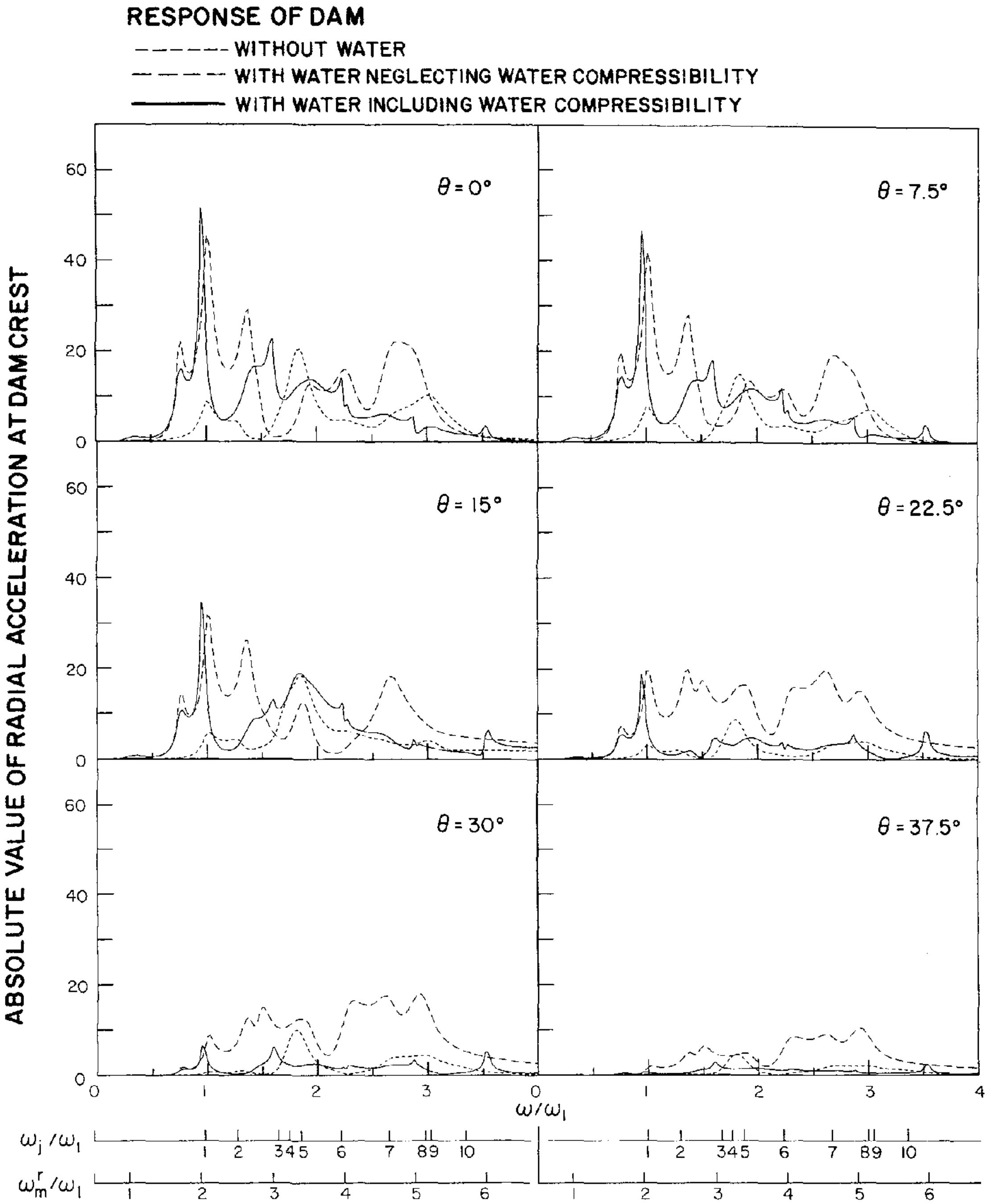

FIG. 7.29 COMPLEX FREQUENCY RESPONSES FOR RADIAL ACCELERATION AT $\Theta = 0^{\circ}$, 7.5°, 15°, 22.5°, 30°, AND 37.5° ALONG CREST OF THE DAM DUE TO VERTICAL GROUND MOTION. RESULTS ARE FOR ARCH DAMS WITH $R/H_d = 0.5$

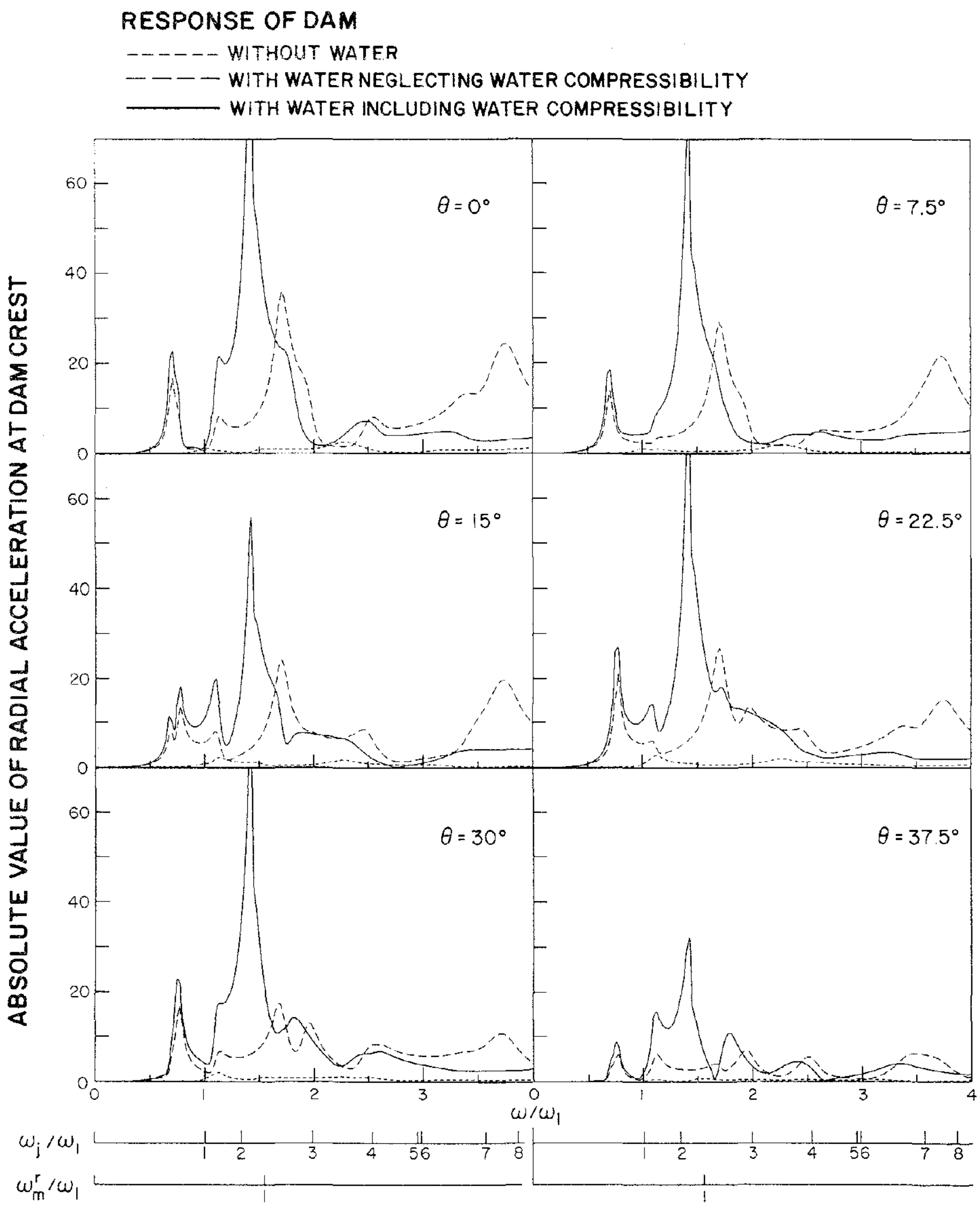

FIG. 7.30 COMPLEX FREQUENCY RESPONSES FOR RADIAL ACCELERATION AT $\Theta = 0^{\circ}$, 7.5°, 15°, 22.5°, 30°, AND 37.5° ALONG CREST OF THE DAM DUE TO VERTICAL GROUND MOTION. RESULTS ARE FOR ARCH DAMS WITH $R/H_d = 1.5$

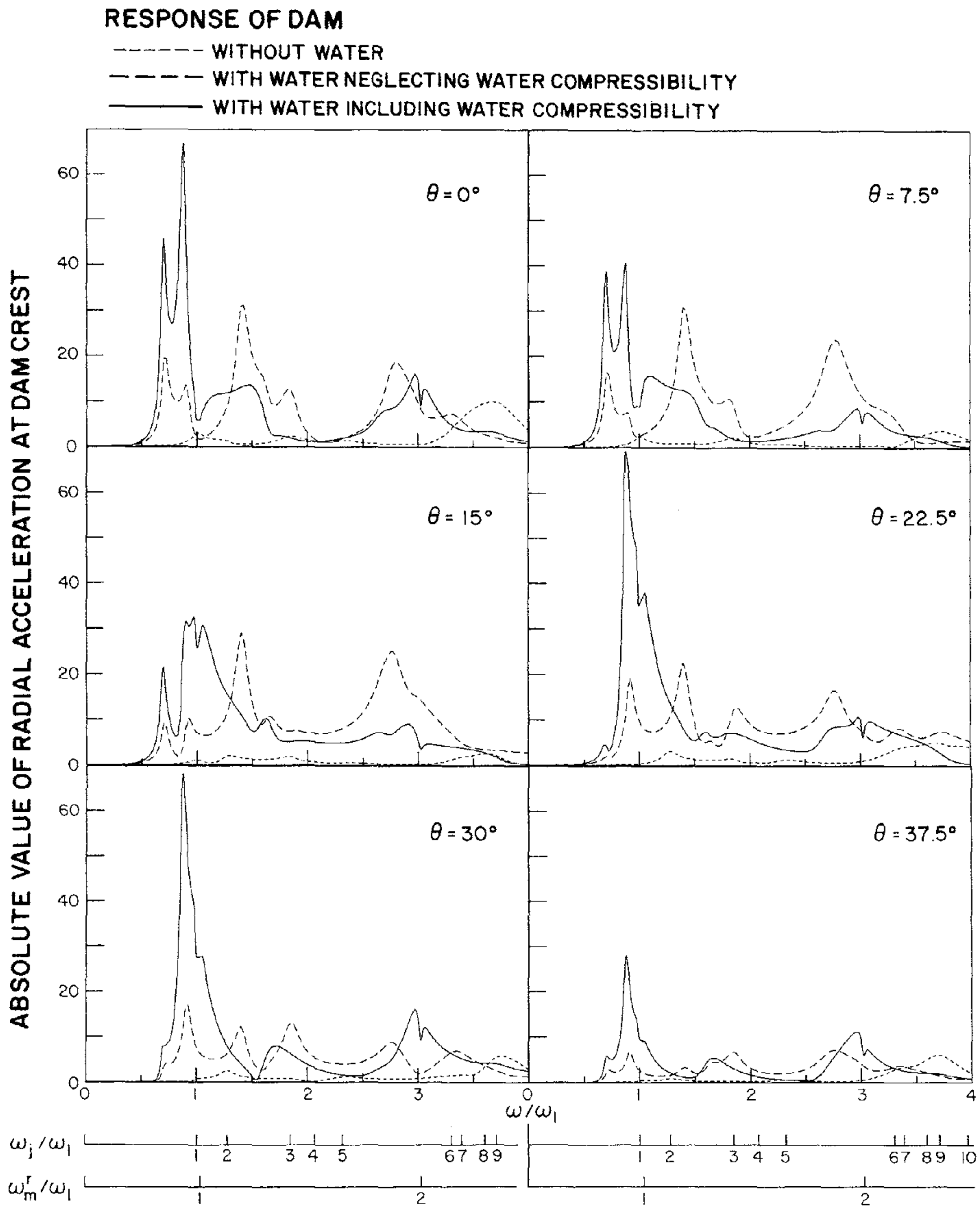

FIG. 7.31 COMPLEX FREQUENCY RESPONSES FOR RADIAL ACCELERATION AT $\Theta = 0^{o}$, 7.5^{o}, 15^{o}, 22.5^{o}, 30^{o}, AND 37.5^{o} ALONG CREST OF THE DAM DUE TO VERTICAL GROUND MOTION. RESULTS ARE FOR ARCH DAMS WITH $R/H_d = 2.5$

modulus of elasticity of mass concrete of the dam. Also included to assist in interpretation of the results are two additional frequency scales, one identifying the natural frequencies of the vibration modes, symmetric or antisymmetric as appropriate, of the dam alone; the other locating the resonant frequencies of the fluid domain.

The absolute value or modulus of the complex frequency response functions in the modal (generalized) coordinates (Eqs. 4.17, 5.16 and 6.13) for the first six ($j = 1, 2, \ldots, 6$) of the ten modes included in the analysis is plotted against normalized excitation frequency. Such plots are presented in Figs. 7.8, 7.9, and 7.10 for dams with $R/H_d = 0.5$, 1.5, and 2.5, respectively, subjected to upstream-downstream ground motion. Similar plots corresponding to cross-stream ground motion are presented in Figs. 7.17 to 7.20, those associated with vertical ground motion in Figs. 7.26 to 7.28. The modal coordinate is defined at the location on the dam where the radial component of the mode shape attains its maximum value. For all of the dams investigated, this maximum mode shape value occurs at the crest of the dam at a location defined by the value of θ given in Figs. 7.2 to 7.4 for the symmetric modes and in Figs. 7.5 to 7.7 for the antisymmetric modes. Thus, the various modal responses are not defined at the same location on the crest and therefore are not directly comparable. However, the response at any location associated with any particular mode is simply the product of the modal coordinate and the value of the normalized mode shape -- maximum value of the radial component of the normalized mode shape is unity -- at that location (Eqs. 4.18, 5.17 and 6.14).

The complex frequency response functions for the accelerations at any nodal point on the dam can be determined from the corresponding functions for the generalized modal accelerations $\bar{\ddot{Y}}^x_j(\omega)$, $\bar{\ddot{Y}}^y_j(\omega)$ or $\bar{\ddot{Y}}^z_j(\omega)$ and Eqs. 4.19, 5.18 or 6.15, respectively. The radial component of acceleration at several locations around the circumference -- $\theta = 0°$, 7.5°, 15°, 22.5°, 30°, and 37.5° measured from the crown -- of the upstream edge of the crest of the dam were computed by combining the contributions of the first 10 modes. The responses due to upstream-downstream ground motion are presented in Figs. 7.11 to 7.13 and those due to vertical ground motion in Fig. 7.29 to 7.31. In both cases, the response is symmetric about the x-z (θ=0) plane. The responses due to cross-stream ground motion, which are antisymmetric about the x-z plane, are presented in Figs. 7.20 to 7.22.

7.5 Discussion of Response Results

7.5.1 Modal Responses

The modal responses of the dam without water ($H/H_d = 0$) are representative of a multidegree of freedom system with constant mass, stiffness, and damping parameters. Each modal response curve is similar to the response behavior of a single-degree-of-freedom (SDOF) system, with resonance at the natural vibration frequency (the effect of damping, $\xi_j = 0.05$, on the resonant frequency is negligible) of the particular mode.

Whereas the responses in the natural modes of vibration of the dam are uncoupled when effects of water on the response of the dam are excluded, the modal responses become coupled when hydrodynamic effects are included (see Sections 4.3.4, 5.3.4 and 6.3.4). Such coupling is apparent in both cases -- with or without water compressibility -- from the response curve for any mode, wherein the primary response is at the resonant frequency of that mode but secondary, smaller peaks appear at the resonant frequencies of the other modes (Figs. 7.8 to 7.10, 7.17 to 7.19, 7.26 to 7.28).

Similar to many structures, the response of arch dams to earthquake ground motion indicates some tendency for larger response in the lower modes of vibration. The peak modal response of arch dams with $R/H_d = 0.5$ and 1.5 to upstream-downstream ground motion (Figs. 7.8 and 7.9) generally decreases with mode number; however, the response of the more flexible arch dams with $R/H_d = 2.5$ (Fig. 7.10) without water or including hydrodynamic effects but ignoring water compressibility, is especially significant in the fifth vibration mode. In the case of cross-stream ground motion, the peak modal responses of arch dams with $R/H_d = 0.5$ and 2.5 generally decrease, although not monotonically, with mode number; however, the response of arch dams with $R/H_d = 1.5$ is rather large in the fifth and sixth modes of vibration (Figs. 7.17 to 7.19). The peak modal responses of arch dams, including hydrodynamic effects and water compressibility, to vertical ground motion similarly do not display any simple trends. For dams with $R/H_d = 0.5$, the peak response in the fifth mode is almost as large as in the first mode; for dams with $R/H_d = 1.5$, the response in the second mode is larger than in the first mode; and for dams with $R/H_d = 2.5$, the response in the fifth mode is much larger than in any other mode (Figs 7.26 to 7.28). That the largest modal response does not appear until the fifth or sixth mode in some cases illustrates the complicated response behavior of arch dams. Thus, although only the first few modes -- compared to the total number of DOF -- will generally suffice for predicting the response, the analysis must include all the modes having significant contributions to the response. In general, many more modes need to be included in predicting the response of arch dams compared to concrete gravity dams or multistory buildings. The number of modes that need to be included depends on the response quantity of interest. Typically, fewer modes suffice for displacements, more modes are generally necessary for accelerations and for stresses.

Since the total response at any nodal point on the dam (Figs. 7.11 to 7.13, 7.20 to 7.22, 7.29 to 7.31) is a linear combination of the responses $\bar{\tilde{Y}}_j(\omega)$ in the first ten modes of vibration, it exhibits many characteristics of the individual modal responses. For example, the first two resonant peaks in the response, including hydrodynamic and water compressibility effects at the crown, $\theta = 0°$ (Fig. 7.12), arise from the contributions of the first and second modes (Fig. 7.9), respectively. The response, including hydrodynamic and water compressibility effects at the fundamental resonant frequency, which is dominated by the first mode, can be seen to vary around the crest-arch (Fig. 7.12) similar to the first mode shape (Fig. 7.3). This variation depends on the excitation frequency. At any other excitation frequency this variation is more complicated, depending on the contributions of the various modes to the response at that frequency. Because the modal contributions vary with θ and each modal contribution varies differently, when they are all combined the distribution of acceleration around the arch is rather irregular, varying strongly with θ.

7.5.2 Hydrodynamic Effects

When water compressibility is neglected the effects of structure-fluid interaction are frequency-independent and are equivalent to an added mass matrix and an added load vector in the modal equations (Eqs. 4.27, 5.25 and 6.19). Because of the added mass effects, the resonant frequencies of arch dams are reduced (Tables 7.1 and 7.2) and

TABLE 7.1: REDUCTION IN RESONANT FREQUENCIES OF SYMMETRIC VIBRATION MODES DUE TO HYDRODYNAMIC EFFECTS

MODE j	$R/H_d = 0.5$			$R/H_d = 1.5$			$R/H_d = 2.5$		
	ω_j/ω_1	PERCENT REDUCTION		ω_j/ω_1	PERCENT REDUCTION		ω_j/ω_1	PERCENT REDUCTION	
		Incompressible Water	Compressible Water		Incompressible Water	Compressible Water		Incompressible Water	Compressible Water
1	1.00	24	25	1.00	30	30	1.00	30	31
2	1.299	23	26	1.272	28	31	1.125	31	31
3	1.660	17	16	1.848	24	26	1.506	26	27
4	1.765	16	17	2.069	21	22	2.245	24	24
5	1.857	1	1	2.324	20	22	2.270	25	38
6	2.220	14	13	3.302	17	18	2.506	22	27

TABLE 7.2: REDUCTION IN RESONANT FREQUENCIES OF ANTISYMMETRIC VIBRATION MODES DUE TO HYDRODYNAMIC EFFECTS

MODE j	$R/H_d = 0.5$			$R/H_d = 1.5$			$R/H_d = 2.5$		
	ω_j/ω_1	PERCENT REDUCTION		ω_j/ω_1	PERCENT REDUCTION		ω_j/ω_1	PERCENT REDUCTION	
		Incompressible Water	Compressible Water		Incompressible Water	Compressible Water		Incompressible Water	Compressible Water
1	1.000	18	18	1.000	28	28	1.000	30	30
2	1.669	15	13	1.861	23	25	1.338	27	29
3	1.816	1	0	2.318	21	23	1.989	24	21
4	2.193	12	20	3.132	19	19	2.530	24	34
5	2.584	9	12	3.352	0	0	2.935	22	22
6	2.755	8	15	3.539	5	6	2.972	22	25

the apparent damping ratios are also reduced. Similar results were obtained earlier for concrete gravity dams [14,15,26]. The added loads are associated with hydrodynamic pressures in the radial direction on the cylindrical upstream face of the dam due to rigid body motion of the dam and banks. Motions in the upstream-downstream direction and the vertical direction cause large pressures compared to those due to cross stream motions (compare the pressures in Figs. 4.1, 5.1 and 6.1 at $\omega = 0$). As a result, when water compressibility is neglected, the resonant response to upstream-downstream or vertical ground motion is increased considerably (Figs. 7.8 - 7.10 and 7.26 - 7.28) whereas the resonant response to cross-stream ground motion is influenced little by hydrodynamic effects (Figs. 7.17 - 7.19).

When the compressibility of water is included, dam-water interaction introduces frequency-dependent terms in the equations of motion of the dam (Sections 4.3.4, 5.3.4 and 6.3.4). This frequency dependence accounts for the complicated shape of the response curves compared to the curves in which the hydrodynamic effects have been neglected or water is assumed to be incompressible. The behavior of the response to upstream-downstream ground motion is especially complicated at excitation frequencies in the neighborhood of ω_m^r, where the hydrodynamic terms become unbounded. This, in contrast to gravity dams [26], results in unbounded response at these frequencies (see Section 4.4 and Appendix E). This response amplification is detectable over only an extremely narrow bandwidth in the neighborhood of ω_m^r (Figs. 7.8 to 7.13). In contrast, the hydrodynamic forces due to cross-stream and vertical ground motions are bounded at the eigen-frequencies ω_m^r of the fluid domain (Sections 5.3.3 and 6.3.3), resulting in bounded response at these excitation frequencies (Figs. 7.17 to 7.22 and 7.26 to 7.31).

Dam-water interaction reduces the j^{th} resonant frequency of the dam from ω_j to $\tilde{\omega}_j$. The following observations can be made from the percentage decrease in resonant frequencies summarized in Tables 7.1 and 7.2. The decrease in a resonant frequency depends on the mode number, whether the mode is symmetric or antisymmetric, and the R/H_d value for the dam. Greater reductions are observed for dams with higher R/H_d values and in the lower modes of vibration. But for a few exceptions, the reduction in resonant frequency is about the same whether compressibility is considered or not.

The resonant response in any vibration mode is influenced by whether $\tilde{\omega}_j$, the resonant frequency of that mode including the effects of compressible water, is less than or greater than ω_1^r, the fundamental resonant frequency of the fluid domain. At excitation frequencies $\omega < \omega_1^r$ the frequency dependent terms in the equations of motion for upstream-downstream and cross-stream ground motions are real valued; the effect of water is equivalent to an added mass and load with their magnitude depending on the excitation frequency. In the equations of motion for vertical ground motion, the added mass term is real valued but the added load term is complex valued for $\alpha \neq 1$. This added mass, in addition to reducing the fundamental resonant frequency of the dam, has the indirect effect of reducing the apparent damping ratio. The reduced damping and added load results in narrower bandwidth and larger response at resonance. Such are the characteristics of response to upstream-downstream or vertical ground motions exhibited by those vibration modes of an arch dam with resonant frequency $\tilde{\omega}_j < \omega_1^r$ (modes 1 and 2 in Figs. 7.9 and 7.27; modes 1, 2, and 3 in Figs. 7.10 and 7.28). The total responses display similar behavior at frequencies where these modes have the more important contributions (Figs. 7.12, 7.13, 7.30 and 7.31). In the case of cross stream ground motion, the added mass reduces the resonant frequency. However, the added load is relatively small compared to the case of upstream-downstream ground motion (compare Figs. 4.1 to 4.3 with 5.1 to 5.3), leading to hardly any increase in resonant response over the value for the dam alone. Such is the response characteristic exhibited by those antisymmetric vibration modes of an arch dam with resonant frequency $\tilde{\omega}_j < \omega_1^r$ (mode 1 in Fig. 7.18 and modes 1 and 2 in Fig. 7.19). The total responses display similar behavior at frequencies where these modes have the more important contributions (Figs. 7.21 and 7.22).

At excitation frequencies $\omega > \omega_1^r$ the additional hydrodynamic terms in the equations of motion of the dam are complex valued for each of the three components of ground motion (Sections 4.3.2, 5.3.2 and 6.3.2). Thus, the effect of water is equivalent to frequency dependent additional mass, damping and load. The added mass is relatively small, and therefore the higher resonant frequencies are not reduced as much as the lower resonant frequencies (Tables 7.1, 7.2). In the case of upstream-downstream ground motion, the added damping is however significant, resulting in decreased resonant response for dams with $R/H_d = 0.5$ and 1.5 in those modes with resonant frequencies $\tilde{\omega}_j > \omega_1^r$ (all modes in Fig. 7.8, modes 3-6 in Fig. 7.9). Thus, the total response is also reduced in the frequency range including the higher resonant frequencies (Figs. 7.11, 7.12). The trends are not clear for arch dams with $R/H_d = 2.5$ but the influence of additional load appears to dominate the effect of additional damping, resulting in slightly increased resonant response (Fig. 7.10). The two competing effects of hydrodynamic interaction, additional damping and load, are also present in the case of cross-stream or vertical ground motions. In the response of some modes to cross-stream ground motions the additional load effect is more significant resulting in larger resonant response (mode 1 in Fig. 7.17; modes 2 and 6 in Fig. 7.18; modes 3 and 4 in Fig. 7.19). For other modes the additional damping effect is dominant resulting in smaller resonant response (modes 2, 4, 5 and 6 in Fig. 7.17; modes 3, 4 and 5 in Fig. 7.18; modes 5 and 6 in Fig. 7.19). The additional load effect is dominant in the response of most vibration modes to vertical ground motion (Figs. 7.26 to 7.28).

The effects of compressibility of water on the dynamic response of an arch dam are also controlled by the values of $\tilde{\omega}_j$, the resonant frequencies of the dam, relative to ω_1^r, the fundamental resonant frequency of the fluid domain. At excitation frequencies ω much smaller than ω_1^r, the compressibility of water has little influence on the hydrodynamic terms in the equations of motion (Section 4.5, 5.4 and 6.4) and thus also on the response of the dam (Figs. 7.8 to 7.13, 7.17 to 7.22 and 7.26 to 7.31). If the resonant frequency of any mode $\tilde{\omega}_j << \omega_1^r$, water compressibility will have little influence on the response in that mode, except in the neighborhood of ω_1^r (modes 1 and 2 in Fig. 7.10, mode 1 in Fig. 7.18, modes 1 and 2 in Fig. 7.19).

The effect of water is equivalent to an added mass and load, independent of excitation frequency, when water compressibility is ignored (Section 4.5, 5.4 and 6.4). However, when water compressibility is included, this effect is equivalent to a frequency dependent added mass and load for $\omega < \omega_1^r$ but to added mass, load and damping at $\omega > \omega_1^r$ with damping increasing with ω. Thus, at excitation frequencies $\omega > \omega_1^r$, the response is reduced when water compressibility is included (Figs. 7.8 to 7.13). At excitation frequencies beyond a certain $\omega > \omega_1^r$, except in the neighborhood of ω_m^r, the hydrodynamic forces on rigid dams due to upstream-downstream and vertical ground motion (Figs. 4.4 and 6.2), and hence added loads in the equations of motions, are smaller than their values at $\omega = 0$, i.e. values corresponding to incompressible water. At these excitation frequencies, the combined effect of reduced load and increased damping associated with water compressibility effects reduces the response of the dam (Figs. 7.8 to 7.13 and 7.26 to 7.31). The response at these excitations frequencies is thus overestimated if water compressibility is neglected. At the above-mentioned excitation frequencies, the hydrodynamic forces due to cross-stream ground motion may be larger or smaller than the forces at $\omega = 0$, which also corresponds to incompressible water, depending on the value of θ and excitation frequency (Figs. 5.1 to 5.4). Thus, water compressibility may lead to an increase or decrease in the response at a particular location depending on the excitation frequency (Figs. 7.17 to 7.22).

7.5.3 Comparison of Response to Various Ground Motion Components

The relative significance of the three components of ground motion in the response of arch dams can be studied by comparing Figs. 7.11, 7.20 and 7.29 for dams with $R/H_d = 0.5$; Figs. 7.12, 7.21 and 7.30 for dams with $R/H_d = 1.5$; and Figs. 7.13, 7.22 and 7.31 for dams with $R/H_d = 2.5$. The radial acceleration response of dams without water is largest due to upstream-downstream ground motion, smaller due to cross-stream ground motion and smallest due to vertical ground motion. Dam-water interaction and water compressibility similarly affect dam response to upstream-downstream and cross-stream ground motions. However, the response to vertical ground motion is greatly increased by these effects, becoming larger than the response to upstream-downstream ground motion for some parameter values. Just as in the case of gravity dams [24], vertical ground motion causes significant hydrodynamic pressures acting in the horizontal plane on a cylindrical dam face, thus causing significant additional response.

7.5.4 Effects of Bank Motion

In all the preceding results, the excitation was simultaneous, identical motions of the ground and reservoir banks. Because it may not be reasonable to assume that the motion of ground and banks is identical, it is of interest to examine the influence of bank motions on the response. The response of arch dams with three different values of $R/H_d = 0.5$, 1.5, and 2.5, computed from two separate analyses are presented. The hydrodynamic effects included are due to motion of the ground only in one case, but due to motion of ground and banks in the other case. Ten modes of vibration and effects of water compressibility were included in the analysis. Results of response due to upstream-downstream ground motion are presented in Figs. 7.14 to 7.16 and those due to cross-stream ground motion in Figs. 7.23 to 7.25.

The hydrodynamic forces due to bank motions may cause an increase or decrease in the response at a particular location on the dam, depending on the direction of ground motion, the excitation frequency ω and the R/H_d value for the dam. At $\omega < \omega_1^r$, the response at all locations on the dam increases in the case of upstream-downstream ground motion but decreases for cross-stream ground motion. At $\omega > \omega_1^r$ no systematic trend is apparent; depending on the excitation frequency the response of the dam at a particular location may increase or decrease. Even for a particular excitation frequency, the response may decrease at some locations and increase at others. The above-observed effects of bank motions on dam response are closely related to the influence of the bank motions on hydrodynamic pressures and forces on rigid dams (Figs. 4.1 to 4.4 and 5.1 to 5.4). The response to upstream-downstream ground motion at excitation frequencies $\omega = \omega_m^r$ is infinite if the effects of bank motions are included but finite otherwise. This is consistent with the analytical results of Section 4.4.

Although the effects of bank motion may be significant on the response at some excitation frequencies, they are generally smaller than the effects of dam-water interaction or of water compressibility. The effects of bank motion on dam response are roughly similar in magnitude for the two horizontal components of ground motion, and they increase as R/H_d increases.

In the case of vertical ground motion, the motion of the vertical banks produces no additional hydrodynamic pressures and hence no influence on the dam response (see Section 6.3.1).

8. CONCLUSIONS

The substructure method has been adapted and generalized for response analysis of arch dams subjected to upstream-downstream, cross-stream and vertical components of ground motion. The arch dam and impounded water are treated as two substructures of the total system and displacements of the dam are represented as a linear combination of the first few natural modes of vibration of the dam alone. Responses to arbitrary ground motion can be obtained by Fourier synthesis procedures applied to the complex frequency response functions determined by the analysis procedures presented in this paper.

Structure-fluid interaction introduces additional terms -- which depend on excitation frequency when water compressibility is considered but are frequency-independent if water is assumed to be incompressible -- in the equations of motion for a finite element idealization of the dam. These hydrodynamic terms in the structural equations are determined as solutions of the wave equation over the fluid domain for appropriate motions of the boundary. Mathematical solutions were possible for the simple geometry of the arch dam and fluid domain assumed in this paper. For pratical problems, numerical solutions of the wave equation would be necessary and are being developed [27].

The analysis procedure presented in this report permits the effects of structure-fluid interaction to be included rationally in dynamic response of arch dams. The simple geometry assumed for the arch dam and fluid domain would not be appropriate for analysis of practical problems but is useful in developing basic understanding of the hydrodynamic effects in the dynamic response of arch dams. The following conclusions are based on the response results presented in Chapter 7.

In general, hydrodynamic effects and water compressibility should be considered in analyzing the dynamic response of arch dams.

Water in the reservoir causes a decrease in the resonant frequencies of the dam; as much as 30 percent reduction was observed in the cases analyzed. The decrease in a resonant frequency depends on the depth of water, mode number, whether the mode is symmetric or anti-symmetric, and the radius to height ratio of the dam. Greater reductions are observed for dams with higher radius to height ratios and in the lower modes of vibration.

When water compressibility is considered, the hydrodynamic terms in the equations of motion are functions of ω, the excitation frequency. At $\omega < \omega_1^r$, the fundamental resonant frequency of the fluid domain, these hydrodynamic terms are real valued for upstream-downstream and cross-stream ground motions, and the effect of water is equivalent to an added mass and load; for vertical ground motion, the added mass term is real valued but the added load term is complex valued if the reflection constant $\alpha \neq 1$. At $\omega > \omega_1^r$ the hydrodynamic terms are complex valued for each of the three components of motion, and the effect of water is equivalent to frequency-dependent additional mass, damping and load. As a result, the hydrodynamic effects in dam response depend on whether ω is less than or greater than ω_1^r, and on the ground motion component. These effects were discussed in some detail in Chapter 7.

For all three components of ground motion, water compressibility has little influence on the response of the dam at excitation frequencies ω much smaller than ω_1^r. At excitation frequencies $\omega > \omega_1^r$ the response to upstream-downstream and vertical components of ground motion is reduced if water compressibility is included. However, water compressibility effects may lead to an increase or decrease in the response to cross-stream ground motion, depending on the excitation frequency.

Dam-water interaction, considering water compressibility, affects the radial acceleration response of dams to upstream-downstream and cross-stream ground motions to a similar degree. However, the response to vertical ground motion is greatly increased by these effects. Just as in the case of gravity dams, vertical ground motion causes significant hydrodynamic pressures. These pressures act in the horizontal plane on a cylindrical dam face, thus causing significant additional response.

The additional hydrodynamic forces caused by bank motions in the upstream-downstream or cross-stream directions may significantly affect the dynamic response of arch dams at some excitation frequencies. However, these effects of bank motions are generally smaller than the effects of dam-water interaction or of water compressibility. The effects of bank motion on dam response are roughly similar in magnitude for the two horizontal compontents of ground motion. In the case of vertical ground motion, the motion of the vertical banks produces no additional hydrodynamic forces and hence has no influence on the dam response.

REFERENCES

1. R.W. Clough, J.M. Raphael, and S. Mojtahedi, "ADAP - A Computer Program for Static and Dynamic Analysis of Arch Dams," Earthquake Engineering Research Center Report No. EERC 73-14, University of California, Berkeley, June 1973.

2. H.M. Westergaard, "Water Pressures on Dams During Earthquakes," Transactions, ASCE, Vol. 98, 1933.

3. C.N. Zangar, "Hydrodynamic Pressures on Dams Due to Horizontal Earthquake Effects," Engineering Monograph No. 11, U.S. Bureau of Reclamation, May 1952.

4. R.W. Clough and A.K. Chopra, "Earthquake Response Analysis of Concrete Dams," in Structural and Geotechnical Mechanics, Editor W.J. Hall, Prentice-Hall, 1977.

5. S. Kotsubo, "External Forces on Arch Dams During Earthquakes," Memoirs Faculty of Engineering, Kyushu University, Fukuoka, Japan, Vol. 20, No. 4, 1961.

6. P.R. Perumulswami and L. Kar, "Earthquake Hydrodynamic Forces on Arch Dams," Journal of Engineering Mechanics Division, ASCE, Vol. 99, No. EM5, October 1973.

7. O.C. Zienkiewicz, and B. Nath, "Earthquake Pressures on Arch Dams - An Electric Analogue Solution," Proceedings, Institute of Civil Engineers, Vol. 25, Proc. Paper 6668, 1963, pp. 165-175.

8. R. Priscu, A. Popovici, L. Ilie, and D. Stematiu, "New Aspects in the Earthquake Analysis of Arch Dams," in Criteria and Assumptions for Numerical Analysis of Dams, Ed. by D.N. Naylor, et al., Proceedings of an International Symposium, Swansea, United Kingdom, Sept. 1975, pp. 709-725.

9. T. Hatano, and K. Hiroshi, "Numerical Solution of Hydrodynamic Pressures During Earthquakes on Arch Dams," Technical Report: C-65002, Technical Laboratory, Central Research Institute of Electric Power Industry, Tokyo, Jan. 1966.

10. A.K. Chopra, E.L. Wilson and I. Farhoomand, "Earthquake Analysis of Reservoir-Dam Systems," Proceedings, Fourth World Conference on Earthquake Engineering, Santiago, Chile, Jan. 1969.

11. O.C. Zienkiewicz and R.E. Newton, "Coupled Vibrations of a Structure Submerged in a Compressible Fluid," International Symposium on Finite Element Techniques, Stuttgart, May 1969.

12. T. Hatano and T. Nakagawa, "Seismic Analysis of Arch Dams - Coupled Vibrations of Dam Body and Reservoir Water," Technical Report, Technical Laboratory No. 1, Central Research Institute of Electric Power Industry, Tokyo, Japan, November 1972.

13. P. Chakrabarti and A.K. Chopra, "Earthquake Analysis of Gravity Dams Including Hydrodynamic Interaction," International Journal of Earthquake Engineering and Structural Dynamics, Vol. 2, pp. 143-160, 1973.

14. A.K. Chopra, "Earthquake Behavior of Reservoir-Dam Systems," Journal of Engineering Mechanics Division, ASCE, Vol. 94, No. EM6, December 1968.

15. A.K. Chopra, "Earthquake Response of Concrete Gravity Dams," Journal of the Engineering Mechanics Division, ASCE, Vol. 96, No. EM4, August 1970.

16. P.R. Perumalswami and L. Kar, "Earthquake Behavior of Arch Dam-Reservoir Systems," Proceedings, Fifth World Conference on Earthquake Engineering, Rome, June 1973.

17. R.W. Clough and J. Penzien, Dynamics of Structures, McGraw-Hill, New York, 1975.

18. R.W. Clough and K.J, Bathe, "Finite Element Analysis of Dynamic Response," Advances in Computational Methods in Structural Mechanics and Design, 2nd U.S.-Japan Seminar, Berkeley, 1972. University of Alabama Huntsville Press, Huntsville, ALA., pp. 153-180.

19. K.J. Bathe, E.L. Wilson, and F.E. Peterson, "SAP IV - A Structural Analysis Program for Static and Dynamic Response of Linear Systems," Earthquake Engineering Research Center Report No. EERC 73-11, University of California, Berkeley, June 1973.

20. O.C. Zienkiewicz, The Finite Element Method in Engineering Science, McGraw-Hill, London, 1971.

21. C.-Y. Liaw and A.K. Chopra, "Earthquake Analysis of Axisymmetric Towers Partially Submerged in Water," International Journal of Earthquake Engineering and Structural Dynamics, Vol. 3, No. 3, Jan.-March 1975, pp. 233-248.

22. A.K. Chopra, "Hydrodynamic Pressures on Dams During Earthquakes," Journal of the Engineering Mechanics Division, ASCE, Vol. 93, No. EM6, Proc. Paper 5695, December 1967, pp. 205-223.

23. J.I. Bustamante, E. Rosenblueth, I. Herrara, and A. Flores, "Prescision Hidrodinamica en Presas Y Depositos," "Boletin Sociedad Mexicana de Ingenieria Sismica," Vol. 1, No. 2, October 1963.

24. P. Chakrabarti, and A.K. Chopra, "Hydrodynamic Pressures and Response of Gravity Dams to Vertical Earthquake Component," International Journal of Earthquake Engineering and Structural Dynamics, Vol. 1, No. 4, April-June 1973, pp. 325-335.

25. E. Rosenblueth, "Presion' hidrodinamica en presas debida a la acceleracion vertical con refraccion' en el fonado," II, Crongreso Nacional de Ingenieria Sismica, Veracruz, Mexico, May 1968.

26. P. Chakrabarti, and A.K. Chopra, "Hydrodynamic Effects in Earthquake Response of Gravity Dams," Journal of the Structural Division, ASCE, Vol. 100, No. ST6, June 1974, pp. 1211-1224.

27. J.F. Hall and A.K. Chopra, EERC Report in preparation.

APPENDIX A - NOTATION

$\left.\begin{array}{l} A_n, B_n, C_n \\ D_n, E_m, F_m, G_n \\ I^j_{mn}, T_n, U_m, V_m \end{array}\right\}$ = quantities defined in Eq. 4.11 for upstream-downstream ground motion or in Eq. 5.11 for cross stream ground motion

B_1 = radial thickness of the dam at the crest

B_2 = radial thickness of the dam at the base

$\underset{\sim}{c}$ = damping matrix for the dam

C = velocity of sound in water

C_j = generalized damping in the j^{th} mode of vibration of the dam (without water)

C_r = P-wave velocity in rock

E = modulus of elasticity for dam material

$\{e^x\}^T$ = < 1,0,0,1,0,0....1,0,0,....1,0,0 >

$\{e^y\}^T$ = < 0,1,0,0,1,0....0,1,0,....0,1,0 >

$\{e^z\}^T$ = < 0,0,1,0,0,1....0,0,1,....0,0,1 >

F_0 = hydrodynamic force acting per unit circumferential length corresponding to P_0

$\bar{F}_0$ = complex frequency response function for F_0

$F_{0\ell}$ = hydrodynamic force per unit circumferential length acting in the radial direction on the upstream face of the dam as defined in Eq. 4.12

$\bar{F}_{0\ell}$ = complex frequency response function for $F_{0\ell}$

F_s = hydrostatic force per unit circumferential length at the base of the dam

g	=	acceleration of gravity
H	=	depth of water in the reservoir
H_d	=	height of the dam
i	=	$\sqrt{-1}$
j,k,ℓ,m,n	=	integer counters in summations
J	=	number of generalized DOF included in an analysis
$J_n(x)$	=	Bessel function of the first kind of order n
$\underline{k}$	=	stiffness matrix for the dam
k	=	$C_r w_r / C w$
K_j	=	generalized stiffness in j^{th} mode of vibration of the dam (without water)
$K_n(x)$	=	modified Bessel function of the second kind of order n
$\underline{L}^x$	=	generalized load vector defined by Eq. 4.15 and 4.16
$\underline{L}^y$	=	generalized load vector defined by Eq. 5.14 and 5.15
$\underline{L}^z$	=	generalized load vector defined by Eq. 6.11 and 6.12
$\underline{L}^{ax}$	=	generalized "added load" vector for incompressible water due to upstream-downstream ground motion
$\underline{L}^{ay}$	=	generalized "added load" vector for incompressible water due to cross stream ground motion
$\underline{L}^{az}$	=	generalized "added load" vector for incompressible water due to vertical ground motion
$\underline{L}^{0x}$	=	generalized load vector associated with the mass of the dam due to upstream-downstream ground motion
$\underline{L}^{0y}$	=	generalized load vector associated with the mass of the dam due to cross-stream ground motion

$\underline{L}^{0z}$ = generalized load vector associated with the mass of the dam due to vertical ground motion

$\underline{m}$ = consistent mass matrix for the dam

m_ℓ = the largest integer "m" satisfying the inequality $\omega/\omega_1^r > (2m-1)$, $m = 1,2,3,\ldots.$

$\underline{M}^a$ = generalized "added mass" for incompressible water

M_j = generalized mass for the j^{th} natural mode of vibration of the dam (without water)

N = number of nodal points on the dam

p = hydrodynamic pressure in excess of hydrostatic

p_c = hydrodynamic pressure on the upstream face of the dam

$\bar{p}_c$ = complex frequency response function for p_c

p_j = hydrodynamic pressure on the upstream face of the dam due to acceleration of the dam in its j^{th} natural mode of vibration

$\bar{p}_j$ = complex frequence response function for p_j

p_0^z = hydrodynamic pressure on the upstream face of the dam due to vertical, rigid-body accelerations of the dam, reservoir bottom and the banks

$\bar{p}_0^z$ = complex frequency response function for p_0^z

p_{0B}^x = hydrodynamic pressure on the upstream face of the dam due to acceleration of only the reservoir banks in the upstream-downstream direction.

$\bar{p}_{0B}^x$ = complex frequency response function for p_{0B}^x

p_{0B}^y = hydrodynamic pressure on the upstream face of the dam due to acceleration of only the reservoir banks in the cross-stream direction

$\bar{p}_{0B}^y$ = complex frequency response function for p_{0B}^y

p^x_{0D} = hydrodynamic pressure on the upstream face of the dam due to acceleration of the rigid dam in the upstream-downstream direction but the banks remain stationary

$\bar{p}^x_{0D}$ = complex frequency response function for p^x_{0D}

p^y_{0D} = hydrodynamic pressure on the upstream face of the dam due to acceleration of the rigid dam in the cross-stream direction but the banks remain stationary.

$\bar{p}^y_{0D}$ = complex frequency response function for p^y_{0D}

p_{0T} = hydrodynamic pressure on the upstream face of the dam due to acceleration of the rigid dam and reservoir banks ($p_{0B} + p_{0D}$)

$\bar{p}_{0T}$ = complex frequency response function for p_{0T}

$\underset{\sim}{Q}$ = vector of nodal point loads associated with hydrodynamic pressures

$\bar{\underset{\sim}{Q}}$ = complex frequency response function for $\underset{\sim}{Q}$

$\underset{\sim}{Q}^f$ = subvector of $\underset{\sim}{Q}(t)$ associated with the DOF of the nodal points, on the upstream face of the dam, in contact with the water

$\bar{\underset{\sim}{Q}}^f$ = complex frequency response function for $\underset{\sim}{Q}^f$

$\bar{\underset{\sim}{Q}}^x_j, \bar{\underset{\sim}{Q}}^y_j, \bar{\underset{\sim}{Q}}^z_j$ = hydrodynamic load vector defined as the static equivalent of the pressure function $\bar{p}^x_j$, $\bar{p}^y_j$, or $\bar{p}^z_j$ respectively

$\bar{\underset{\sim}{Q}}^x_{0B}, \bar{\underset{\sim}{Q}}^y_{0B}$ = hydrodynamic load vector defined as the static equivalent of the pressure function $\bar{p}^x_{0B}$ or $\bar{p}^y_{0B}$ respectively

$\bar{\underset{\sim}{Q}}^x_{0D}, \bar{\underset{\sim}{Q}}^y_{0D}$ = hydrodynamic load vector defined as the static equivalent of the pressure function $\bar{p}^x_{0D}$ or $\bar{p}^y_{0D}$ respectively

r = radial coordinate of reservoir - dam system (see Fig. 2.1)

R	=	radius of upstream face of the dam
$\underset{\sim}{S}$	=	coefficient matrix given in Eq. 4.16 for upstream-downstream ground motion or by Eq. 5.15 for cross stream ground motion
t	=	time variable
$\underset{\sim}{v}$	=	vector of nodal point displacements relative to the ground
$\bar{\ddot{\underset{\sim}{v}}}^{x}$	=	complex frequency response vector for total acceleration of the dam due to upstream-downstream ground motion (Eq. 4.19)
$\bar{\ddot{\underset{\sim}{v}}}^{y}$	=	complex frequency response vector for total acceleration of the dam due to cross-stream ground motion (Eq. 5.18)
$\bar{\ddot{\underset{\sim}{v}}}^{z}$	=	complex frequency response vector for total acceleration of the dam due to vertical ground motion (Eq. 6.15)
$\ddot{v}_{g}^{x}$	=	upstream-downstream component of earthquake ground acceleration
$\ddot{v}_{g}^{y}$	=	cross-stream component of earthquake ground acceleration
$\ddot{v}_{g}^{z}$	=	vectical component of earthquake ground acceleration
$\bar{\ddot{\underset{\sim}{v}}}_{j}^{x}$	=	complex frequency response vector for acceleration of the dam in the j^{th} symmetric mode due to upstream-downstream ground motion (Eq. 4.18)
$\bar{\ddot{\underset{\sim}{v}}}_{j}^{y}$	=	complex frequency response vector for acceleration of the dam in the j^{th} antisymmetric mode due to cross-stream ground motion (Eq. 5.17)
$\bar{\ddot{\underset{\sim}{v}}}_{j}^{z}$	=	complex frequency response vector for acceleration of the dam in the j^{th} symmetric mode of vibration of the dam due to vertical ground motion (Eq. 6.14)
v^{r}	=	the radial component of water partical displacements
v^{θ}	=	the tangential component of water partical displacements
v^{z}	=	the vertical component of water partical displacements

v_n^x = x- component of the displacement of nodal point "n" (Fig. 3.1)

v_n^y = y- component of the displacement of nodal point "n" (Fig. 3.1)

v_n^z = z- component of the displacement of nodal point "n" (Fig. 3.1)

w = unit weight of water

w_r = unit weight of ground rock

x,y,z = orthogonal cartesian coordinates (Fig. 2.1)

Y_j = j^{th} generalized displacement of the dam

$\bar{Y}_j$ = complex frequency response of Y_j

$Y_n(x)$ = Bessel function of the second kind of order n

Y_j^x = generalized displacement of the dam associated with the j^{th} symmetric mode of vibration due to upstream-downstream ground motion

Y_j^y = generalized displacement of the dam associated with the j^{th} atisymmetric mode of vibration due to cross-stream ground motion

Y_j^z = generalized displacement of the dam associated with the j^{th} symmetric mode of vibration due to vertical ground motion

$\bar{Y}_j^x$ = complex frequency response for Y_j^x

$\bar{Y}_j^y$ = complex frequency response for Y_j^y

$\bar{Y}_j^z$ = complex frequency response for Y_j^z

α = reflection constant for the reservoir bottom associated with vertical ground motion $\alpha = (k - 1)/(k + 1)$

α_m = quantity defined in Eq. 4.11a or 5.11a

ξ_j = viscous damping ratio for the j^{th} natural mode of vibration of the dam (without water)

ε_n = numerical multiplier equal to 1 when $n = 0$ but equal to 2 when $n \neq 0$

λ_m = quantity defined in Eq. 4.11b or 5.11b

ν = Poisson's ratio

ϕ_j = continuous function analogue of $\underline{\phi}_j$

$\underline{\phi}_j$ = j^{th} mode shape vector of the dam (without water in the reservoir)

$\underline{\phi}_j^f$ = sub-vector of the j^{th} mode shape $\underline{\phi}_j$ containing elements associatiated with the DOF on the upstream face of the dam

$\underline{\phi}_j^{xf}$ = sub-vector of $\underline{\phi}_j^f$ containing elements associated with the x- DOF of the nodal points on the upstream face of the dam

$\underline{\phi}_j^{yf}$ = sub-vector of $\underline{\phi}_j^f$ containing elements associated with the y- DOF of the nodal points on the upstream face of the dam

θ = angular coordinate of reservoir-dam system (Fig. 2.1)

ω = circular frequency of harmonic ground motion

ω_j = j^{th} natural frequency of vibration of the dam (without water in the reservoir)

ω_m^r = $\frac{\pi C}{2H}(2m - 1)$, $m = 1,2,3,\ldots$; the m^{th} eigen-frequency of the water in the reservoir

μ_n = summation index defined in Eq. 5.11

APPENDIX B - FINITE ELEMENT PROPERTIES

B.1 Introduction

A general form of the stiffness matrix $\underline{k}$ for any finite element is given by

$$\underline{k} = \int_{Vol} \underline{a}^T \underline{c} \underline{a} \, dV \qquad (B.1)$$

where $\underline{a}$ is the strain-displacement relationship and $\underline{c}$ is the stress-strain law, i.e.

$$\underline{\varepsilon} = \underline{a} \, \underline{v} \qquad (B.2)$$

$$\underline{\sigma} = \underline{c} \, \underline{\varepsilon} \qquad (B.3)$$

where $\underline{v}$ is the nodal displacements, $\underline{\varepsilon}$ and $\underline{\sigma}$ are the element strains and corresponding stresses respectively.

B.2 Coordinate System

The shell-element used to descritize the dam is a 16-node curved solid element (see Fig. B1). The locations of the nodes are defined by the right-handed rectangular Cartesian coordinate system (x, y, z) which is referred to as a global system. Within each element a local coordinate system (ξ, η, ζ) is defined such that ξ, η and ζ vary from -1 to 1; (0,0,0) is located at the centroid of the element (see Fig. B1). The global coordinates are given in terms of the local coordinate system by

$$x = \sum_{i=1}^{16} h_i x_i$$

$$y = \sum_{i=1}^{16} h_i y_i$$

$$z = \sum_{i=1}^{16} h_i z_i \tag{B.4}$$

where the interpolation functions h_i are given by

$$h_1 = \frac{1}{8}(1 + \xi)(1 + \eta)(1 + \zeta)(\xi + \eta - 1)$$

$$h_2 = \frac{1}{8}(1 - \xi)(1 + \eta)(1 + \zeta)(-\xi + \eta - 1)$$

$$h_3 = \frac{1}{8}(1 - \xi)(1 - \eta)(1 + \zeta)(-\xi - \eta - 1)$$

$$h_4 = \frac{1}{8}(1 + \xi)(1 - \eta)(1 + \zeta)(\xi - \eta - 1)$$

$$h_5 = \frac{1}{8}(1 + \xi)(1 + \eta)(1 - \zeta)(\xi + \eta - 1)$$

$$h_6 = \frac{1}{8}(1 - \xi)(1 + \eta)(1 - \zeta)(-\xi + \eta - 1)$$

$$h_7 = \frac{1}{8}(1 - \xi)(1 - \eta)(1 - \zeta)(-\xi - \eta - 1)$$

$$h_8 = \frac{1}{8}(1 + \xi)(1 - \eta)(1 - \zeta)(\xi - \eta - 1)$$

$$h_9 = \frac{1}{4}(1 - \xi^2)(1 + \eta)(1 + \zeta)$$

$$h_{10} = \frac{1}{4}(1 - \xi)(1 - \eta^2)(1 + \zeta)$$

$$h_{11} = \frac{1}{4}(1 - \xi^2)(1 - \eta)(1 + \zeta)$$

$$h_{12} = \frac{1}{4}(1 + \xi)(1 - \eta^2)(1 + \zeta)$$

$$h_{13} = \frac{1}{4}(1 - \xi^2)(1 + \eta)(1 - \zeta)$$

$$h_{14} = \frac{1}{4}(1 - \xi)(1 - \eta^2)(1 - \zeta)$$

$$h_{15} = \frac{1}{4}(1 - \xi^2)(1 - \eta)(1 - \zeta)$$

$$h_{16} = \frac{1}{4}(1 + \xi)(1 - \eta^2)(1 - \zeta) \qquad \text{(B.5)}$$

B.3 Strain-Displacement Equations

The x, y and z components of displacements within an element (v^x, v^y, v^z) are assumed to be of the following form:

$$v^x = \sum_{i=1}^{16} h_i v_i^x + h_{17}\alpha_1^x + h_{18}\alpha_2^x + h_{19}\alpha_3^x + h_{20}\alpha_4^x + h_{21}\alpha_5^x$$

$$v^y = \sum_{i=1}^{16} h_i v_i^y + h_{17}\alpha_1^y + h_{18}\alpha_2^y + h_{19}\alpha_3^y + h_{20}\alpha_4^y + h_{21}\alpha_5^y$$

$$v^z = \sum_{i=1}^{16} h_i v_i^z + h_{17}\alpha_1^z + h_{18}\alpha_2^z + h_{19}\alpha_3^z + h_{20}\alpha_4^z + h_{21}\alpha_5^z \qquad \text{(B.6)}$$

where

$$h_{17} = \xi(1 - \xi^2)$$

$$h_{18} = \eta(1 - \eta^2)$$

$$h_{19} = (1 - \zeta^2)$$

$$h_{20} = \xi\eta(1 - \zeta^2)$$

$$h_{21} = \eta\xi(1 - \eta^2) \qquad \text{(B.7)}$$

v_i^x, v_i^y and v_i^z are the x, y and z displacements of nodal point i. The fifteen degrees of freedom α_i^x, α_i^y and α_i^z, i = 1,5, are introduced in the element in addition to the nodal point displacements to impart better bending characteristics.* These additional degrees of freedom will be condensed out at the element level.

The strain-displacement equations are

$$\varepsilon^{xx} = \frac{\partial v^x}{\partial x} = \left\langle \underline{h}_{,x} \right\rangle \begin{Bmatrix} \underline{v}^x \\ \underline{\alpha}^x \end{Bmatrix}$$

$$\varepsilon^{yy} = \frac{\partial v^y}{\partial y} = \left\langle \underline{h}_{,y} \right\rangle \begin{Bmatrix} \underline{v}^y \\ \underline{\alpha}^y \end{Bmatrix}$$

$$\varepsilon^{zz} = \frac{\partial v^z}{\partial z} = \left\langle \underline{h}_{,z} \right\rangle \begin{Bmatrix} \underline{v}^z \\ \underline{\alpha}^z \end{Bmatrix}$$

$$\varepsilon^{xy} = \frac{\partial v^x}{\partial y} + \frac{\partial v^y}{\partial x} = \left\langle \underline{h}_{,y} \right\rangle \begin{Bmatrix} \underline{v}^x \\ \underline{\alpha}^x \end{Bmatrix} + \left\langle \underline{h}_{,x} \right\rangle \begin{Bmatrix} \underline{v}^y \\ \underline{\alpha}^y \end{Bmatrix}$$

$$\varepsilon^{xz} = \frac{\partial v^x}{\partial z} + \frac{\partial v^z}{\partial x} = \left\langle \underline{h}_{,z} \right\rangle \begin{Bmatrix} \underline{v}^x \\ \underline{\alpha}^x \end{Bmatrix} + \left\langle \underline{h}_{,x} \right\rangle \begin{Bmatrix} \underline{v}^z \\ \underline{\alpha}^z \end{Bmatrix}$$

$$\varepsilon^{yz} = \frac{\partial v^y}{\partial z} + \frac{\partial v^z}{\partial y} = \left\langle \underline{h}_{,z} \right\rangle \begin{Bmatrix} \underline{v}^y \\ \underline{\alpha}^y \end{Bmatrix} + \left\langle \underline{h}_{,y} \right\rangle \begin{Bmatrix} \underline{v}^z \\ \underline{\alpha}^z \end{Bmatrix} \qquad \text{(B.8)}$$

*E.L. Wilson, R.L. Taylor, W. Doherty, and J. Ghaboussi, "Incompatible Displacement Models," Numerical and Computer Methods in Structural Mechanics (S.J. Fenves, N. Perrone, J. Robinson, and W.C. Schnobrich, eds.), Academic Press, Inc., New York, 1973, pp. 43-57.

where

$$\left\langle \underline{h}_{,x} \right. = \left\langle h_{1,x} \quad h_{2,x} \quad \cdots\cdots \quad h_{21,x} \right\rangle$$

$$\left\langle \underline{h}_{,y} \right. = \left\langle h_{1,y} \quad h_{2,y} \quad \cdots\cdots \quad h_{21,y} \right\rangle$$

$$\left\langle \underline{h}_{,z} \right. = \left\langle h_{1,z} \quad h_{2,z} \quad \cdots\cdots \quad h_{21,z} \right\rangle \qquad \text{(B.9)}$$

$$\left\{ \underline{v}^{x} \right\}^{T} = \left\langle v_1^x \quad v_2^x \quad \cdots\cdots \quad v_{16}^x \right\rangle$$

$$\left\{ \underline{v}^{y} \right\}^{T} = \left\langle v_1^y \quad v_2^y \quad \cdots\cdots \quad v_{16}^y \right\rangle$$

$$\left\{ \underline{v}^{z} \right\}^{T} = \left\langle v_1^z \quad v_2^z \quad \cdots\cdots \quad v_{16}^z \right\rangle \qquad \text{(B.10)}$$

$$\left\{ \underline{\alpha}^{x} \right\}^{T} = \left\langle \alpha_1^x \quad \alpha_2^x \quad \alpha_3^x \quad \alpha_4^x \quad \alpha_5^x \right\rangle$$

$$\left\{ \underline{\alpha}^{y} \right\}^{T} = \left\langle \alpha_1^y \quad \alpha_2^y \quad \alpha_3^y \quad \alpha_4^y \quad \alpha_5^y \right\rangle$$

$$\left\{ \underline{\alpha}^{z} \right\}^{T} = \left\langle \alpha_1^z \quad \alpha_2^z \quad \alpha_3^z \quad \alpha_4^z \quad \alpha_5^z \right\rangle \qquad \text{(B.11)}$$

The "," denotes partial derivative. Equation B.8 can be written in matrix form as

$$\underline{\varepsilon} = \left[\underline{a}_v \;\middle|\; \underline{a}_\alpha \right] \left\{ \begin{array}{c} \underline{v} \\ \hline \underline{\alpha} \end{array} \right\} \qquad \text{(B.12)}$$

where

$$\underline{v}^T = \left\langle \left\{ \underline{v}^x \right\}^T , \left\{ \underline{v}^y \right\}^T , \left\{ \underline{v}^z \right\}^T \right.$$

$$\underline{\alpha}^T = \left\langle \left\{ \underline{\alpha}^x \right\}^T , \left\{ \underline{\alpha}^y \right\}^T , \left\{ \underline{\alpha}^z \right\}^T \right. \qquad \text{(B.13)}$$

$\underset{\sim}{a}_v$ and $\underset{\sim}{a}_\alpha$ are matrices in terms of the derivatives of the interpolation functions. The sizes of $\underset{\sim}{a}_v$ and $\underset{\sim}{a}_\alpha$ are 6 x 48 and 6 x 15 respectively.

Since the functions h_i are in terms of ξ, η and ζ the chain rule is applied in order to compute the derivatives with respect to the x, y, z system,

$$
\begin{aligned}
h_{i,x} &= h_{i,\xi}\, \xi_{,x} + h_{i,\eta}\, \eta_{,x} + h_{i,\zeta}\, \zeta_{,x} \\
h_{i,y} &= h_{i,\xi}\, \xi_{,y} + h_{i,\eta}\, \eta_{,y} + h_{i,\zeta}\, \zeta_{,y} \\
h_{i,z} &= h_{i,\zeta}\, \xi_{,z} + h_{i,\eta}\, \eta_{,z} + h_{i,\zeta}\, \zeta_{,z}
\end{aligned}
\qquad (B.14)
$$

In general, the chain rule can be written as

$$
\begin{Bmatrix} \frac{\partial}{\partial\xi} \\ \frac{\partial}{\partial\eta} \\ \frac{\partial}{\partial\zeta} \end{Bmatrix}
=
\begin{bmatrix} x_{,\xi} & y_{,\xi} & z_{,\xi} \\ x_{,\eta} & y_{,\eta} & z_{,\eta} \\ x_{,\zeta} & y_{,\zeta} & z_{,\zeta} \end{bmatrix}
\begin{Bmatrix} \frac{\partial}{\partial x} \\ \frac{\partial}{\partial y} \\ \frac{\partial}{\partial z} \end{Bmatrix}
= \left[J\right]
\begin{Bmatrix} \frac{\partial}{\partial x} \\ \frac{\partial}{\partial y} \\ \frac{\partial}{\partial z} \end{Bmatrix}
\qquad (B.15)
$$

The matrix $[J]$ is known as the Jacobian matrix. The elements of the Jacobian matrix can easily be found using Eq. B.4. The derivatives required in Eq. B.15 are obtained using the inverse of Eq. B.16 as

$$
\begin{Bmatrix} h_{i,x} \\ h_{i,y} \\ h_{i,z} \end{Bmatrix}
= \left[J\right]^{-1}
\begin{Bmatrix} h_{i,\xi} \\ h_{i,\eta} \\ h_{i,\zeta} \end{Bmatrix}
\qquad (B.16)
$$

For given numerical values of ξ, η and ζ the derivatives of the interpolation function can be computed. Then from Eq. B.17 and B.16, all derivatives required for the numerical evaluation of the strain-displacement matrix, Eq. B.13, can be obtained.

B.4 Static Condensation

The standard static condensation procedure is applied to condense out the additional degrees of freedom α_i.

From Eq. B.13 and B.1, the element stiffness matrix can be written as

$$\underset{\sim}{\tilde{k}} = \int_{Vol} \begin{Bmatrix} \underline{a}_v^T \\ a_\alpha^T \end{Bmatrix} \underline{c} \left\langle \underline{a}_v \quad \underline{a}_\alpha \right\rangle dV \tag{B.17}$$

In partitioned form

$$\underset{\sim}{\tilde{k}} = \begin{bmatrix} \tilde{\underline{k}}_{vv} & \tilde{\underline{k}}_{v\alpha} \\ \tilde{\underline{k}}_{\alpha v} & \tilde{\underline{k}}_{\alpha\alpha} \end{bmatrix} \tag{B.18}$$

where

$$\tilde{\underline{k}}_{vv} = \int_{Vol} \underline{a}_v^T \, \underline{c} \, \underline{a}_v \, dV$$

$$\tilde{\underline{k}}_{v\alpha} = \tilde{\underline{k}}_{\alpha v} = \int_{Vol} \underline{a}_v^T \, \underline{c} \, \underline{a}_\alpha \, dv$$

$$\tilde{\underline{k}}_{\alpha\alpha} = \int_{Vol} \underline{a}_\alpha^T \, \underline{c} \, \underline{a}_\alpha \, dV \tag{B.19}$$

Nodal forces $\underline{Q}_v$ and $\underline{Q}_\alpha$ are related to the nodal displacements as

$$\begin{Bmatrix} \underline{Q}_v \\ \hline \underline{Q}_\alpha \end{Bmatrix} = \begin{bmatrix} \tilde{\underline{k}}_{vv} & \tilde{\underline{k}}_{v\alpha} \\ \tilde{\underline{k}}_{\alpha v} & \tilde{\underline{k}}_{\alpha\alpha} \end{bmatrix} \begin{Bmatrix} \underline{v} \\ \hline \underline{\alpha} \end{Bmatrix} \tag{B.20}$$

The work done by the nodal forces in deforming the element is

$$W = \frac{1}{2}\left\langle \underline{v}^T,\ \alpha^T \right\rangle \begin{Bmatrix} \underline{Q}_v \\ --- \\ \underline{Q}_\alpha \end{Bmatrix}$$

$$= \frac{1}{2}\ \underline{v}^T\ \underset{\sim}{\underline{k}}_{vv}\ \underline{v} + \alpha^T\ \underset{\sim}{\underline{k}}_{\alpha v}\ \underline{v} + \frac{1}{2}\ \alpha^T\ \underset{\sim}{\underline{k}}_{\alpha\alpha}\ \underline{\alpha} \qquad \text{(B.21)}$$

Minimizing W with respect to the additional degrees of freedom, i.e.

$$\frac{\partial W}{\partial \alpha_i^x} = \frac{\partial W}{\partial \alpha_i^y} = \frac{\partial W}{\partial \alpha_i^z} = 0 \qquad i=1,2,3,4,5 \qquad \text{(B.22)}$$

leads to

$$\underline{\alpha} = -\left[\underset{\sim}{\underline{k}}_{\alpha\alpha}\right]^{-1} \underset{\sim}{\underline{k}}_{\alpha v}\ \underline{v} \qquad \text{(B.23)}$$

Therefore

$$\underline{Q}_v = \left[\underset{\sim}{\underline{k}}_{vv} - \underset{\sim}{\underline{k}}_{v\alpha}\left[\underset{\sim}{\underline{k}}_{\alpha\alpha}\right]^{-1} \underset{\sim}{\underline{k}}_{\alpha v}\right]\ v \qquad \text{(B.24)}$$

The condensed stiffness matrix of the element with respect to the nodal displacement amplitudes $\underline{v}$ is

$$\underline{k} = \underset{\sim}{\underline{k}}_{vv} - \underset{\sim}{\underline{k}}_{v\alpha}\left[\underset{\sim}{\underline{k}}_{\alpha\alpha}\right]^{-1} \underline{k}_{\alpha v} \qquad \text{(B.25)}$$

Similarly the condensed form of the strain-displacement transformation matrix is

$$\underline{a} = \underline{a}_v - \underline{a}_\alpha\left[\underset{\sim}{\underline{k}}_{\alpha\alpha}\right]^{-1} \underset{\sim}{\underline{k}}_{\alpha v} \qquad \text{(B.26)}$$

B.5 Numerical Integration of Element Stiffness Matrix

The element stiffness is given by Eq. B.26. The numerical integration necessary to form $\tilde{\underline{k}}_{vv}$ is briefly discussed. Similar computations are involved in obtaining other matrices in Eq. B.26.

The expression for $\tilde{\underline{k}}_{vv}$ in the local coordinate system (ξ, η, ζ) is

$$\tilde{\underline{k}}_{vv} = \int_{-1}^{1} \int_{-1}^{1} \int_{-1}^{1} \underline{a}_v^T \, \underline{c} \, \underline{a}_v \; J \, d\xi \, d\eta \, d\zeta \tag{B.27}$$

where J is the determinant of the Jacobian matrix (Eq. B.16). The direct application of one-dimensional integration formulas yields

$$\tilde{\underline{k}}_{vv} = \sum_{i=1}^{3} \sum_{j=1}^{3} \sum_{m=1}^{2} W_i W_i W_i \; J(\xi_i, \eta_j, \zeta_m) \left[\underline{a}_v(\xi_i, \eta_j, \zeta_m)\right]^T \underline{c} \left[\underline{a}_v(\xi_i, \eta_j, \zeta_m)\right] \quad \ldots\ldots\ldots (B.28)$$

where (ξ_i, η_j, ζ_m) are the integration points and W_i , W_j , W_m are approximate weight functions.

B.6 Consistent Mass Matrix

The mass matrix formulation for any element is based on the same displacement assumptions as those used to formulate the element stiffness matrix (Eq. B.6). The element displacements can be written is the form

$$\begin{Bmatrix} v^x \\ v^y \\ v^z \end{Bmatrix} = \left[H\right] \left\{\underline{v}\right\} \tag{B.29}$$

where $\underline{v}$ is defined in Eq. B.14 and $\underline{H}$ is a matrix of interpolation functions. The mass matrix for the element $\underline{m}$, is

$$\underline{m} = \int_{Vol} \rho \, \underline{H}^T \, \underline{H} \, dV \qquad \text{(B.30)}$$

The volume integration is carried out analogous to the integration described for the stiffness matrix (Sec. B.5).

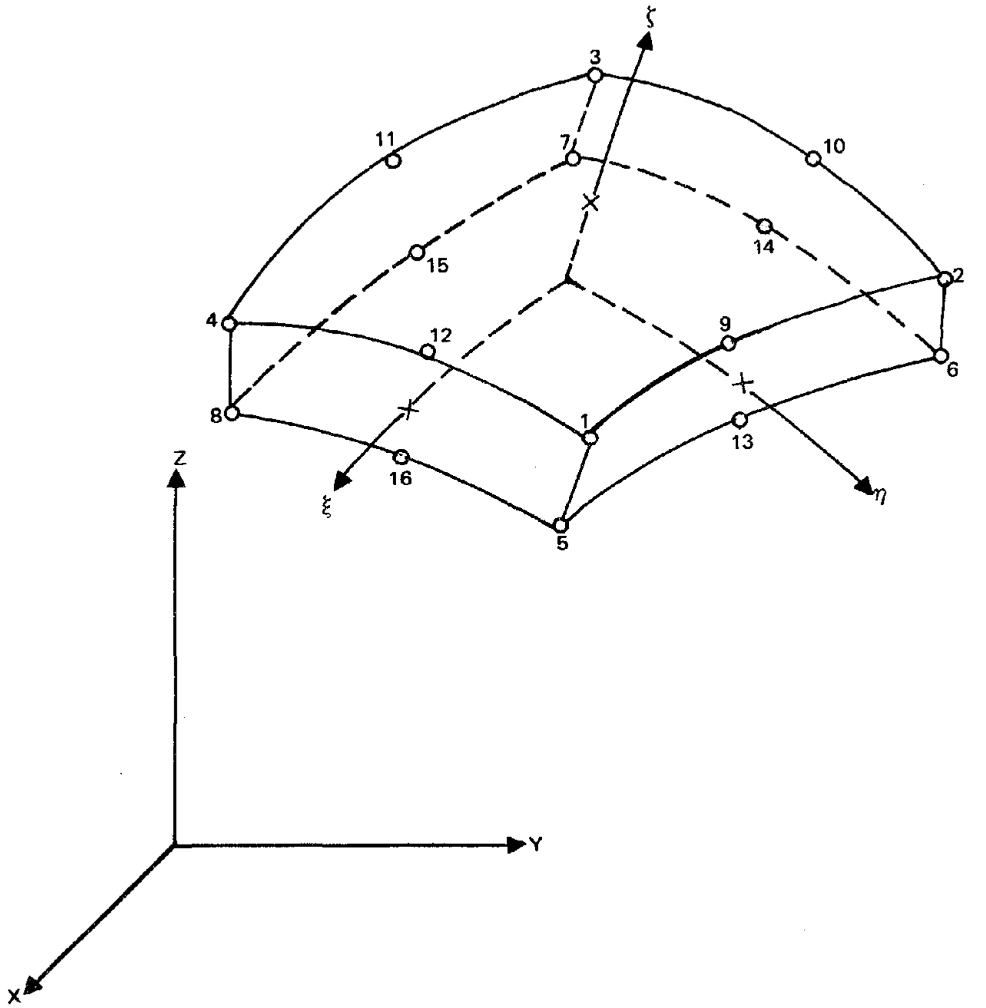

NODE NUMBER	GLOBAL COORDINATE	LOCAL COORDINATE
1	(x_1, y_1, z_1)	(1, 1, 1)
2	(x_2, y_2, z_2)	(-1, 1, 1)
3	(x_3, y_3, z_3)	(-1, -1, 1)
4	(x_4, y_4, z_4)	(1, -1, 1)
5	(x_5, y_5, z_5)	(1, 1, -1)
6	(x_6, y_6, z_6)	(-1, 1, -1)
7	(x_7, y_7, z_7)	(-1, -1, -1)
8	(x_8, y_8, z_8)	(1, -1, -1)
9	(x_9, y_9, z_9)	(0, 1, 1)
10	(x_{10}, y_{10}, z_{10})	(-1, 0, 1)
11	(x_{11}, y_{11}, z_{11})	(0, -1, 1)
12	(x_{12}, y_{12}, z_{12})	(1, 0, -1)
13	(x_{13}, y_{13}, z_{13})	(0, 1, -1)
14	(x_{14}, y_{14}, z_{14})	(-1, 0, -1)
15	(x_{15}, y_{15}, z_{15})	(0, -1, -1)
16	(x_{16}, y_{16}, z_{16})	(1, 0, 1)

FIG. B1. 16 NODE SHELL ELEMENT

APPENDIX C - DERIVATIONS OF THE COMPLEX FREQUENCY RESPONSE FUNCTIONS FOR HYDRODYNAMIC PRESSURE

C.1 Preliminaries

Appendix C presents the solution of the wave equation for the complex frequency response function for hydrodynamic pressures acting on the upstream face of the idealized arch dam. In cylindrical coordinates the governing equation for hydrodynamic pressure p is

$$\frac{\partial^2 p}{\partial r^2} + \frac{1}{r}\frac{\partial p}{\partial r} + \frac{1}{r^2}\frac{\partial^2 p}{\partial \theta^2} + \frac{\partial^2 p}{\partial z^2} = \frac{1}{C^2}\frac{\partial^2 p}{\partial t^2} \tag{C.1}$$

where C is the velocity of sound in water, t is time and r, θ and z are the radial, angular and depth coordinates respectively (see Fig. 2.1). For harmonic ground acceleration $\ddot{v}_g(t) = e^{i\omega t}$, the hydrodynamic pressures $p(r,\theta,z,t)$ can be expressed as

$$p(r,\theta,z,t) = \overline{p}(r,\theta,z)e^{i\omega t} \tag{C.2}$$

where ω is the excitation frequency and $\overline{p}(r,\theta,z)$ is the complex frequency response function for hydrodynamic pressure. In terms of $\overline{p}$ the governing equation becomes

$$\frac{\partial^2 \overline{p}}{\partial r^2} + \frac{1}{r}\frac{\partial \overline{p}}{\partial r} + \frac{1}{r^2}\frac{\partial^2 \overline{p}}{\partial \theta^2} + \frac{\partial^2 \overline{p}}{\partial z^2} = -\frac{\omega^2}{C^2}\overline{p} \tag{C.3}$$

Letting $\overline{p} = \rho(r)\Theta(\theta)\zeta(z)$, Eq. C.3 separates into three equations as follows

$$\zeta''(z) + \alpha^2\zeta(z) = 0 \tag{C.4a}$$

$$\Theta''(\theta) + \mu^2\Theta(\theta) = 0 \tag{C.4b}$$

$$\rho''(r) + \frac{1}{r}\rho'(r) + \left(\frac{\omega^2}{C^2} - \alpha^2 - \frac{\mu^2}{r^2}\right)\rho(r) = 0 \tag{C.4c}$$

where ( )' and ( )" signify the first and second derivative of ( ) with respect to its independent variable. α and μ are separation constants that will be determined from boundary conditions.

The following sections of Appendix C determine expressions for $\overline{p}$ on the upstream face of the dam (r = R) by solving Eq. C.4a to C.4c for boundary conditions associated with horizontal ground motion in the upstream-downstream direction (Sec. C.2), horizontal ground motion in the cross-stream direction (Sec. C.3) and vertical ground motion (Sec. C.4).

C.2 Ground Motion In Upstream-Downstream Direction

C.2.1 Derivation of $\overline{p}^x_{OD}(\theta,z,\omega)$

$\overline{p}^x_{OD}$ is the complex frequency response function for the hydrodynamic pressures on the upstream face of the dam when the excitation is the acceleration of the rigid dam in the x direction but the banks remain stationary. From Chapter 4, Eq. 4.3 and 4.5 the boundary conditions for the governing equation (Eq. C.3) are

$$\frac{\partial \overline{p}}{\partial r}(R,\theta,z) = -\frac{w}{g}\cos\theta \tag{C.5a}$$

$$\frac{\partial \overline{p}}{r\partial \theta}(r,\pi/4,z) = 0 \tag{C.5b}$$

$$\frac{\partial \overline{p}}{\partial z}(r,\theta,o) = 0 \tag{C.5c}$$

$$\overline{p}(r,\theta,H) = 0 \tag{C.5d}$$

$$\frac{\partial \overline{p}}{r\partial \theta}(r,o,z) = 0 \tag{C.5e}$$

where w is the unit weight of water and g is the acceleration due to gravity. In addition to these boundary conditions, no wave reflections at the upstream end of the reservoir (r = B) are permitted.

The solution of Eq. C.4a together with the boundary conditions given in Eq. C.5c and C.5d yield

$$\zeta(z) = A_m \cos \alpha_m z \qquad m = 1,2,\ldots\infty \tag{C.6a}$$

where α_m is the value of α satisfying

$$\alpha_m = \frac{(2m-1)\pi}{2H} \tag{C.6b}$$

and A_m are constants.

The solution of Eq. C.4b together with the boundary conditions given in Eq. C.5b and C.5e result in

$$\Theta(\theta) = B_n \cos \mu_n \theta \qquad n = 0,1,2,3,\ldots \tag{C.7a}$$

where μ_n is the value of μ satisfying

$$\mu_n = 4n \tag{C.7b}$$

and B_n are constants.

Recognizing Eq. C.4c as a form of Bessel's equation, the solution involves the relationship between α_m^2 and $\frac{\omega^2}{C^2}$. If $\frac{\omega^2}{C^2}$ is greater than α_m^2, Hankel functions of the first and second kind of order μ_n, $H_{\mu_n}^{(1)}(\lambda_m r)$ and $H_{\mu_n}^{(2)}(\lambda_m r)$, characterize the solution

$$\rho(r) = C_{mn} H_{\mu_n}^{(1)}(\lambda_m r) + D_{mn} H_{\mu_n}^{(2)}(\lambda_m r) \tag{C.8a}$$

where

$$\lambda_m = \sqrt{\left|\alpha_m^2 - \frac{\omega^2}{C^2}\right|} \tag{C.8b}$$

and C_{mn} and D_{mn} are constants. $H^{(1)}_{\mu_n}(\lambda_m r)$ is associated with a converging wave traveling toward the dam, which can be regarded as a wave reflected from an upstream boundary. Since there is no upstream boundary and thus no reflected waves permitted $C_{mn} = 0$. Therefore, Eq. C.8a becomes

$$\rho(r) = D_{mn}\, H^{(2)}_{\mu_n}(\lambda_m r) \qquad \text{for} \quad \frac{\omega^2}{C^2} < \alpha_m^2 \tag{C.9}$$

If $\frac{\omega^2}{C^2} > \alpha_m^2$, modified Bessel functions of the first and second kind of order μ_n, $I_{\mu_n}(\lambda_m r)$ and $K_{\mu_n}(\lambda_m r)$, characterize the solution

$$\rho(r) = E_{mn}\, I_{\mu_n}(\lambda_m r) + F_{mn}\, K_{\mu_n}(\lambda_m r) \tag{C.10}$$

where E_{mn} and F_{mn} are coefficients determined by the boundary conditions. $I_{\mu_n}(\lambda_m r)$ becomes infinite as r approaches infinity, thus setting $E_{mn} = 0$ eliminates $I_{\mu_n}(\lambda_m r)$ from the solution. Thus,

$$\rho(r) = F_{mn}\, K_{\mu_n}(\lambda_m r) \qquad \text{for} \quad \frac{\omega^2}{C^2} > \alpha_m^2 \tag{C.11}$$

Combining Eq. C.6a, C.7a, C.7b, C.8b, C.9b and C.11, the expression for $\bar{p}_{OD}^{x}$ becomes

$$\bar{p}_{OD}^{x}(r,\theta,z,\omega) = \sum_{m=1}^{m_\ell}\sum_{n=0}^{\infty} D_{mn}\, H_{4n}^{(2)}(\lambda_m r)\cos 4n\theta \cos \alpha_m z$$

$$+ \sum_{m=m_\ell+1}^{\infty}\sum_{n=0}^{\infty} F_{mn}\, K_{4n}(\lambda_m r)\cos 4n\theta \cos \alpha_m z \qquad \text{(C.12)}$$

where m_ℓ is the largest integer "m" satisfying the inequality $\frac{\omega}{C} > \alpha_m$.

The constants D_{mn} and F_{mn} are determined such that $\bar{p}_{OD}^{x}$ satisfies the boundary condition given in Eq. C.5a.

$$\sum_{m=1}^{m_\ell}\sum_{n=0}^{\infty} D_{mn}\frac{d}{dR}\left[H_{4n}^{(2)}(\lambda_m R)\right]\cos 4n\theta \cos \alpha_m z$$

$$+ \sum_{m=m_\ell+1}^{\infty}\sum_{n=0}^{\infty} F_{mn}\frac{d}{dR}\left[K_{4n}(\lambda_m R)\right]\cos 4n\theta \cos \alpha_m z$$

$$= -\frac{w}{g}\cos\theta \qquad \text{(C.13)}$$

Because the set of eigenfunctions $\cos 4n\theta \cos \alpha_m z$, $n = 0, 1, 2,\ldots,$ $m = 1, 2, 3,\ldots$ are an orthogonal set of functions on the interval $(0 \leqslant \theta \leqslant \pi/4)$ $(0 \leqslant z \leqslant H)$, D_{mn} and F_{mn} can be found by classical eigenfunction expansion techniques as

$$D_{mn} = \frac{-\frac{w}{g}\int_{o}^{\pi/4} \cos\theta \cos 4n\theta \, d\theta \int_{o}^{H} \cos \alpha_m z \, dz}{\frac{d}{dR}\left[H_{4n}^{(2)}(\lambda_m R)\right] \int_{o}^{\pi/4} \cos^2 4n\theta \, d\theta \int_{o}^{H} \cos^2 \alpha_m z \, dz} \tag{C.14}$$

$$F_{mn} = \frac{-\frac{w}{g}\int_{o}^{\pi/4} \cos\theta \cos 4n\theta \, d\theta \int_{o}^{H} \cos \alpha_m z \, dz}{\frac{d}{dR}\left[K_{4n}(\lambda_m R)\right] \int_{o}^{\pi/4} \cos^2 4n\theta \, d\theta \int_{o}^{H} \cos^2 \alpha_m z \, dz} \tag{C.15}$$

Evaluation of the integrals in Eq. C.14 and C.15 yields

$$\int_{o}^{H} \cos \alpha_m z \, dz = \frac{(-1)^{m+1}}{\alpha_m} \qquad m = 1,2,3,... \tag{C.16a}$$

$$\int_{o}^{H} \cos^2 \alpha_m z \, dz = \frac{H}{2} \qquad m = 1,2,3,... \tag{C.16b}$$

$$\int_{o}^{\pi/4} \cos\theta \cos 4n\theta \, d\theta = \frac{\sqrt{2}}{2} \frac{(-1)^n}{(1-16n^2)} \qquad n = 0,1,2,... \tag{C.16c}$$

$$\int_{o}^{\pi/4} \cos^2 4n\theta \, d\theta = \frac{\pi}{4\,\varepsilon_n} \qquad n = 0,1,2,... \tag{C.16d}$$

where

$$\varepsilon_n \begin{cases} 1 & n = 0 \\ 2 & n = 1,2,3,... \end{cases} \tag{C.16e}$$

The Hankel function can be expressed in terms of Bessel functions J_{4n} and Y_{4n} and differentiated to obtain

$$\frac{d}{dR}\left[H_{4n}^{(2)}(\lambda_m R)\right] = \frac{\lambda_m}{2}\left[A_n(\lambda_m R) - iB_n(\lambda_m R)\right] \tag{C.17a}$$

where $i = \sqrt{-1}$ and

$$A_n(\lambda_m R) = J_{4n-1}(\lambda_m R) - J_{4n+1}(\lambda_m R) \tag{C.17b}$$

$$B_n(\lambda_m R) = Y_{4n-1}(\lambda_m R) - Y_{4n+1}(\lambda_m R) \tag{C.17c}$$

The derivative of the Modified Bessel function $K_{4n}(\lambda_m R)$ can be expressed as

$$\frac{d}{dR}\left[K_{4n}(\lambda_m R)\right] = -\frac{\lambda_m}{2}\left[K_{4n-1}(\lambda_m R) + K_{4n+1}(\lambda_m R)\right] \tag{C.18}$$

The expressions for D_{mn} and F_{mn} can be rewritten by substituting Eq. C.16 and C.17 into Eq. C.14 for D_{mn} and Eq. C.16 and C.18 into Eq. C.15 for F_{mn}. After some simplification,

$$D_{mn} = -\frac{8\sqrt{2}\ w\ \varepsilon_n(-1)^n\ (-1)^{m+1}}{g\pi H(1-16n^2)\ \alpha_m\ \lambda_m}\left[\frac{A_n(\lambda_m R) + iB_n(\lambda_m R)}{A_n^2(\lambda_m R) + B_n^2(\lambda_m R)}\right] \tag{C.19a}$$

$$F_{mn} = +\frac{8\sqrt{2}\ w\ \varepsilon_n(-1)^n\ (-1)^{m+1}}{g\pi H(1-16n^2)\ \alpha_m\ \lambda_m}\left[\frac{1}{K_{4n-1}(\lambda_m R) + K_{4n+1}(\lambda_m R)}\right] \tag{C.19b}$$

The complex frequency response function for pressure on the upstream face ($r = R$) of the dam, $\bar{\bar{p}}_{OD}^{x}(\theta,z,\omega)$, is obtained by substituting the above expressions for D_{mn} and F_{mn} into Eq. C.12. Noting that

$$H_{4n}^{(2)}(\lambda_m r) = J_{4n}(\lambda_m r) - iY_{4n}(\lambda_m r) \tag{C.20}$$

and rearranging terms, Eq. C.12 becomes

$$\bar{p}_{OD}^{x}(\theta,z,\omega) = \frac{16\sqrt{2}\ w\ R}{g\pi^2}\sum_{m=1}^{\infty}\sum_{n=0}^{\infty}\frac{(-1)^m}{(2m-1)}$$

$$\bullet\ \frac{\varepsilon_n(-1)^n}{(1-16n^2)}\left[C_n(\lambda_m R) + iD_n(\lambda_m R)\right]\cos 4n\theta\ \cos\alpha_m z \tag{C.21}$$

Expressions for C_n and D_n differ depending on whether m is smaller or larger than m_ℓ. For $m \leqslant m_\ell$ they are as follows

$$C_n(\lambda_m R) = \frac{\left[A_n(\lambda_m R)\ J_{4n}(\lambda_m R) + B_n(\lambda_m R)\ Y_{4n}(\lambda_m R)\right]}{\lambda_m R\left[A_n^2(\lambda_m R) + B_n^2(\lambda_m R)\right]} \tag{C.22a}$$

$$D_n(\lambda_m R) = \frac{\left[B_n(\lambda_m R)\ J_{4n}(\lambda_m R) - A_n(\lambda_m R)\ Y_{4n}(\lambda_m R)\right]}{\lambda_m R\left[A_n^2(\lambda_m R) + B_n^2(\lambda_m R)\right]} \tag{C.22b}$$

where $A_n(\lambda_m R)$ and $B_n(\lambda_m R)$ are given in Eq. C.17b and C.17c, respectively. For $m > m_\ell$ the above listed functions are as follows:

$$C_n(\lambda_m R) = -\frac{K_{4n}(\lambda_m R)}{\lambda_m R\left[K_{4n-1}(\lambda_m R) + K_{4n+1}(\lambda_m R)\right]} \tag{C.22c}$$

$$D_n(\lambda_m R) = 0 \tag{C.22d}$$

Kotsubo [5] obtained the pressure on the face of rigid arch dams for excitation $\ddot{v}_g^x(t) = -\alpha g \sin\omega t$. Taking the imaginary part of the pressure (Eq. C.2, C.21, and C.22) and multiplying by $-\alpha g$, the result given for p_{OD}^x specializes to Kotsubo's.

C.2.2 Derivation of $\overline{p}_{OB}^{x}(\theta,z,\omega)$

$\overline{p}_{OB}^{x}(\theta,z,\omega)$ is the complex frequency response function for the hydrodynamic pressures on the upstream face of the dam when the excitation is the acceleration of the reservoir banks in the upstream-downstream direction but the dam remains stationary. From Chapter 4, Eq. 4.3c to 4.3e, 4.6a and 4.6b, the boundary conditions for the governing equation (Eq. C.3) are

$$\frac{\partial \overline{p}}{\partial r}(R,\theta,z) = 0 \tag{C.23a}$$

$$\frac{\partial \overline{p}}{r\partial \theta}(r,\pi/4,z) = \frac{1}{\sqrt{2}}\frac{w}{g} \tag{C.23b}$$

$$\frac{\partial \overline{p}}{\partial z}(r,\theta,o) = 0 \tag{C.23c}$$

$$\overline{p}(r,\theta,H) = 0 \tag{C.23d}$$

$$\frac{\partial \overline{p}}{r\partial \theta}(r,o,z) = 0 \tag{C.23e}$$

In addition to these boundary conditions, no wave reflections at the upstream end of the reservoir ($r = \infty$) are permitted.

Because the governing equation as well as the boundary conditions are linear, the principle of superposition applies. The complex frequency response function, $\overline{p}_{OB}^{x}$, can therefore be expressed as:

$$\overline{p}_{OB}^{x} = \overline{p}_{OB}^{x1} + \overline{p}_{OB}^{x2} \tag{C.24}$$

$\overline{p}_{OB}^{x1}$ and $\overline{p}_{OB}^{x2}$ in Eq. C.24 are defined as follows. $\overline{p}_{OB}^{x1}$ is the solution of Eq. C.3 for motion of the banks with the dam removed. Thus, boundary conditions C.23b to C.23e are satisfied but the boundary condition on the upstream face of the dam, Eq. C.23a, is not satisfied. $\overline{p}_{OB}^{x2}$ is the solution of Eq. C.3 for the following boundary conditions:

$$\frac{\partial \overline{p}}{\partial r} (R,\theta,z) = - \frac{\partial \overline{p}_{OB}^{x1}}{\partial r} (R,\theta,z) \tag{C.25a}$$

$$\frac{\partial \overline{p}}{r\partial \theta} (r,\pi/4,z) = 0 \tag{C.25b}$$

and those specified in Eq. C.23c to C.23e.

The complex frequency response function for hydrodynamic pressure due to motion of the banks with the dam removed $\overline{p}_{OB}^{x1}$ can be obtained by superposing the response due to excitation of each of the two banks acting separately

$$\overline{p}_{OB}^{x1} = \overline{p}_{OB}^{1} + \overline{p}_{OB}^{2} \tag{C.26}$$

Consider the rectangular coordinate system $\widetilde{x}$, $\widetilde{y}$, z where $\widetilde{x}$ is directed along the bank $\theta = -\pi/4$, $\widetilde{y}$ along the bank $\theta = \pi/4$ and z is the vertical coordinate (see Fig. 2.1). The $\widetilde{x}$ and $\widetilde{y}$ coordinates are rotated 45° from the x and y coordinates shown in Fig. 2.1. Expressed in the rectangular coordinates $\widetilde{x}$, $\widetilde{y}$, z, the pressure function $\overline{p}_{OB}^{1}$ associated with excitation of only the bank $\widetilde{x} = 0$ is governed by the two-dimensional equivalent of the equation of motion, Eq. C.3, and the boundary conditions given in Eq. C.23b to C.23d.

$$\frac{\partial^2 \overline{p}(\widetilde{x},z)}{\partial \widetilde{x}^2} + \frac{\partial^2 \overline{p}(\widetilde{x},z)}{\partial z^2} = - \frac{\omega^2}{C^2} \overline{p}(\widetilde{x},z) \tag{C.27}$$

$$\frac{\partial \bar{p}}{\partial \tilde{x}} (o,z) = - \frac{1}{\sqrt{2}} \frac{w}{g} \tag{C.28a}$$

$$\frac{\partial \bar{p}}{\partial z} (\tilde{x},o) = 0 \tag{C.28b}$$

$$\bar{p}(\tilde{x},H) = 0 \tag{C.28c}$$

In addition to these boundary conditions, no wave reflections at the upstream end of the reservoir are permitted.

The application of standard separation of variable techniques yields the following expression

$$\bar{p}^{1}_{OB} = \frac{2\sqrt{2}\, w}{g\pi} \left\{ - \sum_{m=1}^{m_\ell} \frac{i(-1)^{m+1}}{(2m-1)\lambda_m} \cos \alpha_m z \, e^{-i\lambda_m \tilde{x}} + \sum_{m=m_\ell+1}^{\infty} \frac{(-1)^{m+1}}{(2m-1)\lambda_m} \cos \alpha_m z \, e^{-\lambda_m \tilde{x}} \right\} \tag{C.29}$$

where λ_m and m_ℓ have been defined previously.

The complex frequency response for hydrodynamic pressure $\bar{p}^{2}_{OB}$ due to similar excitation of only the bank $\tilde{y} = 0$ is obtained by exchanging $\tilde{y}$ for $\tilde{x}$ in the above equations (Eq. C.27 to C.29). Transforming $\tilde{x}$ and $\tilde{y}$ into the cylindrical coordinates, r and θ, the pressure function $\bar{p}^{x1}_{OB}$ due to excitation of both banks (without dam) is obtained from Eq. C.26 as

$$p_{OB}^{\overline{x}1}(r,\theta,z) = \frac{2\sqrt{2}\ w}{g\pi} \Bigg\{ - \sum_{m=1}^{m_\ell} \frac{i(-1)^{m+1}}{(2m-1)\lambda_m}$$

$$\bullet \cos \alpha_m z \left[e^{-i\lambda_m r \sin(\pi/4-\theta)} + e^{-i\lambda_m r \sin(\pi/4+\theta)} \right]$$

$$+ \sum_{m=m_\ell+1}^{\infty} \frac{(-1)^{m+1}}{(2m-1)\lambda_m} \cos \alpha_m z \left[e^{-\lambda_m r \sin(\pi/4-\theta)} \right.$$

$$\left. + e^{-\lambda_m r \sin(\pi/4+\theta)} \right] \Bigg\} \qquad \text{(C.30)}$$

$\overline{p}_{OB}^{x2}$ is obtained from the solution of Eq. C.3 and the boundary conditions given by Eq. C.23c to C.23e and C.25a to C.25b. The general form of the solution for $\overline{p}_{OD}^{x}$ given in Eq. C.12 also applies to $\overline{p}_{OB}^{x2}$ since all boundary conditions except C.25a are satisfied by Eq. C.12.

$$\overline{p}_{OB}^{x2}(r,\theta,z,\omega) = \sum_{m=1}^{m_\ell} \sum_{n=0}^{\infty} D_{mn}\ H_{4n}^{(2)}(\lambda_m r) \cos 4n\theta \cos \alpha_m z$$

$$+ \sum_{m=m_\ell+1}^{\infty} \sum_{n=0}^{\infty} F_{mn}\ K_{4n}(\lambda_m r) \cos 4n\theta \cos \alpha_m z \qquad \text{(C.31)}$$

The complete solution for $\overline{p}_{OB}^{x2}$ is obtained when the coefficients D_{mn} and F_{mn} are determined so that the remaining boundary condition (Eq. C.25a) is satisfied. Using Eq. C.17a to C.17c, C.18, C.30 and C.31, the boundary condition given in Eq. C.25a becomes

$$\sum_{m=1}^{m_\ell}\sum_{n=0}^{\infty}\frac{D_{mn}\lambda_m}{2}\left[A_n(\lambda_m R) - iB_n(\lambda_m R)\right]\cos 4n\theta \cos \alpha_m z$$

$$-\sum_{m=m_\ell+1}^{\infty}\sum_{n=0}^{\infty}\frac{F_{mn}\lambda_m}{2}\left[K_{4n-1}(\lambda_m R) + K_{4n+1}(\lambda_m R)\right]\cos 4n\theta \cos \alpha_m z$$

$$= \frac{2\sqrt{2}\,w}{g\pi}\left\{\sum_{m=1}^{m_\ell}\frac{(-1)^{m+1}}{(2m-1)}\cos \alpha_m z\left[\sin(\pi/4-\theta)\, e^{-i\lambda_m R\sin(\pi/4-\theta)}\right.\right.$$

$$\left. + \sin(\pi/4+\theta)\, e^{-i\lambda_m R\sin(\pi/4+\theta)}\right] + \sum_{m=m_\ell+1}^{\infty}\frac{(-1)^{m+1}}{(2m-1)}$$

$$\bullet \cos \alpha_m z\left[\sin(\pi/4-\theta)\, e^{-\lambda_m R\sin(\pi/4+\theta)}\right.$$

$$\left.\left. + \sin(\pi/4+\theta)\, e^{-\lambda_m R\sin(\pi/4+\theta)}\right]\right\} \qquad (C.32)$$

Because the set of eigenfunctions $\cos 4n\theta$, $n = 0, 1, 2, 3, \ldots$ form an orthogonal set of functions on the interval $0 \leqslant \theta \leqslant \pi/4$, D_{mn} and F_{mn} can be found by standard eigenfunction expansion techniques.

$$D_{mn} = \frac{16\sqrt{2}\,w\,(-1)^{m+1}\,\varepsilon_n\left[A_n(\lambda_m R) + iB_n(\lambda_m R)\right]}{\pi^2 g(2m-1)\lambda_m\left[A_n^2(\lambda_m R) + B_n^2(\lambda_m R)\right]}\,L_n(\lambda_m R) \qquad (C.33)$$

$$F_{mn} = -\frac{16\sqrt{2}\,w\,(-1)^{m+1}\,\varepsilon_n}{\pi^2 g(2m-1)\lambda_m\left[K_{4n-1}(\lambda_m R) + K_{4n+1}(\lambda_m R)\right]}\,G_n(\lambda_m R) \qquad (C.34)$$

where

$$G_n(\lambda_m R) = \int_0^{\pi/4} \left[\sin(\pi/4-\theta)\ e^{-\lambda_m R \sin(\pi/4-\theta)} + \sin(\pi/4+\theta)\ e^{-\lambda_m R \sin(\pi/4+\theta)}\right] \cos 4n\theta\ d\theta \qquad (C.35)$$

$$L_n(\lambda_m R) = \int_0^{\pi/4} \left[\sin(\pi/4-\theta)\ e^{-i\lambda_m R \sin(\pi/4-\theta)} + \sin(\pi/4+\theta)\ e^{-i\lambda_m R \sin(\pi/4+\theta)}\right] \cos 4n\theta\ d\theta \qquad (C.36)$$

A simplified form for the integral $L_n(\lambda_m R)$ is obtained by expressing the exponential terms of Eq. C.36 as a series of Bessel functions and evaluating the resulting integrals. $L_n(\lambda_m R)$ becomes

$$L_n(\lambda_m R) = (-1)^n \left\{ \frac{i\pi}{4} A_n(\lambda_m R) - \sum_{k=0}^{\infty} \varepsilon_{2k}\ J_{2k}(\lambda_m R) \cdot \frac{[16n^2 + 4k^2 - 1]}{[16n^2 - 4k^2 - 4k - 1][16n^2 - 4k^2 + 4k - 1]} \right\} \qquad (C.37)$$

Thus, $\overline{p}_{OB}^{x2}$ is given by Eq. C.31 with coefficients D_{mn} and F_{mn} defined in Eq. C.33 to C.35 and C.37.

The complex frequency response function for hydrodynamic pressures on the upstream face of the dam ($r = R$) when the excitation is the acceleration of the reservoir banks in the upstream-downstream direction but the dam remains stationary, $\overline{p}_{OB}^{x}(\theta,z,\omega)$, is obtained by superposing -- see Eq. C.24 -- the expressions for $\overline{p}_{OB}^{x1}$ (Eq. C.30) and $\overline{p}_{OB}^{x2}$ (Eq. C.31, C.33 to C.35 and C.37). After rearranging terms, the expression for $\bar{p}^x_{OB}$ becomes

$$\bar{p}^x_{OB}(\theta,z,\omega) = \frac{2\sqrt{2}\,wR}{g\pi}\left\{\sum_{m=1}^{\infty}\left[E_m(\lambda_m R) + iF_m(\lambda_m R)\right]\cos\alpha_m z\right.$$

$$\left. + \frac{8}{\pi}\sum_{m=1}^{\infty}\sum_{n=0}^{\infty}\varepsilon_n\left[U_{mn}(\lambda_m R) + iV_{mn}(\lambda_m R)\right]\cos 4n\theta\cos\alpha_m z\right\} \qquad (C.38)$$

where α_m, λ_m and ε_n are given by Eq. C.6b, C.8b and C.16e respectively. Expressions for functions E_m, F_m, U_{mn}, and V_{mn} differ depending on whether m is smaller or larger than m_ℓ; m_ℓ is the largest integer "m" satisfying the inequality $\frac{\omega}{C} > \alpha_m$. For $m < m_\ell$ they are as follows:

$$E_m(\lambda_m R) = \frac{(-1)^m}{(2m-1)\lambda_m R}\left\{\sin\left[\lambda_m R\sin(\pi/4-\theta)\right]\right.$$

$$\left. + \sin\left[\lambda_m R\sin(\pi/4+\theta)\right]\right\} \qquad (C.39a)$$

$$F_m(\lambda_m R) = \frac{(-1)^m}{(2m-1)\lambda_m R}\left\{\cos\left[\lambda_m R\sin(\pi/4-\theta)\right]\right.$$

$$\left. + \cos\left[\lambda_m R\sin(\pi/4+\theta)\right]\right\} \qquad (C.39b)$$

$$U_{mn}(\lambda_m R) = \frac{(-1)^m(-1)^n}{(2m-1)}\left\{T_n(\lambda_m R)\;C_n(\lambda_m R)\right.$$

$$\left. + \frac{\pi}{4}A_n(\lambda_m R)\;D_n(\lambda_m R)\right\} \qquad (C.39c)$$

$$V_{mn}(\lambda_m R) = \frac{(-1)^m(-1)^n}{(2m-1)} \Big\{ T_n(\lambda_m R)\ D_n(\lambda_m R)$$

$$- \frac{\pi}{4} A_n(\lambda_m R)\ C_n(\lambda_m R) \Big\} \tag{C.39d}$$

where

$$T_n(\lambda_m R) = \sum_{k=0}^{\infty} \varepsilon_{2k}\ J_{2k}(\lambda_m R)$$

$$\bullet \frac{(16n^2 + 4k^2 - 1)}{(16n^2 - 4k^2 - 4k - 1)(16n^2 - 4k^2 + 4k - 1)} \tag{C.39e}$$

$C_n(\lambda_m R)$, $D_n(\lambda_m R)$, $A_n(\lambda_m R)$ and $B_n(\lambda_m R)$ are defined in Eq. C.22a, C.22b, C.17a and C.17b respectively. For $m > m_\ell$ the above listed functions are as follows:

$$E_m(\lambda_m R) = \frac{-(-1)^m}{(2m-1)\lambda_m R} \Big[e^{-\lambda_m R \sin(\pi/4-\theta)}$$

$$+ e^{-\lambda_m R \sin(\pi/4+\theta)} \Big] \tag{C.39f}$$

$$F_m(\lambda_m R) = 0 \tag{C.39g}$$

$$U_{mn}(\lambda_m R) = \frac{-(-1)^m}{(2m-1)} C_n(\lambda_m R)\ G_n(\lambda_m R) \tag{C.39h}$$

$$V_{mn}(\lambda_m R) = 0 \tag{C.39i}$$

where $C_n(\lambda_m R)$ and $G_n(\lambda_m R)$ are defined in Eq. C.22c and C.35 respectively.

Taking the imaginary part of the pressure (Eq. C.2, C.38 and C.39) and multiplying by $-\alpha g$, the result given for p^x_{OB} specializes to results obtained by Kotsubo [5] for excitation $\ddot{v}^y_g(t) = -\alpha g \sin \omega t$.

C.2.3 Derivation of $\bar{p}_j^x(\theta,z,\omega)$

$\bar{p}_j^x$ is the complex frequency response function for the hydrodynamic pressures on the upstream face of the dam when the excitation is the acceleration $\ddot{\bar{Y}}_j^x(\omega) = 1$ (see Chapter 4, Eq. 4.4) in the $j\underline{^{th}}$ symmetric natural mode of vibration of the dam (without water). From Chapter 4, Eq. 4.3 and 4.7, the boundary conditions for the governing equation (Eq. C.3) are

$$\frac{\partial\bar{p}}{\partial r}(R,\theta,z) = -\frac{w}{g}\left[\phi_j^{xf}(\theta,z)\cos\theta + \phi_j^{yf}(\theta,z)\sin\theta\right] \qquad \text{(C.40a)}$$

$$\frac{\partial\bar{p}}{r\partial\theta}(r,\pi/4,z) = 0 \qquad \text{(C.40b)}$$

$$\frac{\partial\bar{p}}{\partial z}(r,\theta,o) = 0 \qquad \text{(C.40c)}$$

$$\bar{p}(r,\theta,H) = 0 \qquad \text{(C.40d)}$$

$$\frac{\partial\bar{p}}{r\partial\theta}(r,o,z) = 0 \qquad \text{(C.40e)}$$

where ϕ_j^{xf} and ϕ_j^{yf} are the x and y components, respectively, of the $j\underline{^{th}}$ mode shape evaluated on the upstream face of the dam. In addition to these boundary conditions, no wave reflections are permitted at the upstream end of the reservoir ($r = \infty$).

The general form of the solution for $\bar{p}_{OD}^x$ given in Eq. C.12 also applies to $\bar{p}_j^x$ since all boundary conditions except Eq. C.40a are satisfied by Eq. C.12. Thus,

$$\overline{p}_j^x(r,\theta,z,\omega) = \sum_{m=1}^{m_\ell} \sum_{n=0}^{\infty} D_{mn} H_{4n}^{(2)}(\lambda_m r) \cos 4n\theta \cos \alpha_m z$$

$$+ \sum_{m=m_\ell+1}^{\infty} \sum_{n=0}^{\infty} F_{mn} K_{4n}(\lambda_m r) \cos 4n\theta \cos \alpha_m z \qquad \text{(C.41)}$$

The complete solution for $\overline{p}_j^x$ is obtained when the coefficients D_{mn} and F_{mn} are determined so that the remaining boundary condition (Eq. C.40a) is satisfied. Using Eq. C.17a to C.17c, C.18 and C.41, the boundary condition becomes

$$\sum_{m=1}^{m_\ell} \sum_{n=0}^{\infty} \frac{D_{mn} \lambda_m}{2} \left[A_n(\lambda_m R) - iB_n(\lambda_m R)\right] \cos 4n\theta \cos \alpha_m z$$

$$- \sum_{m=m_\ell+1}^{\infty} \sum_{n=0}^{\infty} \frac{F_{mn} \lambda_m}{2} \left[K_{4n-1}(\lambda_m R)\right.$$

$$\left. - K_{4n+1}(\lambda_m R)\right] \cos 4n\theta \cos \alpha_m z$$

$$= - \frac{w}{g} \left[\phi_j^{xf}(\theta,z) \cos \theta + \phi_j^{yf}(\theta,z) \sin \theta\right] \qquad \text{(C.42)}$$

Since the set of eigenfunctions $\cos 4n\theta \cos \alpha_m z$, $n = 0, 1, 2, 3, \ldots$, $m = 1, 2, 3\ldots$ form an orthogonal set of functions on the interval $(0 \leqslant \theta \leqslant \pi/4)$ $(0 \leqslant z \leqslant H)$, D_{mn} and F_{mn} can be found by standard eigenfunction expansion techniques.

$$D_{mn} = - \frac{16\, w\, \varepsilon_n}{\pi g \lambda_m} \; \frac{A_n(\lambda_m R) + iB_n(\lambda_m R)}{A_n^2(\lambda_m R) + B_n^2(\lambda_m R)} \; I_{mn}^j \qquad \text{(C.43a)}$$

$$F_{mn} = \frac{16\ w\ \varepsilon_n\ I^j_{mn}}{\pi g \lambda_m \left[K_{4n-1}(\lambda_m R) + K_{4n+1}(\lambda_m R)\right]} \tag{C.43b}$$

where

$$I^j_{mn} = \frac{1}{H} \int_o^{\pi/4} \int_o^{H} \left[\phi^{xf}_j(\theta,z) \cos\theta + \phi^{yf}_j \sin\theta\right]$$

$$\bullet \cos 4n\theta \cos \alpha_m z\ dz\ d\theta \tag{C.43c}$$

Thus, $\overline{p}^x_j$ is given by Eq. C.41 with coefficients D_{mn} and F_{mn} defined in Eq. C.43a and C.43b. After rearranging terms, the expression for $\overline{p}^x_j$ becomes:

$$\overline{p}^x_j(\theta,z,\omega) = -\frac{16\ w\ R}{g\pi} \sum_{m=1}^{\infty} \sum_{n=0}^{\infty} \varepsilon_n\ I^j_{mn}\Big[C_n(\lambda_m R)$$

$$+\ iD_n(\lambda_m R)\Big] \cos 4n\theta \cos \alpha_m z \tag{C.44}$$

where α_m, λ_m, ε_n, and I^j_{mn} are given by Eq. C.6b, C.8b, C.16e and C.43c respectively. Expressions for functions $C_n(\lambda_m R)$ and $D_n(\lambda_m R)$ differ depending on whether m is smaller or larger than m_ℓ. For $m \leqslant m_\ell$ they are given by Eq. C.22a and C.22b. For $m > m_\ell$ $C_n(\lambda_m R)$ is given by Eq. C.22c and $D_n(\lambda_m R) = 0$.

C.3 Ground Motion In Cross-Stream Direction

C.3.1 Derivation of $\overline{p}^y_{OD}(\theta,z,\omega)$

$\overline{p}^y_{OD}$ is the complex frequency response function for the hydrodynamic pressures on the upstream face of the dam when the excitation is the acceleration of the rigid dam in the y direction (cross-stream, Fig. 2.1) but the banks remain stationary. From Chapter 5, Eq. 5.3c to 5.3e, 5.5a and 5.5b, the boundary conditions for the governing equation (Eq. C.3) are

$$\frac{\partial \overline{p}}{\partial r}(R,\theta,z) = -\frac{w}{g}\sin\theta \tag{C.45a}$$

$$\frac{\partial \overline{p}}{r\partial \theta}(r,\pi/4,z) = 0 \tag{C.45b}$$

$$\frac{\partial \overline{p}}{\partial z}(r,\theta,o) = 0 \tag{C.45c}$$

$$\overline{p}(r,\theta,H) = 0 \tag{C.45d}$$

$$\overline{p}(r,o,z) = 0 \tag{C.45e}$$

In addition to these boundary conditions, no wave reflections are permitted at the upstream end of the reservoir ($r = \infty$).

The expression characterizing $\overline{p}^y_{OD}$ is obtained by following the same steps given in Section C.2.1 for determining $\overline{p}^x_{OD}$. The general form of $\overline{p}^y_{OD}$ satisfying all boundary conditions except C.45a is

$$\overline{p}^y_{OD}(r,\theta,z) = \sum_{m=1}^{m_\ell}\sum_{n=0}^{\infty} D_{mn}\, H^{(2)}_{\mu_n}(\lambda_m r)\ \sin\mu_n\theta\ \cos\alpha_m z$$

$$+ \sum_{m=m_\ell+1}^{\infty}\ \sum_{n=0}^{\infty} F_{mn}\, K_{\mu_n}(\lambda_m r)\ \sin\mu_n\theta\ \cos\alpha_m z \tag{C.46a}$$

where

$$\alpha_m = \frac{(2m-1)\pi}{2H} \tag{C.46b}$$

$$\mu_n = 4n + 2 \tag{C.46c}$$

$$\lambda_m = \sqrt{\left|\alpha_m^2 - \frac{\omega^2}{C^2}\right|} \tag{C.46d}$$

and m_ℓ is the largest integer "m" satisfying the inequality $\omega/C > \alpha_m$. The coefficients D_{mn} and F_{mn} are determined such that p_{OD}^y satisfies the boundary condition given in Eq. C.45a. Substituting Eq. C.46 into Eq. C.45a, the boundary condition becomes

$$\sum_{m=1}^{m_\ell} \sum_{n=0}^{\infty} D_{mn} \frac{d}{dR} \left[H_{\mu_n}^{(2)}(\lambda_m R)\right] \sin \mu_n\theta \cos \alpha_m z$$

$$+ \sum_{m=m_\ell+1}^{\infty} \sum_{n=0}^{\infty} F_{mn} \frac{d}{dR} \left[K_{\mu_n}^{(2)}(\lambda_m R)\right] \sin \mu_n\theta \cos \alpha_m z$$

$$= - \frac{\omega}{g} \sin \theta \tag{C.47}$$

The set of eigenfunctions $\sin \mu_n\theta \cos \alpha_m z$, $n = 0, 1, 2, \ldots$, $m = 1, 2, 3, \ldots$ form an orthogonal set of functions on the intervals $(0 \leqslant \theta \leqslant \pi/4)$, $(0 \leqslant z \leqslant H)$. Thus, D_{mn} and F_{mn} can be found by classical eigenfunction expansion techniques as

$$D_{mn} = - \frac{16\sqrt{2}\, w\, (-1)^{m+1}(-1)^n}{g\pi H(\mu_n^2 - 1)\, \alpha_m\, \lambda_m} \left[\frac{A_n(\lambda_m R) + iB_n(\lambda_m R)}{A_n^2(\lambda_m R) + B_n^2(\lambda_m R)}\right] \tag{C.48a}$$

$$F_{mn} = \frac{16\sqrt{2}\ w\ (-1)^{m+1}(-1)^n}{g\pi H(\mu_n^2 - 1)\ \alpha_m\ \lambda_m} \left[\frac{1}{K_{\mu_n-1}(\lambda_m R) - K_{\mu_n+1}(\lambda_m R)}\right] \quad (C.48b)$$

where

$$A_n(\lambda_m R) = J_{\mu_n-1}(\lambda_m R) - J_{\mu_n+1}(\lambda_m R) \quad (C.48c)$$

$$B_n(\lambda_m R) = Y_{\mu_n-1}(\lambda_m R) - Y_{\mu_n+1}(\lambda_m R) \quad (C.48d)$$

After substituting the above expressions for D_{mn} and F_{mn} into Eq. C.46a and rearranging terms, the pressure on the upstream face (r = R) of the dam, $\bar{p}^y_{OD}(\theta,z,\omega)$, becomes:

$$\bar{p}^y_{OD}(\theta,z,\omega) = \frac{32\sqrt{2}\ w\ R}{g\pi^2} \sum_{m=1}^{\infty}\sum_{n=0}^{\infty} \frac{(-1)^m(-1)^n}{(2m-1)(\mu_n^2-1)}$$

$$\bullet \left[C_n(\lambda_m R) + iD_n(\lambda_m R)\right] \sin \mu_n\theta \cos \alpha_m z \quad (C.49)$$

where α_m, μ_n and λ_m are given by Eq. C.46b to C.46d respectively. Expressions for $C_n(\lambda_m R)$ and $D_n(\lambda_m R)$ differ depending on whether m is smaller or larger than "m_ℓ". For $m \leqslant m_\ell$ they are as follows:

$$C_n(\lambda_m R) = \frac{\left[A_n(\lambda_m R)\ J_{\mu_n}(\lambda_m R) + B_n(\lambda_m R)\ Y_{\mu_n}(\lambda_m R)\right]}{\lambda_m R\left[A_n^2(\lambda_m R) + B_n^2(\lambda_m R)\right]} \quad (C.50a)$$

$$D_n(\lambda_m R) = \frac{\left[B_n(\lambda_m R)\ J_{\mu_n}(\lambda_m R) - A_n(\lambda_m R)\ Y_{\mu_n}(\lambda_m R)\right]}{\lambda_m R\left[A_n^2(\lambda_m R) + B_n^2(\lambda_m R)\right]} \quad (C.50b)$$

where $A_n(\lambda_m R)$ and $B_n(\lambda_m R)$ are given by Eq. C.48c and C.48d. For $m > m_\ell$ the above functions are as follows:

$$C_n(\lambda_m R) = - \frac{K_{\mu_n}(\lambda_m R)}{\lambda_m R\left[K_{\mu_n - 1}(\lambda_m R) + K_{\mu_n + 1}(\lambda_m R)\right]} \tag{C.50c}$$

$$D_n(\lambda_m R) = 0 \tag{C.50d}$$

Kotsubo [5] obtained the pressure on the face of rigid arch dams for excitation $\ddot{v}_g^y(t) = -\alpha g \sin \omega t$. Taking the imaginary part of the pressure (Eq. C.2, C.49 and C.50) and multiplying by $-\alpha g$, the result given for p_{OD}^x specializes to Kotsubo's.

C.3.2 Derivation of $\overline{p}_{OB}^y(\theta,z,\omega)$

$\overline{p}_{OB}^y(\theta,z,\omega)$ is the complex frequency response function for hydrodynamic pressures on the upstream face of the dam when the excitation is the acceleration of the reservoir banks in the cross-stream direction but the dam remains stationary. From Chapter 5, Eq. 5.3c to 5.3e, 5.6a and 5.6b the boundary conditions for the governing equation (Eq. C.3) are

$$\frac{\partial \overline{p}}{\partial r}(R,\theta,z) = 0 \tag{C.51a}$$

$$\frac{\partial \overline{p}}{r\partial \theta}(r,\pi/4,z) = -\frac{1}{\sqrt{2}}\frac{w}{g} \tag{C.51b}$$

$$\frac{\partial \overline{p}}{\partial z}(r,\theta,o) = 0 \tag{C.51c}$$

$$\overline{p}(r,\theta,H) = 0 \tag{C.51d}$$

$$\overline{p}(r,o,z) = 0 \tag{C.51e}$$

In addition to these boundary conditions, no wave reflections are permitted at the upstream end of the reservoir ($r = \infty$).

Following the procedure of Section C.2.2, $\overline{p}^{y}_{OB}$ is expressed as the superposition of two functions

$$\overline{p}^{y}_{OB} = \overline{p}^{y1}_{OB} + \overline{p}^{y2}_{OB} \tag{C.52}$$

The functions $\overline{p}^{y1}_{OB}$ and $\overline{p}^{y2}_{OB}$ are defined as follows. $\overline{p}^{y1}_{OB}$ is the solution of Eq. C.3 for motion of the banks in the cross-stream direction with the dam removed. Thus, boundary conditions C.51b to C.51e are satisfied but the boundary condition on the upstream face of the dam, Eq. C.51a, is not satisfied. $\overline{p}^{y2}_{OB}$ is the solution of Eq. C.3 for the following boundary conditions:

$$\frac{\partial \overline{p}}{\partial r} (R,\theta,z) = - \frac{\partial \overline{p}^{y1}_{OB}}{\partial \theta} (R,\theta,z) \tag{C.53a}$$

$$\frac{\partial \overline{p}}{r\partial \theta} (r,\pi/4,z) = 0 \tag{C.53b}$$

and those specified in Eq. C.51c to C.51e.

$\overline{p}^{y1}_{OB}$ can be obtained by combining the response due to excitation of each of the banks acting independently (with the dam removed). As in Appendix C.2.2, define $\overline{p}^{1}_{OB}$ and $\overline{p}^{2}_{OB}$ as the complex frequency response functions for excitation of the banks $\widetilde{x} = 0$ and $\widetilde{y} = 0$ respectively ($\widetilde{x}$ and $\widetilde{y}$ are defined in Appendix C.2.2). For cross-stream excitation

$$\overline{p}^{y1}_{OB} = \overline{p}^{1}_{OB} - \overline{p}^{2}_{OB} \tag{C.54}$$

where $\overline{p}^{1}_{OB}$ is given by Eq. C.29. $\overline{p}^{2}_{OB}$ is obtained by exchanging $\widetilde{y}$ for $\widetilde{x}$ in Eq. C.29. Transforming $\widetilde{x}$ and $\widetilde{y}$ into cylindrical coordinates r and θ, the pressure function $\bar{p}_{OB}^{y1}$ due to excitation of both banks (with dam removed) is obtained from Eq. C.54 and C.29 as

$$\bar{p}_{OB}^{y1}(r,\theta,z,\omega) = \frac{2\sqrt{2}\,w}{g\pi}\left\{-\sum_{m=1}^{m_\ell}\frac{i(-1)^{m+1}}{(2m-1)\lambda_m}\right.$$

$$\bullet \cos\alpha_m z\left[e^{-i\lambda_m r\sin(\pi/4-\theta)} - e^{-i\lambda_m r\sin(\pi/4+\theta)}\right]$$

$$+\sum_{m=m_\ell+1}^{\infty}\frac{(-1)^{m+1}}{(2m-1)\lambda_m}\cos\alpha_m z\left[e^{-\lambda_m r\sin(\pi/4-\theta)}\right.$$

$$\left.\left.- e^{-\lambda_m r\sin(\pi/4+\theta)}\right]\right\} \tag{C.55}$$

$\bar{p}_{OB}^{y2}$ is obtained from the solution of Eq. C.3 and the boundary conditions given by Eq. C.51c to C.51e, C.53a and C.53b. The genral form of the solution for $\bar{p}_{OD}^{y}$ given in Eq. C.46 also applies to $\bar{p}_{OB}^{y2}$ since all boundary except C.53a are satisfied by Eq. C.46.

$$\bar{p}_{OB}^{y2}(r,\theta,z,\omega) = \sum_{m=1}^{m_\ell}\sum_{n=0}^{\infty} D_{mn}\,H_{\mu_n}^{(2)}(\lambda_m r)\,\sin\mu_n\theta\,\cos\alpha_m z$$

$$+\sum_{m=m_\ell+1}^{\infty}\sum_{n=0}^{\infty} F_{mn}\,K_{\mu_n}(\lambda_m r)\,\sin\mu_n\theta\,\cos\alpha_m z \tag{C.56}$$

The complete solution for $\bar{p}_{OB}^{y2}$ is obtained when the coefficients D_{mn} and F_{mn} are determined so that the remaining boundary condition (Eq. C.53a) is satisfied. Substituting Eq. C.55 and C.56 into Eq. C.53a, the boundary condition becomes

$$\sum_{m=1}^{m_\ell}\sum_{n=0}^{\infty}\frac{D_{mn}\ \lambda_m}{2}\left[A_n(\lambda_m R)\ -\ iB_n(\lambda_m R)\right]\ \sin\mu_n\theta\ \cos\alpha_m z$$

$$-\sum_{m=m_\ell+1}^{\infty}\ \sum_{n=0}^{\infty}\frac{F_{mn}\ \lambda_m}{2}\left[K_{\mu_n-1}(\lambda_m R)\ +\ K_{\mu_n+1}(\lambda_m R)\right]\ \sin\mu_n\theta\ \cos\alpha_m z$$

$$=\frac{2\sqrt{2}\ w}{g\pi}\left\{\sum_{m=1}^{m_\ell}\frac{(-1)^{m+1}}{(2m-1)}\cos\alpha_m z\left[\sin(\pi/4-\theta)\ e^{-i\lambda_m R\ \sin(\pi/4-\theta)}\right.\right.$$

$$\left.-\ \sin(\pi/4+\theta)\ e^{-i\lambda_m R\ \sin(\pi/4+\theta)}\right]+\sum_{m=m_\ell+1}^{\infty}\frac{(-1)^{m+1}}{(2m-1)}$$

$$\bullet\ \cos\alpha_m z\left[\sin(\pi/4-\theta)\ e^{-\lambda_m R\ \sin(\pi/4-\theta)}\right.$$

$$\left.\left.-\ \sin(\pi/4+\theta)\ e^{-\lambda_m R\ \sin(\pi/4+\theta)}\right]\right\} \qquad \text{(C.57)}$$

where Eq. C.46c, C.48c and C.48d define μ_n, $A_n(\lambda_m R)$ and $B_n(\lambda_m R)$. Because the set of eigenfunctions $\sin\mu_n\theta$, $n = 0, 1, 2,\ldots$ form an orthogonal set of functions on the interval $0 \leqslant \theta \leqslant \pi/4$, D_{mn} and F_{mn} can be found by standard eigenfunction expansion techniques as

$$D_{mn}=\frac{32\sqrt{2}\ w\ (-1)^{m+1}\left[A_n(\lambda_m R)\ +\ iB_n(\lambda_m R)\right]}{\pi^2 g(2m-1)\left[A_n^2(\lambda_m R)\ +\ B_n^2(\lambda_m R)\right]}\ L_n(\lambda_m R) \qquad \text{(C.58)}$$

$$F_{mn}=-\ \frac{32\sqrt{2}\ w\ (-1)^{m+1}}{\pi^2 g(2m-1)\left[K_{\mu_n-1}(\lambda_m R)\ +\ K_{\mu_n+1}(\lambda_m R)\right]}\ G_n(\lambda_m R) \qquad \text{(C.59)}$$

where

$$G_n(\lambda_m R) = \int_0^{\pi/4} \left[\sin(\pi/4+\theta)\ e^{-\lambda_m R \sin(\pi/4+\theta)} - \sin(\pi/4-\theta)\ e^{-\lambda_m R \sin(\pi/4-\theta)}\right] \sin \mu_n \theta \ d\theta \tag{C.60}$$

$$L_n(\lambda_m R) = \int_0^{\pi/4} \left[\sin(\pi/4+\theta)\ e^{-i\lambda_m R \sin(\pi/4+\theta)} - \sin(\pi/4-\theta)\ e^{-i\lambda_m R \sin(\pi/4-\theta)}\right] \sin \mu_n \theta \ d\theta \tag{C.61}$$

A simplified form for the integral $L_n(\lambda_m R)$ is obtained by expressing the exponential terms as a series of Bessel functions and evaluating the resulting integrals. $L_n(\lambda_m R)$ becomes

$$L_n(\lambda_m R) = (-1)^n \left\{ \sum_{k=0}^{\infty} \varepsilon_{2k}\ J_{2k}(\lambda_m R) \frac{\left(\mu_n^2 + 4k^2 - 1\right)}{\left(\mu_n^2 - 4k^2 - 4k - 1\right)\left(\mu_n^2 - 4k^2 + 4k - 1\right)} - \frac{i\pi}{4} A_n(\lambda_m R) \right\} \tag{C.62}$$

where

$$\varepsilon_{2k} = \begin{cases} 1 & k = 0 \\ 2 & k = 1, 2, 3, \ldots \end{cases} \tag{C.63}$$

Thus, $\bar{p}_{OB}^{y2}$ is given by Eq. C.56 with coefficients D_{mn} and F_{mn} defined in Eq. C.58 to C.60 and C.62.

$\bar{p}_{OB}^{y}$ is obtained by superposing -- see Eq. C.52 -- the expressions for $\bar{p}_{OB}^{y1}$ (Eq. C.55) and $\bar{p}_{OB}^{y2}$ (Eq. C.58 to C.60 and C.62). After rearranging terms, the expression for $\bar{p}_{OB}^{y}(\theta,z,\omega)$ on the upstream face of the dam ($r = R$) becomes

$$\bar{p}_{OB}^{y}(\theta,z,\omega) = \frac{2\sqrt{2}\, w\, R}{g\pi} \left\{ \sum_{m=1}^{\infty} \left[E_m(\lambda_m R) + iF_m(\lambda_m R)\right] \cos \alpha_m z \right.$$

$$\left. + \frac{16}{\pi} \sum_{m=1}^{\infty} \sum_{n-0}^{\infty} \left[U_{mn}(\lambda_m R) + iV_{mn}(\lambda_m R)\right] \sin \mu_n \theta \cos \alpha_m z \right\} \qquad \text{.......(C.64)}$$

where α_m, μ_n, λ_m and ε_n are given by Eq. C.46b, c, d and C.63 respectively. Expressions for functions E_m, F_m, U_{mn} and V_{mn} differ depending on whether m is smaller or larger than m_ℓ. For $m \leqslant m_\ell$ they are as follows

$$E_m(\lambda_m R) = \frac{(-1)^m}{(2m-1)\lambda_m R} \left\{ \sin\left[\lambda_m R \sin(\pi/4+\theta)\right] - \sin\left[\lambda_m R \sin(\pi/4-\theta)\right] \right\} \qquad \text{(C.65a)}$$

$$F_m(\lambda_m R) = \frac{(-1)^m}{(2m-1)\lambda_m R} \left\{ \cos\left[\lambda_m R \sin(\pi/4+\theta)\right] - \cos\left[\lambda_m R \sin(\pi/4-\theta)\right] \right\} \qquad \text{(C.65b)}$$

$$U_{mn}(\lambda_m R) = \frac{(-1)^m(-1)^n}{(2m-1)} \left\{ T_n(\lambda_m R)\ C_n(\lambda_m R) \right.$$

$$\left. + \frac{\pi}{4} A_n(\lambda_m R)\ D_n(\lambda_m R) \right\} \tag{C.65c}$$

$$V_{mn}(\lambda_m R) = - \frac{(-1)^m(-1)^n}{(2m-1)} \left\{ T_n(\lambda_m R)\ D_n(\lambda_m R) \right.$$

$$\left. - \frac{\pi}{4} A_n(\lambda_m R)\ C_n(\lambda_m R) \right\} \tag{C.65d}$$

where

$$T_n(\lambda_m R) = \sum_{k=0}^{\infty} \varepsilon_{2k}\ J_{2k}(\lambda_m R)$$

$$\bullet \frac{(\mu_n^2 + 4k^2 - 1)}{(\mu_n^2 - 4k^2 - 4k - 1)(\mu_n^2 - 4k^2 + 4k - 1)} \tag{C.65e}$$

$A_n(\lambda_m R)$, $B_n(\lambda_m R)$, $C_n(\lambda_m R)$ and $D_n(\lambda_m R)$ are defined in Eq. C.48a, C.48b, C.50a and C.50b respectively. For $m > m_\ell$ the above listed functions are as follows:

$$E_m(\lambda_m R) = - \frac{(-1)^m}{(2m-1)\lambda_m R} \left[e^{-\lambda R \sin(\pi/4-\theta)} \right.$$

$$\left. - e^{-\lambda_m R \sin(\pi/4-\theta)} \right] \tag{C.65f}$$

$$F_m(\lambda_m R) = 0 \tag{C.65g}$$

$$U_{mn}(\lambda_m R) = -\frac{(-1)^m}{(2m-1)} C_n(\lambda_m R)\ G_n(\lambda_m R) \qquad \text{(C.65h)}$$

$$V_{mn}(\lambda_m R) = 0 \qquad \text{(C.65i)}$$

where $C_n(\lambda_m R)$ and $G_n(\lambda_m R)$ are defined in Eq. C.50c and C.60 respectively.

Taking the imaginary part of the pressure (Eq. C.2, C.64 and C.65) and multiplying by $-\alpha g$, the result given for p^y_{OB} specializes to results obtained by Kotsubo [5] for excitation $\ddot{v}^y_g(t) = -\alpha g \sin \omega t$.

C.3.3 Derivation of $\bar{p}^y_j(\theta,z,\omega)$

$\bar{p}^y_j$ is the complex frequency response function for the hydrodynamic pressures on the upstream face of the dam when the excitation is the acceleration $\bar{\ddot{Y}}^y_j(\omega) = 1$ (see Chapter 5, Eq. 5.4) in the j^{th} antisymmetric natural mode of vibration of the dam (without water). From Chapter 5, Eq. 5.3c to 5.3e, 5.7a and 5.7b, the boundary conditions for the governing equation (Eq. C.3) are

$$\frac{\partial \bar{p}}{\partial r}(R,\theta,z) = -\frac{w}{g}\left[\phi^{xf}_j(\theta,z)\cos\theta + \phi^{yf}_j(\theta,z)\sin\theta\right] \qquad \text{(C.66a)}$$

$$\frac{\partial \bar{p}}{r\partial \theta}(r,\pi/4,z) = 0 \qquad \text{(C.66b)}$$

$$\frac{\partial \bar{p}}{\partial z}(r,\theta,o) = 0 \qquad \text{(C.66c)}$$

$$\bar{p}(r,\theta,H) = 0 \qquad \text{(C.66d)}$$

$$\bar{p}(r,o,z) = 0 \qquad \text{(C.66e)}$$

where ϕ_j^{xf} and ϕ_j^{yf} are the x and y components, respectively, of the $j^{\underline{th}}$ antisymmetric mode shape evaluated on the upstream face of the dam. In addition to these boundary conditions, no wave reflections are permitted at the upstream end of the reservoir ($r = \infty$).

The general form of the solution for $\overline{p}_{OB}^{y}$ given in Eq. C.46 also applies to $\overline{p}_j^y$ since all boundary conditions except Eq. C.67a are satisfied by Eq. C.46. Thus

$$\overline{p}_j^y(r,\theta,z) = \sum_{m=1}^{m_\ell} \sum_{n=0}^{\infty} D_{mn} H_{\mu_n}^{(2)}(\lambda_m r) \sin \mu_n\theta \cos \alpha_m z$$

$$+ \sum_{m=m_\ell+1}^{\infty} \sum_{n=0}^{\infty} F_{mn} K_{\mu_n}(\lambda_m r) \sin \mu_n\theta \cos \alpha_m z \tag{C.67}$$

The complete solution for $\overline{p}_j^y$ is obtained when the coefficients D_{mn} and F_{mn} are determined so that the remaining boundary condition (Eq. C.66a) is satisfied. Using Eq. C.67 and Bessel function equalities, the boundary condition becomes

$$\sum_{m=1}^{m_\ell} \sum_{n=0}^{\infty} \frac{D_{mn} \lambda_m}{2} \left[A_n(\lambda_m R) - iB_n(\lambda_m R)\right] \sin \mu_n\theta \cos \alpha_m z$$

$$+ \sum_{m=m_\ell+1}^{\infty} \sum_{n=0}^{\infty} \frac{F_{mn} \lambda_m}{2} \left[K_{\mu_n-1}(\lambda_m R)\right.$$

$$\left. + K_{\mu_n+1}(\lambda_m R)\right] \sin \mu_n\theta \cos \alpha_m z$$

$$= -\frac{w}{g} \left[\phi_j^{xf}(\theta,z) \cos \theta + \phi_j^{yf}(\theta,z) \sin \theta\right] \tag{C.68}$$

Since the set of eigenfunctions $\sin \mu_n \theta \cos \alpha_m z$, $n = 0, 1, 2, \ldots$ form an orthogonal set of functions on the interval $(0 \leqslant \theta \leqslant \pi/4)(0 \leqslant z \leqslant H)$, D_{mn} and F_{mn} can be found by standard eigenfunction expansion techniques as

$$D_{mn} = -\frac{32\ w}{\pi g \lambda_m} \frac{A_n(\lambda_m R) + iB_n(\lambda_m R)}{A_n^2(\lambda_m R) + B_n^2(\lambda_m R)} I_{mn}^j \tag{C.69a}$$

$$F_{mn} = \frac{32\ w}{\pi g \lambda_m} \frac{I_{mn}^j}{K_{\mu_n - 1}(\lambda_m R) + K_{\mu_n + 1}(\lambda_m R)} \tag{C.69b}$$

where

$$I_{mn}^j = \frac{1}{H} \int_0^{\pi/4} \int_0^H \left[\phi_j^{xf}(\theta, z) \cos \theta + \phi_j^{yf}(\theta, z) \sin \theta\right] \sin \mu_n \theta \cos \alpha_m z \; dz \; d\theta \tag{C.69c}$$

Thus, $\overline{p}_j^y$ is given by Eq. C.67 with coefficients D_{mn} and F_{mn} defined in Eq. C.69a and C.69b. After rearranging terms, the expression for $\overline{p}_j^y$ on the upstream face of the dam becomes:

$$\overline{p}_j^y(\theta, z, \omega) = -\frac{32\ w\ r}{g\pi} \sum\sum I_{mn}^j \left[C_n(\lambda_m R) + iD_n(\lambda_m R)\right] \sin \mu_n \theta \cos \alpha_m z \tag{C.70}$$

where α_m, μ_n, λ_m, $A_n(\lambda_m R)$, $B_n(\lambda_m R)$ and I_{mn}^j are given by Eq. C.46b to C.46d, C.48c, C.48d and C.69c respectively. Expressions for $C_n(\lambda_m R)$ and $D_n(\lambda_m R)$ differ depending on whether m is smaller or larger than m_ℓ. For $m \leqslant m_\ell$ they are given by Eq. C.50a and C.50b. For $m > m_\ell$ $C_n(\lambda_m R)$ is given by Eq. C.50c and $D_n(\lambda_m R) = 0$.

C.4 Vertical Ground Motion

C.4.1 Derivation of $\overline{p}_o^z(z,\omega)$

$\overline{p}_o^z(z,\omega)$ is the complex frequency response function for the hydrodynamic pressures on the upstream face of the dam when the excitation is the vertical, rigid-body accelerations of the dam, the reservoir bottom and the banks. From Chapter 6, Eq. 6.3b to 6.3e and 6.4, the boundary conditions for the governing equation (Eq. C.3) are

$$\frac{\partial \overline{p}}{\partial r}(R,\theta,z) = 0 \tag{C.71a}$$

$$\frac{\partial \overline{p}}{r\partial \theta}(r,\pi/4,z) = 0 \tag{C.71b}$$

$$\frac{\partial \overline{p}}{\partial z}(r,\theta,o) = -\frac{w}{g} \tag{C.71c}$$

$$\overline{p}(r,\theta,H) = 0 \tag{C.71d}$$

$$\frac{\partial \overline{p}}{r\partial \theta}(r,o,z) = 0 \tag{C.71e}$$

In addition to these boundary conditions, no wave reflections at the upstream end of the reservoir ($r = \infty$) are permitted.

For ease in satisfying the boundary conditions, the separated equations of motion (Eq. C.4a to C.4c) are rewritten as

$$\zeta''(z) + \left(\frac{\omega^2}{C^2} - \lambda^2\right)\zeta(z) = 0 \tag{C.72a}$$

$$\Theta''(\theta) + \mu^2\Theta(\theta) = 0 \tag{C.72b}$$

$$\rho''(r) + \frac{1}{r}\rho'(r) + \left(\lambda^2 - \frac{\mu^2}{r^2}\right)\rho(r) = 0 \tag{C.72c}$$

where λ and μ are separation constants.

The solution of Eq. C.72b together with the boundary conditions given in Eq. C.71b and C.71e yields

$$\Theta(\theta) = B_n \cos \mu_n \theta \tag{C.73a}$$

where μ_n is the value of μ satisfying

$$\mu_n = 4n \qquad n = 0,1,2,... \tag{C.73b}$$

and B_n are undetermined coefficients.

The solution of Eq. C.72c that satisfies boundary condition C.71a and the condition assuring no wave reflections at the upstream end of the reservoir depends on the form of λ. If λ is an imaginary number, a solution does not exist. When $\lambda = 0$ Eq. C.72c reduces to an equation of the Euler type. The general solution is

$$\rho(r) = \begin{cases} A_o + B_o \ln r & \mu_n = 0,\ \lambda = 0 \\ A_1 r^{\mu_n} + B_1 r^{-\mu_n} & \mu_n \neq 0,\ \lambda = 0 \end{cases} \tag{C.74}$$

where A_o, B_o, A_1 and B_1 are constants and μ_n are the values of μ defined in Eq. C.73b. Evaluating the constants such that $\rho(r)$ satisfies the appropriate boundary condition results in $A_1 = B_0 = B_1 = 0$. Thus when $\lambda = 0$ there is a solution only in the case $n = 0$,

$$\rho(r) = A_o \qquad \text{for } \lambda = 0 \tag{C.75}$$

When λ is a real number Eq. C.72c is a form of Bessel's equation. Hankel functions of the first and second kind of order μ_n, $H^{(1)}_{\mu_n}(\lambda r)$ and $H^{(2)}_{\mu_n}(\lambda r)$, characterize the solution. However, as explained in Section C.2.1, $H^{(1)}_{\mu_n}(\lambda r)$ is omitted from the solution because it can be regarded as a wave reflected from the upstream boundary ($r = \infty$). The solution is

$$\rho(r) = D_{mn} H^{(2)}_{\mu_n}(\lambda_{mn} r) \qquad \begin{matrix} n = 0,1,2\ldots; \\ m = 1,2,3\ldots \end{matrix} \qquad \text{(C.76)}$$

where D_{mn} is a constant and λ_{mn} are the values of λ that satisfy the boundary condition given by Eq. C.71a.

The solution of Eq. C.72a involves the relationship between λ^2_{mn} and ω^2/C^2. If ω^2/C^2 is greater than λ^2_{mn} (including $\lambda_{mn} = 0$) the solution of Eq. C.72a that satisfies boundary condition Eq. C.71d is

$$\zeta(z) = E_{mn} \sin\left[(H - z)\sqrt{\frac{\omega^2}{C^2} - \lambda^2_{mn}}\right] \qquad \text{(C.77)}$$

where E_{mn} is a constant. If ω^2/C^2 is less than λ^2_{mn} the solution that satisfies the boundary condition is

$$\zeta(z) = F_{mn} \sinh\left[(H - z)\sqrt{\lambda^2_{mn} - \frac{\omega^2}{C^2}}\right] \qquad \text{(C.78)}$$

Combining Eq. C.73, C.75, C.76, C.77 and C.78 the expression for $\bar{p}^z_o(r,z,\omega)$ becomes

$$\overline{p}_o^z(r,z,\omega) = A_o \sin\left[\frac{\omega}{C}(H - z)\right]$$

$$+ \sum_{m=1}^{m_\ell} \sum_{n=0}^{\infty} D_{mn} H_{4n}^{(2)}(\lambda_{mn} r)$$

$$\bullet \cos 4n\theta \sin\left[(H - z)\sqrt{\frac{\omega^2}{C^2} - \lambda_{mn}^2}\right]$$

$$+ \sum_{m=m_\ell+1}^{\infty} \sum_{n=0}^{\infty} E_{mn} H_{4n}^{(2)}(\lambda_{mn} r)$$

$$\bullet \cos 4n\theta \sinh\left[(H - z)\sqrt{\frac{\omega^2}{C^2} - \lambda_{mn}^2}\right] \tag{C.79}$$

where m_ℓ is the largest value of m such that $\frac{\omega}{C} > \lambda_{mn}$. $\overline{p}_o^z$ satisfies the remaining boundary condition if the constants are

$$A_o = \frac{w}{g} \bullet \frac{1}{\frac{\omega}{C} \cos\left(\frac{\omega H}{C}\right)} \tag{C.80a}$$

$$D_{mn} = E_{mn} = 0 \tag{C.80b}$$

After substituting Eq. C.80 into Eq. C.79 and rearranging terms, the complex frequency response for pressure $\overline{p}_o^z(z,\omega)$ becomes

$$\overline{p}_o(z,\omega) = \frac{2\ w\ H}{g\pi} \frac{\sin\left[\frac{\pi}{2}\frac{\omega}{\omega_1^r}\left(1 - \frac{z}{H}\right)\right]}{\frac{\omega}{\omega_1^r}\cos\left[\frac{\pi}{2}\left(\frac{\omega}{\omega_1^r}\right)\right]} \tag{C.81a}$$

where

$$\omega_1^r = \frac{\pi C}{2H} \tag{C.81b}$$

Kotsubo [5] obtained the pressure on the face of rigid arch dams for excitation $\ddot{v}_g^z(t) = -\alpha g \sin \omega t$. Taking the imaginary part of the pressure (Eq. C.2 and C.81) and multiplying by $-\alpha g$, the result given for p_o^z specializes to Kotsubo's.

APPENDIX D - COMPUTATION OF HYDRODYNAMIC TERMS

This appendix presents the method used in the computer program (Appendix H) to compute the hydrodynamic loads on the dam due to horizontal excitation of the arch dam - reservoir system.

D.1 Ground Motion in the Upstream-Downstream Direction

The vector of nodal point loads associated with hydrodynamic pressures on the upstream face of the dam due to harmonic ground motion in the upstream-downstream direction (see Chapter 4, Section 4.3.4) is

$$\bar{\underline{Q}}^{f}(\omega) = \bar{\underline{Q}}^{x}_{OD}(\omega) + \bar{\underline{Q}}^{x}_{OB}(\omega) + \sum_{k=1}^{J} \bar{\dot{Y}}^{x}_{k}(\omega)\ \bar{\underline{Q}}_{k}(\omega) \qquad \text{(D.1)}$$

where the force vectors $\bar{\underline{Q}}^{x}_{OD}$, $\bar{\underline{Q}}^{x}_{OB}$ and $\bar{\underline{Q}}^{x}_{k}$ are static equivalents of the corresponding pressure functions $\bar{p}^{x}_{OD}$, $\bar{p}^{x}_{OB}$, and $\bar{p}^{x}_{k}$ (Chapter 4, Eq. 4.8 to 4.10). Taking advantage of the symmetry of the mode shapes, dam geometry and pressure functions and applying the principle of virtual work, the generalized hydrodynamic loads can be expressed in integral form as

$$\left\{\phi^{f}_{j}\right\}^{T} \bar{\underline{Q}}^{x}_{OD} = 2 \int_{0}^{H} \int_{0}^{\pi/4} \phi^{fr}_{j}(\theta,z)\ \bar{p}^{x}_{OD}(\theta,z,\omega)\ R\ d\theta\ dz \qquad \text{(D.2a)}$$

$$\left\{\phi^{f}_{j}\right\}^{T} \bar{\underline{Q}}^{x}_{OB} = 2 \int_{0}^{H} \int_{0}^{\pi/4} \phi^{fr}_{j}(\theta,z)\ \bar{p}^{x}_{OB}(\theta,z,\omega)\ R\ d\theta\ dz \qquad \text{(D.2b)}$$

$$\left\{\phi^{f}_{j}\right\}^{T} \bar{\underline{Q}}^{x}_{k} = 2 \int_{0}^{H} \int_{0}^{\pi/4} \phi^{fr}_{j}(\theta,z)\ \bar{p}^{x}_{k}(\theta,z,\omega)\ R\ d\theta\ dz \qquad \text{(D.2c)}$$

where $\underline{\phi}_j^f$ is a sub-vector of the $j^{\underline{th}}$ symmetric mode shape $\underline{\phi}_j$ of the dam (without water in the reservoir) containing elements associated with DOF on the upstream face of the dam. $\phi^{fr}(\theta,z)$ is the continuous function analogue for the radial component of $\underline{\phi}_j^f$. Since the pressure acts normal to the upstream face of the dam, only the radial component of the mode shape (i.e., the component normal to the upstream face) is required for determining the generalized hydrodynamic loads. Note that in Chapter 4, $\phi_j^{fr}(\theta,z)$ is expressed in terms of its x and y components (see Fig. 2.1) as

$$\phi_j^{fr}(\theta,z) = \phi_j^{fx}(\theta,z) \cos\theta + \phi_j^{fy}(\theta,z) \sin\theta \tag{D.3}$$

Substitution of the expressions for pressure from Chapter 4 (Eq. 4.8 to 4.11) into Eq. D.2 and interchanging integration and summation gives

$$\left\{\phi_j^f\right\}^T \bar{\underline{Q}}_{OB}^x = \frac{32\sqrt{2}\, w\, R^2 H}{g\pi^2} \sum_{m=1}^{\infty}\sum_{n=0}^{\infty} \frac{(-1)^m}{(2m-1)} \frac{\varepsilon_n(-1)}{(1-16n^2)} I_{mn}^j \bullet \left[C_n(\lambda_m R) + iD_n(\lambda_m R)\right] \tag{D.4}$$

$$\left\{\phi_j^f\right\}^T \bar{\underline{Q}}_{OB}^x = \frac{4\sqrt{2}\, w\, R^2 H}{g\pi} \left\{ \frac{1}{H} \int_0^H \int_0^{\pi/4} \phi_j^{fr}(\theta,z) \bullet \left[\sum_{m=1}^{\infty} \left[E_m(\lambda_m R) + iF_m(\lambda_m R)\right] \cos\alpha_m z\right] d\theta\, dz + \frac{8}{\pi} \sum_{m=1}^{\infty}\sum_{n=0}^{\infty} \varepsilon_n I_{mn}^j \left[U_{mn}(\lambda_m R) + iV_{mn}(\lambda_m R)\right] \right\} \tag{D.5}$$

$$\left\{\phi_j^f\right\}^T \bar{Q}_k = \frac{32\ w\ R^2 H}{g\pi} \sum_{m=1}^{\infty}\sum_{n=0}^{\infty} \varepsilon_n I_{mn}^j I_{mn}^k \left[C_n(\lambda_m R) + iD_n(\lambda_m R)\right] \tag{D.6}$$

where $C_n(\lambda_m R)$, $D_n(\lambda_m R)$, $E_m(\lambda_m R)$, $F_m(\lambda_m R)$, $U_{mn}(\lambda_m R)$, $V_{mn}(\lambda_m R)$, α_m, λ_m, ε_n, and I_{mn}^j are given in Eq. 4.11. I_{mn}^j can be rewritten using Eq. 4.11c and D.3 as

$$I_{mn}^j = \frac{1}{H} \int_0^H \int_0^{\pi/4} \phi_j^{fr}(\theta,z) \cos 4n\theta \cos \alpha_m z \; d\theta \; dz \tag{D.7}$$

The expressions C_n, D_n, U_{mn} and V_{mn} needed to compute the generalized loads (Eq. D.4 to D.6) can be obtained using standard Bessel function evaluation techniques. The functions C_n and D_n are discussed further in Appendix E. However, the procedure for determining I_{mn}^j and the integral portion of Eq. D.5 require additional explanation.

Using the finite element descritization of the dam, the mode shapes on the upstream face of the dam, $\underline{\phi}_j^{fr}$, are obtained at the upstream face nodal points. Each sixteen node shell element (Fig. H2 and H3) used in the descritization of the dam is oriented such that one of the eight node surfaces coincides with the upstream face. Since the upstream face is a segment of a circular cylinder of radius R, it is convenient to descritize the dam so that the eight node surface associated with element e is defined in cylindrical coordinates (Fig. 2.1) by two values of the height coordinate (z_1^e, z_2^e) and two values of the angular coordinate (θ_1^e, θ_2^e); the value of the radial coordinate is the constant upstream radius R. Thus, the location of the nodes on the upstream surface are defined by the global coordinate system (θ,z). Within this surface element a local coordinate system (ξ,η) is defined such that ξ and η vary from -1 to 1 (see Fig. D1). The global coordinates are given in terms of the local coordinates as

$$\theta^e = \frac{1}{2}(1 - \xi)\theta_1^e + \frac{1}{2}(1 + \xi)\theta_2^e \tag{D.8a}$$

$$z^e = \frac{1}{2}(1 - \eta)z_1^e + \frac{1}{2}(1 + \eta)z_2^e \tag{D.8b}$$

For a particular element e, the values of the mode shape vectors $\underline{\phi}_j^{rf}$ are given at the eight nodal points on the upstream face of the dam. $\underline{\phi}_j^{rf}$ can be expressed as a continuous function within element e as

$$\phi_j^{fre}(\theta,z) = \sum_{i=1}^{8} N_j(\xi,\eta)\phi_{ji}^{fre} \tag{D.9}$$

where ϕ_{ji}^{fre} is the value of $\underline{\phi}_j^{fr}$ at the $i^{\underline{th}}$ nodal point of element e. The interpolation functions N_i are

$$N_1 = \frac{1}{4}(1 - \xi)(1 - \eta)(-\xi - \eta - 1)$$

$$N_2 = \frac{1}{4}(1 - \xi)(1 - \eta)(\xi - \eta - 1)$$

$$N_3 = \frac{1}{4}(1 + \xi)(1 + \eta)(\xi + \eta - 1)$$

$$N_4 = \frac{1}{4}(1 - \xi)(1 + \eta)(-\xi + \eta - 1)$$

$$N_5 = \frac{1}{2}(1 - \xi^2)(1 - \eta)$$

$$N_6 = \frac{1}{2}(1 + \xi)(1 - \eta^2)$$

$$N_7 = \frac{1}{2}(1 - \xi^2)(1 + \eta)$$

$$N_8 = \frac{1}{2}(1 - \xi)(1 - \eta^2) \tag{D.10}$$

The integral I^j_{mn} (Eq. D.7) can be written as the sum of contributions from each eight node element on the upstream face of the dam within the region acted upon by the hydrodynamic forces $(0 \leq \theta \leq \pi/4), (0 \leq z \leq H)$. Letting NEL represent the number of elements within the integration region and substituting Eq. D.8, D.9, and D.10 into Eq. D.7, the integral becomes

$$I^j_{mn} = \frac{1}{H} \sum_{e=1}^{NEL} \left(\frac{\theta_2^e - \theta_1^e}{2}\right)\left(\frac{z_2^e - z_1^e}{2}\right) \int_{-1}^{1} \int_{-1}^{1}$$

$$\cdot \left[\sum_{i=1}^{8} N_i(\xi,\eta)\phi^{fre}_{ji}\right] \cos \alpha_m \left[\left(\frac{z_1^e + z_2^e}{2}\right) + \left(\frac{z_2^e - z_1^e}{2}\right)\eta\right]$$

$$\cos 4n \left[\left(\frac{\theta_1^e + \theta_2^e}{2}\right) + \left(\frac{\theta_2^e - \theta_1^e}{2}\right)\xi\right] d\xi \, d\eta \qquad \text{(D.11)}$$

In the computer program described in Appendix H the above integral (Eq. D.11) is computed by direct integration within each element e. Although numerical integration schemes (such as Gaussian quadrature) could be used to compute I^j_{mn}, the oscillating nature of $\cos 4n\theta$ and $\cos \alpha_m z$ for large values of m and n is difficult to capture with low order polynomial approximations.

The integral in Eq. D.5, I^j, can be written as

$$I^j = \int_0^H \int_0^{\pi/4} \phi^{fr}_j(\theta,z) \, \psi(z) \, d\theta \, dz \qquad \text{(D.12)}$$

where

$$\psi(z) = \sum_{m=1}^{\infty} \left[E_{mn}(\lambda_m R) + iF_m(\lambda_m R) \right] \cos \alpha_m z \tag{D.13}$$

I^j can be written as the sum of contributions from each eight node element on the upstream face of the dam within the region acted upon by the hydrodynamic forces $(0 \leq \theta \leq \pi/4)(0 \leq z \leq H)$. For a particular eight node element e, $\psi(z)$ can be expressed as

$$\psi^e(z) = \sum_{i=1}^{8} N_i(\xi,\eta)\psi_i = \left\{\underline{N}\right\}^T \left\{\underline{\psi}^e\right\} \tag{D.14}$$

where N_i is the interpolation functions given in Eq. D.10 and ψ_i^e is the values of $\psi(z)$ at nodal point i associated with element e. $\left\{\underline{N}\right\}$ and $\left\{\underline{\psi}^e\right\}$ are column vectors with elements N_i and ψ_i. Substituting Eq. D.8, D.9 and D.14 into Eq. D.12, I^j can be written as

$$I^j = \sum_{e=1}^{NEL} \left(\frac{\theta_2^e - \theta_1^e}{2}\right)\left(\frac{z_2^e - z_1^e}{2}\right) \left\{\underline{\psi}^e\right\}^T$$

$$\cdot \int_{-1}^{1} \int_{-1}^{1} \{\underline{N}\}\{\underline{N}\}^T \, d\xi \, d\eta \left\{\underline{\phi}_j^{fre}\right\} \tag{D.15}$$

The direct application of one-dimensional numerical integration formulas yields the value of the integral in Eq. D.15 as

$$\int_{-1}^{1}\int_{-1}^{1}\{\underline{N}\}\{\underline{N}\}^T\,d\xi\,d\eta = \sum_{i=1}^{3}\sum_{k=1}^{3} W_i\,W_k\left\{\underline{N}(\xi_i,\eta_k)\right\}\left\{\underline{N}(\xi_i,\eta_k)\right\}^T \qquad (D.16)$$

where (ξ_i,η_k) are the integration points and W_i, W_k are appropriate weight functions.

D.2 Ground Motion in the Cross-Stream Direction

The vector of nodal point loads associated with hydrodynamic pressures on the upstream face of the dam due to harmonic ground motion in the cross-stream direction (see Chapter 5, Section 5.3.4) is

$$\bar{\underset{\sim}{Q}}^f(\omega) = \bar{\underset{\sim}{Q}}^y_{OD}(\omega) + \bar{\underset{\sim}{Q}}^y_{OB}(\omega) + \sum_{k=1}^{J}\bar{\dot{Y}}^y_k(\omega)\;\bar{\underset{\sim}{Q}}_k(\omega) \qquad (D.17)$$

where the force vectors $\bar{\underset{\sim}{Q}}^y_{OD}$, $\bar{\underset{\sim}{Q}}^y_{OB}$ and $\bar{\underset{\sim}{Q}}^y_k$ are static equivalents of the corresponding pressure functions $\bar{p}^y_{OD}$, $\bar{p}^y_{OB}$ and $\bar{p}^y_k$ respectively (Chapter 5, Eq. 5.8 to 5.10). The generalized hydrodynamic loads can be expressed in integral form as

$$\left\{\phi^f_j\right\}^T\bar{\underset{\sim}{Q}}^y_{OD} = 2\int_o^H\int_o^{\pi/4}\phi^{fr}_j(\theta,z)\;\bar{p}^y_{OD}(\theta,z,\omega)\;R\,d\theta\,dz \qquad (D.18a)$$

$$\left\{\phi^f_j\right\}^T\bar{\underset{\sim}{Q}}^y_{OB} = 2\int_o^H\int_o^{\pi/4}\phi^{fr}_j(\theta,z)\;\bar{p}^y_{OB}(\theta,z,\omega)\;R\,d\theta\,dz \qquad (D.18b)$$

$$\left\{\phi^f_j\right\}^T\bar{\underset{\sim}{Q}}^y_k = 2\int_o^H\int_o^{\pi/4}\phi^{fr}_j(\theta,z)\;\bar{p}^y_k(\theta,z,\omega)\;R\,d\theta\,dz \qquad (D.18c)$$

where $\underline{\phi}_j^f$ is a sub-vector of the $j^{\underline{th}}$ antisymmetric mode shape $\underline{\phi}_j$ of the dam (without water) containing elements associated with DOF on the upstream face of the dam. $\phi_j^{fr}(\theta,z)$ is the continuous function analogue of $\underline{\phi}_j^f$. Substitution of the expressions for pressure from Chapter 5 (Eq. 5.8 to 5.11) into Eq. D.18 and interchanging integration and summation gives

$$\left\{\phi_j^f\right\}^T \bar{\underline{Q}}_{OD}^y = \frac{64\sqrt{2}\, w\, R^2 H}{g\pi^2} \sum_{m=1}^{\infty}\sum_{n=0}^{\infty} \frac{(-1)^m}{(2m-1)} \frac{(-1)^n}{(\mu_n^2-1)} I_{mn}^j \cdot \left[C_n(\lambda_m R) + iD_n(\lambda_m R)\right] \tag{D.19}$$

$$\left\{\phi_j^f\right\}^T \bar{\underline{Q}}_{OB}^y = \frac{4\sqrt{2}\, w\, R^2 H}{g\pi} \left\{\frac{1}{H} \int_0^H \int_0^{\pi/4} \phi_j^{fr}(\theta,z) \cdot \left[\sum_{m=1}^{\infty} \left[E_m(\lambda_m R) + iF_m(\lambda_m R)\right] \cos \alpha_m z\right] d\theta\, dz + \frac{16}{\pi} \sum_{m=1}^{\infty}\sum_{n=0}^{\infty} I_{mn}^j \left[U_{mn}(\lambda_m R) + iV_{mn}(\lambda_m R)\right]\right\} \tag{D.20}$$

$$\left\{\phi_j^f\right\}^T \bar{\underline{Q}}_k^y = -\frac{64\sqrt{2}\, w\, R^2 H}{g\pi} \sum_{m=1}^{\infty}\sum_{n=0}^{\infty} I_{mn}^j\, I_{mn}^k \cdot \left[C_n(\lambda_m R) + iD_n(\lambda_m R)\right] \tag{D.21}$$

where C_n, D_n, E_m, F_m, U_{mn}, V_{mn}, α_m, λ_m, and I^j_{mn} are given in Eq. 5.11. I^j_{mn} can be rewritten as

$$I^j_{mn} = \frac{1}{H} \int_o^H \int_o^{\pi/4} \phi^{fr}_j(\theta,z)\ \sin \mu_n\theta\ \cos \alpha_m z\ d\theta\ dz \qquad \text{(D.22)}$$

The expressions C_n, D_n, U_{mn}, and V_{mn} can be obtained using standard Bessel function evaluation techniques. The procedures for determining I^j_{mn} and the integral portion of Eq. D.20 parallel those already discussed in the previous section (D.1).

D.3 Vertical Ground Motion

The vector of nodal point loads associated with hydrodynamic pressures on the upstream face of the dam due to harmonic vertical ground motion (see Chapter 6, Section 6.3.4) is

$$\bar{\underset{\sim}{Q}}^f(\omega) = \bar{\underset{\sim}{Q}}^z_o(\omega) + \sum_{k=1}^{J} \bar{\ddot{Y}}^z_k(\omega)\ \bar{\underset{\sim}{Q}}^z_k(\omega) \qquad \text{(D.23)}$$

where the force vectors $\bar{\underset{\sim}{Q}}^z_o(\omega)$ and $\bar{\underset{\sim}{Q}}^z_k(\omega)$ are static equivalents of $\bar{p}^z_o(\omega)$ and $\bar{p}^z_k(\omega)$. Since $\bar{p}^z_k$ is identical to the corresponding function, $\bar{p}^x_k$, associated with upstream-downstream ground motion (see Chapter 6), the generalized hydrodynamic load is given by Eq. D.6. Applying the principle of virtual work, the generalized load associated with $\bar{\underset{\sim}{Q}}^z_o$ can be expressed in the integral form as

$$\left\{\phi^f_j\right\}^T \bar{\underset{\sim}{Q}}^z_o = 2 \int_o^H \int_o^{\pi/4} \phi^{fr}_j(\theta,z)\ \bar{p}^z_o(\theta,z,\omega)\ R\ d\theta\ dz \qquad \text{(D.24)}$$

where $\bar{p}_o^z$ is given by Eq. 6.8 in Chapter 6. The procedures for determining the above integral follow those already presented in Section D.1 for evaluating the integral portion of Eq. D.5.

APPENDIX E - LIMIT ANALYSIS

E.1 Bessel Function Behavior

The analytical expressions for hydrodynamic pressures on arch dams given in Chapters 4, 5 and 6 involve Bessel functions of the first kind $J_n(x)$, Bessel functions of the second kind $Y_n(x)$ and modified Bessel functions of the second kind $K_n(x)$ where n is an integer and the argument x is a real number greater than zero. In the expressions for pressures on the dam (Eq. 4.8 to 4.11 and 5.8 to 5.11), the Bessel functions occur in the following form. For $m \leq m_\ell$

$$C_n(x) = \frac{A_n(x)\ J_{4n}(x) + B_n(x)\ Y_{4n}(x)}{x\left[A_n^2(x) + B_n^2(x)\right]} \qquad n = 0,1,2,\ldots \qquad (E.1)$$

$$D_n(x) = \frac{B_n(x)\ J_{4n}(x) - A_n(x)\ Y_{4n}(x)}{x\left[A_n^2(x) + B_n^2(x)\right]} \qquad n = 0,1,2,\ldots \qquad (E.2)$$

where

$$A_n(x) = J_{4n-1}(x) - J_{4n+1}(x) \qquad (E.3)$$

$$B_n(x) = Y_{4n-1}(x) - Y_{4n+1}(x) \qquad (E.4)$$

For $m > m_\ell$

$$C_n(x) = -\frac{K_{4n}(x)}{x\left[K_{4n-1}(x) + K_{4n+1}(x)\right]} \qquad n = 0,1,2,\ldots \qquad (E.5)$$

$$D_n(x) = 0 \qquad n = 0,1,2,\ldots$$

the function given in Eq. E.1, E.2 and E.5 are plotted in Fig. E1 to E3. Although the individual Bessel functions $J_n(x)$ and $Y_n(x)$ oscillate about their null values, and $Y_n(x)$ and $K_n(x)$ are unbounded at $x = 0$, the composite functions $C_n(x)$ and $D_n(x)$ are very well behaved (Fig. E1 to E3). As shown in the figures, as x approaches zero $C_n(x)$ and $D_n(x)$ have limiting values of

$$\lim_{x\to 0} C_n(x) = -\frac{1}{8n} \qquad n = 0,1,2,... \tag{E.6}$$

$$\lim_{x\to 0} D_n(x) = \begin{cases} \pi/4 & n = 0,\ m \le m_\ell \\ 0 & n = 0,\ m > m_\ell \\ 0 & n = 1,2,3... \end{cases} \tag{E.7}$$

Notice that as x approaches zero $C_o(x)$ is the only unbounded function (Eq. E.6 and E.7). In the expressions for hydrodynamic pressures on the dam (Eq. 4.8 to 4.11 and 5.8 to 5.11) the argument x, of the functions $C_n(x)$ and $D_n(x)$ approaches zero as the frequency of excitation approaches the resonant frequencies of the water in the reservoir.

E.2 Gravity Dam Pressures as Limits of Arch Dam Pressures

This section of Appendix E shows that as the central angle of the dam approaches 180° and $R \to \infty$, representing a straight dam in the limit, $\bar{p}^x_{OD}(\theta,z,\omega)$ approaches the previously obtained [22] two-dimensional solution of the wave equation for a straight gravity dam. For an arch dam with central angle $2\theta_a$, $\bar{p}^x_{OD}(\theta,z,\omega)$ can be found as a generalization of Eq. 4.8.

$$\bar{p}^{x}_{OD}(\theta,z,\omega) = \frac{8\ w\ R}{g\pi}\ \frac{\sin\ \theta_a}{\theta_a} \sum_{m=1}^{\infty} \sum_{n=0}^{\infty} \frac{(-1)^n}{2m-1}\ \frac{\varepsilon_n(-1)^n}{(1-\mu_n^2)}$$

$$\bullet \left[C_n(\lambda_m R)\ +\ iD_n(\lambda_m R) \right]\ \cos\ \mu_n\theta\ \cos\ \alpha_m z \qquad \text{(E.8)}$$

where

$$\mu_n = \frac{n\pi}{\theta_a} \qquad n = 0,1,2,... \qquad \text{(E.9a)}$$

and m_ℓ, w, ε_n, λ_m, α_m are given in Eq. 4.11. Expressions for C_n and D_n differ depending on whether m is smaller than m_ℓ or larger than m_ℓ. For $m \leq m_\ell$ they are as follows

$$C_n(\lambda_m R) = \frac{\left[A_n(\lambda_m R)\ J_{\mu_n}(\lambda_m R)\ +\ B_n(\lambda_m R)\ Y_{\mu_n}(\lambda_m R) \right]}{\lambda_m R \left[A_n^2(\lambda_m R)\ +\ B_n^2(\lambda_m R) \right]} \qquad \text{(E.9b)}$$

$$D_n(\lambda_m R) = \frac{B_n(\lambda_m R)\ J_{\mu_n}(\lambda_m R)\ -\ A_n(\lambda_m R)\ Y_{\mu_n}(\lambda_m R)}{\lambda_m R \left[A_n^2(\lambda_m R)\ +\ B_n^2(\lambda_m R) \right]} \qquad \text{(E.9c)}$$

where

$$A_n(\lambda_m R) = J_{\mu_n-1}(\lambda_m R)\ -\ J_{\mu_n+1}(\lambda_m R) \qquad \text{(E.9d)}$$

$$B_n(\lambda_m R) = Y_{\mu_n-1}(\lambda_m R)\ -\ Y_{\mu_n+1}(\lambda_m R) \qquad \text{(E.9e)}$$

For $m > m_\ell$ the above functions are as follows:

$$C_n(\lambda_m R) = -\frac{K_{\mu_n}(\lambda_m R)}{\lambda_m R\left[K_{\mu_n-1}(\lambda_m R) + K_{\mu_n+1}(\lambda_m R)\right]} \tag{E.9f}$$

$$D_n(\lambda_m R) = 0 \tag{E.9g}$$

The above expressions specialize to those given in Eq. 4.8 and 4.11 for dams with $\theta_a = \pi/4$ (90° included angle from bank to bank).

In order to extract the gravity dam pressure expression, $\bar{p}_g(z,\omega)$, from the above expression for arch dams let $\theta_a = \pi/2$ (giving $\mu_n = 2n$), $R \to \infty$ and $\theta = 0$. In addition multiply the numerator and denominator of Eq. E.8 by λ_m and rearrange terms. $\bar{p}^x_{OD}(o,z,\omega)$ can now be written as

$$\bar{p}^x_{OD}(o,z,\omega) = \frac{32\ w\ H}{g\pi^3}\left\{\sum_{m=1}^{\infty}\frac{(-1)^m \cos \alpha_m z}{(2m-1)\sqrt{\left|(2m-1)^2 - \left(\frac{\omega}{\omega_1^r}\right)^2\right|}}\right.$$

$$\left.\bullet \lim_{R\to\infty}\sum_{m=0}^{\infty}\frac{\varepsilon_n(-1)^n}{(1-4n^2)}\ \lambda_m R\left[C_n(\lambda_m R) + iD_n(\lambda_m R)\right]\right\} \tag{E.10}$$

where, from Eq. 4.11b,

$$\lambda_m R = \frac{\pi R}{2H}\sqrt{\left|(2m-1)^2 - \left(\frac{\omega}{\omega_1^r}\right)^2\right|} \tag{E.11}$$

The limit of $\lambda_m RC_n(\lambda_m R)$ and $\lambda_m RD_n(\lambda_m R)$ as $R\to\infty$ can be obtained from Eq. E.9 by replacing the Bessel functions by their asymptotic expansions and taking the limit of the resulting expression. For $m \le m_\ell$ the limiting process gives

$$\lim_{R\to\infty} \lambda_m R\, C_n(\lambda_m R) = 0 \qquad n = 0,1,2,\ldots \qquad \text{(E.12a)}$$

$$\lim_{R\to\infty} \lambda_m R\, D_n(\lambda_m R) = 1/2 \qquad n = 0,1,2\ldots \qquad \text{(E.12b)}$$

For $m > m_\ell$ the limits are

$$\lim_{R\to\infty} \lambda_m R\, C_n(x) = -1/2 \qquad n = 0,1,2,\ldots \qquad \text{(E.12c)}$$

$$\lim_{R\to\infty} \lambda_m R\, D_n(x) = 0 \qquad n = 0,1,2,\ldots \qquad \text{(E.12d)}$$

Substituting the limiting values from Eq. E.12 into Eq. E.10 and taking the limit within the summation term by term. $p^x_{OD}(o,z,\omega)$ can be written as follows:

$$\bar{p}^x_{OD}(0,z,\omega) = \frac{16\ w\ H}{g\pi^3}\left\{\sum_{m=1}^{m_\ell} \frac{i(-1)^m \cos\alpha_m z}{(2m-1)\sqrt{\left|(2m-1)^2 - \left(\frac{\omega}{\omega_1^r}\right)^2\right|}} \sum_{n=0}^{\infty}\frac{\varepsilon_n(-1)^n}{(1-4n^2)}\right.$$

$$\left. - \sum_{m=m_\ell+1}^{\infty} \frac{(-1)^m \cos\alpha_m z}{(2m-1)\sqrt{\left|(2m-1)^2 - \left(\frac{\omega}{\omega_1^r}\right)^2\right|}} \sum_{n=0}^{\infty}\frac{\varepsilon_n(-1)^n}{(1-4n^2)}\right\} \qquad \text{(E.13)}$$

Removing the absolute value sign and noting that

$$\sum_{n=0}^{\infty}\frac{\varepsilon_n(-1)^n}{(1-4n^2)} = \frac{\pi}{2} \qquad \text{(E.14)}$$

The expression given in Eq. E.13 can be written as

$$\bar{p}^{x}_{OD}(o,z,\omega) = \frac{8\ w\ H}{g\pi^2} \sum_{m=1}^{\infty} \frac{(-1)^{m-1}}{(2m-1)\sqrt{\left|(2m-1)^2 - \left(\frac{\omega}{\omega_1^r}\right)^2\right|}} \cos \alpha_m z \tag{E.15}$$

The above equation is identical to the corresponding expression, $\bar{p}_g(z,\omega)$, for straight gravity dams [22].

E.3 Dam Response at Resonant Frequencies of Fluid Domain

If only the fundamental vibration mode of the dam is included, the response at a resonant frequency of the fluid domain can be obtained through a limiting process. If the excitation is only the motion of the base of the dam in the upstream-downstream direction and the banks are stationary (i.e., $\bar{p}^{x}_{OB}(\theta,z,\omega) = \bar{Q}^{x}_{OB}(\theta,z,\omega) = 0$), the response of the dam (from Chapter 4, Eq. 4.14 and 4.17) can be written as follows:

$$\bar{\ddot{Y}}^{x}_{1}(\omega) = \frac{L_1^{ox} + B_1(\omega)}{M_1\left[-1 + 2i\xi_1\left(\frac{\omega_1}{\omega}\right) + \left(\frac{\omega_1}{\omega}\right)^2\right] - B_2(\omega)} \tag{E.16}$$

where

L_1^{ox} = Generalized force due to the mass of the dam

M_1 = Generalized mass of the dam in its fundamental mode of vibration

ξ = Damping ratio of the dam in its fundamental mode of vibration

$\bar{\ddot{Y}}^{x}_{1}(\omega)$ = Complex frequency response function for generalized acceleration of the dam in its fundamental mode of vibration

ω = Excitation frequency

ω_1 = Fundamental natural frequency of the dam

The functions due to hydrodynamic loads on the dam, $B_1(\omega)$ and $B_2(\omega)$, are given in Appendix D (Eq. D.4 and D.6 respectively) as

$$B_1(\omega) = \frac{32\sqrt{2}\ w\ R^2 H}{g\pi^2} \sum_{m=1}^{\infty}\sum_{n=0}^{\infty} \frac{(-1)^m}{(2m-1)} \ \frac{\varepsilon_n(-1)^n}{(1-16n^2)}\ I^1_{mn}\left[C_n(\lambda_m R) + iD_n(\lambda_m R)\right] \qquad \text{.......(E.17)}$$

$$B_2(\omega) = -\frac{32\ w\ R^2 H}{g\pi} \sum_{m=1}^{\infty}\sum_{n=0}^{\infty} \varepsilon_n \left(I^1_{mn}\right)^2 \left[C_n(\lambda_m R) + iD_n(\lambda_m R)\right] \qquad \text{(E.18)}$$

where I^1_{mn}, ε_n, C_n and D_n are given in Chapter 4, Eq. 4.11. Restating Eq. 4.11b,

$$\lambda_m R = \frac{\pi R}{2H} \sqrt{\left|(2m-1)^2 - \left(\frac{\omega}{\omega^r_1}\right)^2\right|} \qquad \text{(E.19)}$$

where the $m^{\underline{th}}$ resonant frequency of the fluid domain is

$$\omega^r_m = (2m-1)\ \frac{\pi C}{2H} \qquad m = 1,2,3,... \qquad \text{(E.20)}$$

When the excitation frequency ω equals the $M^{\underline{th}}$ resonant frequency ω^r_M,

$$\lambda_m R = \begin{cases} 0 & m = M \\ \sqrt{\left|(2m-1)^2 - (2M-1)^2\right|} & m \neq M \end{cases} \qquad \text{(E.21)}$$

The investigation into Bessel function behavior (Section E.1) shows that

$$\lim_{\omega\to\omega^r_M} C_n(\lambda_m R) = \begin{cases} -\infty & n = 0 \\ -\dfrac{1}{8n} & n = 1,2,3,... \end{cases} \qquad \text{(E.22)}$$

$$\lim_{\omega\to\omega_M^r} D_n(\lambda_m R) = \begin{cases} 0 & n = 1,2,3,\ldots \\ \pi/4 & n = 0 \quad \omega\to(\omega_M^r)^+ \\ 0 & n = 0 \quad \omega\to(\omega_M^r)^- \end{cases} \tag{E.23}$$

where $\omega\to(\omega_M^r)^-$ signifies that $\omega < \omega_M^r$ in the limiting process and conversely $\omega\to(\omega_M^r)^+$ signifies that $\omega > \omega_M^r$ in the limiting process. $C_n(\lambda_m R)$ and $D_n(\lambda_m R)$ are smooth functions and are bounded for all values of $\lambda_m R$ except when $n = 0$ and $\lambda_m R\to 0$ (i.e., when $\omega\to\omega_M^r$). However, the $\lim_{\omega\to\omega_M^r} C_n(\lambda_m R)$ and $\lim_{\omega\to\omega_m^r} D_n(\lambda_m R)$ exist for all $m = 1,2,3,\ldots$ and for $n = 1,2,3,\ldots$.
However, $\lim_{\omega\to\omega_M^r} C_o(\lambda_m R)$ does not exist (i.e., $\lim_{\omega\to\omega_M^r} C_o(\lambda_m R)\to -\infty$). Thus, both the functions $B_1(\omega)$ and $B_2(\omega)$, Eq. E.17 and E.18 and consequently the numerator and denominator of Eq. E.16 contain terms that become unbounded as $\omega\to\omega_M^r$.

The limit of Eq. E.16 as $\omega\to\omega_M^r$ can be obtained by factoring out the term that becomes unbounded, $C_o(\lambda_m R)$. Dividing both numerator and denominator by $C_o(\lambda_m R)$ and taking the limit, Eq. E.16 can be rewritten as

$$\lim_{\omega\to\omega_M^r} \bar{\ddot{Y}}_1^x(\omega) = \frac{\dfrac{L_1^{ox}}{C_o(\lambda_m R)} + \dfrac{B_1(\omega)}{C_o(\lambda_m R)}}{\dfrac{M_1\left[-1 + 2i\xi_1\left(\dfrac{\omega_1}{\omega}\right) + \left(\dfrac{\omega_1}{\omega}\right)^2\right]}{C_o(\lambda_m R)} - \dfrac{B_2(\omega)}{C_o(\lambda_m R)}} \tag{E.24}$$

Referring to Eq. E.17 and E.18, all terms in the numerator and denominator of Eq. E.24 approach zero as $\omega \to \omega_m^r$ except the term in $B_1(\omega)$ and $B_2(\omega)$ associated with m = M, n = 0. Thus, the limiting value of Eq. E.21 is

$$\lim_{\omega \to \omega_M^r} \bar{\dot{Y}}_1^x(\omega) = \frac{\sqrt{2}\ (1)^{M}}{\pi (2M1)\ I_{MO}^{1}} \tag{E.25}$$

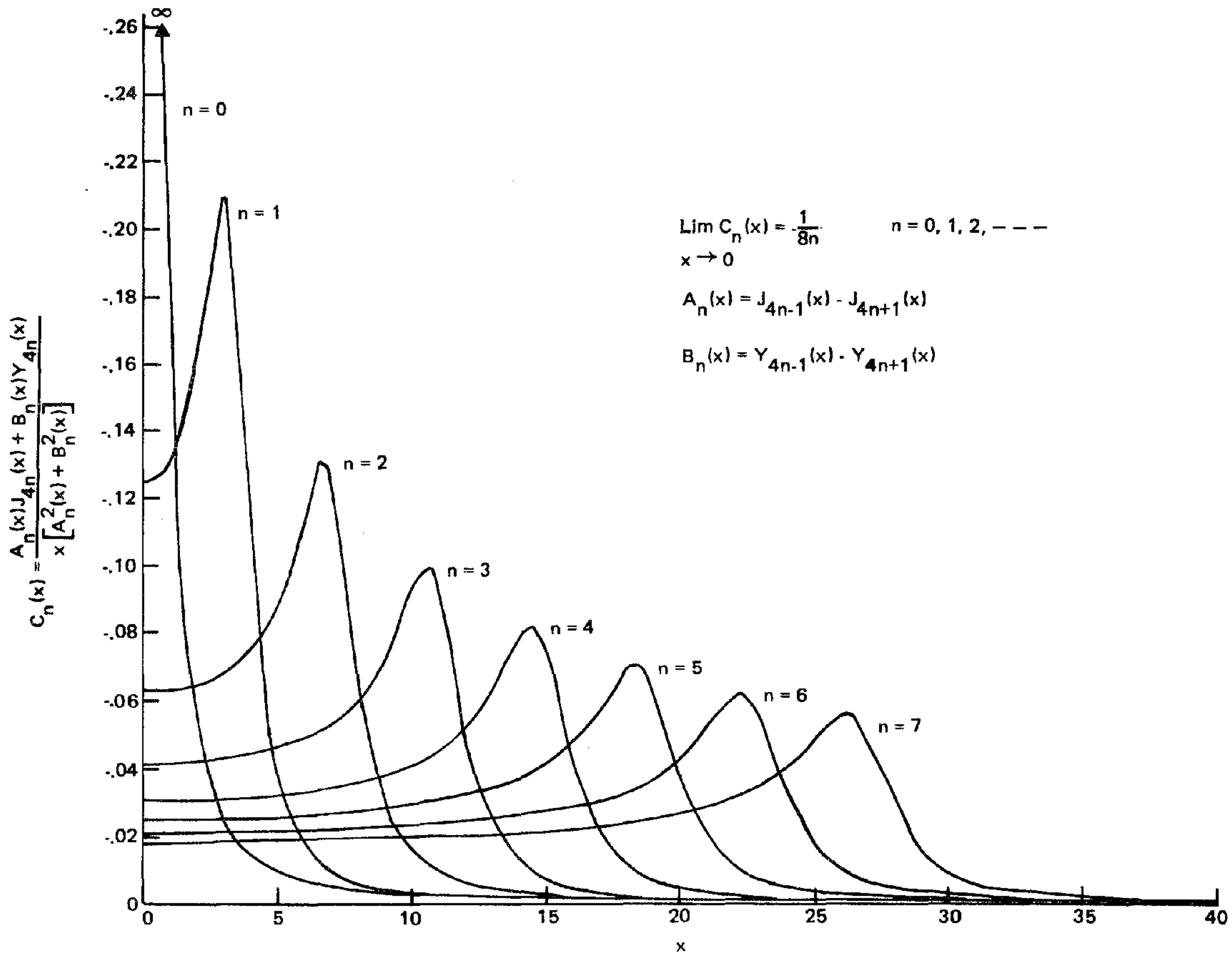

FIG. E1. FUNCTIONS $C_n(x)$ FOR $m \leq m_\ell$

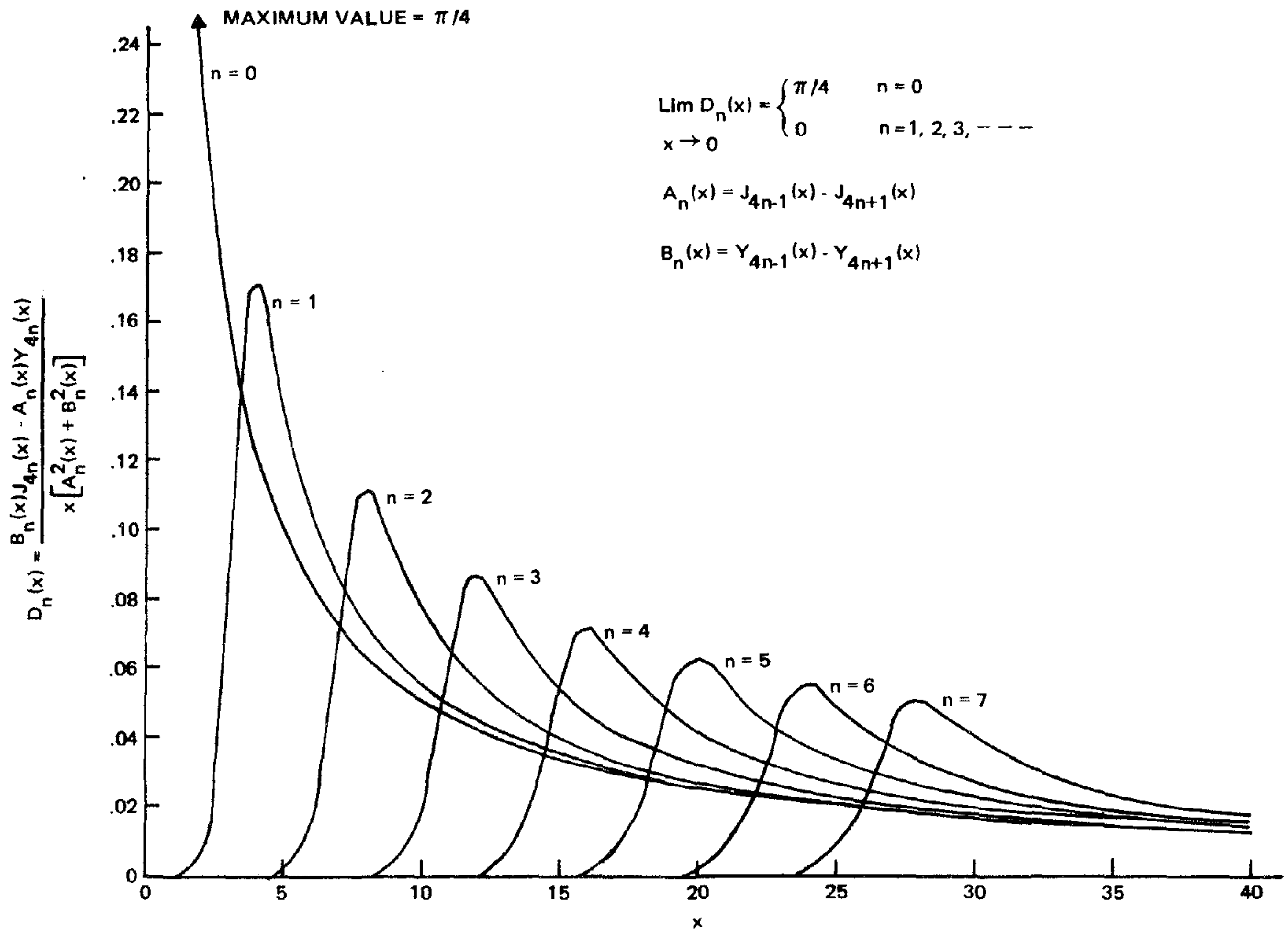

FIG. E2. FUNCTIONS $D_n(x)$ FOR $m \leq m_\ell$

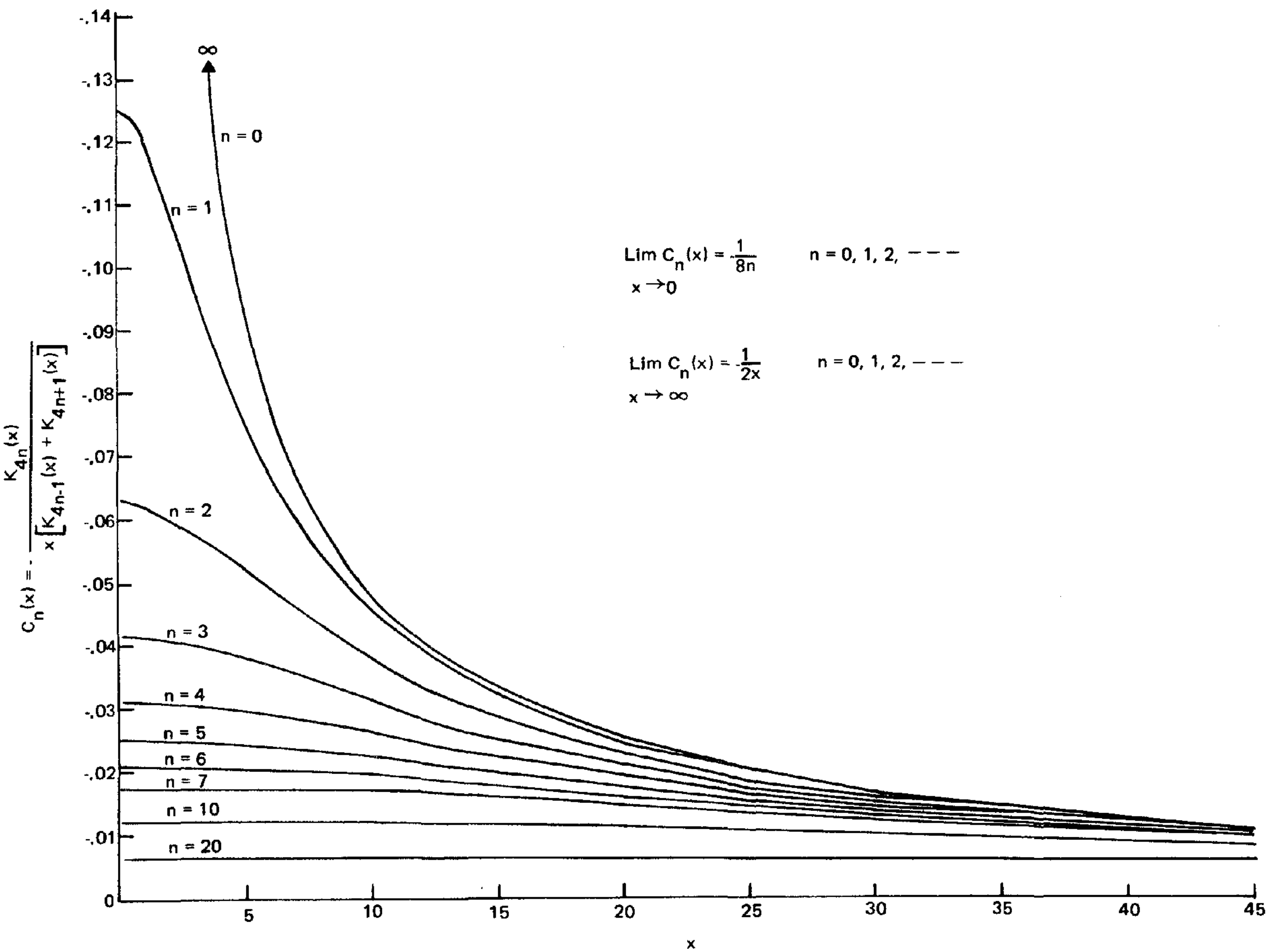

FIG. E3. FUNCTIONS $C_n(x)$ FOR $m > m_\ell$

APPENDIX F - SYMMETRY OF $\underline{S}(\omega)$

F.1 Ground Motion In The Upstream-Downstream Direction

It can be shown that the matrix $\underline{S}(\omega)$ is symmetric. This is most conveniently demonstrated by expressing S_{jk}, for $j \neq k$ (Eq. 4.16) in integral form.

$$S_{jk}(\omega) = +2\omega^2 \int_0^{\pi/4} \int_0^H \phi_j^f(\theta,z)\ \bar{p}_k^x(\theta,z,\omega)\ dz\ d\theta \tag{F.1}$$

The symmetric (with respect to θ) model vector $\underline{\phi}_j^f$ has been replaced by its continuous analogue $\phi_j^f(\theta,z)$ and the continuous pressure distribution $\bar{p}_k^x(\theta,z,\omega)$ replaces the load vector $\underline{\bar{Q}}_k^x(\omega)$. Using expressions for $\bar{p}_k^x$ given in Eq. 4.10, Eq. F.1 may be expressed as

$$S_{jk}(\omega) = -\omega^2\ \frac{32\ w\ R}{g\pi} \int_0^{\pi/4} \int_0^H \left\{ \sum_{m=1}^{\infty} \sum_{n=0}^{\infty} \varepsilon_n\ I_{mn}^k \right.$$

$$\left. \bullet \left[C_n(\lambda_m R) + iD_n(\lambda_m R)\right]\ \cos 4n\theta\ \cos \alpha_m z \right\}$$

$$\phi_j^f(\theta,z)\ dz\ d\theta \tag{F.2}$$

where ε_n, α_m, $\lambda_m R$, I_{mn}^k, C_n and D_n are defined in Eq. 4.11. The term I_{mn}^k (Eq. 4.11c) is an integral involving the mode shape ϕ_k^f. Recognizing that

$$\phi_k^f(\theta,z) = \phi_k^{xf}(\theta,z)\ \cos\theta + \phi_k^{yf}(\theta,z)\ \sin\theta \tag{F.3}$$

where $\phi_k^{xf}(\theta,z)$ and $\phi_k^{yf}(\theta,z)$ are the x and y components of $\phi_k^f(\theta,z)$, I_{mn}^k can be written as

$$I_{mn}^k = \frac{1}{H} \int_o^{\pi/4} \int_o^H \phi_k^f(\theta,z) \cos 4n\theta \cos \alpha_m z \, dz \, d\theta \qquad \text{(F.4)}$$

Substituting Eq. F.4 into F.2 and rearranging,

$$S_{jk}(\omega) = -\omega^2 \frac{32 \; w \; R}{g\pi H} \int_o^{\pi/4} \int_o^H \left\{ \sum_{m=1}^{\infty} \sum_{n=0}^{\infty} \varepsilon_n \right.$$

$$\int_o^{\pi/4} \int_o^H \phi_k^f(\sigma,\tau) \cos 4n\sigma \cos \alpha_m \tau \, d\tau \, d\sigma$$

$$\left. \bullet \left[C_n(\lambda_m R) + iD_n(\lambda_m R) \right] \cos 4n\theta \cos \alpha_m z \right\}$$

$$\phi_j^f(\theta,z) \, dz \, d\theta \qquad \text{(F.5)}$$

Interchanging the integral and summation signs and rearranging,

$$S_{jk}(\omega) = -\omega^2 \frac{32 \; w \; R}{g\pi H} \int_o^{\pi/4} \int_o^H \left\{ \sum_{m=1}^{\infty} \sum_{n=0}^{\infty} \varepsilon_n \right.$$

$$\int_o^{\pi/4} \int_o^H \phi_j^f(\sigma,\tau) \cos 4n\sigma \cos \alpha_m \tau \, d\tau \, d\sigma$$

$$\left. \left[C_n(\lambda_m R) + iD_n(\lambda_m R) \right] \cos 4n\theta \cos \alpha_m z \right\}$$

$$\phi_k^f(\theta,z) \, dz \, d\theta \qquad \text{(F.6)}$$

$$= +2\omega^2 \int_0^{\pi/4} \int_0^H \phi_k^f(\theta,z)\ \overline{p}_j^x(\theta,z,\omega)\ dz\ d\theta \tag{F.7}$$

$$= S_{kj}(\omega) \tag{F.8}$$

Thus, the matrix $\underline{S}(\omega)$ is symmetric.

F.2 Ground Motion In The Cross-Stream Direction

Express S_{jk} for $j \neq k$ (Eq. 5.15) in integral form.

$$S_{jk}(\omega) = +2\omega^2 \int_0^{\pi/4} \int_0^H \phi_j^f(\theta,z)\ \overline{p}_k^y(\theta,z,\omega)\ dz\ d\theta \tag{F.9}$$

in which the antisymmetric (with respect to θ) modal vector $\underline{\phi}_j^f$ has been replaced by its continuous analogue $\phi_j^f\ (\theta,z)$ and the continuous pressure distribution $\overline{p}_k^y(\theta,z,\omega)$ replaces the load vector $\underline{\overline{Q}}_k^y(\omega)$. Using expressions for $\overline{p}_k^y$ given in Eq. 5.10 and the mode shape relationship of Eq. F.3, $\underline{S}(\omega)$ may be expressed

$$S_{jk}(\omega) = -\omega^2\ \frac{64\ w\ R}{g\pi H} \int_0^{\pi/4} \int_0^H \left\{ \sum_{m=1}^{\infty} \sum_{n=0}^{\infty} \right.$$

$$\int_0^{\pi/4} \int_0^H \phi_k^f(\sigma,\tau)\ \sin \mu_n\sigma\ \cos \alpha_m\tau\ d\tau\ d\sigma$$

$$\left. \bullet \left[C_n(\lambda_m R) + iD_n(\lambda_m R) \right]\ \sin \mu_n\theta\ \cos \alpha_m z \right\}$$

$$\phi_j^f(\theta,z)\ dz\ d\theta \tag{F.10}$$

where μ_n, α_m, λ_m, C_n and D_n are defined in Eq. 5.11. Interchanging the integral and summation signs and rearranging,

$$S_{jk}(\omega) = -\omega^2 \frac{64 \; w \; R}{g\pi H} \int_0^{\pi/4} \int_0^H \Bigg\{ \sum_{m=1}^{\infty} \sum_{n=0}^{\infty}$$

$$\int_0^{\pi/4} \int_0^H \phi_j^f(\sigma,\tau) \; \sin \mu_n \sigma \; \cos \alpha_m \tau \; d\tau \; d\sigma$$

$$\bullet \left[C_n(\lambda_m R) + iD_n(\lambda_m R) \right] \; \sin \mu_n \theta \; \cos \alpha_m z \Bigg\}$$

$$\phi_k^f(\theta,z) \; dz \; d\theta \tag{F.11}$$

$$= +2\omega^2 \int_0^{\pi/4} \int_0^H \phi_k^f(\theta,z) \; \bar{p}_j^y(\theta,z,\omega) \; dz \; d\theta \tag{F.12}$$

$$= S_{kj}(\omega) \tag{F.13}$$

Thus, the matrix $\underline{S}(\omega)$ is symmetric.

APPENDIX G - DIMENSIONAL ANALYSIS

In this appendix dimensionless variables will be found for three quantities: the frequency ω_j and mode shape $\underline{\phi}_j$ of the $j^{\underline{th}}$ natural mode of vibration of the dam without water and the complex frequency response function for generalized acceleration of the dam--including hydrodynamic interaction effects--in the $j^{\underline{th}}$ mode of vibration of the dame, $\overline{\ddot{Y}}_j$.

The π theorem assures that any physical quantity can be expressed in terms of dimensionless combinations of variables. This theorem may be stated as follows:

"Any function of N variables

$$f\left(P_1, P_2, P_3, P_4, \ldots P_N\right) = 0 \tag{G.1}$$

may be expressed in terms of (N-K) π products

$$f\left(\pi_1, \pi_2, \pi_3, \ldots \pi_{N-K}\right) = 0 \tag{G.2}$$

where each π product is a dimensionless combination of an arbitrary selected set of K variables and one other; that is,

$$\begin{aligned} \pi_1 &= f\left(P_1, P_2, \ldots P_K, P_{K+1}\right) \\ \pi_2 &= f\left(P_1, P_2, \ldots P_K, P_{K+2}\right) \\ \pi_{N-K} &= f\left(P_1, P_2, \ldots P_K, P_N\right) \end{aligned} \tag{G.3}$$

K is equal to the number of fundamental dimensions required to describe the variables P. If the problem is one in mechanics, all quantities P may be expressed in terms of mass, length and time, and K = 3. In thermodynamics, all quantities may be expressed in terms of mass, length, time and temperature, and K = 4. The arbitrarily selected set of K variables may contain any of the quantities P_i with the restriction that the K set itself may not form a dimensionless combination."*

A set of dimensionless parameters characterizing ω_j, ϕ_j and $\bar{\ddot{Y}}_j$ will be obtained using the π theorem from a set of variables for the specialized arch dam-water system described in Section 7.2. Denoting dimensions M, L and T as mass, length and time respectively, the variablee that describe the system along with their dimensions are:

Symbol	Name	Dimensions
B_1	radial thickness of dam at the crest	L
B_2	radial thickness of dam at the base	L
C	velocity of sound in water	LT^{-2}
E	modulus of elasticity of the dam concrete	$ML^{-1}T^{-2}$
H	depth of water in the reservoir	L
H_d	height of dam	L
R	radius of upstream face of the dam	L
r	radial coordinate of points on the dam	L
θ	angular coordinate of points on the dam	Dimensionless
z	vertical coordinate of points on the dam	L
$\bar{\ddot{Y}}_j$	complex frequency response function for generalized acceleration of the dam including hydrodynamic interaction effects	Dimensionless
α	reflection constant at reservoir bottom for hydrodynamic pressure waves defined in Section 6.3.2; pertinent only for vertical ground motion	Dimensionless
ξ_j	damping ratio for the j^{th} mode of vibration of the dam	Dimensionless

*A.M. Kuethe and J.D. Schetzer, *Foundations of Aerodynamics*, John Wiley and Sons, Inc., New York, second edition, 1959.

$\underline{\phi}_j$	mode shape vector of $j^{\underline{th}}$ natural mode of vibration of the dam	Dimensionless
ρ_d	mass density of dam concrete	ML^{-3}
ρ	mass density of water	ML^{-3}
ν	Poisson's ratio	Dimensionless
ω	excitation frequency	T^{-1}
ω_j	$j^{\underline{th}}$ natural frequency of the dam	T^{-1}

Dimensionless Parameters for ω_j

The $j^{\underline{th}}$ natural frequency of the dam (without water in the reservoir) is a function of the following variables:

$$\omega_j = f(B_1, B_2, R, \nu, E, H_d, \rho_d) \tag{G.4}$$

Write Eq. G.4 in the form of Eq. G.1:

$$f(\omega_j, B_1, B_2, R, \nu, E, H_d, \rho_d) = 0 \tag{G.5}$$

There are eight variables and three fundamental dimensions. Thus, there are five π products. If E, H_d and ρ_d are chosen as the K set denoted in the π theorem, the π products are

$$\pi_i = f(\omega_j, E, H_d, \rho_d)$$

$$\pi_2 = f(B_1, E, H_d, \rho_d)$$

$$\pi_3 = f(B_2, E, H_d, \rho_d)$$

$$\pi_4 = f(R, E, H_d, \rho_d)$$

$$\pi_5 = f(\nu, E, H_d, \rho_d) \tag{G.6}$$

The π theorem guarantees that the π products above can be made dimensionless. As an example, a dimensionless combination of the variables in π_1 can be found in the form $\omega_j E^a H_d^b \rho_d^c$, where a, b and c are constants. In terms of its dimensions the quantity $\omega_j E^a H_d^b \rho_d^c$ becomes

$$\left(T^{-1}\right)\left(ML^{-1}T^{-2}\right)^a\left(L\right)^b\left(ML^{-3}\right)^c \tag{G.7}$$

For π_1 to be dimensionless the exponents of M, L and T must be zero. Thus,

$$\begin{aligned} &M: && a + c = 0 \\ &L: && -a + b - 3c = 0 \\ &T: && -1 - 2a = 0 \end{aligned} \tag{G.8}$$

Solving the above set of simultaneous equations gives a = -1/2, b = 1 and c = 1/2. The π product becomes

$$\pi_1 = \omega_j \; H_d \sqrt{\frac{\rho_d}{E}} \tag{G.9}$$

Following the same procedure, the other π products are

$$\begin{aligned} \pi_2 &= \frac{B_1}{H_d} \\ \pi_3 &= \frac{B_2}{H_d} \\ \pi_4 &= \frac{R}{H_d} \\ \pi_5 &= \nu \end{aligned} \tag{G.10}$$

In terms of the dimensionless π products given above, Eq. G.5 can be written

$$f\left(\omega_j H_d \sqrt{\frac{\rho_d}{E}}\, , \frac{B_1}{H_d}\, , \frac{B_2}{H_d}\, , \frac{R}{H_d}\, , \nu\right) = 0 \tag{G.11}$$

An expression for ω_j is obtained from Eq. G.11 as

$$\omega_j = \frac{1}{H}\sqrt{\frac{E}{\rho_d}}\, f\left(\frac{B_1}{H_d}\, , \frac{B_2}{H_d}\, , \frac{R}{H_d}\, , \nu\right) \tag{G.12}$$

Dimensionless Parameters for $\underline{\phi}_j$

For small damping, the mode shape vector, $\underline{\phi}_j$, is a function of the following variables

$$\underline{\phi}_j = f(B_1, B_2, R, r, \theta, z, \nu, E, H_d, \rho_d) \tag{G.13}$$

Write Eq. G.13 in the form of Eq. G.1:

$$f(\underline{\phi}_j, B_1, B_2, R, r, \theta, z, \nu, E, H_d, \rho_d) = 0 \tag{G.14}$$

There are eleven variables, three fundamental dimensions and, thus, eight π products. Choosing E, H_d and ρ_d as the K set denoted in the π theorem and following the same procedures as used above for ω_j, Eq. G.14 can be written in terms of the eight π products (see Eq. G.2) as

$$f\left(\underline{\phi}_j, \frac{B_1}{H_d}\, , \frac{B_2}{H_d}\, , \frac{R}{H_d}\, , \frac{r}{H_d}\, , \theta, \frac{z}{H_d}\, , \nu\right) = 0 \tag{G.15}$$

An expression for $\underline{\phi}_j$ is obtained from Eq. G.15 as

$$\underline{\phi}_j{}' = f\left(\frac{B_1}{H_d}\, , \frac{B_2}{H_d}\, , \frac{R}{H_d}\, , \frac{r}{H_d}\, , \theta, \frac{z}{H_d}\, , \nu\right) \tag{G.16}$$

Dimensionless Procedures for $\bar{\ddot{Y}}_j$

$\bar{\ddot{Y}}_j$ is a function of the following variables

$$\bar{\ddot{Y}}_j = f(\omega, \nu, B_1, B_2, R, \xi_j, \rho, C, H, \alpha, E, H_d, \rho_d) \qquad (G.17)$$

Write Eq. G.17 in the form of Eq. G.1:

$$f(\bar{\ddot{Y}}_j, \omega, \nu, B_1, B_2, R, \xi_j, \rho, C, H, \alpha, E, H_d, \rho_d) \qquad (G.18)$$

There are fourteen variables, three fundamental dimensions and, thus, eleven π products. Choosing E, H_d and ρ_d as the K set denoted in the π theorem and following the procedures used above for ω_j, Eq. G.18 can be written in terms of the eleven π products (see Eq. G.2) as

$$f\left(\bar{\ddot{Y}}_j, \omega H_d\sqrt{\frac{\rho_d}{E}}, \nu, \frac{B_1}{H_d}, \frac{B_2}{H_d}, \frac{R}{H_d}, \xi_j, \frac{\rho}{\rho_d},\right.$$

$$\left. C\sqrt{\frac{\rho_d}{E}}, \frac{H}{H_d}, \alpha\right) = 0 \qquad (G.19)$$

An alternate form of the above equation can be obtained by substituting the expression for the fundamental natural frequency of the dam ω_1, from Eq. G.12 into Eq. G.19.

$$f\left(\bar{\ddot{Y}}_j, \frac{\omega}{\omega_1}, \nu, \frac{B_1}{H_d}, \frac{B_2}{H_d}, \frac{R}{H_d}, \xi_j, \frac{\rho}{\rho_d},\right.$$

$$\left. C\sqrt{\frac{\rho_d}{E}}, \frac{H}{H_d}, \alpha\right) = 0 \qquad (G.20)$$

The fundamental resonant frequency of the water in the reservoir, $\omega_1^r = \frac{\pi C}{2H}$, normalized with respect to ω_1 (Eq. G.12) can be written as

$$\frac{\omega_1^r}{\omega_1} = C\sqrt{\frac{\rho_d}{E}}\,\frac{H_d}{H}\, f\left(\frac{B_1}{H_d}\,,\ \frac{B_2}{H_d}\,,\ \frac{R}{H_d}\,,\ \nu\right) \tag{G.21}$$

Using Eq. G.21 in place of the π product $C\sqrt{\frac{\rho_d}{E}}$, in Eq. G.20 and rearranging terms, Eq. G.20 yields the following expression for $\overline{\ddot{Y}}_j$:

$$\overline{\ddot{Y}}_j = f\left(\frac{\omega}{\omega_1}\,,\ \nu,\ \frac{B_1}{H_d}\,,\ \frac{B_2}{H_d}\,,\ \frac{R}{H_d}\,,\ \xi_j,\ \frac{\rho}{\rho_d}\,,\ \frac{\omega_1^r}{\omega_1}\,,\ \frac{H}{H_d}\,,\ \alpha\right) \tag{G.22}$$

APPENDIX H - USER'S GUIDE TO COMPUTER PROGRAM

Identification

RADHI: Response of Arch Dams Including Hydrodynamic Interaction To Harmonic Ground Motion

Programmed: Craig Porter, University of California, Berkeley, 1978.

General Description of the Program

The FORTRAN IV computer program RADHI was written for the purpose of investigating the effects of hydrodynamic interaction on the dynamic structural behavior and response of arch dams. The program calculates the modal response of arch dams including hydrodynamic interaction to any of the three components of harmonic ground motion: horizontal ground motion in the upstream-downstream direction, horizontal ground motion in the cross-stream direction and vertical ground motion. The response both including and neglecting the hydrodynamic effects due to motion of the reservoir banks is calculated for the horizontal components of ground motion excitation. The water in the reservoir can be treated as either compressible or incompressible. The response of the dam alone (without water in the reservoir) can also be obtained.

The computer program is based on the sub-structure analysis procedure developed in Chapters 3, 4, 5 and 6 in which the dam-reservoir system is restricted to the special geometries and conditions described in Chapter 2 and Fig. 2.1. Briefly, the upstream face of the dam is a segment of a circular cylinder contained within radially extending banks enclosing a central angle of 90°. The reservoir, which is filled with water of constant depth, extends to infinity in the radial direction. The dam properties are treated as symmetrical about the $x - z$ ($\theta = 0$) plane. The dam is fixed at the base and at the banks.

The overlay feature available for use with CDC computers has been used in the program. The program is composed of several portions which are treated as overlays. Each overlay is loaded into the memory when needed; it is removed from memory when its operations are completed. This feature has resulted in a significant reduction of the storage requirements of the program.

Description of the Overlays

The program is composed of a main overlay, three primary overlays, and three secondary overlays. The functions of the different overlays are described below:

O.L. (0,0) reads in the main control parameters of the problem and directs the control to different primary overlays depending upon the problem type. This main overlay remains in the memory during the entire execution time.

O.L. (1,0) reads in nodal point and element data for the arch dam and forms the element stiffness and consistent mass matrices. The element mass and stiffness matrices are written on tape. This information is later used in forming the global mass and stiffness matrices for the arch dam. The element subroutines utilized in this overlay were taken from the program ADAP [1].

O.L. (2,0) assembles the global mass and stiffness matrices for the dam from the element matrices and solves an eigenvalue problem to compute natural frequencies and mode shapes of the dam (without water in the reservoir). This overlay was taken from the program ADAP [1].

O.L. (3,0) computes the hydrodynamic loads, the inertia loads of the dam due to ground motion excitation, and solves for the complex frequency response for acceleration of the dam in its modal coordinates. Secondary overlays (3,1), (3,2), and (3,3) compute the complex frequency response functions due to excitation in the upstream-downstream, cross-stream, and vertical directions respectively. Note that the response to ground motions in the upstream-downstream and vertical directions require symmetrical mode shapes, while the response to cross-stream ground motion requires anti-symmetric mode shapes.

Saving Mode Shapes and Frequencies

In the dynamic analysis of arch dams, evaluation of the natural frequencies and mode shapes consumes a significant part of the excitation time. Thus, the possibility of using previously evaluated and stored mode shapes and frequencies was built into the program. To utilize this option, the program should be run first to compute the mode shapes and frequencies of the dam (without water in the reservoir). At the end of this job, the data on logical units 1, 8, 9, and 10 should be copied on physical tape(s) and be supplied to the program in subsequent runs for computing the response to harmonic ground motion. The physical tape(s) transfers the following information:

Logical Unit 1 ... Element data

8 ... Nodal point data

9 ... Structure mass matrix

10 ... Mode shapes and frequencies

Subsequent runs require no element and nodal point data cards. Assuming the program exists in binary form, the deck setup and control cards (as required for the CDC 6400 computer at the University of California, Berkeley) for the first and subsequent jobs are shown below:

1. First job

   Job card

   LGO,INPUT.

   REWIND,TAPE1,TAPE2,TAPE3

   REQUEST,SAVE,HI,I,B.(tape number),WRITE,(output user name)

   COPYBF,TAPE1,SAVE

   COPYBF,TAPE8,SAVE

   COPYBF,TAPE9,SAVE

   COPYBF,TAPE10,SAVE

   7-8-9

   Program in binary form

   7-8-9

   Data cards

   6-7-8-9

2. Subsequent jobs

   Job card

   REQUEST,SAVE,HI,I,B.(tape number)

   COPYBF,SAVE,TAPE1

   COPYBF,SAVE,TAPE8

   COPYBF,SAVE,TAPE9

   COPYBF,SAVE,TAPE10

   REWIND,TAPE1,TAPE8,TAPE9,TAPE10

LGO,INPUT

7-8-9

Program in binary form

7-8-9

Data Cards

6-7-8-9

Input Data

A. HEADING CARD (12A6)

This card contains information to be printed as heading for the output

B. MASTER CONTROL CARDS

Two or three of the following cards will be required depending on the type of problem:

Card 1. This card is required for all problems (6I5).

Columns 1-5	NUMNP	Number of nodal points in the system.
6-10	MTOT	Size of available blank common (see note below).
11-15	NF	Number of mode shapes of the dam to be included in the analysis
16-20	NDYN	Parameter identifying type of analysis to be performed. =1 If mode shapes and frequencies are to be computed only. =2 For including the hydrodynamic analysis
21-25	IMODE	=1 If mode shapes and frequencies are to be stored on tape or read from tape.

=0 Otherwise

26-30 IPRM =1 If printout of mode shapes is to be surpressed

=0 Otherwise

Note: The smallest size of the blank common which is required by the program is

MTOT = 7* NUMNP + 4* NMAT + 3970

where NUMNP = Number of nodal points

NMAT = Number of different materials for elements of the dam.

It should be emphasized that the value of MTOT as computed by the above equation, in cases of large structural systems (many degrees of freedom), may be quite inadequate to use. This is because a large number of blocks of equations may be formed and result in excessive exection time. In any problem, the number of blocks of equations (NBLOCK) will be determined from the value of MTOT and other prescribed parameters. In general, larger values of MTOT will result in smaller values of NBLOCK.

In most cases of practical interest (arch dam analysis using a fine mesh) the maximum storage capacity of the computer should be used and the size of blank common (MTOT) should be computed accordingly. This will result in the smallest value of NBLOCK for a particular case. When analyzing small structural systems, partial storage of the computer, and hence a smaller value of MTOT, may be used as long as NBLOCK = 1. In short, the value of NBLOCK should be selected in such a way that the smallest value for NBLOCK is obtained without any waste of computer storage. The user will be able to prescribe MTOT properly after some experience.

Card 2. This card is required for all problems (2F10).

Columns	1-10	RADIUS	Radius of upstream face of dam measured in feet.
	11-20	RADHT	Radius divided by the height of the dam (non-dimensional number).

Card 3. This card is required only when previously computed mode shapes are to be read from tape (3I5).

Columns	1-5	MBAND	Bandwidth of the system of equilibrium equations as computed in the previous run.
	6-10	NUMEL	Total number of elements in the dam.
	11-15	NEQ	Number of equations (degrees of freedom) of the system as computed in the previous run.

C. NODAL POINT COORDINATES AND BOUNDARY CONDITION CARDS (I5, 3F10, 3I5)

No cards are required when mode shapes are to be read from tape. In any other case, one card per nodal point is required unless some nodal points are to be generated.

Columns	1-5	NODE	Nodal point number
	6-15	ANGLE	Angle measured in radians from the center of the dam. The maximum angle occurs at the banks where ANGLE = $\pi/4$.
	16-25	HEIGHT	Vertical coordinate measured in feet

26-35 THICK Radial distance from the vertical upstream face of the dam to the nodal point measured in feet (always a positive number).

36-40 v^x-displacement
41-45 v^y-displacement
46-50 v^z-displacement

fixity code: zero or blank for free component, one for fixed com-component.

Note 1: These cards must be in increasing nodal point numbering sequence. However, if a set of cards is omitted, the corresponding nodal points are generated at equal intervals on a straight line connecting two nodal points for which coordinates are supplied.

Note 2: Due to the symmetry of the problem only half the dam is descritized (see Fig. H1). Input for ground motion in the x direction (upstream-downstream direction) and in the z direction (vertical direction) requires symmetrical boundary conditions for nodal points on the plane of symmetry of the dam. That is, the v^y-displacement for nodal points on the plane of symmetry must be fixed (a one in card column 41-45). Input for ground motion in the y direction (cross-stream direction) requires anti-symmetrical boundary conditions for nodal points on the plane of symmetry of the dam. That is, the v^x-displacement for nodal points on the plane of symmetry must be fixed (a one in card column 36-40).

Note 3: The dam must be descritized such that all elements have the same included angle and the same height on the upstream surface. Hydrodynamic considerations impose this requirement.

Note 4: The dam is only one element thick.

D. THREE-DIMENSIONAL THICK SHELL ELEMENT DATA

No cards are required if mode shapes are to be read from tape. Otherwise supply the following cards:

1. Control Card (3I5)

Columns	5	The number 2
	6-10	Total number of elements
	11-15	Number of different materials (NMAT)

2. Material Properties Cards (I5, 3F10)

One card is required for each material type:

Columns	1-5	Material identification number ($\leq$ NMAT)
	6-15	Modulus of elasticity (pounds/(foot)^2)
	16-25	Poisson's ratio
	26-35	Weight density of material (pounds/(foot)^3)

3. Acceleration of Gravity Card (F10)

One card is required

Columns	1-10	Acceleration due to gravity (ft/sec^2)

4. Element Cards

Arch dam elements are numbered from one to the total number of elements. Element cards must be in ascending order. Two cards are required for each element:

Card 1. (3I5)

Columns	1-5	Element number
	10	The number 3 (integration order)
	11-15	Material number (if left blank material number equals 1).

Card 2. (16I5)

Columns	Description	Node
1-5	Global nodal point numbers of nodes (See Fig. H2)	1
6-10		2
11-15		3
16-20		4
21-25		5
26-30		6
31-35		7
36-40		8
41-45		9
46-50		10
51-55		11
56-60		12
61-65		13
66-70		14
71-75		15
76-80		16

Note 1: A typical 20 element mesh is shown in Fig. H1. Element number one must be adjacent to the base and plane of symmetry of the dam. Elements in the z direction must be numbered in ascending order. After reaching the top element in a column of elements the next element numbered must be the base element of the next column of elements associated with an increase in θ.

Note 2: Due to the way that the hydrodynamic terms couple to the arch dam nodal points, the global nodal points correspond to the local element nodal points in a specific manner. The element surface containing the local element nodal points 5, 6, 7, 8, 13, 14, 15, and 16 corresponds to the upstream face of the dam (i.e., the face of the dam in contact with the water in the reservoir). Local nodal point 5 has the largest ANGLE (angle from the center of the dam) and the largest HEIGHT (vertical coordinate) of any nodal point associated with a particular element. Loosely speaking, the axis (Fig. H2) of each element must be lined up approximately with the vertical, z, axis of the arch dam (Fig. H1).

E. HYDRODYNAMIC CARDS

The following cards are required only if hydrodynamic loads are included in the analysis.

Card 1. (2I5, 3F10, 3I5)

Column	1-5	NUMELZ	Number of elements in z direction
	6-10	NUMELT	Number of elements in θ direction
	11-20	TW	Half the included angle of the element (radians)
	21-30	ZW	Element half height (ft)
	31-40	HWATER	Depth of the reservoir (ft)
	41-45	NTERM	Number of terms associated with the ζ direction in the series solution for hydrodynamic loads (see Eq. 4.8 to 4.10 and 5.8 to 5.10)
	46-50	MTERM	Number of terms associated with the z direction in the series solution for hydrodynamic loads (see Eq. 4.8 to 4.10 and 5.8 to 5.10)

-55 IXYZ Parameter identifying the direction of ground motion

=1 Horizontal ground motion in upstream-downstream direction (along x axis in Fig. 2.1)

=2 Horizontal ground motion in cross-stream direction (along y axis in Fig. 2.1)

=3 Ground motion in vertical direction

Note 1: (NUMELZ)*(NUMELT) = Total number of elements

(NUMELZ)*(zw + zw) = Height of dam

(NUMELT)*(tw + tw) = $\pi/4$ radians (dam half angle)

Note 2: The number of terms, NTERM and MTERM, required to approximate the infinite series solution varies with the reservoir natural frequency, the radius of the dam, and the frequency of excitation. For most earthquake excitation problems NTERM = MTERN = 10 is adequate.

CARD 2. (2F10, 2I5)

Columns 1-10 DAMP Damping factor to be applied to all modes

11-20 ALPHA Coefficient of refraction between water and ground rock below reservoir. This may be computed as ALPHA = (k-1)/(k+1), where k = $C_r w_r / cw$ with w_r and w being the unit weights of rock and water respectively, C_r the P-wave velocity in rock and C the velocity of sound in water (4720 ft/sec). ALPHA < 1. Used only for vertical excitations.

-25 INCOMP Parameter for incompressible water solution

=0 Water treated as compressible

=1 Water assumed to be incompressible

-30 NPUNCH Parameter for punching complex frequency response results (see note below)

=0 Does not punch results

≥ 1 Punches results

Note: If NPUNCH ≥ 1, a set of complex frequency response results are punched for each excitation frequency. For horizontal ground motion in the upstream-downstream direction and in the cross-stream direction, two cards are punched for every mode shape included in the analysis. Thus, if 10 modes are included (NF = 10) and if results are required for 50 excitations, the total number of punched cards equals 1000. Punched results for vertical ground motion have only one card per mode shape per excitation frequency.

F. EXCITATION FREQUENCY CARDS

One card with format F10 is required for each excitation frequency. A negative frequency card terminates the program.

Column 1-10 WW1DAM Excitation Frequency, ω, normalized with respect to the fundamental natural frequency of the dam, ω_1^d.

Output

The following is printed by the program:

1. Program control information
2. Coordinates of nodal points on the dam
3. Material property parameters

4. Nodal point - shell element connectivity information
5. Natural frequencies and mode shapes of the dam (without water in the reservoir) unless surpressed according to the options provided in Card B.
6. Hydrodynamic input parameters
7. The real and imaginary components together with the absolute value of the complex frequency response function for modal acceleration ($\ddot{Y}_j(\omega)$, $j = 1, 2, \ldots$ NF) of the dam in each mode for each input excitation frequency.

EXAMPLE

The response of an arch dam-reservoir system to vertical ground motion with 58 nodal points descritizing half the dam illustrates the preparation of input data for this program. Figure H3 shows the nodal point numbering scheme for the example. The input data is obtained from the following parameters.

Radius to upstream face = 450 ft.

Height of dam = 300 ft.

Depth of water in the reservoir = 300 ft.

Modulus of elasticity of dam = 720 x 10^6 psf

Poisson's ratio of dam = .17

Weight density of dam = 150 psf

Acceleration due to gravity = 32.2 ft/sec^2

Modal damping ratio = 5%

Coefficient of refraction between water and ground rock = 0.85

Size of available blank common = 12,000

Number of frequencies for modal analysis = 1

Radial width of the dam at the crest = 12.6 ft.

Radial width of the dam at the base = 50.0 ft.

The dam has a constant cross-section normal to the radial coordinate

Excitation frequencies are ω/ω_1 = 0.100 and 0.500

Half the dam is divided into six elements

Ten terms for each summation are used to approximate the infinite series for the hydrodynamic loads.

The input data required for the dynamic response analysis of the dam is presented on the following page.

```
EXAMPLE PROBLEM - 58 NODE ARCH DAM MESH - MARCH 1978
  5812000     1     2
     450.        1.5
    1    .0          0.0        0.0     1     1     1
    5    .0        300.0        0.0           1
    6    .0          0.0       50.0     1     1     1
   10    .0        300.0       12.6           1
   11    .1309       0.0        0.0     1     1     1
   13    .1309     300.0        0.0
   14    .1309       0.0       50.0     1     1     1
   16    .1309     300.0       12.6
   17    .2618       0.0        0.0     1     1     1
   21    .2618     300.0        0.0
   22    .2618       0.0       50.0     1     1     1
   26    .2618     300.0       12.6
   27    .3927       0.0        0.0     1     1     1
   29    .3927     300.0        0.0
   30    .3927       0.0       50.0     1     1     1
   32    .3927     300.0       12.6
   33    .5236       0.0        0.0     1     1     1
   37    .5236     300.0        0.0
   38    .5236     0.0         50.0     1     1     1
   42    .5236     300.0       12.6
   43    .6545       0.0      0.0       1     1     1
   45    .6545     300.0      0.0
   46    .6545      0.0      50.0       1     1     1
   48    .6545     300.0     12.6
   49    .78540      0.0        0.0     1     1     1
   53    .78540    300.0        0.0     1     1     1
   54    .78540      0.0       50.0     1     1     1
   58    .78540    300.0       12.6     1     1     1
    2     6     1
   1720000000.       .17      150.0
  32.2
    1     3
   24    22     6     8    19    17     1     3    23    14     7    15    18    11     2    12
    2     3
   26    24     8    10    21    19     3     5    25    15     9    16    20    12     4    13
    3     3
   40    38    22    24    35    33    17    19    39    30    23    31    34    27    18    28
    4     3
   42    40    24    26    37    35    19    21    41    31    25    32    36    28    20    29
    5     3
   56    54    38    40    51    49    33    35    55    46    39    47    50    43    34    44
    6     3
   58    56    40    42    53    51    35    37    57    47    41    48    52    44    36    45
    2     3      .1309     75.      300.      10    10     3
  0.05      0.85
.100
.500
-1.
```

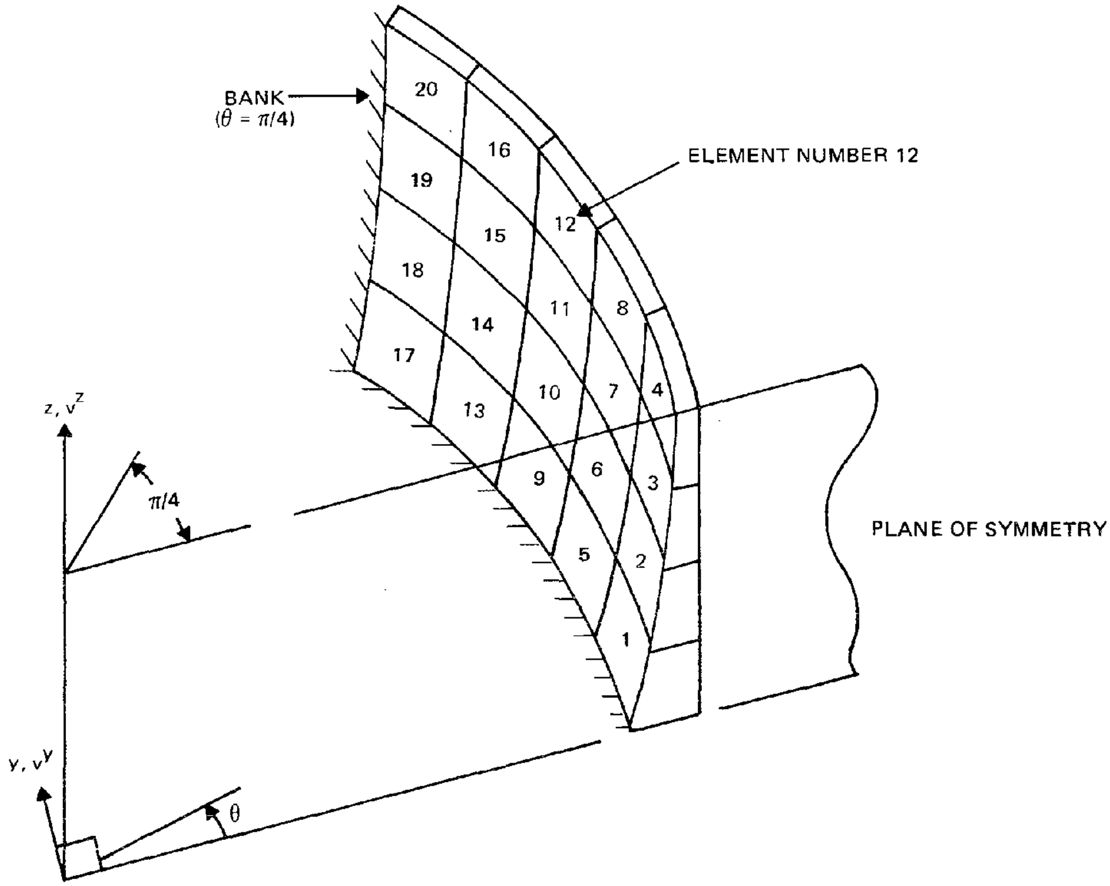

FIG. H1. ELEMENT NUMBERING OF AN ARCH DAM DEMONSTRATED WITH A 20 ELEMENT MESH

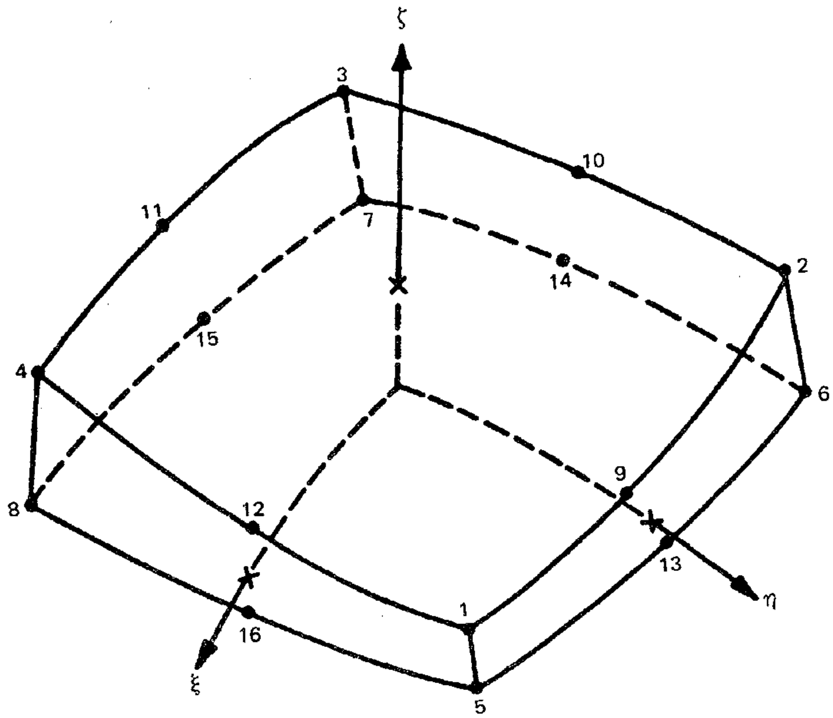

FIG. H2. LOCAL ELEMENT NUMBERING - THREE DIMENSIONAL THICK SHELL

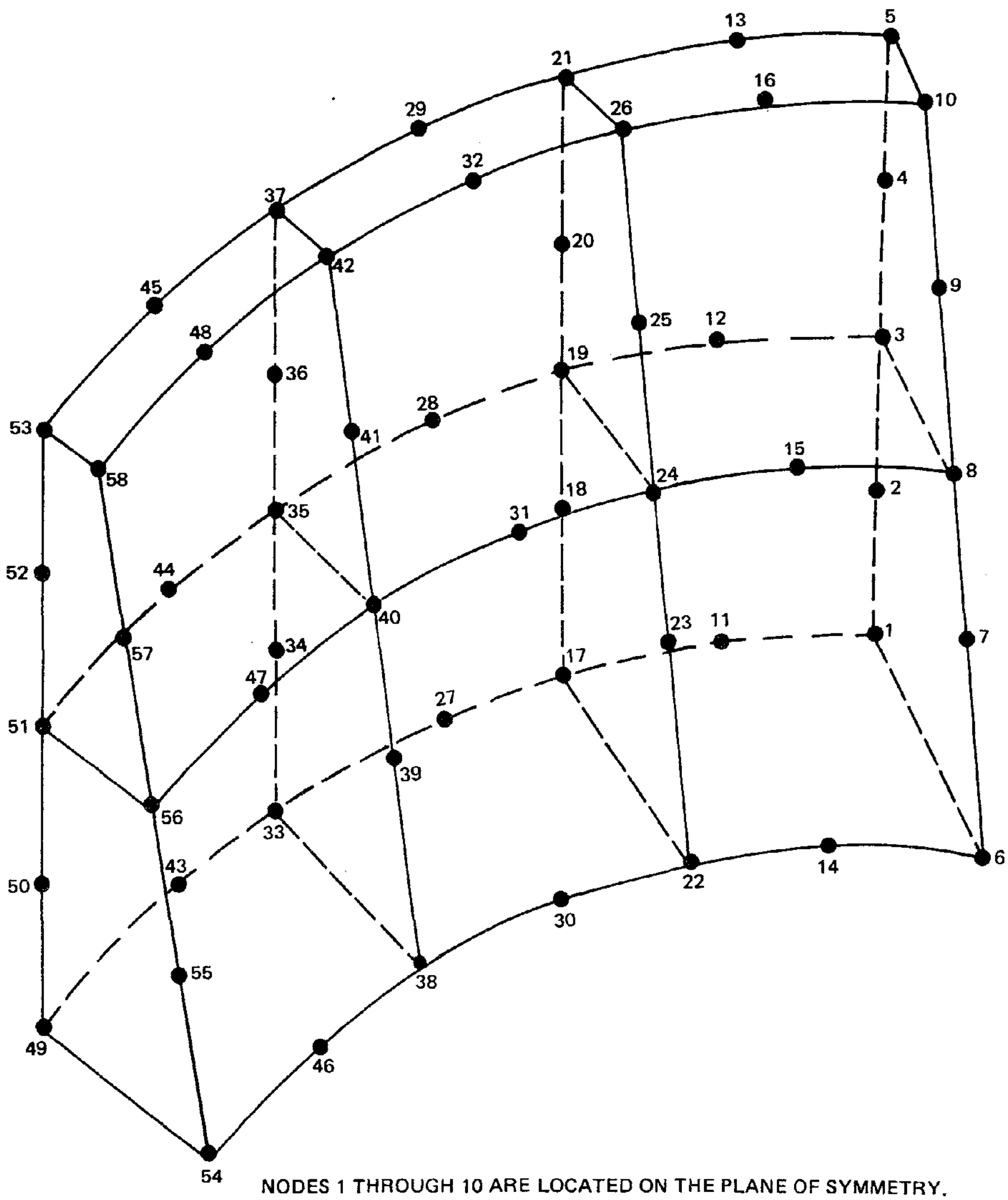

NODES 1 THROUGH 10 ARE LOCATED ON THE PLANE OF SYMMETRY.
NODES 49 THROUGH 58 ARE LOCATED ON THE BANK.

FIG. H3. EXAMPLE PROBLEM - NODAL POINT NUMBERING OF 58 NODE, 6 ELEMENT ARCH DAM

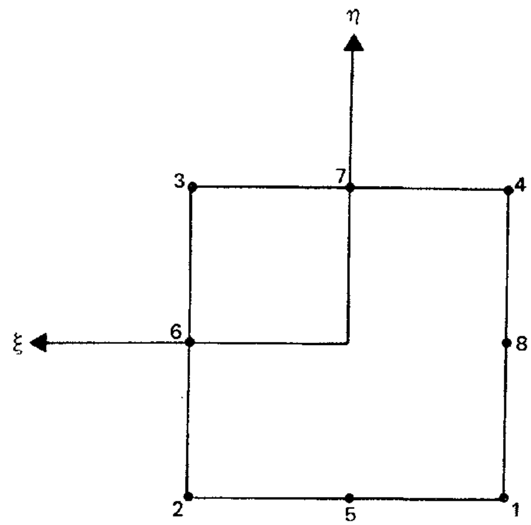

LOCAL NODAL POINT NUMBER	GLOBAL COORDINATES (θ^e, z^e)	LOCAL COORDINATES (ξ, η)
1	(θ_1^e, z_1^e)	(-1, -1)
2	(θ_2^e, z_1^e)	(1, -1)
3	(θ_2^e, z_2^e)	(1, 1)
4	(θ_1^e, z_2^e)	(-1, 1)
5	$\left(\frac{\theta_1^e + \theta_2^e}{2}, z_1^e\right)$	(0, -1)
6	$\left(\theta_2^e, \frac{z_1^e + z_2^e}{2}\right)$	(1, 0)
7	$\left(\frac{\theta_1^e + \theta_2^e}{2}, z_2^e\right)$	(0, 1)
8	$\left(\theta_1^e, \frac{z_1^e + z_2^e}{2}\right)$	(-1, 0)

FIG. D1. Local Global Corrdinates of Eight Node Surface Element on Upstream Face of the Dam

APPENDIX I - COMPUTER PROGRAM LISTING

```
EXAMPLE PROBLEM - 58 NODE ARCH DAM MESH - MARCH 1978
   5812000     1     2
     450.        1.5
    1     .0          0.0       0.0     1     1     1
    5     .0        300.0       0.0           1
    6     .0          0.0      50.0     1     1     1
   10     .0        300.0      12.6           1
   11     .1309       0.0       0.0     1     1     1
   13     .1309     300.0       0.0
   14     .1309       0.0      50.0     1     1     1
   16     .1309     300.0      12.6
   17     .2618       0.0       0.0     1     1     1
   21     .2618     300.0       0.0
   22     .2618       0.0      50.0     1     1     1
   26     .2618     300.0      12.6
   27     .3927       0.0       0.0     1     1     1
   29     .3927     300.0       0.0
   30     .3927       0.0      50.0     1     1     1
   32     .3927     300.0      12.6
   33     .5236       0.0       0.0     1     1     1
   37     .5236     300.0       0.0
   38     .5236     0.0        50.0     1     1     1
   42     .5236     300.0      12.6
   43     .6545      0.0      0.0       1     1     1
   45     .6545     300.0      0.0
   46     .6545      0.0     50.0       1     1     1
   48     .6545     300.0      12.6
   49     .78540      0.0       0.0     1     1     1
   53     .78540    300.0       0.0     1     1     1
   54     .78540      0.0      50.0     1     1     1
   58     .78540    300.0      12.6     1     1     1
    2     6     1
    1720000000.         .17      150.0
   32.2
    1     3
   24    22     6     8    19    17     1     3    23    14     7    15    18    11     2    12
    2     3
   26    24     8    10    21    19     3     5    25    15     9    16    20    12     4    13
    3     3
   40    38    22    24    35    33    17    19    39    30    23    31    34    27    18    28
    4     3
   42    40    24    26    37    35    19    21    41    31    25    32    36    28    20    29
    5     3
   56    54    38    40    51    49    33    35    55    46    39    47    50    43    34    44
    6     3
   58    56    40    42    53    51    35    37    57    47    41    48    52    44    36    45
    2     3       .1309      75.      300.       10    10     3
   0.05       0.85
  .100
  .500
  -1.
```

```
      OVERLAY(XFILE,0,0)
      PROGRAM RADHI(INPUT,OUTPUT,PUNCH,TAPE5=INPUT,TAPE6=OUTPUT,TAPE1,
     . TAPE2,TAPE3,TAPE4,TAPE7,TAPE8,TAPE9,TAPE10,TAPE11,TAPE99)
      COMMON/JUNK/HED(12),DUM(388)
      COMMON / MISC / NBLOCK,NEQB,LL,NF,LB ,NDYN
      COMMON /ELPAR/ NPAR(14),NUMNP,MBAND,NELTYP,N1,N2,N3,N4,N5,MTOT,NEQ
     . ,N6, NUMNPF   ,IPRINT ,NLM ,NUMEL,WATL, IMASS,TVOL,NEQEST,IMODE
     . ,IPRM  ,MESH ,MESHFN ,ISYM,WDEN,T(10)
      COMMON/RADDD/RADIUS,RADHT
C
C     PROGRAM CONTROL DATA
C
      READ(5,100) HED,NUMNP,MTOT,NF,NDYN,IMODE,IPRM
      NELTYP= 1
      LL=0
      NLM=0
      NEQEST=0
      ESTVOL= 0.0
      MESH=0
      MESHFN=0
      WATL=0.0
      WDEN=0.0
      WRITE(6,200)HED,NUMNP,MTOT,NF
      READ 1500,RADIUS,RADHT
      PRINT 1600,RADIUS,RADHT
    2 TVOL=0.0
      NUMNPF=NUMNP
      IF(IMODE.LE.0.OR.NDYN.LE.1) GO TO 3
      READ(5,400)MBAND,NUMEL,NEQ
      WRITE(6,201)MBAND,NUMEL,NEQ
    3 IMASS=1
      IF(IMODE.GT.0.AND.NDYN.GT.1) GO TO 4
C
C     INPUT JOINT DATA AND ELEMENT DATA
C     FORM ELEMENT STIFFNESSES--STIFF. ON TAPE 2 -
C     FORM CONSISTANT MASS MATRIX
C
      CALL OVERLAY(5HXFILE,1,0,6HRECALL)
C
C     SOLVE FOR NATURAL FREQUENCIES AND MODE SHAPES DIRECTLY BY SUBSPACE
C     ITERATION......
C
    4 CALL OVERLAY(5HXFILE,2,0,6HRECALL)
      IF(NDYN.LE.1)STOP
C
C    SOLVE FOR HYDRODYNAMIC FREQUENCY RESPONSE FUNCTIONS
C
      CALL OVERLAY(5HXFILE,3,0,6HRECALL)
C
      STOP
  100 FORMAT(12A6/6I5)
  200 FORMAT(1H1, 12A6///
     . 28H  NUMBER OF NODAL POINTS    =  ,I5//
     1 28H  REQD. BLANK COMM. STORAGE=  ,I5//
     1 28H  NUMBER OF FREQUENCIES     =  ,I5////)
  201 FORMAT(37H0HALF BANDWIDTH...................... ,I4//
     .       37H TOTAL NO. OF ELEMENTS............... ,I4//
     .       37H NO. OF EQUATIONS.................... ,I4//)
  400 FORMAT(3I5)
 1500 FORMAT(2F10.0)
 1600 FORMAT(//9H RADIUS =,F10.3,10X,8H RADHT =,F10.4///)
      END
```

```
      SUBROUTINE ERROR(N)
      WRITE(6,2000)N
 2000 FORMAT(21HSTORAGE EXCEEDED BY  ,I5)
      STOP
      END
```

```
      SUBROUTINE PRINTD(ID,D,B,NEQB,NUMNPF,LL,NBLOCK,NEQ,NT,NF)
      DIMENSION              B(NEQB,LL),D(5,LL) ,ID(NUMNPF,3)
      REWIND NT
      READ(NT)
    2 REWIND 8
      READ (8) ID
      M=NEQ
      NN=NEQB*NBLOCK
      WRITE(6,2005)
      N=NUMNPF
C
      DO 500 KK=1,NUMNPF
      I=3
      DO 250 II=1,3
      DO 100 L=1,LL
  100 D(I,L)=0.
      IF(M.GT.NN) GO TO 150
      IF (M.EQ.0) GO TO 150
      READ (NT) B
      NN=NN-NEQB
  150 IF(ID(N,I).LT.1) GO TO 250
      K=M-NN
      M=M-1
C
      DO 200 L=1,LL
  200 D(I,L)=B(K,L)
  250 I=I-1
C
      DO 251 K=1, 3
      IF(ID(N,K).NE.0) GO TO 252
  251 CONTINUE
      GO TO 253
  252 WRITE(6,2004) N,(L,(D(I,L),I=1,3),L=1,LL)
  253 CONTINUE
  500 N=N-1
      RETURN
 2004 FORMAT(1H0,I3,I5,7X,1P3E12.3/(I9,7X,,3E12.3))
 2005 FORMAT(17H1.....MODE SHAPES///,5H NODE,11X,1HX,11X,1HY,11X,1HZ)
      END
```

```
      OVERLAY(XFILE,1,0)
      PROGRAM MAIN1
      COMMON A(1)
      COMMON/RADDD/RADIUS,RADHT
      COMMON /ELPAR/ NPAR(14),NUMNP,MBAND,NELTYP,N1,N2,N3,N4,N5,MTOT,NEQ
     .  ,N6, NUMNPF    ,IPRINT ,NLM ,NUMEL,WATL,DUM(2),NEQEST,IMODE
     .  ,MASTIF,MESH,MESHFN    ,ISYM,WDEN
      COMMON /JUNK/ MM,L,K,NTAG,SIG(318)
      N1=1
      N2=N1+3*NUMNP
      N3=N2+NUMNP
      N4=N3+NUMNP
      N5=N4+NUMNP
      N6=N5+NUMNP
      IF(N6.GT.MTOT) CALL ERROR(N6-MTOT)
      CALL INPUTNS(A(N1), A(N2), NUMNP, NUMNPF, NEQ, NEQEST)
      MBAND=0
      NUMEL=0
      REWIND 1
      REWIND 2
      READ  (5,1001) NPAR
      WRITE (1) NPAR
      NUMEL=NUMEL+NPAR(2)
      N7=N6+NPAR(3)
      N8=N7+NPAR(3)
      N9=N8+NPAR(3)
      N10=N9 +NPAR(3)
      N11=N10+63*63
      IF(N11.GT.MTOT) CALL ERROR(N11-MTOT)
      CALL ELST3D(A(N10),NPAR(2), NPAR(3), NPAR(4), A(N1), A(N2), A(N3),
     .               A(N4), A(N6), A(N7), A(N8), A(N9), NUMNPF, A(N5))
      RETURN
 1001 FORMAT (14I5)
      END
```

```
      SUBROUTINE INPUTNS(ID,COORD,NUMNP,NUMNPF,NEQ,NEQEST)
C
      COMMON/RADDD/RADIUS,RADHT
      COMMON A(1)
      DIMENSION ID(NUMNP ,3), COORD(NUMNP,4), DXYZ(3)
C
C READ COORDINATE ARRAY
C
      NODE=1
    5 NOD=NODE
      IF(NODE.EQ.NUMNP)GOTO 11
      READ 2000,NODE,ANGLE,HEIGHT,THICK,(ID(NODE,K),K=1,3)
      COORD(NODE,1)= (RADIUS - THICK)*COS(ANGLE)
      COORD(NODE,2)= (RADIUS - THICK)*SIN(ANGLE)
      COORD(NODE,3)= HEIGHT
      IF(NODE - NOD.LE.1) GOTO 5
      INT= NODE - NOD -1
      STEP = INT+1
      DO 6 J=1,3
    6 DXYZ(J)= (COORD(NODE,J) - COORD(NOD,J))/STEP
      NODG= NOD
      DO 10 I=1,INT
      NODG= NODG + 1
      DO 9 J=1,3
      COORD(NODG,J)= COORD(NOD,J) + DXYZ(J)
    9 ID(NODG,J)= ID(NODE,J)
   10 NOD= NOD + 1
      IF(NODE.LT.NUMNP) GOTO 5
   11 DO 20 I=1,NUMNP
      COORD(I,4)= 0.0
   20 CONTINUE
      PRINT  35,(NODE,(COORD(NODE,J),J=1,4),(ID(NODE,K),K=1,3),NODE=1,NU
     1MNP)
C
C NUMBER UNKNOWNS
  144 NEQ = 0
      DO 140 I = 1,NUMNPF
      DO 140 J = 1,3
      IF(ID(I,J)-1) 137,138,138
  137 NEQ = NEQ + 1
      ID(I,J) = NEQ
      GO TO 140
  138 ID(I,J) = 0
  140 CONTINUE
      IF(NEQEST.EQ.0) GO TO 160
      IF(NEQEST.EQ.NEQ) GO TO 160
      WRITE(6,1000) NEQ,NEQEST
      STOP
  160 CONTINUE
      REWIND 8
      WRITE (8) ID
      WRITE(8) COORD
      RETURN
   35 FORMAT(//////18H NODAL COORDINATES  //
     1 5H NODE 8X,  1HX,11X,1HY,11X,1HZ,11X,1HT,5X,13HIDX  IDY  IDZ/
     2(I5,4(3X,F9.3),3I5))
 1000 FORMAT(25H CALCULATED NO. OF EQNS.=I5/
     .       25H ESTIMATED  NO. OF EQNS.=I5)
 2000 FORMAT(I5,3F10.0,3I5)
      END
```

```
      SUBROUTINE ELST3D (S,N3DEL,NMAT,NLD,ID,X,Y,Z,EE,ENU,RHO,ALPT,
     .          NUMNP,TEMR)
C
C     STIFNESS SUBROUTINE FOR 48 D.F. ISOPARAMETRIC3D THICK SHELL ELEM.
C     LINEAR ELASTIC ISOTROPIC MATERIAL
C     NINT*NINT*(NINT-1)   GAUSSIAN INTEGRATION RULE USED
C     NINT=1,2,3,4
C
      DIMENSION S(63,63)
      DIMENSION X(NUMNP),Y(NUMNP),Z(NUMNP),ID(NUMNP,3) ,TEMR(NUMNP)
      DIMENSION EE(1),ENU(1),RHO(1),ALPT(1)
      DIMENSION STPTS(10,3) ,NDIR(10), IPP(6,2)
      COMMON/EM/LM(48),ND,NS,SS(48,48),RF(48,4),XM(48,48),SA(40,48),
     .    SF(40,4)
      COMMON /GASS/ XK(4,4),WGT(4,4),IPERM(3)
      COMMON /JUNK/ E1,E2,E3,DET,MLD(4),KLD(4),MULT(4),NP(16),INP(16),
     +              A(3,3),P(3,21),B(3,3),XX(16,4),Q(19),DL(16),
```

```
     .              TT(48),XLF(4),YLF(4),ZLF(4),TLF(4),PLF(4),
     .              REFT,INEL,ININT,IMAT,IINC,TTEMP,NEL,ML,NINT,MAT,
     .              INC,TAG,TEMP,SKIP,I,J,K,L,FAC,CC1,CC2,CC3,CC4,G,
     .              DEN,FACT,GT,GG,C1,C2,C3,C,K1,K2 ,TR(4),THICK(8)
      COMMON /ELPAR/ NPAR(14),NUMN ,MBAND,NELTYP,N1,N2,N3,N4,N5,MTOT,NEQ
     .  ,N6,NUMNPF      ,IPRINT ,NLM ,NUMLL,WATL,IMASS,TVOL,DMM(6),WDEN
C
      DATA XK /      0.,              0.,              0.,            0.,
     1 -.577350269189б, .5773502691896,                0.,            0.,
     2 -.7745966692415, .0000000000000, .7745966692415,              0.,
     3 -.8611363115941,-.3399810435849, .3399810435849, .8611363115941/
      DATA WGT / 2.000,               0.,              0.,            0.,
     1 1.0000000000000,1.0000000000000,                0.,            0.,
     2  .5555555555556, .8888888888889, .5555555555556,              0.,
     3  .3478548451375, .6521451548625, .6521451548625, .3478548451375/
      DATA IPERM / 2,3,1 /
      DATA STPTS /   1. , 1. ,-1. ,-1. , 0. , 0. , 0. , 0. , 0. , 0. ,
     .               0. , 0. , 0. , 0. , 1. , 1. ,-1. ,-1. , 0. , 0. ,
     .               1. ,-1. , 1. ,-1. , 1. ,-1. , 1. ,-1. , 1. ,-1. /
      DATA IPP/1,2,3,1,2,3,1,2,3,2,3,1/
C
C
      DO 9 I=1, 6930
    9 LMU+D=0
      ITP=3
      WRITE(6,3002) N3DEL,NMAT
C
C     MATERIAL PROPERTIES
      WRITE (6,1300)
      DO 1 I=1,NMAT
      READ  (5,1001) N,EE(N),ENU(N),RHO(N)
      ALPT(N)= 0.0
    1 WRITE (6,2001) N,EE(N),ENU(N),RHO(N)
      READ(5,1003) GRAV
      REFT= 0.0
      IF(GRAV.EQ.0.) GRAV=386.0
      WRITE(6,2003) GRAV
C
      WRITE (6,1301)
      NEL=0
   30 READ  (5,1000)      INEL,ININT,IMAT,IINC,MLD,IG,IGG,INP
      DO 39 I=1,4
   39 MULT(I)=1
      IF(IINC.EQ.0) IINC=1
      IF(IMAT.EQ.0) IMAT=1
   40 NEL=NEL+1
      ML=INEL-NEL
      IF(ML) 50,55,60
   50 WRITE (6,4003) INEL
      STOP
   55 DO 56 I=1,16
   56 NP(I)=INP(I)
      NINT=ININT
      MAT=IMAT
      INC=IINC
      TAG=1HI
      SKIP=999.
      IF(NINT) 33,33,57
   33 NINT=IABS(NINT)
      SKIP=1.
      IF(NINT.EQ.0) SKIP=0.
   57 CONTINUE
```

```
      DO 59 I=1,4
      KLD(I)=IABS(MLD(I))
      IF(MLD(I)) 58,58,59
   58 MULT(I)=0
   59 CONT+NUE
      GO TO 62
C
   60 DO 61 I=1,16
   61 NP(I)=NP(I)+INC
      TAG=1H
      DO 64 I=1,4
   64 KLD(I)=KLD(I)*MULT(I)
   62 WRITE(6,2000) NEL,NP,NINT,MAT
C
      DO 10  I = 1,16
      K=NP(I)
      XX(I,1)=X(K)
      XX(I,2)=Y(K)
      XX(I,3)=Z(K)
      XX(I,4)=TEMR(K)
   10 CONTINUE
      K=MAT
      FAC = EE(K)/((1.-2.*ENU(K))*(1.+ENU(K)))
      CCTT=FAC*(1.+ENU(K))
      IF(SKIP) 70,70,63
   63 SKIP=SKIP-1.
      CC1=1.-ENU(K)
      CC2=ENU(K)
      CC3=.5-ENU(K)
      DEN = RHO(K)
C
      L3=63*63
      DO 100 I=1,L3
  100 S(I)=0.
      DO 110 I=1,48
  110 TT(I)=0.
      DO 120 I=1,16
  120 DL(I)=0.
      L3=48*48
      DO 121 I=1, L3
  121 XM(I)=0.0
      DO 123 I=1, 160
  123 SF(I)=0.0
      VOL=0.0
C
C     LOOP OVER NINT**3 INTEGRATION POINTS
C
      MINT=NINT-1
      DO 300  LX = 1,NINT
      E1=XK(LX,NINT)
      E2=XK(LY,NINT)
      DO 300  LZ = 1,MINT
      E3=XK(LZ,MINT)
C
      CALL FUNCT(1.SA)
C
      G = WGT(LX,NINT)*WGT(LY,NINT)*WGT(LZ,MINT)
      GV=G*DET
      GT=G
      GG=G*DET*DEN
      GGG=GG/GRAV
      G=G*FAC/DET
```

```
      C1=G*CC1
      C2=G*CC2
      C3=G*CC3
C
C     CONSISTENT MASS MATRIX
C
      DO 130 I=1, 16
       II=(I-1)*3
      DO 130 J=I, 16
      JJ=(J-1)*3
      HH=Q(I)*Q(J)*GGG
      DO 130 K=1,3
      KI=II+K
      KJ=JJ+K
      XM(KI,KJ)=XM(KI,KJ)+HH
  130 XM(KJ,KI)=XM(KI,KJ)
C
C     ADD CONTRIBUTION TO STIFFNESS MATRIX
C
  311 VOL=VOL+GV
      DO 300 I=1,21
      K3 = 3*I
      K2 = K3 - 1
      K1 = K2 - 1
      UI=SA(I,1)
      VI=SA(I,2)
      WI=SA(I,3)
      DO 300 J=1,21
      L3 = 3*J
      L2 = L3 - 1
      L1 = L2 - 1
      UJ=SA(J,1)
      VJ=SA(J,2)
      WJ=SA(J,3)
      UU=UI*UJ
      VV=VI*VJ
      WW=WI*WJ
      UV=UI*VJ
      VU=VI*UJ
      UW=UI*WJ
      WU=WI*UJ
      VW=VI*WJ
      WV=WI*VJ
      S(K1,L1) = S(K1,L1) + C1*UU + C3*(VV+WW)
      S(K2,L2) = S(K2,L2) + C1*VV + C3*(WW+UU)
      S(K3,L3) = S(K3,L3) + C1*WW + C3*(UU+VV)
      S(K1,L2) = S(K1,L2) + C2*UV + C3*VU
      S(K1,L3) = S(K1,L3) + C2*UW + C3*WU
      S(K2,L3) = S(K2,L3) + C2*VW + C3*WV
      IF (I.EQ.J)  GO TO 300
      S(K2,L1) = S(K2,L1) + C2*VU + C3*UV
      S(K3,L1) = S(K3,L1) + C2*WU + C3*UW
      S(K3,L2) = S(K3,L2) + C2*WV + C3*VW
  300 CONTINUE
      TVOL=TVOL+VOL
 3000 FORMAT(14H ELEM. VOL.  =  E15.7)
      PRINT 3000, VOL
C
C     STATIC CONDENSATION
C
  406 DO 710 M=1, 15
      MN=64-M
      MO=MN-1
C
C      STIFFNESS MATRIX - S
C
      SP=S(MN,MN)
      DO 650 I=1,MO
  650 S(MN,I)=S(I,MN)/SP
      DO 700 K=1,MO
      SP=S(MN,K)
      DO 700 J=1,K
  700 S(J,K)=S(J,K) - SP*S(J,MN)
  710 CONTINUE
C
  711 DO 760 I=1,48
      DO 760 J=I,48
      SS(I,J)=S(I,J)
  760 SS(J,I)=SS(I,J)
C
C      SAVE ELASTIC PROPERTIES
C
      SA(17,1)=CC1
      SA(17,2)=CC2
      SA(17,3)=CC3
      SA(17,4)=FAC
      DO 505 I=1,7
  505 SA(I)=SF(I)
 70   CONTINUE
C
C     DISTRIBUTED LOAD
C
      DO 410 J=1,48
      DO 410 I=1,4
  410 RF(J,I)=0.
C
  468 IJ=0
      DO 551 I=1, 16
      II=NP(I)
      DO 550 J=1,3
      IJ=IJ+1
      LM(IJ)=ID(II,J)
  550 CONTINUE
  551 CONTINUE
      NS=1
      ND=48
C
  701 CONTINUE
      CALL WRITET (MBAND,NDIF)
C
C     CHECK IF LAST ELEMENT
C
      IF(N3DEL-NEL) 50,600,590
  590 IF(ML) 30,30,40
C
  600 RETURN
C
 1000 FORMAT (4I5,4I2,2X,40X    ,2I5/16I5)
 1001 FORMAT (I5,3F10.0)
 1003 FORMAT(F10.2)
 2000 FORMAT(I6,X,8I5/7X,8I5,I9,I12/)
 2001 FORMAT (X,I5,3E15.4)
 2003 FORMAT(///35H .....ACCELERATION DUE TO GRAVITY =,F10.2///)
 1300 FORMAT (9H1MATERIAL 10X 1HE 12X 2HNU 10X 3HRHO,/8H  NUMBER,/)
```

```
 1301 FORMAT (30H1...16 NODE SOLID ELEMENT DATA ///
     . 8H ELEMENT 10X 15HCONNECTED NODES 17X 21HINTEGRATION  MATERIAL/
     . 8H  NUMBER 3X,36H1     2     3     4     5     6     7     8 6X,5HORDER
     . 7X,  3HNO./
     .11X,36H9    10    11    12    13    14    15    16 //     )
 4003 FORMAT (36H0ELEMENT CARD ERROR, ELEMENT NUMBER= I6)
 3002 FORMAT ( 31H1.....16 - NODE SOLID ELEMENTS  ///
     . 24H  NUMBER OF ELEMENTS.... ,I5 //
     . 24H  NUMBER OF MATERIALS... ,I5 ///)
      END
```

```
      SUBROUTINE FUNCT (KK,D)
C
      DIMENSION D(40,1),BB(3)
      COMMON /GASS/ XK(4,4),WGT(4,4),IPERM(3)
      COMMON /JUNK/ R ,S ,T ,DET,MLD(4),KLD(4),MULT(4),NP(16),INP(16),
     .              A(3,3),P(3,21),B(3,3),XZ(16,4),Q(19),DL(16)
C
      R2=2.*(1.-(R**2))
      S2=2.*(1.-(S**2))
      RN=.125*(1.-R)
      SP=1.+S
      SN=1.-S
      TP=1.+T
      TN=1.-T
      RPSP= R+S-1.
      RPSN= R-S-1.
      RNSP=-R+S-1.
      RNSN=-R-S-1.
      XPP= 2.*R+S
      XPN= 2.*R-S
      XNP=-2.*R+S
      XNN=-2.*R-S
      YPP= R+(2.*S)
      YPN= R-(2.*S)
      YNN=-R-(2.*S)
      XX=.125
C
C      SHAPE FUNCTIONS
C
      Q( 1)=RP*SP*TP*RPSP
      Q( 2)=RN*SP*TP*RNSP
      Q( 3)=RN*SN*TP*RNSN
      Q( 4)=RP*SN*TP*RPSN
      Q( 5)=RP*SP*TN*RPSP
      Q( 6)=RN*SP*TN*RNSP
      Q( 7)=RN*SN*TN*RNSN
      Q( 8)=RP*SN*TN*RPSN
      Q( 9)=R2*SP*TP*XX
      Q(10)=RN*S2*TP
      Q(11)=R2*SN*TP*XX
      Q(12)=RP*S2*TP
      Q(13)=R2*SP*TN*XX
      Q(14)=RN*S2*TN
      Q(15)=R2*SN*TN*XX
      Q(16)=RP*S2*TN
C
C      DERIVATIVES OF SHAPE FUNCTIONS
C
  100 XR=-.5*R
      XS=-4.*S
      P(1,1)= XX*SP*TP*XPP
      P(1,2)=-XX*SP*TP*XNP
      P(1,3)=-XX*SN*TP*XNN
      P(1,4)= XX*SN*TP*XPN
      P(1,5)= XX*SP*TN*XPP
      P(1,6)=-XX*SP*TN*XNP
      P(1,7)=-XX*SN*TN*XNN
      P(1,8)= XX*SN*TN*XPN
      P(1,9)= XR*SP*TP
      P(1,10)=-XX*S2*TP
      P(1,11)= XR*SN*TP
      P(1,12)= XX*S2*TP
      P(1,13)= XR*SP*TN
      P(1,14)=-XX*S2*TN
      P(1,15)= XR*SN*TN
      P(1,16)= XX*S2*TN
      P(1,17)=1.-(3.*R*R)
      P(1,18)=0.
      P(1,19)=0.
      P(1,20)=S*(1.0-(3.0*R*R))
      P(1,21)=S*(1.0-(S*S))
C
      P(2,1)= RP*TP*YPP
      P(2,2)= RN*TP*YNP
      P(2,3)=-RN*TP*YNN
      P(2,4)=-RP*TP*YPN
      P(2,5)= RP*TN*YPP
      P(2,6)= RN*TN*YNP
      P(2,7)=-RN*TN*YNN
      P(2,8)=-RP*TN*YPN
      P(2,9)= R2*TP*XX
      P(2,10)= XS*TP*RN
      P(2,11)=-R2*TP*XX
      P(2,12)= XS*TP*RP
      P(2,13)= R2*TN*XX
      P(2,14)= XS*TN*RN
      P(2,15)=-R2*TN*XX
      P(2,16)= XS*TN*RP
      P(2,17)=0.
      P(2,18)=1.-(3.*S*S)
      P(2,19)=0.
      P(2,20)=R*(1.0-(R*R))
      P(2,21)=R*(1.0-(3.0*S*S))
C
      P(3,1)= RP*SP*RPSP
      P(3,2)= RN*SP*RNSP
      P(3,3)= RN*SN*RNSN
      P(3,4)= RP*SN*RPSN
      P(3,5)=-RP*SP*RPSP
      P(3,6)=-RN*SP*RNSP
      P(3,7)=-RN*SN*RNSN
      P(3,8)=-RP*SN*RPSN
      P(3,9)= R2*SP*XX
      P(3,10)= RN*S2
      P(3,11)= R2*SN*XX
      P(3,12)= RP*S2
      P(3,13)=-R2*SP*XX
      P(3,14)=-RN*S2
```

```
      P(3,15)=-R2*SN*XX
      P(3,16)=-RP*S2
      P(3,17)=0.
      P(3,18)=0.
      P(3,19)=-2.*T
      P(3,20)=0.0
      P(3,21)=0.0
C
C      JACOBIAN MATRIX A
C
      DO 200 I=1,3
      DO 200 J=1,3
      C=0.
      DO 150 K=1,16
  150 C=C+P(I,K)*XZ(K,J)
  200 A(I,J)=C
      IF (KK.EQ.3) GO TO 600
C
C      INVERT JACOBIAN
C
      DO 300 I=1,3
      J=IPERM(I)
      K=IPERM(J)
      B(I,I)=A(J,J)*A(K,K)-A(K,J)*A(J,K)
      B(I,J)=A(K,J)*A(I,K)-A(I,J)*A(K,K)
  300 B(J,I)=A(J,K)*A(K,I)-A(J,I)*A(K,K)
      DET=A(1,1)*B(1,1)+A(1,2)*B(2,1)+A(1,3)*B(3,1)
C
C      MATRIX OF X-Y-Z DERIVATIVES
C
      DO 400 I=1,3
      DO 400 J=1,22
      C=0.
      DO 350 K=1,3
  350 C=C+B(I,K)*P(K,J)
  400 D(J,I)=C
C
  600 RETURN
C
      END
```

```
      SUBROUTINE WRITET(MBAND,NDIF)
      COMMON/EM/LM(48),ND,NS,S(48,48),P(48,4),XM(48,48),ST(40,48),
     1   TT(40,4)
C
C     CALCULATION OF BAND WIDTH AND WRITES ELEMENT MATRICES ON TAPES
      MIN=100000
      MAX=0
      DO 450 L=1,ND
      IF (LM(L).EQ.0) GO TO 450
      IF (LM(L).GT.MAX) MAX=LM(L)
      IF (LM(L).LT.MIN) MIN=LM(L)
  450 CONTINUE
      NDIF=MAX-MIN+1
      IF (NDIF.GT.MBAND) MBAND=NDIF
      PRINT 2, NDIF
    2 FORMAT(7H MBAND=I5)
C
      DO 1 I=1, 48
      IF(XM(I,I).LT.0.0) STOP
    1 CONTINUE
      WRITE (1) NS,ND,LM,ST,TT,XM
      WRITE (2) LM,ND,NS,S,P, XM
      RETURN
      END
```

```
      OVERLAY(XFILE,2,0)
      PROGRAM EIGSSP
C
C    PROGRAM TO COMPUTE SMALLEST EIGENVALUES AND ASSOCIATED VECTORS IN
C    THE GENERALIZED EIGENVALUE PROBLEM
C                    A*V=RT*B*V  (A POS DEF,B DIAG NONNEG DEF)
C
C
      COMMON /ELPAR/ NPAR(14),NUMNP,MBAND,NELTYP,N1,N2,N3,N4,N5,MTOT,NEQ
     .  ,N6, NUMNPF   ,IPRINT ,NLM ,NUMEL,WATL, IMASS,TVOL,NEQEST,IMODE
     .  ,IPRM  ,MESH ,MESHFN ,ISYM,WDEN
      COMMON /JUNK/ HED(12)
      COMMON / MISC / NBLOCK,NEQB,LL,NF,LB,NDYN
       COMMON /TAPES/NSTIF,NRED,NL,NR,NT,NMASS
      COMMON A(16000)
C
C
      MTEMP=MTOT
      IF(MTOT.EQ.0) MTOT=MTEMP
       NSTIF=4
       NMASS=9
       NRED=10
       NL=2
       NR=3
       NT=7
      LL=0
      II=0
       NV=2*NF
       IF (NF.GT.8) NV=NF+12
      NEQB=MTOT/(2*MBAND+1)
    5 NBLOCK=(NEQ-1)/NEQB+1
      II=II+1
      IF(II.GT.100) STOP
      IF(NEQB.GT.NEQ)  NEQB=NEQ
       NWA=NEQB*MBAND
       NWV=NV*NEQB
       NTB=(MBAND-2)/NEQB+1
       IF (NTB.GE.NBLOCK) NTB=NBLOCK-1
       NWVV=NWV*(NTB+1)
       N2=NWV+NEQB+NV
      IF(N2.LE.MTOT) GO TO 10
      NEQB=(MTOT-NV)/(1+NV)
      GO TO 5
   10  N3=NWA+NWV+NWVV+NEQB+2*NV
      IF(N3.LE.MTOT) GO TO 20
      NEQB=(MTOT-2*NV)/(MBAND+NV+NV*(1+NTB)+1)
      GO TO 5
   20  N4=NV*(3*NV+2*NEQB+3)+NEQB*MBAND
```

```
      IF(N4.LE.MTOT) GO TO 40
      NEQB=(MTOT-NV*(3+3*NV))/(MBAND+2*NV)
      GO TO 5
   40 NE2B=2*NEQB
       PRINT 1000,NEQ,MBAND,NBLOCK,NEQB,NF
      IF(IMODE.GT.0.AND.NDYN.GT.1) GO TO 50
   45 N2=N1+MBAND*NE2B
      CALL ASMBLB(A(N1),A(N2),NUMEL,NBLOCK,NE2B,LL,MBAND,NEQ,MASWAT)
   50 IF(IMODE.EQ.0.OR.NDYN.EQ.1) GO TO 300
      IMODE=10
      REWIND 7
      REWIND IMODE
      READ(IMODE) NBTP,NEQBTP,NEQTP,NFTP,MBTP
      IF(NBTP.NE.NBLOCK)    GO TO 2
      IF(NEQBTP.NE.NEQB)    GO TO 2
      IF(NEQTP.NE.NEQ)      GO TO 2
      IF(NFTP.NE.NF)        GO TO 2
      IF(MBTP.NE.MBAND)GOTO 2
      READ(IMODE)   (A(I), I=1, NF)
      WRITE(7)      (A(I), I=1, NF)
      WRITE(6,1001) ((I,A(I)), I=1, NF)
      NQF=NEQB*NF
      DO 1 I=1, NBLOCK
      READ(IMODE)   (A(K), K=1, NQF)
    1 WRITE(7)      (A(K), K=1, NQF)
      N1=1
      N2=N1+5*NUMNP
      N3=N2+5*NF
      IF(IPRM  .NE.0) GO  TO 3
      CALL PRINTD(A(N1),A(N2),A(N3),NEQB,NUMNP,NF,NBLOCK,NEQ ,7,NF)
    3 CONTINUE
      RETURN
    2 WRITE(6,1000)   NEQTP,MBTP,NBTP,NEQBTP,NFTP
      STOP
C
 300   NWA=NEQB*MBAND
       NWV=NV*NEQB
       NTB=(MBAND-2)/NEQB+1
       IF (NTB.GE.NBLOCK) NTB=NBLOCK-1
       NWVV=NWV*(NTB+1)
       N=2*NWA+NEQB
       N2=NWV+NEQB+NV
       N3=NWA+NWV+NWVV+NEQB+2*NV
       N4=NV*(3*NV+2*NEQB+3)+NEQB*MBAND
       N5=NWA+6*NV+NEQB
C
       IF (N2.GT.N) N=N2
       IF (N3.GT.N) N=N3
       IF (N4.GT.N) N=N4
       IF (N5.GT.N) N=N5
       IF (MTOT-N) 400,500,500
 400   PRINT 1010,N
       STOP
C
 500   CALL SSPACEB (NEQ,MBAND,NBLOCK,NEQB,NF,NV,NWA,NWV,NWVV,NTB)
      ITP=0
      IF(IMODE.NE.0) ITP=10
      IF(ITP.EQ.0) GO TO 700
      REWIND 7
      REWIND ITP
  550 WRITE(ITP)  NBLOCK,NEQB,NEQ,NF ,MBAND
      NQF=NEQB*NF
      READ(7) (A(I), I=1, NF)
      WRITE(ITP)  (A(I), I=1, NF)
      DO 600 N=1, NBLOCK
      READ(7) (A(I), I=1, NQF)
  600 WRITE(ITP)  (A(I), I=1, NQF)
C
  700 RETURN
C
 1000  FORMAT (1H1,20HPROBLEM INFORMATION  //
     1          /30H NO OF EQUATIONS .............  I4
     2          /30H 1/2 BANDWIDTH OF A ..........  I4
     3          /30H NO OF BLOCKS ................  I4
     4          /30H NO OF EQNS PER BLOCK ........  I4
     5          /30H NO OF FREQUENCIES REQD ......  I4  )
 1001 FORMAT( 9H FREQS.  /(I5,F12.6))
 1010  FORMAT (40HOFOR EXECUTION NEED TO INCREASE MTOT TO  I6)
      END
```

```
       SUBROUTINE SSPACEB (NEQ,MBAND,NBLOCK,NEQB,NF,NV,NWA,NWV,NWVV,NTB)
C
       COMMON /TAPES/NSTIF,NRED,NL,NR,NT,NMASS
       COMMON A(1)
      COMMON /ELPAR/ NPAR(14),NUMNP,MB    ,NELTYP,N1,N2,N3,N4,N5,MTOT,NQQ
     .  ,N6, NUMNPF    ,IPRINT ,INOD,NUMEL, DUM(5),IPRM
C
      NITEM=10
C   FACTORIZE STIFFNESS MATRIX
       N2=1+NWA
       N3=N2+NWA
       CALL SECOND (TIM1)
       CALL DECOMP (A(1),A(N2),A(N3),NEQB,MBAND,NBLOCK,NWA,NTB,NSCH,NEQ)
       CALL SECOND (TIM2)
C
C   ESTABLISH STARTING TRANSFORMATION VECTORS ON TAPE NR
       N2=1+NWV
       N3=N2+NEQB
       CALL INVECT (A(1),A(N2),A(N3),NBLOCK,NEQB,NV)
       CALL SECOND (TIM3)
       TIM1=TIM2-TIM1
       TIM2=TIM3-TIM2
       PRINT 1000,TIM1
       PRINT 1010,TIM2
C
C   PERFORM SUBSPACE ITERN
       DO 100 I=1,NV
 100   A(I)=0.0
       NITE=0
 200   NITE=NITE+1
       PRINT 1020,NITE
       CALL SECOND (TIM1)
       N1=1+2*NV
       N2=N1+NWA
       N3=N2+NWV
       N4=N3+NWVV
       CALL REDBAK (A(N1),A(N2),A(N3),A(N4),NEQB,NV,NWA,NWV,NWVV,NTB,
      1NBLOCK)
C
```

```
C     SOLVE SUBSPACE EIGENVALUE PROBLEM
        N2=1+NV
        N3=N2+NV
        N4=N3+NV*NV
        N5=N4+NV*NV
        N6=N5+NV*NV
        N7=N6+NWV
        N8=N7+NWV
        N9=N8+NV
        CALL SECOND (TIM2)
        CALL EIGSOL (A(1),A(N2),A(N3),A(N4),A(N5),A(N6),A(N7),A(N8),A(N9)
     1,NF,NV,NBLOCK,NEQB,NITE,MBAND)
        CALL SECOND (TIM3)
        TIM1=TIM3-TIM1
        TIM2=TIM3-TIM2
        PRINT 1030,TIM1
        PRINT 1040,TIM2
C
        IF (NITE.LT.NITEM) GO TO 200
C
      PII=ATAN(1.)*4.
      PRINT 1055
      DO 210 I=1, NF
      FREQ=A(I)
      FREQ=SQRT(FREQ)/2./PII
      PRINT 1056,I,FREQ
  210 CONTINUE
        PRINT 1050
        PRINT 1060,(A(I),I=1,NF)
 300    CONTINUE
      IF(IPRM.NE.0) GO TO 310
      N1=1
      N2=N1+5*NUMNP
      N3=N2+5*NF
      CALL PRINTD(A(N1),A(N2),A(N3),NEQB,NUMNPF,NF,NBLOCK,NEQ,NR,NF )
  310   RETURN
C
 1000   FORMAT (34HOTIME FOR STIFFNESS FACTORIZATION  F6.2)
 1010   FORMAT (42HOTIME FOR GENERATION OF INITIAL TR-VECTORS  F6.2)
 1020   FORMAT (1H1,11HNO OF ITERN  I4)
 1030   FORMAT (24HOTIME USED IN ITERN STEP  F6.2)
 1040   FORMAT (25HOTIME FOR EIGENVALUE SOLN  F6.2)
 1050   FORMAT (1H1,26HTHE FINAL EIGENVALUES ARE /)
 1055 FORMAT(37H1 FREQUENCIES IN CYCLE PER SECOND ARE// )
 1056 FORMAT(10X,I5,5H-----F10.4)
 1060   FORMAT (1H0,6E22.14)
      END
```

```
        SUBROUTINE EIGSOL (DL,RTOLV,AR,BR,VEC,VL,VR,D,XM,NF,NV,NBLOCK,
     1NEQB,NITE,MB)
C
        COMMON /TAPES/NSTIF,NRED,NL,NR,NT,NMASS
        DIMENSION AR(NV,NV),BR(NV,NV),VEC(NV,NV),VL(NEQB,NV),VR(NEQB,NV)
        DIMENSION D(NV),DL(NV),RTOLV(NV),XM(NEQB,MB)
       COMMON /ELPAR/ NPAR(14),NUMNP,MBAND,NELTYP,N1,N2,N3,N4,N5,MTOT,NEQ
     . ,N6, NUMNPF   ,IPRINT ,NLM ,NUMEL,WATL ,IMASS,TVOL
C
      NITEM=10
      RTOL=1.0E-04
       TOLJ=1.0E-12
        REWIND NMASS
        REWIND NT
        REWIND NR
C
C     FIND PROJECTIONS OF MASS AND STIFFNESS OPERATORS
        DO 100 I=1,NV
        DO 100 J=I,NV
        AR(I,J)=0.0
 100    BR(I,J)=0.0
        DO 200 N=1,NBLOCK
        BACKSPACE NL
        READ (NL) VL
        BACKSPACE NL
        READ (NR) VR
  101 DO 220 I=1,NV
        DO 220 J=I,NV
        ART=0.0
        DO 230 K=1,NEQB
 230    ART=ART+VL(K,I)*VR(K,J)
 220    AR(I,J)=AR(I,J)+ART
  200 CONTINUE
        DO 290 I=1,NV
        DO 290 J=1,I
      BR(I,J)=BR(J,I)
  290  AR(I,J)=AR(J,I)
C
      DO 291 N=1, NBLOCK
  291 READ(NL)
      CALL TRANSM(XM,VL,VR,BR,NEQB,MB,NV,NMASS,NL,NT,NBLOCK)
C
C
C     SOLVE EIGENVALUE PROBLEM
  289 CONTINUE
        CALL JACOBI (AR,BR,VEC,D,VL,NV,TOLJ)
        DO 295 J=1,NV
        XMM=SQRT(BR(J,J))
        DO 295 K=1,NV
 295    VEC(K,J)=VEC(K,J)/XMM
C
C     ARRANGE EIGENVALUES
        NV1=NV-1
 440    IS=0
        DO 400 I=1,NV1
        IF (D(I+1).GE.D(I)) GO TO 400
        IS=IS+1
        BT=BR(I+1,I+1)
        DT=D(I+1)
        BR(I+1,I+1)=BR(I,I)
        D(I+1)=D(I)
        BR(I,I)=BT
        D(I)=DT
        DO 420 K=1,NV
        TEMP=VEC(K,I+1)
        VEC(K,I+1)=VEC(K,I)
 420    VEC(K,I)=TEMP
 400    CONTINUE
        IF (IS.GT.0) GO TO 440
C
C     CHECK FOR CONVERGENCE
```

```
      DO 300 I=1,NV
      DIF=ABS(DL(I)-D(I))
  300 RTOLV(I)=DIF/D(I)
      PRINT 1040
      PRINT 1000,(RTOLV(I),I=1,NV)
      DO 320 I=1,NF
      IF (RTOLV(I).GT.RTOL) GO TO 340
  320 CONTINUE
      PRINT 1050,RTOL
      NITE=NITEM
      GO TO 350
  340 IF (NITE.LT.NITEM) GO TO 360
      PRINT 1060
  350 DO 354 I=1,NV
     DL(I)=D(I)
     IF(D(I).LE.0.0) STOP
  354 D(I)=SQRT(D(I))
      M=NT
      NT=NL
      NL=M
     M=NR
     NR=NL
     NL=M
     REWIND NR
     WRITE(NR) (D(I), I=1, NF)
     PRINT 1055, ((I,D(I)), I=1, NF)
 1055 FORMAT(7H FREQS./14H      N    FREQ.   /(I5,F10.4))
      GO TO 430
C
C   CALCULATE APPROXIMATE EIGEN DIRECTIONS
  360 DO 410 I=1,NV
  410 DL(I)=D(I)
      REWIND NR
  430 REWIND NT
      DO 460 N=1,NBLOCK
      READ (NT) VR
      DO 480 J=1,NV
      DO 480 I=1,NEQB
      TEMP=0.0
      DO 500 K=1,NV
  500 TEMP=TEMP+VR(I,K)*VEC(K,J)
  480 VL(I,J)=TEMP
  460 WRITE (NR) VL
C
      RETURN
 1000 FORMAT (1H ,12E11.4)
 1040 FORMAT (32H0REL TOL REACHED ON EIGENVALUES   )
 1050 FORMAT (21H0CONVERGENCE FOR RTOL  E10.4)
 1060 FORMAT (31H0WE ACCEPT CURRENT ITERN VALUES   )
     END



     SUBROUTINE TRANSM(XM,A,C,B,NEQB,MB,NV,NMASS,ND,NT,NBLOCK)
C
C    THIS SUBROUTINE FORMS B=AT*XM*A, WRITES  C=XM*A ON TAPE NT.
C    A AND XM  ARE READ FROM TAPES ND AND NMASS.
C
     DIMENSION XM(NEQB,MB),A(NEQB,NV),B(NV,NV),C(NEQB,NV)
C
      REWIND NT
      NMAX=MB/NEQB+2
      IF(NMAX.GT.NBLOCK) NMAX=NBLOCK
      NEV=NEQB*NV
      ITT=0
      CALL SECOND(T1)
      DO 400 N=1, NBLOCK
      REWIND NMASS
      DO 5 I=1, NEV
    5 C(I)=0.0
      NR=N-NMAX
      IF(NR.GT.0) GO TO 6
      NR=0
      GO TO 20
    6 DO 10 I=1, NR
      BACKSPACE ND
      ITT=ITT+1
   10 READ(NMASS)
   20 READ(NMASS) XM
      NR=NR+1
      BACKSPACE ND
      READ (ND) A
      BACKSPACE ND
      ITT=ITT+1
      IF(NR.EQ.N) GO TO 100
      ISTART=(N-NR-1)*NEQB +1
      DO 50 I=1, NEQB
      NXM=ISTART*NEQB+1
      ISTART=ISTART+1
      NDIF=MB-ISTART +1
      IF(NDIF.LT.1) GO TO 20
      NM=NEQB
      IF(NDIF.LT.NM) NM=NDIF
      DO 40 K=1, NM
      NA=1-K
      NC=I-NEQB
      NXM=NXM-1+NEQB
      IF(XM(NXM).EQ.0.0) GO TO 40
      DO 30 J=1, NV
      NA=NA+NEQB
      NC=NC+NEQB
   30 C(NC)=C(NC)+XM(NXM)*A(NA)
   40 CONTINUE
   50 CONTINUE
      GO TO 20
  100 CONTINUE
C
      DO 150 I=1, NEQB
      NXM=NEQB*I
      DO 140 K=1, I
      NXM=NXM+1-NEQB
      II=I+1-K
      IF(II.GT.MB) GO TO 140
      IF(XM(NXM).EQ.0.0) GO TO 140
      NA=K-NEQB
      NC=I-NEQB
      DO 130 J=1, NV
      NA=NA+NEQB
      NC=NC+NEQB
  130 C(NC)=C(NC)+XM(NXM)*A(NA)
  140 CONTINUE
```

```
      IF(I.EQ.NEQB) GO TO 150
      II=I+1
      DO 145 K=II, NEQB
      IJ=K-I+1
      IF(IJ.GT.MB) GO TO 150
      NXM=NXM+NEQB
      IF(XM(NXM).EQ.0.0) GO TO 145
      NA=K-NEQB
      NC=I-NEQB
      DO 155 J=1, NV
      NA=NA+NEQB
      NC=NC+NEQB
  155 C(NC)=C(NC)+XM(NXM)*A(NA)
  145 CONTINUE
  150 CONTINUE
      IB=N
      DO 300 L=2, NMAX
      IB=IB+1
      IF(IB.GT.NBLOCK) GO TO 350
      BACKSPACE ND
      READ (ND) A
      BACKSPACE ND
      ITT=ITT+1
      ISTART=(IB-N)*NEQB +2
      DO 180 I=1, NEQB
      ISTART=ISTART-1
      NDIF=MB-ISTART+1
      IF(NDIF.LT.1) GO TO 180
      NXM=(ISTART-2)*NEQB+I
      NM=NEQB
      IF(NDIF.LT.NM) NM=NDIF
      DO 160 K=1, NM
      NXM=NXM+NEQB
      IF(XM(NXM).EQ.0.0) GO TO 160
      NA=K-NEQB
      NC=I-NEQB
      DO 170 J=1, NV
      NA=NA+NEQB
      NC=NC+NEQB
  170 C(NC)=C(NC)+XM(NXM)*A(NA)
  160 CONTINUE
  180 CONTINUE
  300 CONTINUE
  350 DO 310 I=1, ITT
  310 READ(ND)
      WRITE(NT) C
  400 ITT=0
      NEV=NV*NV
      DO 410 I=1, NEV
  410 B(I)=0.0
      REWIND NT
      DO 450 N=1, NBLOCK
      BACKSPACE ND
      READ(ND) A
      BACKSPACE ND
      READ (NT) C
      DO 440 I=1, NV
      DO 440 J=1, NV
      CT=0.0
      DO 430 K=1, NEQB
  430 CT=CT+A(K,I)*C(K,J)
  440 B(I,J)=B(I,J)+CT
  450 CONTINUE
      DO 460 I=1, NV
      DO 460 J=1, NV
  460 B(J,I)=B(I,J)
      CALL SECOND(T2)
      T2=T2-T1
      PRINT 2000
      PRINT 1000, T2
      RETURN
 1000 FORMAT(F10.4)
 2000 FORMAT(41H TIME FOR FORMING GENERALIZED MASS MATRIX)
      END
```

```
      SUBROUTINE ASMBLB(A,SMS,NUMEL,NBLOCK,NE2B,LL,MBAND,NEQ,MASWAT)
C
C     FORMS GLOBAL EQUILIBRIUM EQUATIONS IN BLOCKS
C
C
C     THIS VERSION ASSEMBLES GLOBAL MASS MATRIX..
C
      DIMENSION A(NE2B,MBAND),STIF(4850) ,SMS(NEQ)
      COMMON/EM/LM(48),ND,NS,S(48,48),P(48,4),XM(48,48),ST(22,48),
     1   TT(12,4)
      EQUIVALENCE (STIF,LM)
      NEQB=NE2B/2
      K=NEQB+1
      X=NBLOCK
      MB=SQRT(X)
      MB=MB/2+1
      NEBB=MB*NE2B
      MM=1
C
      NSHIFT=0
      REWIND 4
      REWIND 9
C
C     FORM EQUATIONS IN BLOCKS     ( 2 BLOCKS AT A TIME)
C
      DO 1000 M=1,NBLOCK ,2
      DO 100 I=1,NE2B
      DO 100 J=1,MBAND
  100 A(I,J)=0.
C
      REWIND 7
      REWIND 2
      NA=7
      NUME=NUM7
      IF (MM.NE.1) GO TO 75
      NA=2
      NUME=NUMEL
      NUM7 =0
C
   75 DO 700 N=1,NUME
      READ (NA)  STIF
      DO 600 I=1,ND
      LMN=1-LM(I)
      II=LM(I)-NSHIFT
```

```
      IF (II.LE.0.OR.II.GT.NE2B) GO TO 600
      DO 500 J=1,ND
      JJ=LM(J)+LMN
      IF(JJ) 500,500,400
  400 A(II,JJ)=A(II,JJ)+S(I,J)
  500 CONTINUE
  600 CONTINUE
C
C     DETERMINE IF STIFFNESS IS TO BE PLACED ON TAPE 7
C
      IF (MM.GT.1) GO TO 700
      DO 650 I=1,ND
      II=LM(I) -NSHIFT
      IF(II.GT.NE2B.AND.II.LE.NEBB) GO TO 660
  650 CONTINUE
      GO TO 700
  660 WRITE (7) STIF
      NUM7=NUM7+1
C
  700 CONTINUE
      WRITE(4) ((A(I,J),I=1,NEQB),J=1,MBAND)
      IF(M.EQ.NBLOCK) GO TO 1000
      WRITE(4) ((A(I,J),I=K,NE2B),J=1,MBAND)
      IF (MM.EQ.MB) MM=0
      MM=MM+1
 1000 NSHIFT=NSHIFT+NE2B
C
      MM=1
      NSHIFT=0
      DO 1001 M=1,NBLOCK,2
      DO 101 I=1, NE2B
      DO 101 J=1, MBAND
  101 A(I,J)=0.0
      REWIND 7
      REWIND 2
      NA=7
      NUME=NUM7
      IF(MM.NE.1) GO TO 76
      NA=2
      NUME=NUMEL
      NUM7=0
   76 DO 701 N=1, NUMEL
      READ(NA) STIF
      DO 601 I=1, ND
      LMN=1-LM(I)
      II=LM(I)-NSHIFT
      IF (II.LE.0.OR.II.GT.NE2B) GO TO 601
      DO 501 J=1, ND
      JJ=LM(J)+LMN
      IF(JJ) 501,501,401
  401 A(II,JJ)=A(II,JJ)+XM(I,J)
  501 CONTINUE
  601 CONTINUE
      IF(MM.GT.1) GO TO 701
      DO 651 I=1, ND
      II=LM(I)-NSHIFT
      IF(II.GT.NE2B.AND.II.LE.NEBB) GO TO 661
  651 CONTINUE
      GO TO 701
  661 WRITE(7) STIF
      NUM7=NUM7+1
  701 CONTINUE
      WRITE(9) ((A(I,J),I=1,NEQB),J=1,MBAND)
      IF(M.EQ.NBLOCK) GO TO 1001
      WRITE(9) ((A(I,J),I=K,NE2B),J=1,MBAND)
 1001 NSHIFT=NSHIFT+NE2B
      RETURN
      END
```

```
      SUBROUTINE INVECT (VA,XM,IEQ,NBLOCK,NEQB,NV)
C
      COMMON /TAPES/NSTIF,NRED,NL,NR,NT,NMASS
      DIMENSION VA(NEQB,NV),XM(NEQB),IEQ(1)
C
      NV1=NV-1
      KK=1
      IND=0
 90   NBV=KK*((NV1-1)/NBLOCK+1)
      IF (NBV.GT.NEQB) NBV=NEQB
      IF (NBV.EQ.NEQB) IND=1
      IF (NBV.GT.NEQB) NBV=NEQB
      IF (NBV.EQ.NEQB) IND=1
      NBVN=0
      ICOUNT=0
      LL=0
C
      REWIND NMASS
      REWIND NSTIF
 60   READ (NMASS) XM
      READ (NSTIF) VA
      ICOUNT=ICOUNT+1
      DO 20 I=1,NEQB
      IF (VA(I).EQ.0.0) GO TO 20
      VA(I)=XM(I)/VA(I)
 20   CONTINUE
C
      NNV=NEQB/NBV
      DO 40 L=1,NBV
      RT=0.0
      NN=L*NNV
      DO 34 I=1,NN
      IF (VA(I).LT.RT) GO TO 34
      RT=VA(I)
      IJ=I
 34   CONTINUE
      DO 30 I=NN,NEQB
      IF (VA(I).LE.RT) GO TO 30
      RT=VA(I)
      IJ=I
 30   CONTINUE
      IF (VA(IJ).NE.0.0) GO TO 32
      NBVN=NBVN+1
      GO TO 40
 32   LL=LL+1
      IEQ(LL)=(ICOUNT-1)*NEQB+IJ
      IF (LL.GE.NV1) GO TO 50
      VA(IJ)=0.0
 40   CONTINUE
      IF (IND.EQ.1) GO TO 45
```

```
      IF ((NBVN.EQ.0).OR.(ICOUNT.EQ.NBLOCK)) GO TO 45
      NBV=KK*((NV1-LL-1)/(NBLOCK-ICOUNT)+1)
      IF (NBV.GT.NEQB) NBV=NEQB
      NBVN=0
C
 45   IF (ICOUNT.LT.NBLOCK) GO TO 60
      IF (IND.EQ.1) GO TO 47
      KK=2*KK
      GO TO 90
 47   PRINT 1000
      STOP
C
 50   REWIND NMASS
      REWIND NR
      DO 100 L=1,NBLOCK
      READ (NMASS) XM
      DO 120 I=1,NEQB
      VA(I,1)=XM(I)
      DO 120 J=2,NV
 120  VA(I,J)=0.0
      DO 140 K=2,NV
      II=IEQ(K-1)
      NLE=(L-1)*NEQB
      NRI=L*NEQB
      IF (II-NLE) 140,140,160
 160  IF (NRI-II) 140,180,180
 180  II=II-NLE
      VA(II,K)=1.
 140  CONTINUE
      WRITE (NR) VA
 100  CONTINUE
      PRINT 1010
      PRINT 1020,(IEQ(I),I=1,NV1)
C
      RETURN
 1000 FORMAT (42H0WE DO NOT HAVE ENOUGH FINITE EIGENVALUES  )
 1010 FORMAT (20H0PRINT OF VECTOR IEQ  )
 1020 FORMAT (1H0,20I6)
     END
```

```
      SUBROUTINE REDBAK (A,VA,VV,MAXB,NEQB,NV,NWA,NWV,NWVV,NTB,NBLOCK)
C
      COMMON /TAPES/NSTIF,NRED,NL,NR,NT,NMASS
      DIMENSION A(NWA),VA(NWV),VV(NWVV),MAXB(NEQB)
C
      NEB=NTB*NEQB
      NEBT=NEB+NEQB
C
C   REDUCE VECTORS ON TAPE NR
      REWIND NRED
      REWIND NR
      REWIND NL
      REWIND NT
      READ (NRED) A,MAXB
      ISV=NTB+1
      LL=0
      DO 10 L=1,ISV
      READ (NR) VA
      K=0
      KK=LL
      DO 20 J=1,NV
      DO 30 I=1,NEQB
      K=K+1
      KK=KK+1
 30   VV(KK)=VA(K)
 20   KK=KK+NEB
 10   LL=LL+NEQB
      ISA=1
C
 500  DO 100 I=1,NEQB
      IL=I+NEQB
      MAX=MAXB(I)
      J=0
      DO 120 II=IL,MAX,NEQB
      J=J+1
      C=A(II)
      IF (C) 110,120,110
 110  KK=I+J
      JJ=I
      DO 140 L=1,NV
      VV(KK)=VV(KK)-C*VV(JJ)
      KK=KK+NEBT
 140  JJ=JJ+NEBT
 120  CONTINUE
 100  CONTINUE
      DO 200 I=1,NEQB
      C=A(I)
      IF (C) 180,200,180
 180  KK=I
      DO 210 L=1,NV
      VV(KK)=VV(KK)/C
 210  KK=KK+NEBT
 200  CONTINUE
      IF (ISA.EQ.NBLOCK) GO TO 400
      READ (NRED) A,MAXB
      ISA=ISA+1
C
C    STORE REDUCED VECTORS ON TAPE NT
      K=0
      KK=0
      DO 240 J=1,NV
      DO 220 I=1,NEQB
      K=K+1
      KK=KK+1
 220  VA(K)=VV(KK)
 240  KK=KK+NEB
      WRITE (NT) VA
      K=1
      DO 310 J=1,NV
      DO 300 I=1,NEB
      KK=K+NEQB
      VV(K)=VV(KK)
 300  K=K+1
 310  K=K+NEQB
      IF (ISV.EQ.NBLOCK) GO TO 500
      READ (NR) VA
      ISV=ISV+1
      KK=NEB
      K=0
```

```
      DO 330 J=1,NV
      DO 320 I=1,NEQB
      K=K+1
      KK=KK+1
  320 VV(KK)=VA(K)
  330 KK=KK+NEB
      GO TO 500
C
C     BACKSUBSTITUTE VECTORS ON TAPE NT
  400 BACKSPACE NRED
      ISA=1
  420 DO 600 I=1,NEQB
      J=NEQB+1-I
      MAX=MAXB(J)
      IF (A(J)) 440,600,440
  440 KK=J
      DO 620 L=1,NV
      JJ=KK+1
      IL=J+NEQB
      C=VV(KK)
      DO 640 II=IL,MAX,NEQB
      C=C-A(II)*VV(JJ)
  640 JJ=JJ+1
      VV(KK)=C
  620 KK=KK+NEBT
  600 CONTINUE
      KK=0
      K=0
      DO 660 J=1,NV
      DO 670 I=1,NEQB
      K=K+1
      KK=KK+1
  670 VA(K)=VV(KK)
  660 KK=KK+NEB
      WRITE (NL) VA
      IF (ISA.EQ.NBLOCK) GO TO 800
      BACKSPACE NRED
      READ (NRED) A,MAXB
      BACKSPACE NRED
      ISA=ISA+1
      BACKSPACE NT
      READ (NT) VA
      BACKSPACE NT
      K=NEBT
      DO 700 J=1,NV
      DO 720 I=1,NEB
      KK=K-NEQB
      VV(K)=VV(KK)
  720 K=K-1
  700 K=K+NEBT+NEB
      K=0
      KK=0
      DO 740 J=1,NV
      DO 760 I=1,NEQB
      K=K+1
      KK=KK+1
  760 VV(KK)=VA(K)
  740 KK=KK+NEB
      GO TO 420
  800 RETURN
      END
```

```
      SUBROUTINE JACOBI (A,B,X,EIGV,D,N,RTOL)
C
      DIMENSION A(N,N),B(N,N),X(N,N),EIGV(N),D(N)
C
      NSMAX=15
      DO 10 I=1,N
      D(I)=A(I,I)/B(I,I)
   10 EIGV(I)=D(I)
      IF (N.EQ.1) RETURN
      DO 30 I=1,N
      DO 20 J=1,N
   20 X(I,J)=0.
   30 X(I,I)=1.0
      NSWEEP=0
      NR=N-1
C
C     WE START ITERATION
   40 NSWEEP=NSWEEP+1
      PRINT 1000,NSWEEP
      EPS=(0.01**NSWEEP)**2
      DO 50 J=1,NR
      JJ=J+1
      DO 50 K=JJ,N
      TT=A(J,K)*A(J,K)
      TB=A(J,J)*A(K,K)
      EPTOLA=ABS(TT/TB)
      TT=B(J,K)*B(J,K)
      TB=B(J,J)*B(K,K)
      EPTOLB=TT/TB
      IF ((EPTOLA.LT.EPS).AND.(EPTOLB.LT.EPS)) GO TO 50
      AKK=A(K,K)*B(J,K)-B(K,K)*A(J,K)
      AJJ=A(J,J)*B(J,K)-B(J,J)*A(J,K)
      AB=A(J,J)*B(K,K)-A(K,K)*B(J,J)
      CHECK=(AB*AB+4.0*AKK*AJJ)/4.0
      IF (CHECK) 60,70,70
   60 PRINT 1004,CHECK
      STOP
   70 SQCH=SQRT(CHECK)
      D1=AB/2.0+SQCH
      D2=AB/2.0-SQCH
      DEN=D1
      IF (ABS(D2).GT.ABS(D1)) DEN=D2
      IF (DEN) 90,80,90
   80 CA=0.
      CG=-A(J,K)/A(K,K)
      GO TO 100
   90 CA=AKK/DEN
      CG=-AJJ/DEN
C
C     WE PERFORM THE GENERALIZED ROTATION
  100 IF (N-2) 95,180,95
   95 JP1=J+1
      JM1=J-1
      KP1=K+1
      KM1=K-1
C
      IF (JM1-1) 120,110,110
```

```
  110 DO 105 I=1,JM1
      AJ=A(I,J)
      BJ=B(I,J)
      AK=A(I,K)
      BK=B(I,K)
      A(I,J)=AJ+CG*AK
      B(I,J)=BJ+CG*BK
      A(I,K)=AK+CA*AJ
  105 B(I,K)=BK+CA*BJ
C
  120 IF (KP1-N) 130,130,140
  130 DO 125 I=KP1,N
      AJ=A(J,I)
      BJ=B(J,I)
      AK=A(K,I)
      BK=B(K,I)
      A(J,I)=AJ+CG*AK
      B(J,I)=BJ+CG*BK
      A(K,I)=AK+CA*AJ
  125 B(K,I)=BK+CA*BJ
C
  140 IF (JP1-KM1) 150,150,180
  150 DO 160 I=JP1,KM1
      AJ=A(J,I)
      BJ=B(J,I)
      AK=A(I,K)
      BK=B(I,K)
      A(J,I)=AJ+CG*AK
      B(J,I)=BJ+CG*BK
      A(I,K)=AK+CA*AJ
  160 B(I,K)=BK+CA*BJ
  180 AK=A(K,K)
      BK=B(K,K)
      A(K,K)=AK+2*CA*A(J,K)+CA*CA*A(J,J)
      B(K,K)=BK+2*CA*B(J,K)+CA*CA*B(J,J)
      A(J,J)=A(J,J)+2*CG*A(J,K)+CG*CG*AK
      B(J,J)=B(J,J)+2*CG*B(J,K)+CG*CG*BK
      A(J,K)=0.0
      B(J,K)=0.0
C
C     UPDATE EIGENVECTORS
      DO 190 I=1,N
      XJ=X(I,J)
      XK=X(I,K)
      X(I,J)=XJ+CG*XK
  190 X(I,K)=XK+CA*XJ
C
   50 CONTINUE
C
      DO 220 I=1,N
  220 EIGV(I)=A(I,I)/B(I,I)
      PRINT 1005
      PRINT 1002,(EIGV(I),I=1,N)
C
C     CHECK FOR CONVERGENCE
      DO 240 I=1,N
      TOL=RTOL*D(I)
      DIF=ABS(EIGV(I)-D(I))
  240 IF (DIF.GT.TOL) GO TO 300
C
C     CHECK IF ALL OFF-DIAG ELEMENTS ARE SATISFACTORILY SMALL
      EPS=RTOL**2
      DO 260 J=1,NK
      JJ=J+1
      DO 260 K=JJ,N
      TT=A(J,K)*A(J,K)
      TB=A(J,J)*A(K,K)
      EPSA=ABS(TT/TB)
      TT=B(J,K)*B(J,K)
      TB=B(J,J)*B(K,K)
      EPSB=TT/TB
      IF ((EPSA.LT.EPS).AND.(EPSB.LT.EPS)) GO TO 260
      GO TO 300
  260 CONTINUE
C
      DO 310 I=1,N
      DO 310 J=I,N
      B(J,I)=B(I,J)
  310 A(J,I)=A(I,J)
      RETURN
C
  300 DO 320 I=1,N
  320 D(I)=EIGV(I)
      IF (NSWEEP.LT.NSMAX) GO TO 40
      DO 330 I=1,N
      DO 330 J=I,N
      B(J,I)=B(I,J)
  330 A(J,I)=A(I,J)
      RETURN
C
 1000 FORMAT (1H0,14HNO OF SWEEP =  I4)
 1002 FORMAT (1H ,12E11.4)
 1004 FORMAT (8H0CHECK =  E20.14)
 1005 FORMAT (24H0CURRENT EIGENVALUES ARE  )
     END
```

```
      SUBROUTINE DECOMP (A,B,MAXB,NEQB,MBAND,NBLOCK,NWA,NTB,NSCH,NEQ)
C
      COMMON /TAPES/NSTIF,NRED,NL,NR,NT,NMASS
      DIMENSION A(NWA),B(NWA),MAXB(NEQB)
C
      NEQB1=NEQB-1
      N1=NL
      N2=NR
      REWIND NSTIF
      REWIND NRED
      REWIND N1
      REWIND N2
      NSCH=0
C
      DO 600 N=1,NBLOCK
      IF (N.NE.1) GO TO 10
      READ (NSTIF) A
      GO TO 110
   10 IF (NTB.EQ.1) GO TO 110
      REWIND N1
      REWIND N2
      READ (N1) A
C
```

```
C    FACTORIZE LEADING BLOCK
 110    DO 300 I=1,NEQBI
        PIV=A(I)
        IF (PIV) 120,115,130
 115    II=(N-1)*NEQB+I
        IF (II.GT.NEQ) GO TO 520
        PRINT 1000,II
        STOP
 120    NSCH=NSCH+1
 130    IH=I+NWA-NEQB
 140    IF (A(IH)) 160,150,160
 150    IH=IH-NEQB
        GO TO 140
 160    MAXB(I)=IH
        JL=I+1
        II=I
        DO 200 J=JL,NEQB
        II=II+NEQB
        IF (II-NWA) 170,170,300
 170    C=A(II)
        IF (C) 180,200,180
 180    C=C/PIV
        KK=J
        MAX=MAXB(I)
        DO 250 JJ=II,MAX,NEQB
        A(KK)=A(KK)-C*A(JJ)
 250    KK=KK+NEQB
 200    A(II)=C
 300    CONTINUE
        IF (A(NEQB)) 80,60,70
 60     II=N*NEQB
        IF (II.GT.NEQ) GO TO 520
        PRINT 1000,II
        STOP
 80     NSCH=NSCH+1
 70     DO 50 J=NEQB,NWA,NEQB
 50     IF (A(J).NE.0.0) MAXB(NEQB)=J
C
C    CARRY OVER INTO TRAILING BLOCKS
        DO 400 NN=1,NTB
        IF ((NN+N).GT.NBLOCK) GO TO 400
        NI=N1
        IF ((N.EQ.1).OR.(NN.EQ.NTB)) NI=NSTIF
        READ (NI) B
        DO 420 I=1,NEQB
        II=IL
        DO 440 K=1,NEQB
        IF (II-NWA) 410,410,440
 410    C=A(II)
        IF (C) 430,440,430
 430    C=C/A(K)
        MAX=MAXB(K)
        KK=I
        DO 460 JJ=II,MAX,NEQB
        B(KK)=B(KK)-C*A(JJ)
 460    KK=KK+NEQB
        A(II)=C
 440    II=II-NEQBI
 420    IL=IL+NEQB
        IF (NTB.NE.1) GO TO 480
        WRITE (NRED) A,MAXB
        DO 500 I=1,NWA
 500    A(I)=B(I)
        GO TO 600
 480    WRITE (N2) B
 400    CONTINUE
        M=N1
        N1=N2
        N2=M
 520    WRITE (NRED) A,MAXB
 600    CONTINUE
C
        RETURN
 1000   FORMAT (22HOPIVOT IS ZERO IN ROW  I4)
        END
```

```
      OVERLAY(XFILE,3,0)
      PROGRAM HYDRO
      COMMON / MISC / NBLOCK,NEQB,LL,NF,LB ,NDYN
      COMMON /ELPAR/ NPAR(14),NUMNP,MBAND,NELTYP,N1,N2,N3,N4,N5,MTOT,NEQ
     .  ,N6, NUMNPF    ,IPRINT ,NLM ,NUMEL,WATL, IMASS,TVOL,NEQEST,IMODE
     .  ,IPRM  ,MESH ,MESHFN ,ISYM,WDEN,T(10)
      COMMON/RADOD/RADIUS,RADHT
      COMMON/HYD/NUMELZ,NUMELT,TW,ZW,HWATER,NTERM,MTERM,IXYZ
C
      READ(5,1000)NUMELZ,NUMELT,TW,ZW,HWATER,NTERM,MTERM,IXYZ
      WRITE(6,2000)NUMELZ,NUMELT,TW,ZW,HWATER,NTERM,MTERM
      NTERM= NTERM + 1
  500 GOTO(1,2,3) IXYZ
C
C     HORIZONTAL EXCITATION IN X DIRECTION
C
    1 CALL OVERLAY(5HXFILE,3,1,6HRECALL)
      GOTO 600
C
C     HORIZONTAL EXCITATION IN Y DIRECTION
C
    2 CALL OVERLAY(5HXFILE,3,2,6HRECALL)
      GOTO 600
C
C     VERTICAL EXCITATION
C
    3 CALL OVERLAY(5HXFILE,3,3,6HRECALL)
  600 RETURN
 1000 FORMAT(2I5,3F10.0,3I5)
 2000 FORMAT(///33H NUMBER ELEMENTS IN Z DIRECTION =,I5,
     1        //37H NUMBER ELEMENTS IN THETA DIRECTION =,I5,
     2        //29H ELEMENT HALF ANGLE -RADIANS=,F10.5,
     3        //22H ELEMENT HALF HEIGHT =,F10.5,
     4        //22H DEPTH OF RESERVOIR = ,F12.6,
     5        //28H NUMBER OF N TERMS - NTERM =,I5,
     6        //28H NUMBER OF M TERMS - MTERM =,I5///)
      END
```

```
      SUBROUTINE GMTNX(GLOAD,FF,ID,IRX,XM,NUMNP,NUMEL,NEQB,
     1     MBAND,NF,NBLOCK,NEQ,IXYZ)
      DIMENSION GLOAD(NF),FF(NEQ),ID(NUMNP,3),IRX(NEQ),XM(NEQB,MBAND)
C
C*********************************************************************
C     THIS SUBROUTINE FORMS THE NODAL LOADS DUE TO GROUND MOTION
C     EXCITATION OF THE DAM ALONE -  FF= (MASS)*(INFLUENCE COEFF  IRX)
C*********************************************************************
C
      REWIND 9
      REWIND 8
      READ (8) ID
      DO 50 I=1,NEQ
   50 IRX(I)= 0
      DO 100 J=1,NUMNP
      NNN= ID(J,IXYZ)
      IF(NNN.LT.1)GOTO 100
      IRX(NNN)=1
  100 CONTINUE
      DO 200 I=1,NEQ
  200 FF(I)= 0.0
      NLOC= 0
      DO 400 N=1,NBLOCK
      READ (9) XM
      DO 375 I=1,NEQB
      IR= I + NLOC
      IF(IR.GT.NEQ)GOTO 500
      DO 275 J=1,MBAND
      JJ= IR + J - 1
      IF(JJ.GT.NEQ)GOTO 300
      K= IRX(JJ)
      IF(K.EQ.0)GOTO 275
      FF(IR)= FF(IR) -XM(I,J)
  275 CONTINUE
  300 K= IRX(IR)
      IF(K.EQ.0)GOTO 350
      DO 325 J=2,MBAND
      IR= IR+1
      IF(IR.GT.NEQ)GOTO 350
  325 FF(IR)= FF(IR) - XM(I,J)
  350 CONTINUE
  375 CONTINUE
  400 NLOC= NLOC + NEQB
  500 CONTINUE
      RETURN
      END
```

```
      SUBROUTINE LOAD1(GLOAD,FF,B,NEQB,NBLOCK,NF,NEQ)
      DIMENSION GLOAD(NF),FF(NEQ),B(NEQB,NF)
C
C*********************************************************************
C     THIS SUBROUTINE TRANSFORMS THE NODAL LOADS (STORED IN FF) TO
C     MODAL LOADS (STORED IN GLOAD). THESE LOADS ARE DUE TO GROUND
C     MOTION EXCITATION OF THE DAM ALONE.
C*********************************************************************
C
      REWIND 7
      READ (7)
      DO 50 I=1,NBLOCK
   50 READ (7)
      DO 100 I=1,NF
  100 GLOAD(I)= 0.0
      NN= -NEQB
      DO 500 N=1,NBLOCK
      BACKSPACE 7
      READ (7) B
      BACKSPACE 7
      NN= NN + NEQB
      DO 250 I=1,NF
      DO 200 L=1,NEQB
      NNN= NN + L
      IF(NNN.GT.NEQ)GOTO 200
      GLOAD(I)= GLOAD(I) + B(L,I)*FF(NNN)
  200 CONTINUE
  250 CONTINUE
  500 CONTINUE
      DO 600 L=1,NF
  600 WRITE(6,2000)L,GLOAD(L)
      RETURN
 2000 FORMAT(7X,I7,8X,F12.3)
      END
```

```
      SUBROUTINE BEV(PHIR,LLM,B,LMTEMP,NEQBT,NUMEL,NF,NBLOCK,NEQB,
     1     NUMELZ,NUMELT,NZ,ZWH,ZWHTOP,ZW,TW,HWATER)
      DIMENSION PHIR(NUMEL,8,NF),LLM(NUMEL,24),B(NEQBT,NF),LMTEMP(50)
      DIMENSION SC(8,2),SHAPE(5,8),PMODE(5)
      REWIND 7
      READ(7)
      REWIND 1
      READ(1)
C
C     READ ELEMENT-NODE LOCATION MATRIX FOR EACH ELEMENT INTO MATRIX LLM
C
      DO 100 I=1,NUMEL
      READ(1) LMTEMP
      DO 90 J=1,3
      J1= J
      K= 20+J
      LLM(I,J1)= LMTEMP(K)
      J1= J1+3
      K= 17+J
      LLM(I,J1)= LMTEMP(K)
      J1= J1+3
      K= 14+J
      LLM(I,J1)= LMTEMP(K)
      J1= J1+3
      K= 23+J
      LLM(I,J1)= LMTEMP(K)
      J1= J1+3
      K= 41+J
      LLM(I,J1)= LMTEMP(K)
      J1= J1+3
      K= 38+J
      LLM(I,J1)= LMTEMP(K)
```

```
      J1= J1+3
      K= 47+J
      LLM(I,J1)= LMTEMP(K)
      J1= J1+3
      K= 44+J
      LLM(I,J1)= LMTEMP(K)
   90 CONTINUE
  100 CONTINUE
C
C     READ MODE SHAPE FROM TAPE 7 INTO MATRIX B
C
      NN= (NBLOCK-1)*NEQB + 1
      DO 200 K=1,NBLOCK
      NNEQB= NN + NEQB - 1
      READ(7)((B(N,L),N=NN,NNEQB),L=1,NF)
  200 NN= NN - NEQB
C
C     FORM MODE SHAPE IN RADIAL DIRECTION AT EACH UPSTREAM NODE-
C     STORE RADIAL MODE SHAPE IN MATRIX PHIR
C
      NN= 0
      THETA1= 0.0
      THETA2= TW
      THETA3= TW + TW
      DO 900 I=1,NUMELT
      SC(1,1)= SIN(THETA1)
      SC(1,2)= COS(THETA1)
      SC(2,1)= SIN(THETA3)
      SC(2,2)= COS(THETA3)
      SC(3,1)= SC(2,1)
      SC(3,2)= SC(2,2)
      SC(4,1)= SC(1,1)
      SC(4,2)= SC(1,2)
      SC(5,1)= SIN(THETA2)
      SC(5,2)= COS(THETA2)
      SC(6,1)= SC(2,1)
      SC(6,2)= SC(2,2)
      SC(7,1)= SC(5,1)
      SC(7,2)= SC(5,2)
      SC(8,1)= SC(1,1)
      SC(8,2)= SC(1,2)
      DO 800 J=1,NUMELZ
      K= J + NN
      DO 700 L=1,NF
      L1= 1
      L2= L1 + 1
      DO 550 NNN=1,8
      PHIR(K,NNN,L)= 0.0
      LLX= LLM(K,L1)
      LLY= LLM(K,L2)
      IF(LLY.LT.1)GOTO 510
      PHIR(K,NNN,L)=B(LLY,L)*SC(NNN,1)
  510 IF(LLX.LT.1)GOTO 520
      PHIR(K,NNN,L)= PHIR(K,NNN,L) + B(LLX,L)*SC(NNN,2)
  520 L1= L1 + 3
      L2= L1 + 1
  550 CONTINUE
  700 CONTINUE
  800 CONTINUE
      NN= NN + NUMELZ
      THETA1= THETA3
      THETA2= THETA1 + TW
      THETA3= THETA2 + TW
  900 CONTINUE
C
C     ADJUST RADIAL MODE SHAPES TO ACCOUNT FOR DIFFERENCES
C     BETWEEN DAM HEIGHT AND RESERVOIR HEIGHT
C
      HT= 0.0
      DO 990 I=1,NUMELZ
      H=HT
      HT= H+ZW+ZW
      NZ= I
      ZWHTOP= (HWATER-H)/(2.0*HWATER)
      C1= ABS((ZWH-ZWHTOP)/ZWH)
      IF(C1.LT.0.10)GOTO 991
      IF(HWATER.LT.HT)GOTO 930
      GOTO 990
  930 SC(1,1)= 1.0
      SC(2,1)= -1.0
      SC(3,1)= 1.0
      SC(4,1)= 0.0
      SC(5,1)= -1.0
      SC(1,2)= (ZWHTOP+ZWHTOP-ZWH)/ZWH
      SC(2,2)= SC(1,2)
      SC(3,2)= (ZWHTOP-ZWH)/ZWH
      SC(4,2)= SC(1,2)
      SC(5,2)= SC(3,2)
      DO 940 J=1,5
      S=SC(J,1)
      T= SC(J,2)
      SHAPE(J,1)= 0.25*(1.0-S)*(1.-T)*(-S-T-1.)
      SHAPE(J,2)= 0.25*(1.+S)*(1.-T)*(S-T-1.)
      SHAPE(J,3)= 0.25*(1.+S)*(1.+T)*(S+T-1.)
      SHAPE(J,4)= 0.25*(1.-S)*(1.+T)*(-S+T-1.)
      SHAPE(J,5)= 0.5*(1.-S*S)*(1.-T)
      SHAPE(J,6)= 0.5*(1.+S)*(1.-T*T)
      SHAPE(J,7)= 0.5*(1.-S*S)*(1.+T)
      SHAPE(J,8)= 0.5*(1.-S)*(1.-T*T)
  940 CONTINUE
      K= NZ
      DO 970 J=1,NUMELT
      DO 960 L=1,NF
      DO 950 N=1,5
      PMODE(N)= 0.0
      DO 950 M=1,8
      PMODE(N)= PMODE(N) + PHIR(K,M,L)*SHAPE(N,M)
  950 CONTINUE
      PHIR(K,3,L)= PMODE(1)
      PHIR(K,4,L)= PMODE(2)
      PHIR(K,6,L)= PMODE(3)
      PHIR(K,7,L)= PMODE(4)
      PHIR(K,8,L)= PMODE(5)
  960 CONTINUE
      K= K + NUMELZ
  970 CONTINUE
      GOTO 991
  990 CONTINUE
  991 CONTINUE
      RETURN
      END
```

```
      SUBROUTINE BESSJY(X,BESJ,BESY,NMAX,NYMAX)
      DIMENSION BESJ(200),BESY(200),TJ(200)
      EULER=0.577215664901533
      PI=2.0/3.14159265358 98
      NU22=20
      IF(10.-X) 2,2,3
    2 HATN=(1.05)*X+25.
      GOTO 4
    3 HATN=35./(3.5-ALOG(X))
    4 NU=HATN
      N=IABS(NMAX)+1
      NU2 = NU + 2
      DO 5 J = NU2,N
      TJ(J) = 0.
    5 CONTINUE
      TJ(NU+1)=0.000001
      DO 6 J=1,NU
      K=NU+1-J
      FK=K+K
    6 TJ(K)=FK*TJ(K+1)/X-TJ(K+2)
      SUM=0.0
      DO 7 J=3,NU,2
    7 SUM=SUM+TJ(J)
      SUM=SUM+SUM
      TK=1./(TJ(1)+SUM)
      DO 8 J=1,N
    8 BESJ(J)=TK*TJ(J)
      IF(NMAX)98,98,55
   55 L=X/5.0
      IF(L-1)300,300,301
  301 X82=1./(64.*X*X)
      X84=X82*X82
      POX=1.-4.5*X82+459.375*X84-150077.8125*X84*X82
      X8=.125/X
      X83=X8*X82
      QOX=-X8+37.5*X83-7441.875*X83*X82+3623307.1875*X83*X84
      XP4=X-0.5/PI
      TI=SQRT(PI/X)
      BESY(1)=TI*(POX*SIN(XP4)+QOX*COS(XP4))
      GOTO 302
  300 DX=X
      DSUM1=0.0
      DSUM2=0.0
      DX2= .25*DX*DX
      DXX=1.0
      DT=1.0
      DO 99 M=1,NU22
      DT=-DT
      DFFM= M
      DFM=1.0/(DFFM*DFFM)
      DX3=DX2*DFM
      DXX=DXX*DX3
      DSUM2=DSUM2 + 1./DFFM
   99 DSUM1=DSUM1+DT*DXX*DSUM2
      BESY(1)=PI*(BESJ(1)*(EULER+ALOG(.5*DX))-DSUM1)
  302 BESY(2)= (BESJ(2)*BESY(1)-(PI/X))/BESJ(1)
      N= NYMAX + 1
      DO 10 J=3,N
      FM=(J+J-4)
   10 BESY(J)=FM*BESY(J-1)/X-BESY(J-2)
   98 RETURN
      END
```

```
      SUBROUTINE BESNKS(X,KMAX,FK)
      DIMENSION FI(50),FK(200)
      IF(X-2.) 2,3,3
    2 T=.5*X
      T=T*T
      FK(1)= (((((.00000740*T+.00010750)*T+.00262698)*T+.03488590)*T+
     1 .23069756)*T+.42278420)*T-.57721566
      FK(2)= (((((-.00004686*T-.00110404)*T-.01919402)*T-.18156897)*T-
     1  .67278579)*T+.15443144)*T+1.
      CALL BESNIS (X,2,FI)
      T2=.5*ALOG(T)
      FK(1)=FK(1)-T2*FI(1)
      FK(2)=FK(2)/X+T2*FI(2)
      T=2./X
      GO TO 1
    3 T=2./X
      FK(1)= (((((.00053208*T-.00251540)*T+.00587872)*T-.01062446)*T+
     1 .02189568)*T-.07832358)*T+1.25331414
      FK(2)= (((((-.00068245*T+.00325614)*T-.00780353)*T+.01504268)*T-
     1 .03655620)*T+.23498619)*T+1.25331414
      T1=EXP(-X)/SQRT(X)
      FK(1)=FK(1)*T1
      FK(2)=FK(2)*T1
    1 CONTINUE
      AA= 1.0
      IF(X.LE.1.0)AA=1.0E-275
      FK(1)= AA*FK(1)
      FK(2)=AA*FK(2)
      DO 4 N=3,KMAX
      DK=N-2
    4 FK(N)=T*DK*FK(N-1)+FK(N-2)
      RETURN
      END
```

```
      SUBROUTINE BESNIS(X,NMAX,FI)
      DIMENSION FI(50), PI(200)
      SUM=0.
      I=X
      JMAX=I+21
      TZ=2./X
      JM2 = JMAX + 2
      DO 4 J = JM2,NMAX
      PI(J) = 0.
    4 CONTINUE
      PI(JMAX+1)=1.E-20
      DO 1 J=1,JMAX
      K=JMAX+2-J
      DK=K-1
```

```
      PI(K-1)=DK*TZ*PI(K)+PI(K+1)
    1 SUM=SUM+PI(K)
      SUM=SUM+SUM
      A=EXP(X)/(PI(1)+SUM)
      DO 2 N=1,NMAX
    2 FI(N)=A*PI(N)
      RETURN
      END
```

```
      SUBROUTINE CSYMEQ(A,B,NN,LL)
C
      COMPLEX A(15,15),B(15,2)
C
      DO 475 N=1,NN
      N1= N+1
C
C     FORM D(N,L)
C
      DO 150 L=1,LL
  150 B(N,L)= B(N,L)/A(N,N)
C
C     CHECK FOR LAST EQUATION
C
      IF(N-NN) 200,500,200
C
  200 DO 450 J=N1,NN
C
C     FORM H(N,J)
C
      IF(CABS(A(N,J))) 250,450,250
  250 A(N,J)= A(N,J)/A(N,N)
C
C     MODIFY A(I,J)
C
      DO 300 I=J,NN
      A(I,J)= A(I,J) - A(I,N)*A(N,J)
  300 A(J,I)=A(I,J)
C
C     MODIFY B(I,L)
C
      DO 400 L=1,LL
  400 B(J,L)= B(J,L) - A(J,N)*B(N,L)
  450 CONTINUE
  475 CONTINUE
C
C     BACK-SUBSTITUTION
C
  500 N1=N
      N= N-1
      IF(N) 700,700,550
C
  550 DO 600 L=1,LL
      DO 600 J= N1,NN
  600 B(N,L)= B(N,L) - A(N,J)*B(J,L)
C
      GOTO 500
C
  700 RETURN
      END
```

```
      SUBROUTINE HINML(PHIR,HINM,CDN,AA,CDM,
     1      NUMELZ,NUMELT,NZ,ZWH,ZWHTOP,TW,NTERM,MTERM,NF,NUMEL)
      DIMENSION PHIR(NUMEL,8,NF),HINM(NTERM,MTERM,NF),
     1      CDN(NUMELT,NTERM,3),AA(NTERM,3),CDM(NUMELZ,MTERM,3)
      DIMENSION CC(3)
C
C*********************************************************************
C     THIS SUBROUTINE FORMS THE INTEGRAL I(N,M,L)
C*********************************************************************
C
      DO 100 N=1,NTERM
      DO 100 M=1,MTERM
      DO 100 L=1,NF
      HINM(N,M,L)= 0.0
  100 CONTINUE
      TW4= 4.0*TW
      ANGLE= TW4
      DO 200 N=2,NTERM
      AN=N-1
      C1= SIN(ANGLE)
      C2= COS(ANGLE)
      CC(1)= (C2-C1/ANGLE)/AN
      CC(2)= 2.0*CC(1)/ANGLE
      CC(3)= C1/AN
      DO 150 I=1,NUMELT
      DO 150 J=1,3
  150 CDN(I,N,J)= CC(J)
  200 ANGLE= ANGLE + TW4
      ANGLEC= TW4
      DO 300 I=1,NUMELT
      ANGLE= ANGLEC
      DO 250 N=2,NTERM
      C1= SIN(ANGLE)
      C2= COS(ANGLE)
      CDN(I,N,1)=CDN(I,N,1)*C1
      CDN(I,N,2)=CDN(I,N,2)*C2
      CDN(I,N,3)=CDN(I,N,3)*C2
      ANGLE= ANGLE + ANGLEC
  250 CONTINUE
      ANGLEC= ANGLEC + TW4 + TW4
  300 CONTINUE
      PI= 3.1415926536
      PIZ= PI*ZWHTOP
      PLM= 0.5*PI
      ANGLE= 0.5*PIZ
      DO 350 M=1,MTERM
      C1= SIN(ANGLE)
      C2= COS(ANGLE)
      CDM(NZ,M,1)= (C2 - C1/ANGLE)/PLM
      CDM(NZ,M,2)= 2.0*CDM(NZ,M,1)/ANGLE
      CDM(NZ,M,3)= C1/PLM
      ANGLE= ANGLE + PIZ
      PLM= PLM + PI
  350 CONTINUE
```

```
      IF(NZ.EQ.1)GOTO 400
      NNZ= NZ-1
      PIZ= PI*ZWH
      PLM= 0.5*PI
      ANGLE= 0.5*PIZ
      DO 375 M=1,MTERM
      C1= SIN(ANGLE)
      C2= COS(ANGLE)
      CC(1)= (C2 - C1/ANGLE)/PLM
      CC(2)= 2.0*CC(1)/ANGLE
      CC(3)= C1/PLM
      DO 370 I=1,NNZ
      DO 370 J=1,3
  370 CDM(I,M,J)= CC(J)
      ANGLE= ANGLE + PIZ
      PLM= PLM + PI
  375 CONTINUE
  400 PIZ= 0.5*PI*ZWH
      PIZ2= PIZ
      ANGLEC= -PIZ
      DO 500 I=1,NZ
      IF(I.EQ.NZ)PIZ2= 0.5*PI*ZWHTOP
      ANGLEC= ANGLEC + PIZ + PIZ2
      ANGLE= ANGLEC
      DO 450 M=1,MTERM
      C1= SIN(ANGLE)
      C2= COS(ANGLE)
      CDM(I,M,1)= CDM(I,M,1)*C1
      CDM(I,M,2)= CDM(I,M,2)*C2
      CDM(I,M,3)= CDM(I,M,3)*C2
      ANGLE= ANGLE + ANGLEC + ANGLEC
  450 CONTINUE
  500 CONTINUE
      NN= 0
      DO 900 I=1,NUMELT
      DO 800 J=1,NZ
      K=J + NN
      DO 700 L=1,NF
      C1= 0.25*(PHIR(K,1,L)+PHIR(K,2,L)+PHIR(K,3,L)+PHIR(K,4,L))
      C5= C1
      C6= C1
      C1= 0.5*(PHIR(K,5,L) +PHIR(K,6,L) + PHIR(K,7,L) +PHIR(K,8,L))-C1
      C2= 0.5*(PHIR(K,7,L) - PHIR(K,5,L))
      C3= 0.5*(PHIR(K,6,L) - PHIR(K,8,L))
      C4= 0.25*(PHIR(K,1,L) - PHIR(K,2,L) + PHIR(K,3,L) - PHIR(K,4,L))
      C5= C5 - 0.5*(PHIR(K,6,L) + PHIR(K,8,L))
      C6= C6 - 0.5*(PHIR(K,5,L) + PHIR(K,7,L))
      C7= 0.25*(PHIR(K,3,L) + PHIR(K,4,L) - PHIR(K,1,L) - PHIR(K,2,L))
      C7= C7 + 0.5*(PHIR(K,5,L) - PHIR(K,7,L))
      C8= 0.25*(PHIR(K,2,L) + PHIR(K,3,L) - PHIR(K,1,L) - PHIR(K,4,L))
      C8= C8 + 0.5*(PHIR(K,8,L) - PHIR(K,6,L))
      AA(1,1)= TW4*(C1+C6/3.0)
      AA(1,2)= TW4*(C2+ C7/3.0)
      AA(1,3)= TW4*C5
      DO 600 N=2,NTERM
      AA(N,1)= C6*CDN(I,N,2) + (C1+C6)*CDN(I,N,3) + C3*CDN(I,N,1)
      AA(N,2)= C7*CDN(I,N,2) + (C2+C7)*CDN(I,N,3) + C4*CDN(I,N,1)
      AA(N,3)= C5*CDN(I,N,3) + C8*CDN(I,N,1)
  600 CONTINUE
      DO 650 N=1,NTERM
      DO 650 M=1,MTERM
      HINM(N,M,L)= HINM(N,M,L) + AA(N,2)*CDM(J,M,1) +
     1              AA(N,3)*CDM(J,M,2) + (AA(N,3) + AA(N,1))*CDM(J,M,3)
  650 CONTINUE
  700 CONTINUE
  800 CONTINUE
      NN= NN + NUMELZ
  900 CONTINUE
      RETURN
      END
```

```
      SUBROUTINE BEV2(PHIR,POB,LLM,TNN,NUMEL,NF,NUMELZ,NUMELT,NZ,ZWH,
     1      ZWHTOP,TW,NEQW)
      DIMENSION PHIR(NUMEL,8,NF),POB(NEQW,NF),LLM(NUMEL,8),TNN(8,8,2)
      DIMENSION ST(3),H(3),SHAPE(8)
C
C*********************************************************************
C     THIS SUBROUTINE FORMS THE INTEGRAL ASSOCIATED WITH THE PRESSURE
C     DUE TO THE MOVEMENT OF THE RESERVOIR BANKS - POB
C*********************************************************************
C
      DATA ST/.774596669,0.0,-.774596669/
      DATA H/.555555556,.888888889,.555555556/
C
C     FORM THE LLM ARRAY WHICH ASSIGNS A LOCATION TO EACH NODAL POINT
C     IN EACH ELEMENT COVERED BY WATER
C
      NN= -NUMELZ
      NEQ2= 0
      DO 100 I=1,NUMELT
      NN= NN + NUMELZ
      NEQ1= NEQ2 + 1
      NEQ2= NEQ1 +NZ + NZ + 1
      NEQ3= NEQ2 + NZ + 1
      DO 100 J=1,NZ
      K= NN + J
      LLM(K,1)= NEQ1
      LLM(K,2)= NEQ3
      LLM(K,3)= NEQ3 + 2
      LLM(K,4)= NEQ1 + 2
      LLM(K,5)= NEQ2
      LLM(K,6)= NEQ3 + 1
      LLM(K,7)= NEQ2 + 1
      LLM(K,8)= NEQ1 + 1
      NEQ1= NEQ1 + 2
      NEQ2= NEQ2 + 1
      NEQ3= NEQ3 + 2
  100 CONTINUE
C
C     FORM THE TNN ARRAY - 64 ELEMENT ARRAY FORMED BY INTEGRATING
C     SHAPE(I)*SHAPE(J) OVER THE -1. TO 1. RECTANGLE
C
      DO 200 K=1,8
      DO 200 L=K,8
  200 TNN(K,L,1)= 0.0
      DO 400 I=1,3
      S= ST(I)
      DO 400 J=1,3
      T= ST(J)
```

```
      HST= H(I)*H(J)
      SHAPE(1)= 0.25*(1.-S)*(1.-T)*(-S-T-1.)
      SHAPE(2)= 0.25*(1.+S)*(1.-T)*(S-T-1.)
      SHAPE(3)= 0.25*(1.+S)*(1.+T)*(S+T-1.)
      SHAPE(4)= 0.25*(1.-S)*(1.+T)*(-S+T-1.)
      SHAPE(5)= 0.5*(1.-S*S)*(1.-T)
      SHAPE(6)= 0.5*(1.+S)*(1.-T*T)
      SHAPE(7)= 0.5*(1.-S*S)*(1.+T)
      SHAPE(8)= 0.5*(1.-S)*(1.-T*T)
      DO 300 K=1,8
      C1= HST*SHAPE(K)
      DO 300 L=K,8
  300 TNN(K,L,1)= TNN(K,L,1) + C1*SHAPE(L)
  400 CONTINUE
      C1= ZWH*TW
      C2= ZWHTOP*TW
      DO 500 K=1,8
      DO 500 L=K,8
      TNN(K,L,2)= C2*TNN(K,L,1)
      TNN(K,L,1)= C1*TNN(K,L,1)
      TNN(L,K,1)= TNN(K,L,1)
  500 TNN(L,K,2)= TNN(K,L,2)
C
C     FORM POB ARRAY - THIS ARRAY RESULTS FROM MULTIPLYING TNN BY THE
C     MODE SHAPES.  THE RESULTS FOR EACH ELEMENT ARE STORED IN POB AT
C     LOCATIONS GIVEN BY THE LLM ARRAY
C
      DO 600 I=1,NEQW
      DO 600 L=1,NF
  600 POB(I,L)= 0.0
      NN= -NUMELZ
      DO 900 I=1,NUMELT
      NN= NN + NUMELZ
      DO 900 J=1,NZ
      K= NN + J
      M= 1
      IF(J.EQ.NZ)M=2
      DO 750 L=1,NF
      DO 700 KK=1,8
      NEQ1= LLM(K,KK)
      C1= 0.0
      DO 650 NNN=1,8
      C2= PHIR(K,NNN,L)
      IF(C2.EQ.0.0)GOTO 650
      C1= C1 + C2*TNN(KK,NNN,M)
  650 CONTINUE
  700 POB(NEQ1,L)= POB(NEQ1,L) + C1
  750 CONTINUE
  900 CONTINUE
      RETURN
      END
```

```
      OVERLAY(XFILE,3,1)
      PROGRAM XHYDRO
      COMMON / MISC / NBLOCK,NEQB,LL,NF,LB ,NDYN
      COMMON /ELPAR/ NPAR(14),NUMNP,MBAND,NELTYP,N1,N2,N3,N4,N5,MTOT,NEQ
     . ,N6, NUMNPF    ,IPRINT ,NLM ,NUMEL,WATL, IMASS,TVOL,NEQEST,IMODE
     .  ,IPRM   ,MESH ,MESHFN ,ISYM,WDEN,T(10)
      COMMON/RADOD/RADIUS,RADHT
      COMMON/HYD/NUMELZ,NUMELT,TW,ZW,HWATER,NTERM,MTERM,IXYZ
      COMMON A(1)
C
      NEQBT= NEQB*NBLOCK
      NEQW= 1
      NODEZ= 1
      N1= 1
      N2= N1 + NF
      N3= N2 + NEQ
      N4= N3 + NUMNP*3
      N5= N4 + NEQ
      N6= N5 + NEQB*MBAND
      IF(N6.GT.MTOT)CALL ERROR(N6-MTOT)
C
      CALL GMINX(A(N1),A(N2),A(N3),A(N4),A(N5),NUMNP,NUMEL,NEQB,
     1      MBAND,NF,NBLOCK,NEQ,IXYZ)
C
      N4= N3 + NEQB*NF
      IF(N4.GT.MTOT)CALL ERROR(N4-MTOT)
      WRITE(6,3000)
C
      CALL LOAD1(A(N1),A(N2),A(N3),NEQB,NBLOCK,NF,NEQ)
C
      IF(HWATER.EQ.0.0)GOTO 500
      ZWH= ZW/HWATER
      N3= N2 + 8*NUMEL*NF
      N4= N3 + 24*NUMEL
      N5= N4 + NEQBT*NF
      N6= N5 + 50
      IF(N6.GT.MTOT)CALL ERROR(N6-MTOT)
C
      CALL BEV(A(N2),A(N3),A(N4),A(N5),NEQBT,NUMEL,NF,NBLOCK,NEQB,
     1      NUMELZ,NUMELT,NZ,ZWH,ZWHTOP,ZW,TW,HWATER)
C
      N4= N3 + MTERM*NTERM*NF
      N5= N4 + NTERM*NUMELT*3
      N6= N5 + NTERM*3
      N7= N6 + MTERM*NUMELZ*3
      IF(N7.GT.MTOT)CALL ERROR(N7-MTOT)
C
      CALL HINML(A(N2),A(N3),A(N4),A(N5),A(N6),
     1      NUMELZ,NUMELT,NZ,ZWH,ZWHTOP,TW,NTERM,MTERM,NF,NUMEL)
C
      NEQW=(3*NZ+2)*NUMELT + NZ +NZ + 1
      N5= N4 + NEQW*NF
      N6= N5 + 8*NUMEL
      N7= N6 + 128
      IF(N7.GT.MTOT)CALL ERROR(N7-MTOT)
C
      CALL BEV2(A(N2),A(N4),A(N5),A(N6),NUMEL,NF,NUMELZ,NUMELT,NZ,
     1       ZWH,ZWHTOP,TW,NEQW)
C
      NODEZ= NZ + NZ + 1
  500 KKMAX= NTERM + NTERM + 14
      N1= 1
      N2= N1 + NF
      N3= N2 + 8*NUMEL*NF
      N4= N3 + MTERM*NTERM*NF
      N5= N4 + NEQW*NF
      N6= N5 + NTERM*KKMAX
```

```
      N7= N6 + NODEZ*MTERM
      N8= N7 + MTERM
      N9= N8 + MTERM
      N10= N9 + NEQW
      N11= N10 + NEQW
      IF(N11.GT.MTOT)CALL ERROR(N11-MTOT)
C
      CALL XHORIZ(A(N1),A(N3),A(N4),A(N5),A(N6),A(N7),A(N8),A(N9),
     1     A(N10),RADIUS,HWATER,NF,NTERM,MTERM,NODEZ,KKMAX,NEQW,NUMELT,
     2     ZWH,ZWHTOP,TW)
C
      RETURN
 3000 FORMAT(///78H GENERALIZED LOAD FOR HORIZONTAL GROUND MOTION IN X D
     1IRECTION - STRUCTURE ONLY,//7X,24H FREQ NUMBER        LOAD)
      END
```

```
      SUBROUTINE XHORIZ(GLOAD,HINM,PDB,FNK,COSLAM,AB,BB,PBR,PBI,
     1     RADIUS,HWATER,NF,NTERM,MTERM,NODEZ,KKMAX,NEQW,NUMELT,
     2     ZWH,ZWHTOP,TW)
      DIMENSION HINM(NTERM,MTERM,NF),PDB(NEQW,NF),FNK(NTERM,KKMAX),
     2  COSLAM(NODEZ,MTERM),AB(MTERM),BB(MTERM),PBR(NEQW),PBI(NEQW),
     3     GLOAD(NF)
      DIMENSION BJK(200),BY(200),GMN(31),WDAM(15)
      REAL JMR(31)
      COMPLEX S(15,15),F(15,2),SS(15,15),FF(15,2)
C
C**********************************************************************
C     THIS SUBROUTINE CALCULATES THE COMPLEX FREQUENCY RESPONSE
C     FUNCTIONS FOR HORIZONTAL GROUND MOTION IN X DIRECTION
C**********************************************************************
C
      REWIND 7
      READ(7)(WDAM(L),L=1,NF)
      READ(5,1000)DAMP,ALPHA,INCOMP,NPUNCH
      WRITE(6,2000)DAMP
      PI= 3.141592653
      RHO1= 9.88540019*RADIUS*RADIUS*HWATER
      RHO2= -.4501581579*RHO1
      RHO3= -.1767766953*RHO1
      IF(HWATER.EQ.0.0)GOTO 24
C
      RCONST= 0.5*PI*RADIUS/HWATER
      W1= 4720.0*PI/(HWATER + HWATER)
      IF(INCOMP.GT.0)GOTO 8
      WRITE(6,3000)W1
      DO 7 M=1,MTERM
    7 WRITE(6,3500)M,HINM(1,M,1)
      GOTO 9
    8 WRITE(6,6000)
      INCOMP= 1
    9 DO 10 NN=1,NTERM
      N= NN - 1
      AN= 16*N*N
      KMAX= N + N + 16
      DO 10 KK= 1,KMAX
      C1=KK - 1
      C2= 4.0*C1
      C3= C2*C1
   10 FNK(NN,KK)= (AN+C3-1.0)/((AN-C3-C2-1.0)*(AN-C3+C2-1.0))
C
      ZH= -ZWH
      DO 15 J=1,NODEZ
      C1= -0.5*PI
      C2= ZWH
      IF(J.GT.(NODEZ-2))C2= ZWHTOP
      ZH= ZH + C2
      C3= 1.0
      DO 15 M=1,MTERM
      C1= C1 + PI
      C3= -C3
      EM= M+M-1
      COSLAM(J,M)= (C3/EM)*(COS(C1*ZH))
   15 CONTINUE
C
   24 WRITE(6,4000)
C
C
   25 READ(5,1000)WW1DAM
C
      IF(WW1DAM.LT.0.0)GOTO 900
      W= WDAM(1)*WW1DAM
      IF(INCOMP.EQ.2)GOTO 860
      C1= 0.0
      C2= 0.0
      DO 40 L=1,NF
      F(L,1)= CMPLX(C1,C2)
      F(L,2)= CMPLX(C1,C2)
      DO 40 K=1,NF
      S(L,K)= CMPLX(C1,C2)
   40 CONTINUE
      IF(HWATER.EQ.0.0)GOTO 860
      WW1= W/W1
      IF(INCOMP.EQ.1)WW1=0.0
      MAX= 0.5*(WW1 + 1.0)
      EM= 1.0
      DO 100 M=1,MTERM
      ARG= ABS((WW1-EM)*(WW1+EM))
      JMR(M)= RCONST*SQRT(ARG)
      IF(JMR(M).LT.0.00001)JMR(M)= 0.00001
  100 EM= EM+2.0
      C1M= 1.0
      DO 500 M=1,MTERM
      C1M= -C1M
      EM= M+M-1
      C2M= -C1M/EM
      X= JMR(M)
      IF(MAX.LT.M)GOTO 300
      NBESSY= 4*(NTERM-1) + 1
      NBESSJ= NBESSY + 30
      IF(X.LT.0.1.AND.NTERM.GT.11)NBESSY= 41
      CALL BESSJY(X,BJK,BY,NBESSJ,NBESSY)
      C1N= C2M
      DO 200 NN=1,NTERM
      C1N= -C1N
      N= NN-1
      N4= 4*N
      KMAX= N+N+15
      FL= 0.5*BJK(1)*FNK(NN,1)
      NX= 0.5*(1.05*X+25.)
```

```
      DO 125 K=1,KMAX
      IF(K.GT.NX)GOTO 130
      KK= K+1
  125 FL= FL + BJK(KK+K)*FNK(NN,KK)
  130 FL= FL + FL
      IF(X.LT.0.1.AND.NN.GT.11)GOTO 176
      IF(NN.EQ.1)GOTO 150
      AMN= BJK(N4) - BJK(N4+2)
      BMN= BY(N4) - BY(N4+2)
      C2= 2.0
      GOTO 175
  150 AMN= -2.0*BJK(2)
      BMN= -2.0*BY(2)
      C2= 1.0
  175 C111= AMN/BMN
      C2= C2/((AMN*C111 + BMN)*JMR(M))
      CMN= C2*(C111*BJK(N4+1) + BY(N4+1))
      DMN= C2*(BJK(N4+1)- C111*BY(N4+1))
      GOTO 177
  176 CMN=-1.0/FLOAT(N4)
      DMN= 0.0
      AMN= 0.0
  177 C3= C1N*CMN
      C4= C1N*DMN
      C5= 0.78539816*AMN
      EB= FL*C3 + C5*C4
      HB= FL*C4 - C5*C3
      ED= -C3*FNK(NN,1)
      HD= -C4*FNK(NN,1)
      DO 180 L=1,NF
      F(L,1)= F(L,1) + HINM(NN,M,L)*CMPLX(EB,HB)
      F(L,2)= F(L,2) + HINM(NN,M,L)*CMPLX(ED,HD)
      DO 180 K=L,NF
      C1= HINM(NN,M,L)*HINM(NN,M,K)
      S(L,K)= S(L,K) + C1*CMPLX(CMN,DMN)
  180 CONTINUE
  200 CONTINUE
      GOTO 500
  300 NBESK= 4*(NTERM-1) + 2
      CALL BESNKS(X,NBESK,BJK)
      CALL G(X,NTERM,100,GMN)
      C1N= -C2M
      DO 400 NN=1,NTERM
      C1N= -C1N
      N4= 4*(NN-1)
      IF(NN.EQ.1)GOTO 350
      CMN= -BJK(N4+1)/((BJK(N4) + BJK(N4+2))*JMR(M))
      CMN= CMN + CMN
      GOTO 355
  350 CMN= -BJK(1)/((BJK(2) + BJK(2))*JMR(M))
  355 EB= C2M*CMN*GMN(NN)
      ED= C1N*CMN*FNK(NN,1)
      C1= 0.0
      DO 375 L=1,NF
      C2= EB*HINM(NN,M,L)
      C3= ED*HINM(NN,M,L)
      F(L,1)= F(L,1) + CMPLX(C2,C1)
      F(L,2)= F(L,2) + CMPLX(C3,C1)
      DO 375 K=L,NF
      C2= CMN*HINM(NN,M,L)*HINM(NN,M,K)
      S(L,K)= S(L,K) + CMPLX(C2,C1)
  375 CONTINUE
  400 CONTINUE
  500 CONTINUE
      DO 600 L=1,NF
      F(L,1)= RHO2*F(L,1)
  600 F(L,2)= RHO2*F(L,2)
C
C-----------------------------------------------------------------------
C     CALCULATE THE LOAD ASSOCIATED WITH THE INTEGRAL TERM FOR
C     PRESSURE DUE TO THE MOVEMENT OF THE RESERVOIR BANKS
C
      NEQ1= 0
      ANG= -TW
      NODET= NUMELT + NUMELT + 1
      NNN= 2
      NCONST= 1
      DO 750 NTHETA= 1,NODET
      NCONST= -NCONST
      NNN= NNN + NCONST
      ANG= ANG + TW
      C1= SIN(.7853981635 - ANG)
      C2= SIN(.7853981635 + ANG)
      DO 710 M=1,MTERM
      C3= C1*JMR(M)
      C4= C2*JMR(M)
      IF(MAX.LT.M)GOTO 700
      AB(M)= (SIN(C3) + SIN(C4))/JMR(M)
      BB(M)= (COS(C3) + COS(C4))/JMR(M)
      GOTO 710
  700 AB(M)= -(EXP(-C3) + EXP(-C4))/JMR(M)
      BB(M)= 0.0
  710 CONTINUE
      DO 740 I=1,NODEZ,NNN
      NEQ1= NEQ1 + 1
      C3= 0.0
      C4= 0.0
      DO 730 M=1,MTERM
      C3=C3 + AB(M)*COSLAM(I,M)
      IF(MAX.LT.M) GOTO 730
      C4= C4 + BB(M)*COSLAM(I,M)
  730 CONTINUE
      PBR(NEQ1)= C3
      PBI(NEQ1)= C4
  740 CONTINUE
  750 CONTINUE
C
      DO 850 L=1,NF
      C3= 0.0
      C4= 0.0
      DO 800 N=1,NEQW
      C3= C3 + PBR(N)*POB(N,L)
      C4= C4 + PBI(N)*POB(N,L)
  800 CONTINUE
      F(L,1)= F(L,1) + RHO3*CMPLX(C3,C4)
  850 CONTINUE
C-----------------------------------------------------------------------
C
  860 RHO1W= RHO1*W*W
      DO 865 L=1,NF
      DO 865 K=L,NF
      SS(L,K)= RHO1W*S(L,K)
      SS(K,L)= SS(L,K)
  865 CONTINUE
```

```
      WW= -W*W
      DO 875 L=1,NF
      FF(L,2)= F(L,2) + GLOAD(L)
      FF(L,1)= F(L,1)
      C1= WW + WDAM(L)*WDAM(L)
      C2= W*WDAM(L)*(DAMP+DAMP)
      SS(L,L)= SS(L,L) + CMPLX(C1,C2)
  875 CONTINUE
      CALL CSYMEQ(SS,FF,NF,2)
C
C     PRINT COMPLEX FREQUENCY RESPONSE FUNCTIONS FOR ACCELERATION---
C     THE COMPLEX FREQUENCY RESPONSE FOR DISPLACEMENT OF DAM ARE STORED
C     IN VECTOR FF AS FOLLOWS-- FF(L,1)= DISPLACEMENT DUE TO
C     HYDRODYNAMIC PRESSURE ON THE DAM CAUSED BY MOVEMENT OF
C     RESERVOIR BANKS.  FF(L,2)= DISPLACEMENT DUE TO GROUND MOTION PLUS
C     DISPLACEMENT DUE TO HYDRODYNAMIC PRESSURE CAUSED BY DAM MOVEMENT.
C
      DO 885 L=1,NF
      C1= WW*REAL(FF(L,1))
      C2= WW*AIMAG(FF(L,1))
      C3= WW*REAL(FF(L,2))
      C4= WW*AIMAG(FF(L,2))
      C5= C1+C3
      C6= C2+C4
      C7= C5*C5 + C6*C6
      C8= SQRT(C7)
      WRITE(6,5000)WW1DAM,WDAM(L),C1,C2,C3,C4,C5,C6,C8
      IF(NPUNCH.GT.0)PUNCH 7000,WW1DAM,WDAM(L),C1,C2,C3,C4,C5,C6,C8
  885 CONTINUE
      IF(INCOMP.GT.0)INCOMP= 2
C
      GOTO 25
C
  900 RETURN
 1000 FORMAT(2F10.0,2I5)
 2000 FORMAT(////22H MODAL DAMPING RATIO =,F10.4,//)
 3000 FORMAT(////41H FUNDAMENTAL FREQUENCY OF THE RESERVOIR =,F12.6,////
     .       /39H INTEGRAL I(M,O) FOR CALCULATING LIMITS)
 3500 FORMAT(/10X,3H I(,I2,4H O)=,E13.6)
 4000 FORMAT(///10X,87H COMPLEX FREQUENCY RESPONSE FOR ACCELERATION -- H
     1ORIZONTAL GROUND MOTION IN X DIRECTION,//16H EXCITATION FREQ,
     2       12H   DAM FREQ ,24H     HACCEL - BANK MOTION,
     3       24H      HACCEL - GMTN+DMTN,
     4       36H      -----------HACCEL - TOTAL------,
     5       /3X,10H W/WDAM(1),7X,9H RAD/SEC ,
     6       24H       REAL          IMAG   ,
     7       24H       REAL          IMAG   ,
     8       36H       REAL          IMAG       ABS VALUE)
 5000 FORMAT(//2F13.6,2X,7E12.4)
 6000 FORMAT(////30H INCOMPRESSIBLE WATER SOLUTION,
     1            /30H ------------- ----- --------,//)
 7000 FORMAT(2F13.6,/7E11.4)
      END
```

```
      SUBROUTINE G(X,NTERM,II,GMN)
C
C     THIS SUBROUTINE COMPUTES GMN USING SIMPSONS RULE
C
      DIMENSION GMN(NTERM),AAA(201)
      JJ= II + II + 1
      H= II+II
      H= 0.7853981635/H
      ANG= 0.0
      DO 20 J=1,JJ
      C1= SIN(0.7853981635 - ANG)
      C2= SIN(0.7853981635 + ANG)
      AAA(J)= C1*EXP(-X*C1) + C2*EXP(-X*C2)
   20 ANG= ANG + H
      DO 50 N=1,NTERM
      GMN(N)= 0.0
      IF(N.EQ.1)GOTO 35
      HN4= 4*(N-1)
      HN4= HN4*H
      ANG2= HN4
      ANG3= HN4 + HN4
      C3= AAA(1)
      DO 30 I=1,II
      J= I+I-1
      C1= C3
      C2= 4.0*AAA(J+1)*COS(ANG2)
      C3= AAA(J+2)*COS(ANG3)
      GMN(N)= GMN(N) + C1+C2+C3
      ANG2= ANG3 + HN4
   30 ANG3= ANG2 + HN4
      GOTO 45
   35 DO 40 I=1,II
      J= I+I-1
   40 GMN(N)= GMN(N) + AAA(J) + 4.0*AAA(J+1) + AAA(J+2)
   45 GMN(N)= (H/3.0)*GMN(N)
   50 CONTINUE
      RETURN
      END
```

```
      OVERLAY(XFILE,3,2)
      PROGRAM YHYDRO
      COMMON / MISC / NBLOCK,NEQB,LL,NF,LB ,NDYN
      COMMON /ELPAR/ NPAR(14),NUMNP,MBAND,NELTYP,N1,N2,N3,N4,N5,MTOT,NEQ
     .  ,N6, NUMNPF    ,IPRINT ,NLM ,NUMEL,WATL, IMASS,TVOL,NEQEST,IMODE
     .  ,IPRM  ,MESH ,MESHFN ,ISYM,WDEN,T(10)
      COMMON/RADDD/RADIUS,RADHT
      COMMON/HYD/NUMELZ,NUMELT,TW,ZW,HWATER,NTERM,MTERM,IXYZ
      COMMON A(1)
C
      NEQBT= NEQB*NBLOCK
      NEQW= 1
      NODEZ= 1
      N1= 1
      N2= N1 + NF
      N3= N2 + NEQ
      N4= N3 + NUMNP*3
      N5= N4 + NEQ
      N6= N5 + NEQB*MBAND
      IF(N6.GT.MTOT)CALL ERROR(N6-MTOT)
C
```

```
      CALL GMTNX(A(N1),A(N2),A(N3),A(N4),A(N5),NUMNP,NUMEL,NEQB,
     1     MBAND,NF,NBLOCK,NEQ,IXYZ)
C
      N4= N3 + NEQB*NF
      IF(N4.GT.MTOT)CALL ERROR(N4-MTOT)
      WRITE(6,3000)
C
      CALL LOAD1(A(N1),A(N2),A(N3),NEQB,NBLOCK,NF,NEQ)
C
      IF(HWATER.EQ.0.0)GOTO 500
      ZWH= ZW/HWATER
      N3= N2 + 8*NUMEL*NF
      N4= N3 + 24*NUMEL
      N5= N4 + NEQBT*NF
      N6= N5 + 50
      IF(N6.GT.MTOT)CALL ERROR(N6-MTOT)
C
      CALL BEV(A(N2),A(N3),A(N4),A(N5),NEQBT,NUMEL,NF,NBLOCK,NEQB,
     1     NUMELZ,NUMELT,NZ,ZWH,ZWHTOP,ZW,TW,HWATER)
C
      N4= N3 + MTERM*NTERM*NF
      N5= N4 + NTERM*NUMELT*3
      N6= N5 + NTERM*3
      N7= N6 + MTERM*NUMELZ*3
      IF(N7.GT.MTOT)CALL ERROR(N7-MTOT)
C
      CALL HYINHL(A(N2),A(N3),A(N4),A(N5),A(N6),
     1     NUMELZ,NUMELT,NZ,ZWH,ZWHTOP,TW,NTERM,MTERM,NF,NUMEL)
C
      NEQW=(3*NZ+2)*NUMELT + NZ +NZ + 1
      N5= N4 + NEQW*NF
      N6= N5 + 8*NUMEL
      N7= N6 + 128
      IF(N7.GT.MTOT)CALL ERROR(N7-MTOT)
C
      CALL BEV2(A(N2),A(N4),A(N5),A(N6),NUMEL,NF,NUMELZ,NUMELT,NZ,
     1     ZWH,ZWHTOP,TW,NEQW)
C
      NODEZ= NZ + NZ + 1
  500 KKMAX= NTERM + NTERM + 14
      N1= 1
      N2= N1 + NF
      N3= N2 + 8*NUMEL*NF
      N4= N3 + MTERM*NTERM*NF
      N5= N4 + NEQW*NF
      N6= N5 + NTERM*KKMAX
      N7= N6 + NODEZ*MTERM
      N8= N7 + MTERM
      N9= N8 + MTERM
      N10= N9 + NEQW
      N11= N10 + NEQW
      IF(N11.GT.MTOT)CALL ERROR(N11-MTOT)
C
      CALL YHORIZ(A(N1),A(N3),A(N4),A(N5),A(N6),A(N7),A(N8),A(N9),
     1     A(N10),RADIUS,HWATER,NF,NTERM,MTERM,NODEZ,KKMAX,NEQW,NUMELT,
     2     ZWH,ZWHTOP,TW)
C
      RETURN
 3000 FORMAT(///78H GENERALIZED LOAD FOR HORIZONTAL GROUND MOTION IN Y D
     1IRECTION - STRUCTURE ONLY,/7X,24H FREQ NUMBER          LOAD)
      END
```

```
      SUBROUTINE HYINHL(PHIR,HINM,CON,AA,COM,
     1     NUMELZ,NUMELT,NZ,ZWH,ZWHTOP,TW,NTERM,MTERM,NF,NUMEL)
      DIMENSION PHIR(NUMEL,8,NF),HINM(NTERM,MTERM,NF),
     1     CON(NUMELT,NTERM,3),AA(NTERM,3),COM(NUMELZ,MTERM,3)
      DIMENSION CC(3)
C
C***********************************************************************
C     THIS SUBROUTINE FORMS THE INTEGRAL I(N,M,L) FOR Y EXCITATION
C***********************************************************************
C
      DO 100 N=1,NTERM
      DO 100 M=1,MTERM
      DO 100 L=1,NF
      HINM(N,M,L)= 0.0
  100 CONTINUE
      TW4= 4.0*TW
      ANGLE= TW + TW
      DO 200 N=1,NTERM
      AN=N-1
      AN = AN + 0.5
      C1= SIN(ANGLE)
      C2= COS(ANGLE)
      CC(1)= (C2-C1/ANGLE)/AN
      CC(2)= 2.0*CC(1)/ANGLE
      CC(3)= C1/AN
      DO 150 I=1,NUMELT
      DO 150 J=1,3
  150 CON(I,N,J)= CC(J)
  200 ANGLE= ANGLE + TW4
      ANGLEC= TW
      DO 300 I=1,NUMELT
      DO 250 N=1,NTERM
      AN= N - 1
      AN= 4.0*AN + 2.0
      ANGLE= AN*ANGLEC
      C1= COS(ANGLE)
      C2= SIN(ANGLE)
      CON(I,N,1)=CON(I,N,1)*C1
      CON(I,N,2)=CON(I,N,2)*C2
      CON(I,N,3)=CON(I,N,3)*C2
  250 CONTINUE
  300 ANGLEC= ANGLEC + TW + TW
      PI= 3.1415926536
      PIZ= PI*ZWHTOP
      PLM= 0.5*PI
      ANGLE= 0.5*PIZ
      DO 350 M=1,MTERM
      C1= SIN(ANGLE)
      C2= COS(ANGLE)
      COM(NZ,M,1)= (C2 - C1/ANGLE)/PLM
      COM(NZ,M,2)= 2.0*COM(NZ,M,1)/ANGLE
      COM(NZ,M,3)= C1/PLM
      ANGLE= ANGLE + PIZ
      PLM= PLM + PI
  350 CONTINUE
      IF(NZ.EQ.1)GOTO 400
      NNZ= NZ-1
```

```
      PIZ= PI*ZWH
      PLM= 0.5*PI
      ANGLE= 0.5*PIZ
      DO 375 M=1,MTERM
      C1= SIN(ANGLE)
      C2= COS(ANGLE)
      CC(1)= (C2 - C1/ANGLE)/PLM
      CC(2)= 2.0*CC(1)/ANGLE
      CC(3)= C1/PLM
      DO 370 I=1,NNZ
      DO 370 J=1,3
  370 CDM(I,M,J)= CC(J)
      ANGLE= ANGLE + PIZ
      PLM= PLM + PI
  375 CONTINUE
  400 PIZ= 0.5*PI*ZWH
      PIZ2= PIZ
      ANGLEC= -PIZ
      DO 500 I=1,NZ
      IF(I.EQ.NZ)PIZ2= 0.5*PI*ZWHTOP
      ANGLEC= ANGLEC + PIZ + PIZ2
      ANGLE= ANGLEC
      DO 450 M=1,MTERM
      C1= SIN(ANGLE)
      C2= COS(ANGLE)
      CDM(I,M,1)= CDM(I,M,1)*C1
      CDM(I,M,2)= CDM(I,M,2)*C2
      CDM(I,M,3)= CDM(I,M,3)*C2
      ANGLE= ANGLE + ANGLEC + ANGLEC
  450 CONTINUE
  500 CONTINUE
      NN= 0
      DO 900 I=1,NUMELT
      DO 800 J=1,NZ
      K=J + NN
      DO 700 L=1,NF
      C1= 0.25*(PHIR(K,1,L)+PHIR(K,2,L)+PHIR(K,3,L)+PHIR(K,4,L))
      C5= C1
      C6= C1
      C1= 0.5*(PHIR(K,5,L) +PHIR(K,6,L) + PHIR(K,7,L) +PHIR(K,8,L))-C1
      C2= 0.5*(PHIR(K,7,L) - PHIR(K,5,L))
      C3= 0.5*(PHIR(K,6,L) - PHIR(K,8,L))
      C4= 0.25*(PHIR(K,1,L) - PHIR(K,2,L) + PHIR(K,3,L) - PHIR(K,4,L))
      C5= C5 - 0.5*(PHIR(K,6,L) + PHIR(K,8,L))
      C6= C6 - 0.5*(PHIR(K,5,L) + PHIR(K,7,L))
      C7= 0.25*(PHIR(K,3,L) + PHIR(K,4,L) - PHIR(K,1,L) - PHIR(K,2,L))
      C7= C7 + 0.5*(PHIR(K,5,L) - PHIR(K,7,L))
      C8= 0.25*(PHIR(K,2,L) + PHIR(K,3,L) - PHIR(K,1,L) - PHIR(K,4,L))
      C8= C8 + 0.5*(PHIR(K,8,L) - PHIR(K,6,L))
      DO 600 N=1,NTERM
      AA(N,1)= C6*CON(I,N,2) + (C1+C6)*CON(I,N,3) - C3*CON(I,N,1)
      AA(N,2)= C7*CON(I,N,2) + (C2+C7)*CON(I,N,3) - C4*CON(I,N,1)
      AA(N,3)= C5*CON(I,N,3) + C8*CON(I,N,1)
  600 CONTINUE
      DO 650 N=1,NTERM
      DO 650 M=1,MTERM
      HINM(N,M,L)= HINM(N,M,L) + AA(N,2)*CDM(J,M,1) +
     1          AA(N,3)*CDM(J,M,2) + (AA(N,3) + AA(N,1))*CDM(J,M,3)
  650 CONTINUE
  700 CONTINUE
  800 CONTINUE
      NN= NN + NUMELZ
  900 CONTINUE
      RETURN
      END


      SUBROUTINE YHORIZ(GLOAD,HINM,POB,FNK,COSLAM,AB,BB,PBR,PBI,
     1     RADIUS,HWATER,NF,NTERM,MTERM,NODEZ,KKMAX,NEQW,NUMELT,
     2      ZWH,ZWHTOP,TW)
      DIMENSION HINM(NTERM,MTERM,NF),POB(NEQW,NF),FNK(NTERM,KKMAX),
     2  COSLAM(NODEZ,MTERM),AB(MTERM),BB(MTERM),PBR(NEQW),PBI(NEQW),
     3     GLOAD(NF)
      DIMENSION BJK(200),BY(200),GMN(31),WDAM(15)
      REAL JMR(31)
      COMPLEX S(15,15),F(15,2),SS(15,15),FF(15,2)
C
C*************************************************************************
C     THIS SUBROUTINE CALCULATES THE COMPLEX FREQUENCY RESPONSE
C      FUNCTIONS FOR HORIZONTAL GROUND MOTION IN Y DIRECTION
C*************************************************************************
C
      REWIND 7
      READ(7)(WDAM(L),L=1,NF)
      READ(5,1000)DAMP,ALPHA,INCOMP,NPUNCH
      WRITE(6,2000)DAMP
      PI= 3.141592653
      RHO1= 19.77080038*RADIUS*RADIUS*HWATER
      RHO2= -.4501581579*RHO1
      RHO3= -.0883883476*RHO1
      IF(HWATER.EQ.0.0)GOTO 24
C
      RCONST= 0.5*PI*RADIUS/HWATER
      W1= 4720.0*PI/(HWATER + HWATER)
      IF(INCOMP.GT.0)GOTO 8
      WRITE(6,3000)W1
      GOTO 9
    8 WRITE(6,6000)
      INCOMP= 1
    9 DO 10 NN=1,NTERM
      N= NN - 1
      AN= 16*N*N + 16*N + 4
      KMAX= N + N + 16
      DO 10 KK= 1,KMAX
      C1=KK - 1
      C2= 4.0*C1
      C3= C2*C1
   10 FNK(NN,KK)= (AN+C3-1.0)/((AN-C3-C2-1.0)*(AN-C3+C2-1.0))
C
      ZH= -ZWH
      DO 15 J=1,NODEZ
      C1= -0.5*PI
      C2= ZWH
      IF(J.GT.(NODEZ-2))C2= ZWHTOP
      ZH= ZH + C2
      C3= 1.0
      DO 15 M=1,MTERM
      C1= C1 + PI
      C3= -C3
      EM= M+M-1
```

```
      COSLAM(J,M)= (C3/EM)*(COS(C1*ZH))
   15 CONTINUE
C
   24 WRITE(6,4000)
C
C
   25 READ(5,1000)WWIDAM
C
      IF(WWIDAM.LT.0.0)GOTO 900
      W= WDAM(1)*WWIDAM
      IF(INCOMP.EQ.2)GOTO 860
      C1= 0.0
      C2= 0.0
      DO 40 L=1,NF
      F(L,1)= CMPLX(C1,C2)
      F(L,2)= CMPLX(C1,C2)
      DO 40 K=1,NF
      S(L,K)= CMPLX(C1,C2)
   40 CONTINUE
      IF(HWATER.EQ.0.0)GOTO 860
      WW1= W/W1
      IF(INCOMP.EQ.1)WW1=0.0
      MAX= 0.5*(WW1 + 1.0)
      EM= 1.0
      DO 100 M=1,MTERM
      ARG= ABS((WW1-EM)*(WW1+EM))
      JMR(M)= RCONST*SQRT(ARG)
      IF(JMR(M).LT.0.00001)JMR(M)= 0.00001
  100 EM= EM+2.0
      C1M= 1.0
      DO 500 M=1,MTERM
      C1M= -C1M
      EM= M+M-1
      C2M= -C1M/EM
      X= JMR(M)
      IF(MAX.LT.M)GOTO 300
      NBESSY= 4*(NTERM-1) + 3
      NBESSJ= NBESSY + 30
      IF(X.LT.0.1.AND.NTERM.GT.11)NBESSY= 43
      CALL BESSJY(X,BJK,BY,NBESSJ,NBESSY)
      C1N= C2M
      DO 200 NN=1,NTERM
      C1N= -C1N
      N= NN-1
      N4= 4*N + 2
      KMAX= N+N+15
      FL= 0.5*BJK(1)*FNK(NN,1)
      NX= 0.5*(1.05*X+25.)
      DO 125 K=1,KMAX
      IF(K.GT.NX)GOTO 130
      KK= K+1
  125 FL= FL + BJK(KK+K)*FNK(NN,KK)
  130 FL= FL + FL
      IF(X.LT.0.1.AND.NN.GT.11)GOTO 176
      AMN= BJK(N4) - BJK(N4+2)
      BMN= BY(N4) - BY(N4+2)
      C2= 1.0
  175 C111= AMN/BMN
      C2= C2/((AMN*C111 + BMN)*JMR(M))
      CMN= C2*(C111*BJK(N4+1) + BY(N4+1))
      DMN= C2*(BJK(N4+1)- C111*BY(N4+1))
      GOTO 177
  176 CMN= -0.5/FLOAT(N4)
      DMN= 0.0
      AMN= 0.0
  177 C3= C1N*CMN
      C4= C1N*DMN
      C5= 0.78539816*AMN
      EB= FL*C3 + C5*C4
      HB= FL*C4 - C5*C3
      ED= C3*FNK(NN,1)
      HD= C4*FNK(NN,1)
      DO 180 L=1,NF
      F(L,1)= F(L,1) - HINM(NN,M,L)*CMPLX(EB,HB)
      F(L,2)= F(L,2) + HINM(NN,M,L)*CMPLX(ED,HD)
      DO 180 K=L,NF
      C1= HINM(NN,M,L)*HINM(NN,M,K)
      S(L,K)= S(L,K) + C1*CMPLX(CMN,DMN)
  180 CONTINUE
  200 CONTINUE
      GOTO 500
  300 NBESK= 4*(NTERM-1) + 4
      CALL BESNKS(X,NBESK,BJK)
      CALL GY(X,NTERM,100,GMN)
      C1N= C2M
      DO 400 NN=1,NTERM
      C1N= -C1N
      N4= 4*(NN-1) + 2
      CMN= -BJK(N4+1)/((BJK(N4) + BJK(N4+2))*JMR(M))
  355 EB= C2M*CMN*GMN(NN)
      ED= C1N*CMN*FNK(NN,1)
      C1= 0.0
      DO 375 L=1,NF
      C2= EB*HINM(NN,M,L)
      C3= ED*HINM(NN,M,L)
      F(L,1)= F(L,1) + CMPLX(C2,C1)
      F(L,2)= F(L,2) + CMPLX(C3,C1)
      DO 375 K=L,NF
      C2= CMN*HINM(NN,M,L)*HINM(NN,M,K)
      S(L,K)= S(L,K) + CMPLX(C2,C1)
  375 CONTINUE
  400 CONTINUE
  500 CONTINUE
      DO 600 L=1,NF
      F(L,1)= RHO2*F(L,1)
  600 F(L,2)= RHO2*F(L,2)
C
C-----------------------------------------------------------------------
C     CALCULATE THE LOAD ASSOCIATED WITH THE INTEGRAL TERM FOR
C     PRESSURE DUE TO THE MOVEMENT OF THE RESERVOIR BANKS
C
      NEQ1= 0
      ANG= -TW
      NODET= NUMELT + NUMELT + 1
      NNN= 2
      NCONST= 1
      DO 750 NTHETA= 1,NODET
      NCONST= -NCONST
      NNN= NNN + NCONST
      ANG= ANG + TW
      C1= SIN(.7853981635 - ANG)
      C2= SIN(.7853981635 + ANG)
      DO 710 M=1,MTERM
      C3= C1*JMR(M)
```

```
      C4= C2*JMR(M)
      IF(MAX.LT.M)GOTO 700
      AB(M)= (SIN(C4) - SIN(C3))/JMR(M)
      BB(M)= (COS(C4) - COS(C3))/JMR(M)
      GOTO 710
  700 AB(M)= -(EXP(-C4) - EXP(-C3))/JMR(M)
      BB(M)= 0.0
  710 CONTINUE
      DO 740 I=1,NODEZ,NNN
      NEQ1= NEQ1 + 1
      C3= 0.0
      C4= 0.0
      DO 730 M=1,MTERM
      C3=C3 + AB(M)*COSLAM(I,M)
      IF(MAX.LT.M) GOTO 730
      C4= C4 + BB(M)*COSLAM(I,M)
  730 CONTINUE
      PBR(NEQ1)= C3
      PBI(NEQ1)= C4
  740 CONTINUE
  750 CONTINUE
C
      DO 850 L=1,NF
      C3= 0.0
      C4= 0.0
      DO 800 N=1,NEQW
      C3= C3 + PBR(N)*POB(N,L)
      C4= C4 + PBI(N)*POB(N,L)
  800 CONTINUE
      F(L,1)= F(L,1) + RHO3*CMPLX(C3,C4)
  850 CONTINUE
C------------------------------------------------------------------------
C
  860 RHO1W= RHO1*W*W
      DO 865 L=1,NF
      DO 865 K=L,NF
      SS(L,K)= RHO1W*S(L,K)
      SS(K,L)= SS(L,K)
  865 CONTINUE
      WW= -W*W
      DO 875 L=1,NF
      FF(L,2)= F(L,2) + GLOAD(L)
      FF(L,1)= F(L,1)
      C1= WW + WDAM(L)*WDAM(L)
      C2= W*WDAM(L)*(DAMP+DAMP)
      SS(L,L)= SS(L,L) + CMPLX(C1,C2)
  875 CONTINUE
      CALL CSYMEQ(SS,FF,NF,2)
C
C     PRINT COMPLEX FREQUENCY RESPONSE FUNCTIONS FOR ACCELERATION---
C     THE COMPLEX FREQUENCY RESPONSE FOR DISPLACEMENT OF DAM ARE STORED
C     IN VECTOR FF AS FOLLOWS-- FF(L,1)= DISPLACEMENT DUE TO
C     HYDRODYNAMIC PRESSURE ON THE DAM CAUSED BY MOVEMENT OF
C     RESERVOIR BANKS.  FF(L,2)= DISPLACEMENT DUE TO GROUND MOTION PLUS
C     DISPLACEMENT DUE TO HYDRODYNAMIC PRESSURE CAUSED BY DAM MOVEMENT.
C
      DO 885 L=1,NF
      C1= WW*REAL(FF(L,1))
      C2= WW*AIMAG(FF(L,1))
      C3= WW*REAL(FF(L,2))
      C4= WW*AIMAG(FF(L,2))
      C5= C1+C3
      C6= C2+C4
      C7= C5*C5 + C6*C6
      C8= SQRT(C7)
      WRITE(6,5000)WW(DAM,WDAM(L),C1,C2,C3,C4,C5,C6,C8
      IF(NPUNCH.GT.0)PUNCH 7000,WWIDAM,WDAM(L),C1,C2,C3,C4,C5,C6,C8
  885 CONTINUE
      IF(INCOMP.GT.0)INCOMP= 2
C
      GOTO 25
C
  900 RETURN
 1000 FORMAT(2F10.0,2I5)
 2000 FORMAT(////22H MODAL DAMPING RATIO =,F10.4,//)
 3000 FORMAT(////41H FUNDAMENTAL FREQUENCY OF THE RESERVOIR =,F12.6,//)
 4000 FORMAT(///10X,87H COMPLEX FREQUENCY RESPONSE FOR ACCELERATION -- H
     1ORIZONTAL GROUND MOTION IN Y DIRECTION,//16H EXCITATION FREQ,
     2      12H    DAM FREQ ,24H      HACCEL - BANK MOTION,
     3      24H        HACCEL - GMTN+DMTN,
     4      36H       -----------HACCEL - TOTAL------,
     5      /3X,10H W/WDAM(1),7X,9H RAD/SEC ,
     6      24H        REAL           IMAG   ,
     7      24H        REAL           IMAG   ,
     8      36H        REAL           IMAG        ABS VALUE)
 5000 FORMAT(//2F13.6,2X,7E12.4)
 6000 FORMAT(////30H INCOMPRESSIBLE WATER SOLUTION,
     1            /30H ------------- ----- --------,//)
 7000 FORMAT(2F13.6,/7E11.4)
      END
```

```
      SUBROUTINE GY(X,NTERM,II,GMN)
      DIMENSION GMN(NTERM),AAA(201)
C
C     THIS SUBROUTINE CALCULATES GMN(ASSOCIATED WITH THE EXCITATION
C     IN THE Y DIRECTION) USING SIMPSONS RULE
C
      JJ= II + II + 1
      H= II+II
      H= 0.7853981635/H
      ANG= 0.0
      DO 20 J=1,JJ
      C1= SIN(0.7853981635 - ANG)
      C2= SIN(0.7853981635 + ANG)
      AAA(J)= C2*EXP(-X*C2) - C1*EXP(-X*C1)
   20 ANG= ANG + H
      DO 50 N=1,NTERM
      GMN(N)= 0.0
      HN4= 4*(N-1) + 2
      HN4= HN4*H
      ANG2= HN4
      ANG3= HN4 + HN4
      C3= 0.0
      DO 30 I=1,II
      J= I+I-1
      C1= C3
      C2= 4.0*AAA(J+1)*SIN(ANG2)
      C3= AAA(J+2)*SIN(ANG3)
      GMN(N)= GMN(N) + C1+C2+C3
```

```
      ANG2= ANG3 + HN4
   30 ANG3= ANG2 + HN4
      GMN(N)= (H/3.0)*GMN(N)
   50 CONTINUE
      RETURN
      END
```

```
      OVERLAY(XFILE,3,3)
      PROGRAM ZHYDRO
      COMMON / MISC / NBLOCK,NEQB,LL,NF,LB ,NDYN
      COMMON /ELPAR/ NPAR(14),NUMNP,MBAND,NELTYP,N1,N2,N3,N4,N5,MTOT,NEQ
     . ,N6, NUMNPF   ,IPRINT ,NLM ,NUMEL,WATL, IMASS,TVOL,NEQEST,IMODE
     . ,IPRN  ,MESH ,MESHFN ,ISYM,WDEN,T(10)
      COMMON/RADDD/RADIUS,RADHT
      COMMON/HYD/NUMELZ,NUMELT,TW,ZW,HWATER,NTERM,MTERM,IXYZ
      COMMON A(1)
C
      NEQBT= NEQB*NBLOCK
      N1= 1
      N2= N1 + NF
      N3= N2 + NEQ
      N4= N3 + NUMNP*3
      N5= N4 + NEQ
      N6= N5 + NEQB*MBAND
      IF(N6.GT.MTOT)CALL ERROR(N6-MTOT)
C
      CALL GMTNX(A(N1),A(N2),A(N3),A(N4),A(N5),NUMNP,NUMEL,NEQB,
     1      MBAND,NF,NBLOCK,NEQ,IXYZ)
C
      N4= N3 + NEQB*NF
      IF(N4.GT.MTOT)CALL ERROR(N4-MTOT)
      WRITE(6,3000)
C
      CALL LOAD1(A(N1),A(N2),A(N3),NEQB,NBLOCK,NF,NEQ)
C
      IF(HWATER.EQ.0.0)GOTO 500
      ZWH= ZW/HWATER
      N3= N2 + 8*NUMEL*NF
      N4= N3 + 24*NUMEL
      N5= N4 + NEQBT*NF
      N6= N5 + 50
      IF(N6.GT.MTOT)CALL ERROR(N6-MTOT)
C
      CALL BEV(A(N2),A(N3),A(N4),A(N5),NEQBT,NUMEL,NF,NBLOCK,NEQB,
     1      NUMELZ,NUMELT,NZ,ZWH,ZWHTOP,ZW,TW,HWATER)
C
      N4= N3 + MTERM*NTERM*NF
      N5= N4 + NTERM*NUMELT*3
      N6= N5 + NTERM*3
      N7= N6 + MTERM*NUMELZ*3
      IF(N7.GT.MTOT)CALL ERROR(N7-MTOT)
C
      CALL HINML(A(N2),A(N3),A(N4),A(N5),A(N6),NUMELZ,NUMELT,NZ,ZWH,
     1      ZWHTOP,TW,NTERM,MTERM,NF,NUMEL)
C
  500 N3= N2 + 8*NUMEL*NF
      CALL VERTIC(A(N1),A(N2),A(N3),NUMELT,NUMELZ,NUMEL,NZ,TW,
     1      ZWH,ZWHTOP,NF,NTERM,MTERM,RADIUS,HWATER)
C
      RETURN
 3000 FORMAT(///61H GENERALIZED LOAD FOR VERTICAL GROUND MOTION - STRUCT
     1URE ONLY,/7X,24H FREQ NUMBER          LOAD)
      END
```

```
      SUBROUTINE VERTIC(GLOAD,PHIR,HINM,NUMELT,NUMELZ,NUMEL,NZ,TW,
     1      ZWH,ZWHTOP,NF,NTERM,MTERM,RADIUS,HWATER)
      DIMENSION BJK(200),BY(200),GMN(31),WDAM(15)
      DIMENSION GLOAD(NF),PHIR(NUMEL,8,NF),HINM(NTERM,MTERM,NF)
      REAL JMR(31)
      COMPLEX S(15,15),F(15),SS(15,15),FF(15)
C
C**********************************************************************
C     THIS SUBROUTINE CALCULATES THE COMPLEX FREQUENCY RESPONSE
C     FUNCTIONS FOR VERTICAL GROUND MOTION
C**********************************************************************
C
      REWIND 7
      READ(7)(WDAM(L),L=1,NF)
      READ(5,1000)DAMP,ALPHA,INCOMP,NPUNCH
      IF(ALPHA.EQ.0.0)ALPHA=1.0
      WRITE(6,2000)DAMP,ALPHA
      PI= 3.141592653
      RHO1= 9.88540019*RADIUS*RADIUS*HWATER
      VRHO= -1.573310304*RADIUS*HWATER*HWATER*TW
      IF(HWATER.EQ.0.0)GOTO 24
C
      RCONST= 0.5*PI*RADIUS/HWATER
      W1= 4720.0*PI/(HWATER + HWATER)
      IF(INCOMP.GT.0)GOTO 8
      WRITE(6,3000)W1
      GOTO 24
    8 WRITE(6,6000)
      INCOMP= 1
C
   24 WRITE(6,4000)
C
C
   25 READ(5,1000)WW1DAM
C
      IF(WW1DAM.LT.0.0)GOTO 900
      W= WDAM(1)*WW1DAM
      IF(INCOMP.EQ.2)GOTO 860
      C1= 0.0
      C2= 0.0
      DO 40 L=1,NF
      F(L)= CMPLX(C1,C2)
      DO 40 K=1,NF
   40 S(L,K)= CMPLX(C1,C2)
      IF(HWATER.EQ.0.0)GOTO 860
      WW1= W/W1
      IF(INCOMP.EQ.1)WW1=0.0
      IF(WW1.LT.1.0E-05)WW1= 1.0E-05
      MAX= 0.5*(WW1 + 1.0)
      EM= 1.0
```

```
      DO 100 M=1,MTERM
      ARG= ABS((WW1-EM)*(WW1+EM))
      JMR(M)= RCONST*SQRT(ARG)
      IF(JMR(M).LT.0.00001)JMR(M)= 0.00001
  100 EM= EM + 2.0
      DO 500 M=1,MTERM
      X= JMR(M)
      IF(MAX.LT.M)GOTO 300
      NBESSY= 4*(NTERM-1) + 1
      IF(X.LT.0.1.AND.NTERM.GT.11)NBESSY= 41
      CALL BESSJY(X,BJK,BY,NBESSY,NBESSY)
      DO 200 NN=1,NTERM
      N4= 4*(NN-1)
      IF(X.LT.0.1.AND.NN.GT.11)GOTO 176
      IF(NN.EQ.1)GOTO 150
      AMN= BJK(N4) - BJK(N4+2)
      BMN= BY(N4) - BY(N4+2)
      C2= 2.0
      GOTO 175
  150 AMN= -2.0*BJK(2)
      BMN= -2.0*BY(2)
      C2= 1.0
  175 C111= AMN/BMN
      C2= C2/((AMN*C111 + BMN)*JMR(M))
      CMN= C2*(C111*BJK(N4+1) + BY(N4+1))
      DMN= C2*(BJK(N4+1) - C111*BY(N4+1))
      GOTO 177
  176 CMN= -1.0/FLOAT(N4)
      DMN= 0.0
  177 DO 180 L=1,NF
      DO 180 K=L,NF
      C1= HINM(NN,M,L)*HINM(NN,M,K)
      S(L,K)= S(L,K) + C1*CMPLX(CMN,DMN)
  180 CONTINUE
  200 CONTINUE
      GOTO 500
C
C
  300 NBESK= 4*(NTERM - 1) + 2
      CALL BESNKS(X,NBESK,BJK)
      DO 400 NN=1,NTERM
      N4= 4*(NN-1)
      IF(NN.EQ.1)GOTO 350
      CMN= -BJK(N4+1)/((BJK(N4) + BJK(N4+2))*JMR(M))
      CMN= CMN + CMN
      GOTO 355
  350 CMN= -BJK(1)/((BJK(2) + BJK(2))*JMR(M))
  355 C1= 0.0
      DO 375 L=1,NF
      DO 375 K=L,NF
      C2= CMN*HINM(NN,M,L)*HINM(NN,M,K)
      S(L,K)= S(L,K) + CMPLX(C2,C1)
  375 CONTINUE
  400 CONTINUE
  500 CONTINUE
C
      CALL VZLOAD(PHIR,F,NUMELT,NUMELZ,NZ,ZWH,ZWHTOP,TW,NUMEL,NF,
     1      WW1,VRHO,ALPHA)
C
C
  860 RHO1W= RHO1*W*W
      DO 865 L=1,NF
      DO 865 K=L,NF
      SS(L,K)= RHO1W*S(L,K)
      SS(K,L)= SS(L,K)
  865 CONTINUE
      WW= -W*W
      DO 875 L=1,NF
      FF(L)= F(L) + GLOAD(L)
      C1= WW + WDAM(L)*WDAM(L)
      C2= W*WDAM(L)*(DAMP + DAMP)
      SS(L,L)= SS(L,L) + CMPLX(C1,C2)
  875 CONTINUE
C
      CALL CSYMEQ(SS,FF,NF,1)
C
      DO 885 L=1,NF
      C1= WW*REAL(FF(L))
      C2= WW*AIMAG(FF(L))
      C3= C1*C1 + C2*C2
      C4= SQRT(C3)
      WRITE(6,5000)W,WW1DAM,WDAM(L),C1,C2,C4
      IF(NPUNCH.GT.0)PUNCH 7000,W,WW1DAM,WDAM(L),C1,C2,C4
  885 CONTINUE
      IF(INCOMP.GT.0)INCOMP= 2
C
      GOTO 25
C
  900 RETURN
 1000 FORMAT(2F10.0,2I5)
 2000 FORMAT(////22H MODAL DAMPING RATIO =,F10.4,
     1      //39H RESERVOIR BOTTOM REFRACTION CONSTANT =,F10.4,//)
 3000 FORMAT(////41H FUNDAMENTAL FREQUENCY OF THE RESERVOIR =,F12.6,//)
 4000 FORMAT(/////7X,70H COMPLEX FREQUENCY RESPONSE FOR ACCELERATION -- V
     1ERTICAL GROUND MOTION,//16H EXCITATION FREQ,12H     W/WLDAM ,
     2      12H  DAM FREQ  ,
     3      45H     ----------COMPLEX FREQ RESPONSE----------,
     4      /6X,8H RAD/SEC,16X,8H RAD/SEC,8X,5H REAL,10X,5H IMAG,
     5      7X,10H ABS VALUE)
 5000 FORMAT(//1X,F13.6,2F12.4,2X,3E15.4)
 6000 FORMAT(////30H INCOMPRESSIBLE WATER SOLUTION,
     1            /30H ------------- ----- --------,//)
 7000 FORMAT(3F13.6,3E11.4)
      END
```

```
      SUBROUTINE VZLOAD(PHIR,F,NUMELT,NUMELZ,NZ,ZWH,ZWHTOP,TW,NUMEL,NF,
     1      WW1,VRHO,ALPHA)
      DIMENSION PHIR(NUMEL,8,NF),VLOAD(15),V(8)
      COMPLEX F(NF)
C
C*********************************************************************
C     THIS SUBROUTINE FORMS THE GENERALIZED LOAD ASSOCIATED WITH
C     HYDRODYNAMIC PRESSURE DUE TO VERTICAL GROUND MOTION ACTING
C     ON THE RIGID DAM.
C*********************************************************************
C
      DO 100 L=1,NF
  100 VLOAD(L)= 0.0
      A= 1.570796327*WW1
```

```
      C1= (1.0 + ALPHA)*COS(A)
      C2= (1.0 - ALPHA)*SIN(A)
      VRHO1= (VRHO*(1.0+ALPHA))/(WW1*WW1*(C1*C1 + C2*C2))
      VRHOR= VRHO1*C1
      VRHOI= -VRHO1*C2
      NN= -NUMELZ
      DO 900 NTHETA= 1,NUMELT
      NN= NN + NUMELZ
      ZC= -ZWH
      DO 900 N= 1,NZ
      NNUMEL= NN + N
      ZC= ZC + ZWH + ZWH
      A1= A*ZWH
      IF(N.EQ.NZ)A1=A*ZWHTOP
      IF(N.EQ.NZ)ZC=ZC-ZWH+ZWHTOP
      A2= A*(1.-ZC)
      SC1= SIN(A1)
      SC2= COS(A1)
      C1= SC1*SIN(A2)
      C2= (SC2 - SC1/A1)*COS(A2)
      C3= ((2.0/A1)*(SC2 - SC1/A1) + SC1)*SIN(A2)
      V(1)= C3/2.0 - C1/3.0 - C2/6.0
      V(2)= V(1)
      V(3)= C3/2.0 - C1/3.0 + C2/6.0
      V(4)= V(3)
      V(5)= 0.6666666667*(C1 - C2)
      V(6)= C1 - C3
      V(7)= 0.6666666667*(C1 + C2)
      V(8)= V(6)
      DO 800 L=1,NF
      DO 800 I=1,8
      VLOAD(L)= VLOAD(L) + V(I)*PHIR(NNUMEL,I,L)
  800 CONTINUE
  900 CONTINUE
      DO 950 L=1,NF
      C1= VRHOR*VLOAD(L)
      C2= VRHOI*VLOAD(L)
  950 F(L)= CMPLX(C1,C2)
      RETURN
      END
```

EARTHQUAKE ENGINEERING RESEARCH CENTER REPORTS

NOTE: Numbers in parenthesis are Accession Numbers assigned by the National Technical Information Service; these are followed by a price code. Copies of the reports may be ordered from the National Technical Information Service, 5285 Port Royal Road, Springfield, Virginia, 22161. Accession Numbers should be quoted on orders for reports (PB --- ---) and remittance must accompany each order. Reports without this information were not available at time of printing. Upon request, EERC will mail inquirers this information when it becomes available.

EERC 67-1 "Feasibility Study Large-Scale Earthquake Simulator Facility," by J. Penzien, J.G. Bouwkamp, R.W. Clough and D. Rea - 1967 (PB 187 905)A07

EERC 68-1 Unassigned

EERC 68-2 "Inelastic Behavior of Beam-to-Column Subassemblages Under Repeated Loading," by V.V. Bertero - 1968 (PB 184 888)A05

EERC 68-3 "A Graphical Method for Solving the Wave Reflection-Refraction Problem," by H.D. McNiven and Y. Mengi - 1968 (PB 187 943)A03

EERC 68-4 "Dynamic Properties of McKinley School Buildings," by D. Rea, J.G. Bouwkamp and R.W. Clough - 1968 (PB 187 902)A07

EERC 68-5 "Characteristics of Rock Motions During Earthquakes," by H.B. Seed, I.M. Idriss and F.W. Kiefer - 1968 (PB 188 338)A03

EERC 69-1 "Earthquake Engineering Research at Berkeley," - 1969 (PB 187 906)A11

EERC 69-2 "Nonlinear Seismic Response of Earth Structures," by M. Dibaj and J. Penzien - 1969 (PB 187 904)A08

EERC 69-3 "Probabilistic Study of the Behavior of Structures During Earthquakes," by R. Ruiz and J. Penzien - 1969 (PB 187 886)A06

EERC 69-4 "Numerical Solution of Boundary Value Problems in Structural Mechanics by Reduction to an Initial Value Formulation," by N. Distefano and J. Schujman - 1969 (PB 187 942)A02

EERC 69-5 "Dynamic Programming and the Solution of the Biharmonic Equation," by N. Distefano - 1969 (PB 187 941)A03

EERC 69-6 "Stochastic Analysis of Offshore Tower Structures," by A.K. Malhotra and J. Penzien - 1969 (PB 187 903)A09

EERC 69-7 "Rock Motion Accelerograms for High Magnitude Earthquakes," by H.B. Seed and I.M. Idriss - 1969 (PB 187 940)A02

EERC 69-8 "Structural Dynamics Testing Facilities at the University of California, Berkeley," by R.M. Stephen, J.G. Bouwkamp, R.W. Clough and J. Penzien - 1969 (PB 189 111)A04

EERC 69-9 "Seismic Response of Soil Deposits Underlain by Sloping Rock Boundaries," by H. Dezfulian and H.B. Seed 1969 (PB 189 114)A03

EERC 69-10 "Dynamic Stress Analysis of Axisymmetric Structures Under Arbitrary Loading," by S. Ghosh and E.L. Wilson 1969 (PB 189 026)A10

EERC 69-11 "Seismic Behavior of Multistory Frames Designed by Different Philosophies," by J.C. Anderson and V. V. Bertero - 1969 (PB 190 662)A10

EERC 69-12 "Stiffness Degradation of Reinforcing Concrete Members Subjected to Cyclic Flexural Moments," by V.V. Bertero, B. Bresler and H. Ming Liao - 1969 (PB 202 942)A07

EERC 69-13 "Response of Non-Uniform Soil Deposits to Travelling Seismic Waves," by H. Dezfulian and H.B. Seed - 1969 (PB 191 023)A03

EERC 69-14 "Damping Capacity of a Model Steel Structure," by D. Rea, R.W. Clough and J.G. Bouwkamp - 1969 (PB 190 663)A06

EERC 69-15 "Influence of Local Soil Conditions on Building Damage Potential during Earthquakes," by H.B. Seed and I.M. Idriss - 1969 (PB 191 036)A03

EERC 69-16 "The Behavior of Sands Under Seismic Loading Conditions," by M.L. Silver and H.B. Seed - 1969 (AD 714 982)A07

EERC 70-1 "Earthquake Response of Gravity Dams," by A.K. Chopra - 1970 (AD 709 640)A03

EERC 70-2 "Relationships between Soil Conditions and Building Damage in the Caracas Earthquake of July 29, 1967," by H.B. Seed, I.M. Idriss and H. Dezfulian - 1970 (PB 195 762)A05

EERC 70-3 "Cyclic Loading of Full Size Steel Connections," by E.P. Popov and R.M. Stephen - 1970 (PB 213 545)A04

EERC 70-4 "Seismic Analysis of the Charaima Building, Caraballeda, Venezuela," by Subcommittee of the SEAONC Research Committee: V.V. Bertero, P.F. Fratessa, S.A. Mahin, J.H. Sexton, A.C. Scordelis, E.L. Wilson, L.A. Wyllie, H.B. Seed and J. Penzien, Chairman - 1970 (PB 201 455)A06

EERC 70-5 "A Computer Program for Earthquake Analysis of Dams," by A.K. Chopra and P. Chakrabarti - 1970 (AD 723 994)A05

EERC 70-6 "The Propagation of Love Waves Across Non-Horizontally Layered Structures," by J. Lysmer and L.A. Drake 1970 (PB 197 896)A03

EERC 70-7 "Influence of Base Rock Characteristics on Ground Response," by J. Lysmer, H.B. Seed and P.B. Schnabel 1970 (PB 197 897)A03

EERC 70-8 "Applicability of Laboratory Test Procedures for Measuring Soil Liquefaction Characteristics under Cyclic Loading," by H.B. Seed and W.H. Peacock - 1970 (PB 198 016)A03

EERC 70-9 "A Simplified Procedure for Evaluating Soil Liquefaction Potential," by H.B. Seed and I.M. Idriss - 1970 (PB 198 009)A03

EERC 70-10 "Soil Moduli and Damping Factors for Dynamic Response Analysis," by H.B. Seed and I.M. Idriss - 1970 (PB 197 869)A03

EERC 71-1 "Koyna Earthquake of December 11, 1967 and the Performance of Koyna Dam," by A.K. Chopra and P. Chakrabarti 1971 (AD 731 496)A06

EERC 71-2 "Preliminary In-Situ Measurements of Anelastic Absorption in Soils Using a Prototype Earthquake Simulator," by R.D. Borcherdt and P.W. Rodgers - 1971 (PB 201 454)A03

EERC 71-3 "Static and Dynamic Analysis of Inelastic Frame Structures," by F.L. Porter and G.H. Powell - 1971 (PB 210 135)A06

EERC 71-4 "Research Needs in Limit Design of Reinforced Concrete Structures," by V.V. Bertero - 1971 (PB 202 943)A04

EERC 71-5 "Dynamic Behavior of a High-Rise Diagonally Braced Steel Building," by D. Rea, A.A. Shah and J.G. Bouwkamp 1971 (PB 203 584)A06

EERC 71-6 "Dynamic Stress Analysis of Porous Elastic Solids Saturated with Compressible Fluids," by J. Ghaboussi and E. L. Wilson - 1971 (PB 211 396)A06

EERC 71-7 "Inelastic Behavior of Steel Beam-to-Column Subassemblages," by H. Krawinkler, V.V. Bertero and E.P. Popov 1971 (PB 211 335)A14

EERC 71-8 "Modification of Seismograph Records for Effects of Local Soil Conditions," by P. Schnabel, H.B. Seed and J. Lysmer - 1971 (PB 214 450)A03

EERC 72-1 "Static and Earthquake Analysis of Three Dimensional Frame and Shear Wall Buildings," by E.L. Wilson and H.H. Dovey - 1972 (PB 212 904)A05

EERC 72-2 "Accelerations in Rock for Earthquakes in the Western United States," by P.B. Schnabel and H.B. Seed - 1972 (PB 213 100)A03

EERC 72-3 "Elastic-Plastic Earthquake Response of Soil-Building Systems," by T. Minami - 1972 (PB 214 868)A08

EERC 72-4 "Stochastic Inelastic Response of Offshore Towers to Strong Motion Earthquakes," by M.K. Kaul - 1972 (PB 215 713)A05

EERC 72-5 "Cyclic Behavior of Three Reinforced Concrete Flexural Members with High Shear," by E.P. Popov, V.V. Bertero and H. Krawinkler - 1972 (PB 214 555)A05

EERC 72-6 "Earthquake Response of Gravity Dams Including Reservoir Interaction Effects," by P. Chakrabarti and A.K. Chopra - 1972 (AD 762 330)A08

EERC 72-7 "Dynamic Properties of Pine Flat Dam," by D. Rea, C.Y. Liaw and A.K. Chopra - 1972 (AD 763 928)A05

EERC 72-8 "Three Dimensional Analysis of Building Systems," by E.L. Wilson and H.H. Dovey - 1972 (PB 222 438)A06

EERC 72-9 "Rate of Loading Effects on Uncracked and Repaired Reinforced Concrete Members," by S. Mahin, V.V. Bertero, D. Rea and M. Atalay - 1972 (PB 224 520)A08

EERC 72-10 "Computer Program for Static and Dynamic Analysis of Linear Structural Systems," by E.L. Wilson, K.-J. Bathe, J.E. Peterson and H.H.Dovey - 1972 (PB 220 437)A04

EERC 72-11 "Literature Survey - Seismic Effects on Highway Bridges," by T. Iwasaki, J. Penzien and R.W. Clough - 1972 (PB 215 613)A19

EERC 72-12 "SHAKE-A Computer Program for Earthquake Response Analysis of Horizontally Layered Sites," by P.B. Schnabel and J. Lysmer - 1972 (PB 220 207)A06

EERC 73-1 "Optimal Seismic Design of Multistory Frames," by V.V. Bertero and H. Kamil - 1973

EERC 73-2 "Analysis of the Slides in the San Fernando Dams During the Earthquake of February 9, 1971," by H.B. Seed, K.L. Lee, I.M. Idriss and F. Makdisi - 1973 (PB 223 402)A14

EERC 73-3 "Computer Aided Ultimate Load Design of Unbraced Multistory Steel Frames," by M.B. El-Hafez and G.H. Powell 1973 (PB 248 315)A09

EERC 73-4 "Experimental Investigation into the Seismic Behavior of Critical Regions of Reinforced Concrete Components as Influenced by Moment and Shear," by M. Celebi and J. Penzien - 1973 (PB 215 884)A09

EERC 73-5 "Hysteretic Behavior of Epoxy-Repaired Reinforced Concrete Beams," by M. Celebi and J. Penzien - 1973 (PB 239 568)A03

EERC 73-6 "General Purpose Computer Program for Inelastic Dynamic Response of Plane Structures," by A. Kanaan and G.H. Powell - 1973 (PB 221 260)A08

EERC 73-7 "A Computer Program for Earthquake Analysis of Gravity Dams Including Reservoir Interaction," by P. Chakrabarti and A.K. Chopra - 1973 (AD 766 271)A04

EERC 73-8 "Behavior of Reinforced Concrete Deep Beam-Column Subassemblages Under Cyclic Loads," by O. Küstü and J.G. Bouwkamp - 1973 (PB 246 117)A12

EERC 73-9 "Earthquake Analysis of Structure-Foundation Systems," by A.K. Vaish and A.K. Chopra - 1973 (AD 766 272)A07

EERC 73-10 "Deconvolution of Seismic Response for Linear Systems," by R.B. Reimer - 1973 (PB 227 179)A08

EERC 73-11 "SAP IV: A Structural Analysis Program for Static and Dynamic Response of Linear Systems," by K.-J. Bathe, E.L. Wilson and F.E. Peterson - 1973 (PB 221 967)A09

EERC 73-12 "Analytical Investigations of the Seismic Response of Long, Multiple Span Highway Bridges," by W.S. Tseng and J. Penzien - 1973 (PB 227 816)A10

EERC 73-13 "Earthquake Analysis of Multi-Story Buildings Including Foundation Interaction," by A.K. Chopra and J.A. Gutierrez - 1973 (PB 222 970)A03

EERC 73-14 "ADAP: A Computer Program for Static and Dynamic Analysis of Arch Dams," by R.W. Clough, J.M. Raphael and S. Mojtahedi - 1973 (PB 223 763)A09

EERC 73-15 "Cyclic Plastic Analysis of Structural Steel Joints," by R.B. Pinkney and R.W. Clough - 1973 (PB 226 843)A08

EERC 73-16 "QUAD-4: A Computer Program for Evaluating the Seismic Response of Soil Structures by Variable Damping Finite Element Procedures," by I.M. Idriss, J. Lysmer, R. Hwang and H.B. Seed - 1973 (PB 229 424)A05

EERC 73-17 "Dynamic Behavior of a Multi-Story Pyramid Shaped Building," by R.M. Stephen, J.P. Hollings and J.G. Bouwkamp - 1973 (PB 240 718)A06

EERC 73-18 "Effect of Different Types of Reinforcing on Seismic Behavior of Short Concrete Columns," by V.V. Bertero, J. Hollings, O. Küstü, R.M. Stephen and J.G. Bouwkamp - 1973

EERC 73-19 "Olive View Medical Center Materials Studies, Phase I," by B. Bresler and V.V. Bertero - 1973 (PB 235 986)A06

EERC 73-20 "Linear and Nonlinear Seismic Analysis Computer Programs for Long Multiple-Span Highway Bridges," by W.S. Tseng and J. Penzien - 1973

EERC 73-21 "Constitutive Models for Cyclic Plastic Deformation of Engineering Materials," by J.M. Kelly and P.P. Gillis 1973 (PB 226 024)A03

EERC 73-22 "DRAIN - 2D User's Guide," by G.H. Powell - 1973 (PB 227 016)A05

EERC 73-23 "Earthquake Engineering at Berkeley - 1973," (PB 226 033)A11

EERC 73-24 Unassigned

EERC 73-25 "Earthquake Response of Axisymmetric Tower Structures Surrounded by Water," by C.Y. Liaw and A.K. Chopra 1973 (AD 773 052)A09

EERC 73-26 "Investigation of the Failures of the Olive View Stairtowers During the San Fernando Earthquake and Their Implications on Seismic Design," by V.V. Bertero and R.G. Collins - 1973 (PB 235 106)A13

EERC 73-27 "Further Studies on Seismic Behavior of Steel Beam-Column Subassemblages," by V.V. Bertero, H. Krawinkler and E.P. Popov - 1973 (PB 234 172)A06

EERC 74-1 "Seismic Risk Analysis," by C.S. Oliveira - 1974 (PB 235 920)A06

EERC 74-2 "Settlement and Liquefaction of Sands Under Multi-Directional Shaking," by R. Pyke, C.K. Chan and H.B. Seed 1974

EERC 74-3 "Optimum Design of Earthquake Resistant Shear Buildings," by D. Ray, K.S. Pister and A.K. Chopra - 1974 (PB 231 172)A06

EERC 74-4 "LUSH - A Computer Program for Complex Response Analysis of Soil-Structure Systems," by J. Lysmer, T. Udaka, H.B. Seed and R. Hwang - 1974 (PB 236 796)A05

EERC 74-5 "Sensitivity Analysis for Hysteretic Dynamic Systems: Applications to Earthquake Engineering," by D. Ray 1974 (PB 233 213)A06

EERC 74-6 "Soil Structure Interaction Analyses for Evaluating Seismic Response," by H.B. Seed, J. Lysmer and R. Hwang 1974 (PB 236 519)A04

EERC 74-7 Unassigned

EERC 74-8 "Shaking Table Tests of a Steel Frame - A Progress Report," by R.W. Clough and D. Tang - 1974 (PB 240 869)A03

EERC 74-9 "Hysteretic Behavior of Reinforced Concrete Flexural Members with Special Web Reinforcement," by V.V. Bertero, E.P. Popov and T.Y. Wang - 1974 (PB 236 797)A07

EERC 74-10 "Applications of Reliability-Based, Global Cost Optimization to Design of Earthquake Resistant Structures," by E. Vitiello and K.S. Pister - 1974 (PB 237 231)A06

EERC 74-11 "Liquefaction of Gravelly Soils Under Cyclic Loading Conditions," by R.T. Wong, H.B. Seed and C.K. Chan 1974 (PB 242 042)A03

EERC 74-12 "Site-Dependent Spectra for Earthquake-Resistant Design," by H.B. Seed, C. Ugas and J. Lysmer - 1974 (PB 240 953)A03

EERC 74-13 "Earthquake Simulator Study of a Reinforced Concrete Frame," by P. Hidalgo and R.W. Clough - 1974 (PB 241 944)A13

EERC 74-14 "Nonlinear Earthquake Response of Concrete Gravity Dams," by N. Pal - 1974 (AD/A 006 583)A06

EERC 74-15 "Modeling and Identification in Nonlinear Structural Dynamics - I. One Degree of Freedom Models," by N. Distefano and A. Rath - 1974 (PB 241 548)A06

EERC 75-1 "Determination of Seismic Design Criteria for the Dumbarton Bridge Replacement Structure, Vol. I: Description, Theory and Analytical Modeling of Bridge and Parameters," by F. Baron and S.-H. Pang - 1975 (PB 259 407)A15

EERC 75-2 "Determination of Seismic Design Criteria for the Dumbarton Bridge Replacement Structure, Vol. II: Numerical Studies and Establishment of Seismic Design Criteria," by F. Baron and S.-H. Pang - 1975 (PB 259 408)A11 (For set of EERC 75-1 and 75-2 (PB 259 406))

EERC 75-3 "Seismic Risk Analysis for a Site and a Metropolitan Area," by C.S. Oliveira - 1975 (PB 248 134)A09

EERC 75-4 "Analytical Investigations of Seismic Response of Short, Single or Multiple-Span Highway Bridges," by M.-C. Chen and J. Penzien - 1975 (PB 241 454)A09

EERC 75-5 "An Evaluation of Some Methods for Predicting Seismic Behavior of Reinforced Concrete Buildings," by S.A. Mahin and V.V. Bertero - 1975 (PB 246 306)A16

EERC 75-6 "Earthquake Simulator Study of a Steel Frame Structure, Vol. I: Experimental Results," by R.W. Clough and D.T. Tang - 1975 (PB 243 981)A13

EERC 75-7 "Dynamic Properties of San Bernardino Intake Tower," by D. Rea, C.-Y. Liaw and A.K. Chopra - 1975 (AD/A008 406) A05

EERC 75-8 "Seismic Studies of the Articulation for the Dumbarton Bridge Replacement Structure, Vol. I: Description, Theory and Analytical Modeling of Bridge Components," by F. Baron and R.E. Hamati - 1975 (PB 251 539)A07

EERC 75-9 "Seismic Studies of the Articulation for the Dumbarton Bridge Replacement Structure, Vol. 2: Numerical Studies of Steel and Concrete Girder Alternates," by F. Baron and R.E. Hamati - 1975 (PB 251 540)A10

EERC 75-10 "Static and Dynamic Analysis of Nonlinear Structures," by D.P. Mondkar and G.H. Powell - 1975 (PB 242 434)A08

EERC 75-11 "Hysteretic Behavior of Steel Columns," by E.P. Popov, V.V. Bertero and S. Chandramouli - 1975 (PB 252 365)A11

EERC 75-12 "Earthquake Engineering Research Center Library Printed Catalog," - 1975 (PB 243 711)A26

EERC 75-13 "Three Dimensional Analysis of Building Systems (Extended Version)," by E.L. Wilson, J.P. Hollings and H.H. Dovey - 1975 (PB 243 989)A07

EERC 75-14 "Determination of Soil Liquefaction Characteristics by Large-Scale Laboratory Tests," by P. De Alba, C.K. Chan and H.B. Seed - 1975 (NUREG 0027)A08

EERC 75-15 "A Literature Survey - Compressive, Tensile, Bond and Shear Strength of Masonry," by R.L. Mayes and R.W. Clough - 1975 (PB 246 292)A10

EERC 75-16 "Hysteretic Behavior of Ductile Moment Resisting Reinforced Concrete Frame Components," by V.V. Bertero and E.P. Popov - 1975 (PB 246 388)A05

EERC 75-17 "Relationships Between Maximum Acceleration, Maximum Velocity, Distance from Source, Local Site Conditions for Moderately Strong Earthquakes," by H.B. Seed, R. Murarka, J. Lysmer and I.M. Idriss - 1975 (PB 248 172)A03

EERC 75-18 "The Effects of Method of Sample Preparation on the Cyclic Stress-Strain Behavior of Sands," by J. Mulilis, C.K. Chan and H.B. Seed - 1975 (Summarized in EERC 75-28)

EERC 75-19 "The Seismic Behavior of Critical Regions of Reinforced Concrete Components as Influenced by Moment, Shear and Axial Force," by M.B. Atalay and J. Penzien - 1975 (PB 258 842)A11

EERC 75-20 "Dynamic Properties of an Eleven Story Masonry Building," by R.M. Stephen, J.P. Hollings, J.G. Bouwkamp and D. Jurukovski - 1975 (PB 246 945)A04

EERC 75-21 "State-of-the-Art in Seismic Strength of Masonry - An Evaluation and Review," by R.L. Mayes and R.W. Clough 1975 (PB 249 040)A07

EERC 75-22 "Frequency Dependent Stiffness Matrices for Viscoelastic Half-Plane Foundations," by A.K. Chopra, P. Chakrabarti and G. Dasgupta - 1975 (PB 248 121)A07

EERC 75-23 "Hysteretic Behavior of Reinforced Concrete Framed Walls," by T.Y. Wong, V.V. Bertero and E.P. Popov - 1975

EERC 75-24 "Testing Facility for Subassemblages of Frame-Wall Structural Systems," by V.V. Bertero, E.P. Popov and T. Endo - 1975

EERC 75-25 "Influence of Seismic History on the Liquefaction Characteristics of Sands," by H.B. Seed, K. Mori and C.K. Chan - 1975 (Summarized in EERC 75-28)

EERC 75-26 "The Generation and Dissipation of Pore Water Pressures during Soil Liquefaction," by H.B. Seed, P.P. Martin and J. Lysmer - 1975 (PB 252 648)A03

EERC 75-27 "Identification of Research Needs for Improving Aseismic Design of Building Structures," by V.V. Bertero 1975 (PB 248 136)A05

EERC 75-28 "Evaluation of Soil Liquefaction Potential during Earthquakes," by H.B. Seed, I. Arango and C.K. Chan - 1975 (NUREG 0026)A13

EERC 75-29 "Representation of Irregular Stress Time Histories by Equivalent Uniform Stress Series in Liquefaction Analyses," by H.B. Seed, I.M. Idriss, F. Makdisi and N. Banerjee - 1975 (PB 252 635)A03

EERC 75-30 "FLUSH - A Computer Program for Approximate 3-D Analysis of Soil-Structure Interaction Problems," by J. Lysmer, T. Udaka, C.-F. Tsai and H.B. Seed - 1975 (PB 259 332)A07

EERC 75-31 "ALUSH - A Computer Program for Seismic Response Analysis of Axisymmetric Soil-Structure Systems," by E. Berger, J. Lysmer and H.B. Seed - 1975

EERC 75-32 "TRIP and TRAVEL - Computer Programs for Soil-Structure Interaction Analysis with Horizontally Travelling Waves," by T. Udaka, J. Lysmer and H.B. Seed - 1975

EERC 75-33 "Predicting the Performance of Structures in Regions of High Seismicity," by J. Penzien - 1975 (PB 248 130)A03

EERC 75-34 "Efficient Finite Element Analysis of Seismic Structure - Soil - Direction," by J. Lysmer, H.B. Seed, T. Udaka, R.N. Hwang and C.-F. Tsai - 1975 (PB 253 570)A03

EERC 75-35 "The Dynamic Behavior of a First Story Girder of a Three-Story Steel Frame Subjected to Earthquake Loading," by R.W. Clough and L.-Y. Li - 1975 (PB 248 841)A05

EERC 75-36 "Earthquake Simulator Study of a Steel Frame Structure, Volume II - Analytical Results," by D.T. Tang - 1975 (PB 252 926)A10

EERC 75-37 "ANSR-I General Purpose Computer Program for Analysis of Non-Linear Structural Response," by D.P. Mondkar and G.H. Powell - 1975 (PB 252 386)A08

EERC 75-38 "Nonlinear Response Spectra for Probabilistic Seismic Design and Damage Assessment of Reinforced Concrete Structures," by M. Murakami and J. Penzien - 1975 (PB 259 530)A05

EERC 75-39 "Study of a Method of Feasible Directions for Optimal Elastic Design of Frame Structures Subjected to Earthquake Loading," by N.D. Walker and K.S. Pister - 1975 (PB 257 781)A06

EERC 75-40 "An Alternative Representation of the Elastic-Viscoelastic Analogy," by G. Dasgupta and J.L. Sackman - 1975 (PB 252 173)A03

EERC 75-41 "Effect of Multi-Directional Shaking on Liquefaction of Sands," by H.B. Seed, R. Pyke and G.R. Martin - 1975 (PB 258 781)A03

EERC 76-1 "Strength and Ductility Evaluation of Existing Low-Rise Reinforced Concrete Buildings - Screening Method," by T. Okada and B. Bresler - 1976 (PB 257 906)A11

EERC 76-2 "Experimental and Analytical Studies on the Hysteretic Behavior of Reinforced Concrete Rectangular and T-Beams," by S.-Y.M. Ma, E.P. Popov and V.V. Bertero - 1976 (PB 260 843)A12

EERC 76-3 "Dynamic Behavior of a Multistory Triangular-Shaped Building," by J. Petrovski, R.M. Stephen, E. Gartenbaum and J.G. Bouwkamp - 1976 (PB 273 279)A07

EERC 76-4 "Earthquake Induced Deformations of Earth Dams," by N. Serff, H.B. Seed, F.I. Makdisi & C.-Y. Chang - 1976 (PB 292 065)A08

EERC 76-5 "Analysis and Design of Tube-Type Tall Building Structures," by H. de Clercq and G.H. Powell - 1976 (PB 252 220) A10

EERC 76-6 "Time and Frequency Domain Analysis of Three-Dimensional Ground Motions, San Fernando Earthquake," by T. Kubo and J. Penzien (PB 260 556)A11

EERC 76-7 "Expected Performance of Uniform Building Code Design Masonry Structures," by R.L. Mayes, Y. Omote, S.W. Chen and R.W. Clough - 1976 (PB 270 098)A05

EERC 76-8 "Cyclic Shear Tests of Masonry Piers, Volume 1 - Test Results," by R.L. Mayes, Y. Omote, R.W. Clough - 1976 (PB 264 424)A06

EERC 76-9 "A Substructure Method for Earthquake Analysis of Structure - Soil Interaction," by J.A. Gutierrez and A.K. Chopra - 1976 (PB 257 783)A08

EERC 76-10 "Stabilization of Potentially Liquefiable Sand Deposits using Gravel Drain Systems," by H.B. Seed and J.R. Booker - 1976 (PB 258 820)A04

EERC 76-11 "Influence of Design and Analysis Assumptions on Computed Inelastic Response of Moderately Tall Frames," by G.H. Powell and D.G. Row - 1976 (PB 271 409)A06

EERC 76-12 "Sensitivity Analysis for Hysteretic Dynamic Systems: Theory and Applications," by D. Ray, K.S. Pister and E. Polak - 1976 (PB 262 859)A04

EERC 76-13 "Coupled Lateral Torsional Response of Buildings to Ground Shaking," by C.L. Kan and A.K. Chopra - 1976 (PB 257 907)A09

EERC 76-14 "Seismic Analyses of the Banco de America," by V.V. Bertero, S.A. Mahin and J.A. Hollings - 1976

EERC 76-15 "Reinforced Concrete Frame 2: Seismic Testing and Analytical Correlation," by R.W. Clough and J. Gidwani - 1976 (PB 261 323)A08

EERC 76-16 "Cyclic Shear Tests of Masonry Piers, Volume 2 - Analysis of Test Results," by R.L. Mayes, Y. Omote and R.W. Clough - 1976

EERC 76-17 "Structural Steel Bracing Systems: Behavior Under Cyclic Loading," by E.P. Popov, K. Takanashi and C.W. Roeder - 1976 (PB 260 715)A05

EERC 76-18 "Experimental Model Studies on Seismic Response of High Curved Overcrossings," by D. Williams and W.G. Godden - 1976 (PB 269 548)A08

EERC 76-19 "Effects of Non-Uniform Seismic Disturbances on the Dumbarton Bridge Replacement Structure," by F. Baron and R.E. Hamati - 1976 (PB 282 981)A16

EERC 76-20 "Investigation of the Inelastic Characteristics of a Single Story Steel Structure Using System Identification and Shaking Table Experiments," by V.C. Matzen and H.D. McNiven - 1976 (PB 258 453)A07

EERC 76-21 "Capacity of Columns with Splice Imperfections," by E.P. Popov, R.M. Stephen and R. Philbrick - 1976 (PB 260 378)A04

EERC 76-22 "Response of the Olive View Hospital Main Building during the San Fernando Earthquake," by S. A. Mahin, V.V. Bertero, A.K. Chopra and R. Collins - 1976 (PB 271 425)A14

EERC 76-23 "A Study on the Major Factors Influencing the Strength of Masonry Prisms," by N.M. Mostaghel, R.L. Mayes, R. W. Clough and S.W. Chen - 1976 (Not published)

EERC 76-24 "GADFLEA - A Computer Program for the Analysis of Pore Pressure Generation and Dissipation during Cyclic or Earthquake Loading," by J.R. Booker, M.S. Rahman and H.B. Seed - 1976 (PB 263 947)A04

EERC 76-25 "Seismic Safety Evaluation of a R/C School Building," by B. Bresler and J. Axley - 1976

EERC 76-26 "Correlative Investigations on Theoretical and Experimental Dynamic Behavior of a Model Bridge Structure," by K. Kawashima and J. Penzien - 1976 (PB 263 388)A11

EERC 76-27 "Earthquake Response of Coupled Shear Wall Buildings," by T. Srichatrapimuk - 1976 (PB 265 157)A07

EERC 76-28 "Tensile Capacity of Partial Penetration Welds," by E.P. Popov and R.M. Stephen - 1976 (PB 262 899)A03

EERC 76-29 "Analysis and Design of Numerical Integration Methods in Structural Dynamics," by H.M. Hilber - 1976 (PB 264 410)A06

EERC 76-30 "Contribution of a Floor System to the Dynamic Characteristics of Reinforced Concrete Buildings," by L.E. Malik and V.V. Bertero - 1976 (PB 272 247)A13

EERC 76-31 "The Effects of Seismic Disturbances on the Golden Gate Bridge," by F. Baron, M. Arikan and R.E. Hamati - 1976 (PB 272 279)A09

EERC 76-32 "Infilled Frames in Earthquake Resistant Construction," by R.E. Klingner and V.V. Bertero - 1976 (PB 265 892)A13

UCB/EERC-77/01 "PLUSH - A Computer Program for Probabilistic Finite Element Analysis of Seismic Soil-Structure Interaction," by M.P. Romo Organista, J. Lysmer and H.B. Seed - 1977

UCB/EERC-77/02 "Soil-Structure Interaction Effects at the Humboldt Bay Power Plant in the Ferndale Earthquake of June 7, 1975," by J.E. Valera, H.B. Seed, C.F. Tsai and J. Lysmer - 1977 (PB 265 795)A04

UCB/EERC-77/03 "Influence of Sample Disturbance on Sand Response to Cyclic Loading," by K. Mori, H.B. Seed and C.K. Chan - 1977 (PB 267 352)A04

UCB/EERC-77/04 "Seismological Studies of Strong Motion Records," by J. Shoja-Taheri - 1977 (PB 269 655)A10

UCB/EERC-77/05 "Testing Facility for Coupled-Shear Walls," by L. Li-Hyung, V.V. Bertero and E.P. Popov - 1977

UCB/EERC-77/06 "Developing Methodologies for Evaluating the Earthquake Safety of Existing Buildings," by No. 1 - B. Bresler; No. 2 - B. Bresler, T. Okada and D. Zisling; No. 3 - T. Okada and B. Bresler; No. 4 - V.V. Bertero and B. Bresler - 1977 (PB 267 354)A08

UCB/EERC-77/07 "A Literature Survey - Transverse Strength of Masonry Walls," by Y. Omote, R.L. Mayes, S.W. Chen and R.W. Clough - 1977 (PB 277 933)A07

UCB/EERC-77/08 "DRAIN-TABS: A Computer Program for Inelastic Earthquake Response of Three Dimensional Buildings," by R. Guendelman-Israel and G.H. Powell - 1977 (PB 270 693)A07

UCB/EERC-77/09 "SUBWALL: A Special Purpose Finite Element Computer Program for Practical Elastic Analysis and Design of Structural Walls with Substructure Option," by D.Q. Le, H. Peterson and E.P. Popov - 1977 (PB 270 567)A05

UCB/EERC-77/10 "Experimental Evaluation of Seismic Design Methods for Broad Cylindrical Tanks," by D.P. Clough (PB 272 280)A13

UCB/EERC-77/11 "Earthquake Engineering Research at Berkeley - 1976," - 1977 (PB 273 507)A09

UCB/EERC-77/12 "Automated Design of Earthquake Resistant Multistory Steel Building Frames," by N.D. Walker, Jr. - 1977 (PB 276 526)A09

UCB/EERC-77/13 "Concrete Confined by Rectangular Hoops Subjected to Axial Loads," by J. Vallenas, V.V. Bertero and E.P. Popov - 1977 (PB 275 165)A06

UCB/EERC-77/14 "Seismic Strain Induced in the Ground During Earthquakes," by Y. Sugimura - 1977 (PB 284 201)A04

UCB/EERC-77/15 "Bond Deterioration under Generalized Loading," by V.V. Bertero, E.P. Popov and S. Viwathanatepa - 1977

UCB/EERC-77/16 "Computer Aided Optimum Design of Ductile Reinforced Concrete Moment Resisting Frames," by S.W. Zagajeski and V.V. Bertero - 1977 (PB 280 137)A07

UCB/EERC-77/17 "Earthquake Simulation Testing of a Stepping Frame with Energy-Absorbing Devices," by J.M. Kelly and D.F. Tsztoo - 1977 (PB 273 506)A04

UCB/EERC-77/18 "Inelastic Behavior of Eccentrically Braced Steel Frames under Cyclic Loadings," by C.W. Roeder and E.P. Popov - 1977 (PB 275 526)A15

UCB/EERC-77/19 "A Simplified Procedure for Estimating Earthquake-Induced Deformations in Dams and Embankments," by F.I. Makdisi and H.B. Seed - 1977 (PB 276 820)A04

UCB/EERC-77/20 "The Performance of Earth Dams during Earthquakes," by H.B. Seed, F.I. Makdisi and P. de Alba - 1977 (PB 276 821)A04

UCB/EERC-77/21 "Dynamic Plastic Analysis Using Stress Resultant Finite Element Formulation," by P. Lukkunapvasit and J.M. Kelly - 1977 (PB 275 453)A04

UCB/EERC-77/22 "Preliminary Experimental Study of Seismic Uplift of a Steel Frame," by R.W. Clough and A.A. Huckelbridge 1977 (PB 278 769)A08

UCB/EERC-77/23 "Earthquake Simulator Tests of a Nine-Story Steel Frame with Columns Allowed to Uplift," by A.A. Huckelbridge - 1977 (PB 277 944)A09

UCB/EERC-77/24 "Nonlinear Soil-Structure Interaction of Skew Highway Bridges," by M.-C. Chen and J. Penzien - 1977 (PB 276 176)A07

UCB/EERC-77/25 "Seismic Analysis of an Offshore Structure Supported on Pile Foundations," by D.D.-N. Liou and J. Penzien 1977 (PB 283 180)A06

UCB/EERC-77/26 "Dynamic Stiffness Matrices for Homogeneous Viscoelastic Half-Planes," by G. Dasgupta and A.K. Chopra - 1977 (PB 279 654)A06

UCB/EERC-77/27 "A Practical Soft Story Earthquake Isolation System," by J.M. Kelly, J.M. Eidinger and C.J. Derham - 1977 (PB 276 814)A07

UCB/EERC-77/28 "Seismic Safety of Existing Buildings and Incentives for Hazard Mitigation in San Francisco: An Exploratory Study," by A.J. Meltsner - 1977 (PB 281 970)A05

UCB/EERC-77/29 "Dynamic Analysis of Electrohydraulic Shaking Tables," by D. Rea, S. Abedi-Hayati and Y. Takahashi 1977 (PB 282 569)A04

UCB/EERC-77/30 "An Approach for Improving Seismic - Resistant Behavior of Reinforced Concrete Interior Joints," by B. Galunic, V.V. Bertero and E.P. Popov - 1977 (PB 290 870)A06

UCB/EERC-78/01 "The Development of Energy-Absorbing Devices for Aseismic Base Isolation Systems," by J.M. Kelly and D.F. Tsztoo - 1978 (PB 284 978)A04

UCB/EERC-78/02 "Effect of Tensile Prestrain on the Cyclic Response of Structural Steel Connections, by J.G. Bouwkamp and A. Mukhopadhyay - 1978

UCB/EERC-78/03 "Experimental Results of an Earthquake Isolation System using Natural Rubber Bearings," by J.M. Eidinger and J.M. Kelly - 1978 (PB 281 686)A04

UCB/EERC-78/04 "Seismic Behavior of Tall Liquid Storage Tanks," by A. Niwa - 1978 (PB 284 017)A14

UCB/EERC-78/05 "Hysteretic Behavior of Reinforced Concrete Columns Subjected to High Axial and Cyclic Shear Forces," by S.W. Zagajeski, V.V. Bertero and J.G. Bouwkamp - 1978 (PB 283 858)A13

UCB/EERC-78/06 "Inelastic Beam-Column Elements for the ANSR-I Program," by A. Riahi, D.G. Row and G.H. Powell - 1978

UCB/EERC-78/07 "Studies of Structural Response to Earthquake Ground Motion," by O.A. Lopez and A.K. Chopra - 1978 (PB 282 790)A05

UCB/EERC-78/08 "A Laboratory Study of the Fluid-Structure Interaction of Submerged Tanks and Caissons in Earthquakes," by R.C. Byrd - 1978 (PB 284 957)A08

UCB/EERC-78/09 "Model for Evaluating Damageability of Structures," by I. Sakamoto and B. Bresler - 1978

UCB/EERC-78/10 "Seismic Performance of Nonstructural and Secondary Structural Elements," by I. Sakamoto - 1978

UCB/EERC-78/11 "Mathematical Modelling of Hysteresis Loops for Reinforced Concrete Columns," by S. Nakata, T. Sproul and J. Penzien - 1978

UCB/EERC-78/12 "Damageability in Existing Buildings," by T. Blejwas and B. Bresler - 1978

UCB/EERC-78/13 "Dynamic Behavior of a Pedestal Base Multistory Building," by R.M. Stephen, E.L. Wilson, J.G. Bouwkamp and M. Button - 1978 (PB 286 650)A08

UCB/EERC-78/14 "Seismic Response of Bridges - Case Studies," by R.A. Imbsen, V. Nutt and J. Penzien - 1978 (PB 286 503)A10

UCB/EERC-78/15 "A Substructure Technique for Nonlinear Static and Dynamic Analysis," by D.G. Row and G.H. Powell - 1978 (PB 288 077)A10

UCB/EERC-78/16 "Seismic Risk Studies for San Francisco and for the Greater San Francisco Bay Area," by C.S. Oliveira - 1978

UCB/EERC-78/17 "Strength of Timber Roof Connections Subjected to Cyclic Loads," by P. Gülkan, R.L. Mayes and R.W. Clough - 1978

UCB/EERC-78/18 "Response of K-Braced Steel Frame Models to Lateral Loads," by J.G. Bouwkamp, R.M. Stephen and E.P. Popov - 1978

UCB/EERC-78/19 "Rational Design Methods for Light Equipment in Structures Subjected to Ground Motion," by J.L. Sackman and J.M. Kelly - 1978 (PB 292 357)A04

UCB/EERC-78/20 "Testing of a Wind Restraint for Aseismic Base Isolation," by J.M. Kelly and D.E. Chitty - 1978 (PB 292 833)A03

UCB/EERC-78/21 "APOLLO - A Computer Program for the Analysis of Pore Pressure Generation and Dissipation in Horizontal Sand Layers During Cyclic or Earthquake Loading," by P.P. Martin and H.B. Seed - 1978 (PB 292 835)A04

UCB/EERC-78/22 "Optimal Design of an Earthquake Isolation System," by M.A. Bhatti, K.S. Pister and E. Polak - 1978 (PB 294 735)A06

UCB/EERC-78/23 "MASH - A Computer Program for the Non-Linear Analysis of Vertically Propagating Shear Waves in Horizontally Layered Deposits," by P.P. Martin and H.B. Seed - 1978 (PB 293 101)A05

UCB/EERC-78/24 "Investigation of the Elastic Characteristics of a Three Story Steel Frame Using System Identification," by I. Kaya and H.D. McNiven - 1978

UCB/EERC-78/25 "Investigation of the Nonlinear Characteristics of a Three-Story Steel Frame Using System Identification," by I. Kaya and H.D. McNiven - 1978

UCB/EERC-78/26 "Studies of Strong Ground Motion in Taiwan," by Y.M. Hsiung, B.A. Bolt and J. Penzien - 1978

UCB/EERC-78/27 "Cyclic Loading Tests of Masonry Single Piers: Volume 1 - Height to Width Ratio of 2," by P.A. Hidalgo, R.L. Mayes, H.D. McNiven and R.W. Clough - 1978

UCB/EERC-78/28 "Cyclic Loading Tests of Masonry Single Piers: Volume 2 - Height to Width Ratio of 1," by S.-W.J. Chen, P.A. Hidalgo, R.L. Mayes, R.W. Clough and H.D. McNiven - 1978

UCB/EERC-78/29 "Analytical Procedures in Soil Dynamics," by J. Lysmer - 1978

UCB/EERC-79/01 "Hysteretic Behavior of Lightweight Reinforced Concrete Beam-Column Subassemblages," by B. Forzani, E.P. Popov, and V.V. Bertero - 1979

UCB/EERC-79/02 "The Development of a Mathematical Model to Predict the Flexural Response of Reinforced Concrete Beams to Cyclic Loads, Using System Identification," by J.F. Stanton and H.D. McNiven - 1979

UCB/EERC-79/03 "Linear and Nonlinear Earthquake Response of Simple Torsionally Coupled Systems," by C.L. Kan and A.K. Chopra - 1979

UCB/EERC-79/04 "A Mathematical Model of Masonry for Predicting Its Linear Seismic Response Characteristics," by Y. Mengi and H.D. McNiven - 1979

UCB/EERC-79/05 "Mechanical Behavior of Lightweight Concrete Confined by Different Types of Lateral Reinforcement," by M.A. Manrique, V.V. Bertero and E.P. Popov - 1979

UCB/EERC-79/06 "Static Tilt Tests of a Tall Cylindrical Liquid Storage Tank," by R.W. Clough and A. Niwa - 1979

UCB/EERC-79/07 "The Design of Steel Energy Absorbing Restrainers and Their Incorporation Into Nuclear Power Plants for Enhanced Safety: Volume 1 - Summary Report," by P.N. Spencer, V.F. Zackay, and E.R. Parker - 1979

UCB/EERC-79/08 "The Design of Steel Energy Absorbing Restrainers and Their Incorporation Into Nuclear Power Plants for Enhanced Safety: Volume 2 - The Development of Analyses for Reactor System Piping," "Simple Systems" by M.C. Lee, J. Penzien, A.K. Chopra, and K. Suzuki "Complex Systems" by G.H. Powell, E.L. Wilson, R.W. Clough and D.G. Row - 1979

UCB/EERC-79/09 "The Design of Steel Energy Absorbing Restrainers and Their Incorporation Into Nuclear Power Plants for Enhanced Safety: Volume 3 - Evaluation of Commerical Steels," by W.S. Owen, R.M.N. Pelloux, R.O. Ritchie, M. Faral, T. Ohhashi, J. Toplosky, S.J. Hartman, V.F. Zackay, and E.R. Parker - 1979

UCB/EERC-79/10 "The Design of Steel Energy Absorbing Restrainers and Their Incorporation Into Nuclear Power Plants for Enhanced Safety: Volume 4 - A Review of Energy-Absorbing Devices," by J.M. Kelly and M.S. Skinner - 1979

UCB/EERC-79/11 "Conservatism In Summation Rules for Closely Spaced Modes," by J.M. Kelly and J.L. Sackman - 1979

UCB/EERC-79/12 "Cyclic Loading Tests of Masonry Single Piers Volume 3 - Height to Width Ratio of 0.5," by P.A. Hidalgo, R.L. Mayes, H.D. McNiven and R.W. Clough - 1979

UCB/EERC-79/13 "Cyclic Behavior of Dense Coarse-Grained Materials in Relation to the Seismic Stability of Dams," by N.G. Banerjee, H.B. Seed and C.K. Chan - 1979

UCB/EERC-79/14 "Seismic Behavior of Reinforced Concrete Interior Beam-Column Subassemblages," by S. Viwathanatepa, E.P. Popov and V.V. Bertero - 1979

UCB/EERC-79/15 "Optimal Design of Localized Nonlinear Systems with Dual Performance Criteria Under Earthquake Excitations," by M.A. Bhatti - 1979

UCB/EERC-79/16 "OPTDYN - A General Purpose Optimization Program for Problems with or without Dynamic Constraints," by M.A. Bhatti, E. Polak and K.S. Pister - 1979

UCB/EERC-79/17 "ANSR-II, Analysis of Nonlinear Structural Response, Users Manual," by D.P. Mondkar and G.H. Powell - 1979

UCB/EERC-79/18 "Soil Structure Interaction in Different Seismic Environments," A. Gomez-Masso, J. Lysmer, J.-C. Chen and H.B. Seed - 1979

UCB/EERC-79/19 "ARMA Models for Earthquake Ground Motions," by M.K. Chang, J.W. Kwiatkowski, R.F. Nau, R.M. Oliver and K.S. Pister - 1979

UCB/EERC-79/20 "Hysteretic Behavior of Reinforced Concrete Structural Walls," by J.M. Vallenas, V.V. Bertero and E.P. Popov - 1979

UCB/EERC-79/21 "Studies on High-Frequency Vibrations of Buildings I: The Column Effects," by J. Lubliner - 1979

UCB/EERC-79/22 "Effects of Generalized Loadings on Bond Reinforcing Bars Embedded in Confined Concrete Blocks," by S. Viwathanatepa, E.P. Popov and V.V. Bertero - 1979

UCB/EERC-79/23 "Shaking Table Study of Single-Story Masonry Houses, Volume 1: Test Structures 1 and 2," by P. Gülkan, R.L. Mayes and R.W. Clough - 1979

UCB/EERC-79/24 "Shaking Table Study of Single-Story Masonry Houses, Volume 2: Test Structures 3 and 4," by P. Gülkan, R.L. Mayes and R.W. Clough - 1979

UCB/EERC-79/25 "Shaking Table Study of Single-Story Masonry Houses, Volume 3: Summary, Conclusions and Recommendations," by R.W. Clough, R.L. Mayes and P. Gülkan - 1979

UCB/EERC-79/26 "Recommendations for a U.S.-Japan Cooperative Research Program Utilizing Large-Scale Testing Facilities," by U.S.-Japan Planning Group - 1979

UCB/EERC-79/27 "Earthquake-Induced Liquefaction Near Lake Amatitlan, Guatemala," by H.B. Seed, I. Arango, C.K. Chan, A. Gomez-Masso and R. Grant de Ascoli - 1979

UCB/EERC-79/28 "Infill Panels: Their Influence on Seismic Response of Buildings," by J.W. Axley and V.V. Bertero - 1979

UCB/EERC-79/29 "3D Truss Bar Element (Type 1) for the ANSR-II Program," by D.P. Mondkar and G.H. Powell - 1979

UCB/EERC-79/30 "2D Beam-Column Element (Type 5 - Parallel Element Theory) for the ANSR-II Program," by D.G. Row, G.H. Powell and D.P. Mondkar

UCB/EERC-79/31 "3D Beam-Column Element (Type 2 - Parallel Element Theory) for the ANSR-II Program," by A. Riahi, G.H. Powell and D.P. Mondkar - 1979

UCB/EERC-79/32 "On Response of Structures to Stationary Excitation," by A. Der Kiureghian - 1979

UCB/EERC-79/33 "Undisturbed Sampling and Cyclic Load Testing of Sands," by S. Singh, H.B. Seed and C.K. Chan - 1979

UCB/EERC-79/34 "Interaction Effects of Simultaneous Torsional and Compressional Cyclic Loading of Sand," by P.M. Griffin and W.N. Houston - 1979

UCB/EERC-80/01 "Earthquake Response of Concrete Gravity Dams Including Hydrodynamic and Foundation Interaction Effects," by A.K. Chopra, P. Chakrabarti and S. Gupta - 1980

UCB/EERC-80/02 "Rocking Response of Rigid Blocks to Earthquakes," by C.S. Yim, A.K. Chopra and J. Penzien - 1980

UCB/EERC-80/03 "Optimum Inelastic Design of Seismic-Resistant Reinforced Concrete Frame Structures," by S.W. Zagajeski and V.V. Bertero - 1980

UCB/EERC-80/04 "Effects of Amount and Arrangement of Wall-Panel Reinforcement on Hysteretic Behavior of Reinforced Concrete Walls," by R. Iliya and V.V. Bertero - 1980

UCB/EERC-80/05 "Shaking Table Research on Concrete Dam Models," by R.W. Clough and A. Niwa - 1980

UCB/EERC-80/06 "Piping With Energy Absorbing Restrainers: Parameter Study on Small Systems," by G.H. Powell, C. Oughourlian and J. Simons - 1980

UCB/EERC-80/07 "Inelastic Torsional Response of Structures Subjected to Earthquake Ground Motions," by Y. Yamazaki - 1980

UCB/EERC-80/08 "Study of X-Braced Steel Frame Structures Under Earthquake Simulation," by Y. Ghanaat - 1980

UCB/EERC-80/09 "Hybrid Modelling of Soil-Structure Interaction," by S. Gupta, T.W. Lin, J. Penzien and C.S. Yeh - 1980

UCB/EERC-80/10 "General Applicability of a Nonlinear Model of a One Story Steel Frame," by B.I. Sveinsson and H. McNiven - 1980

UCB/EERC-80/11 "A Green-Function Method for Wave Interaction with a Submerged Body," by W. Kioka - 1980

UCB/EERC-80/12 "Hydrodynamic Pressure and Added Mass for Axisymmetric Bodies," by F. Nilrat - 1980

UCB/EERC-80/13 "Treatment of Non-Linear Drag Forces Acting on Offshore Platforms," by B.V. Dao and J. Penzien - 1980

UCB/EERC-80/14 "2D Plane/Axisymmetric Solid Element (Type 3 - Elastic or Elastic-Perfectly Plastic) for the ANSR-II Program," by D.P. Mondkar and G.H. Powell - 1980

UCB/EERC-80/15 "A Response Spectrum Method for Random Vibrations," by A. Der Kiureghian - 1980

UCB/EERC-80/16 "Cyclic Inelastic Buckling of Tubular Steel Braces," by V.A. Zayas, E.P. Popov and S.A. Mahin - June 1980

UCB/EERC-80/17 "Dynamic Response of Simple Arch Dams Including Hydrodynamic Interaction," by C.S. Porter and A.K. Chopra - July 1980